CONTROL OF UNCERTAIN NONLINEAR SYSTEMS USING EVENT-TRIGGERED ADAPTIVE DYNAMIC PROGRAMMING

Raju Dahal

CONTROL OF UNCERTAIN NONLINEAR SYSTEMS USING EVENT-TRIGGERED ADAPTIVE DYNAMIC PROGRAMMING

A
Thesis submitted in
partial fulfilment of the requirements
for the dual degree of

Master of Science (Engineering)

and

Doctor of Philosophy

By

Raju Dahal

DEPARTMENT OF ELECTRONICS AND ELECTRICAL ENGINEERING
INDIAN INSTITUTE OF TECHNOLOGY GUWAHATI
GUWAHATI - 781039, ASSAM, INDIA

MAY 2025

DEPARTMENT OF ELECTRONICS AND ELECTRICAL ENGINEERING
INDIAN INSTITUTE OF TECHNOLOGY GUWAHATI
GUWAHATI - 781039, ASSAM, INDIA

Certificate

This is to certify that the thesis entitled "**Control of Uncertain Nonlinear Systems using Event-Triggered Adaptive Dynamic Programming** ", submitted by **Raju Dahal** (Registration number: 166302008), a research scholar in the *Department of Electronics and Electrical Engineering, Indian Institute of Technology Guwahati*, for the award of the dual degree of **Master of Science (Engineering) and Doctor of Philosophy**, is a record of an original research work carried out by him under my supervision and guidance. The thesis has fulfilled all requirements as per the regulations of the institute and has reached the standard needed for submission. The results embodied in this thesis have not been submitted to any other University or Institute for the award of any degree or diploma.

Dated:
Guwahati.

Dr. Indrani Kar
Associate Professor
Dept. of Electronics and Electrical Engg.
Indian Institute of Technology Guwahati
Guwahati - 781039, Assam, India.

Dedicated To

My Beloved Parents

Uma Kanta Dahal and Naramaya Devi

for their endless blessings, love, support, and the countless sacrifices they have made.

Acknowledgements

I would like to express my sincere gratitude to my supervisor, Dr. Indrani Kar, for her invaluable guidance throughout my research endeavors. I am deeply thankful for the constant support and patience she has shown to me. I am particularly grateful for her detailed and thoughtful reviews of all my manuscripts, including this thesis, which have contributed significantly to the quality of my work.

I am thankful to my doctoral committee members, Prof. Somanath Majhi, Prof. Chitralekha Mahanta, and Dr. Srinivasan Krishnaswamy, for their suggestions and constructive criticism of my research work, which has helped to shape the research work to its current form. I would also like to thank Dr. Chayan Bhawal and Dr. Parijat Bhowmick for their support and guidance.

I want to thank the staff members of the EEE department, Mrs. Khurshida Yasmin and Mrs. Chayanika Borah Majumdar, for maintaining the Control and Instrumentation (C&I) Lab and providing various resources necessary for the research work.

I want to thank all of my seniors from C&I Lab for their guidance and help. Thanks to Dr. Trusna Meher, Dr. Gautam Sethia, Dr. Abhijit Mazumdar, Dr. Arghya Chakrabarty, Dr. Sushanta Kundu, Mr. Mandar Maitra, and Mr. Bhim Singh. I thank my friends Dr. Manmohan Sharma, Dr. Sami Al-Issa, and Dr. Kasturi Das for helping me with technical and non-technical challenges. I would also like to thank all my juniors, including Anindya, Shiv Santosh, Tamen, Adino, Gangadari, Sanjeev, Athoibi, Nitisha, Biswanath, and Narendra, for their love and support.

I thank all my friends at IITG for making my stay pleasant and memorable. Special thanks to Nishant, Mog, Sibasis, Aditya, Atanu, Samarjeet, Upasana, Manoj, Nayan, Bhale, Harish, Sumit, and Birjit for the beautiful memories and support. I would also like to acknowledge my friends Upasana, Dinesh, Matap, Samten, and Nedup for the moments we shared.

I would like to express my profound appreciation to my family. I thank my parents, siblings, sister-in-law, and cousin Nanu for their unconditional love, sacrifices, and encouragement throughout this long journey. I would also like to thank my cousins and extended family for supporting me in countless ways.

I extend my gratitude to everyone else who has contributed to my academic and personal growth in one way or another. Finally, I thank the Almighty God for granting me this incredible opportunity and for His blessings, which helped me overcome every challenge successfully.

Raju Dahal

Abstract

This thesis presents novel tracking control strategies by utilizing the event-triggered adaptive dynamic programming (ADP) approach for diverse nonlinear systems, addressing matched uncertainties, unmatched uncertainties, control constraints, and state constraints. The first part focuses on event-triggered guaranteed cost tracking control of nonlinear matched uncertain systems. The original problem is transformed into an optimal control problem of the nominal augmented system. A critic neural network (NN) within the framework of ADP is employed to solve the Hamilton-Jacobi-bellman (HJB) equation associated with the optimal control problem. The event-based guaranteed cost is derived, and its relation with the time-based one is discussed. Furthermore, it is proved that the derived event-based controller can make the tracking error uniformly ultimately bounded (UUB). In the second part, the robust tracking control problem for systems with unmatched uncertainties is investigated using an event-based ADP approach. First, an augmented system is constructed based on the nonlinear system and the reference trajectory. Then, by forming an auxiliary system and introducing a discounted cost function, the event-based robust tracking control problem is transformed into the event-based optimal control problem of the auxiliary system. A novel weight tuning rule for the critic network is formulated to avoid the necessity of an initial admissible control at the beginning of the weight tuning process. The obtained event-based controller is updated only at the triggering instants decided by the designed triggering condition. Meanwhile, it is demonstrated that the obtained event-based controller can guarantee the tracking error's uniform ultimate boundedness. The third part introduces an event-triggered robust guaranteed cost tracking controller for continuous-time systems with control constraints and unmatched uncertainty, utilizing the ADP framework. Detailed Lyapunov analysis guarantees the ultimate boundedness of the closed-loop event-triggered system. The derivation of event-based guaranteed cost and its relation with the time-based counterpart is presented. The exclusion of the infamous Zeno behavior is guaranteed. The uniform ultimate boundedness of the critic weight estimation error is established. The fourth part addresses safety-critical control of partially unknown nonlinear uncertain systems with input and state constraints. The unknown part of the system dynamics is approximated using a neural network. A novel safe HJB equation is formulated by incorporating a control barrier function (CBF) and a nonquadratic term into the cost function to penalize violations of safety regulations. Solving the new safe HJB equation involves employing a critic neural network to approximate the solution. The applicability of the proposed frameworks is demonstrated through simulation studies on nonlinear systems, including a robotic arm and other benchmark nonlinear models.

Contents

List of Figures

List of Tables

List of Abbreviations

ACD	Adaptive Critic Design
ADP	Adaptive Dynamic Programming
ARE	Algebraic Ricatti Equation
ANN	Artificial Neural Network
CBF	Control Barrier Function
DP	Dynamic Programming
HJB	Hamilton Jacobi Bellman
LQR	Linear Quadratic Regulator
NN	Neural Network
PDE	Partial Differential Equation
PE	Persistence of Excitation
RL	Reinforcement Learning
UUB	Uniformly Ultimately Bounded
ZOH	Zero Order Hold

List of Symbols

$\mathbb{R}$	The set of all real numbers
$\mathbb{R}^n$	The Euclidean space of n-dimensional real vectors
$\mathbb{R}^{n\times m}$	The space of all $n \times m$ real matrices
I_n	$n \times n$ Identity matrix
$0_{n\times n}$	$n \times n$ Zero matrix
$\|\cdot\|$	The vector norm or the matrix norm
$\top$	Transpose operator
$\nabla(\cdot)$	Gradient operator
$\lambda_M(\cdot)$	Maximum eigenvalue of a matrix
$\lambda_m(\cdot)$	Minimum eigenvalue of a matrix
$\mathrm{tr}(\cdot)$	Trace of a matrix
$\mathrm{diag}(a_1, a_2)$	Diagonal matrix composed of a_1 and a_2
$\triangleq$	Equal by definition
ω_c	Actual weight of critic network
$\hat{\omega}_c$	Approximated weight of critic network
$\tilde{\omega}_c$	Weight approximation error of critic network
$\sigma_c(\zeta)$	Activation function of critic network
ϵ_c	Reconstruction error of critic network
l_c	Learning rate of critic network
l_s	Design parameter
$e_r(t)$	Tracking error
$\mathcal{L}$	Lipschitz constant
γ	Discount factor

List of Publications

Journal Publications:

1. **Raju Dahal** and Indrani Kar,"Robust Tracking Control of Nonlinear Unmatched Uncertain Systems via Event-Based Adaptive Dynamic Programming," *Nonlinear Dynamics*, vol. 109, no. 4, pp. 2831-2850, 2022.

2. **Raju Dahal** and Indrani Kar, "Guaranteed Cost Tracking Control of Constrained Input Nonlinear Uncertain Systems Using Event-Based ADP," *Neurocomputing*, vol. 572, p.127179, 2024.

3. **Raju Dahal** and Indrani Kar."Event-Triggered ADP-Based Tracking Controller for Partially Unknown Nonlinear Uncertain Systems with Input and State Constraints." **Accepted for publication** in *Neural Networks*, 2025.

Conference Publications:

1. **Raju Dahal** and Indrani Kar, "Event-Triggered Robust Tracking Controller for Uncertain Nonlinear Systems Using Adaptive Critic," *17th IEEE India Council International Conference (INDICON)*, NSUT Delhi, 11-13 December 2020.

2. **Raju Dahal** and Indrani Kar, "Event-Triggered Adaptive Dynamic Programming Based Guaranteed Cost Tracking Controller for Uncertain Nonlinear Systems," *8th Indian Control Conference (ICC)*, IIT Madras, 14-16 December 2022.

1

Introduction

Contents

1.1 Background

Nonlinear systems, such as mobile robots, autonomous vehicles, mass-spring-damper systems, chemical reactors, etc., are widely encountered in various engineering disciplines due to the fundamental nonlinearity inherent in numerous physical systems. Controlling nonlinear systems is often challenging due to the difficulties in precisely modeling the system behavior and dealing with uncertainties in parameters and external disturbances. Robust control strategies provide a systematic approach to address these challenges and ensure the stability and performance of nonlinear systems in real-world applications. So, considering the requirement of the robustness of the designed feedback controller to uncertainties, many robust control design schemes have been developed over the past several decades [1–3]. Especially, the method developed by Lin [3], in which an indirect approach is utilized to obtain the robust controller, got remarkable attention [4, 5]. This indirect approach involves transforming the robust control problem into an optimal control problem by carefully choosing a cost function tailored to compensate for the impact of uncertainties. The reason behind adopting this approach lies in the observation that, in numerous instances, solving an optimal control problem offers a more structured framework compared to directly addressing a robust control problem. This indirect strategy presents an effective alternative to the other methodologies extensively explored in existing literature [6].

The optimal control methodology is firmly established and has been applied to both linear and nonlinear systems. It involves finding the control input that optimizes a specific performance criterion while considering the system dynamics and constraints. These performance criteria include minimizing costs, maximizing efficiency, or achieving other performance goals. While designing an optimal controller for linear systems, the linear quadratic regulator (LQR) approach is commonly employed due to its simple and systematic design approach. The solution to the LQR problem involves solving the algebraic Riccati equation (ARE) to find the optimal controller. However, for nonlinear systems, instead of the ARE, one needs to find the solution of the Hamilton-Jacobi-Bellman (HJB) equation [7]. The optimal control problem for continuous-time nonlinear systems is discussed below.

1.1.1 The Optimal Control Problem

Consider the following continuous-time nonlinear systems

$$\dot{x}(t) = f(x(t)) + g(x(t))u(x(t)), \tag{1.1}$$

where $x(t) \in \mathbb{R}^n$ is the state vector and $u(x(t)) \in \mathbb{R}^m$ is the control input. $f(\cdot)$ and $g(\cdot)$ are smooth functions in their arguments with $f(0) = 0$. Let $f(x)+g(x)u(x)$ be Lipschitz continuous on a set $\bar{\Omega}$ in $\mathbb{R}^n$ containing the origin and (1.1) is controllable in the sense that there exists a continuous control policy on $\bar{\Omega}$ that asymptotically stabilizes (1.1). While addressing the optimal control problem, the objective is to derive the feedback control law $u(x)$ that minimizes the cost function

$$J(x) = \int_0^\infty \{U(x(\tau), u(x(\tau)))\}\mathrm{d}\tau, \tag{1.2}$$

where U is known as the utility function, $U(0,0) = 0$, and $U(x,u) \geq 0$ for all x and u. Here, the utility function is selected as the quadratic form $U(x, u(x)) = x^\top Qx + u^\top(x)Ru(x)$, where Q and R represent positive definite matrices, with $Q \in \mathbb{R}^{n\times n}$ and $R \in \mathbb{R}^{m\times m}$.

Let $\tilde{\Psi}(\bar{\Omega})$ be the set of admissible controls on $\bar{\Omega}$. If the associated cost function $J(x)$ is continuously differentiable, then an infinitesimal version of (1.2) is the nonlinear Lyapunov equation written as

$$U(x, u(x)) + (\nabla J(x))^\top(f(x) + g(x)u(x)) = 0 \tag{1.3}$$

with $J(0) = 0$, where ∇ signifies the gradient operator. Before proceeding further, the following definition is stated.

Definition 1.1. (Admissible control). A control policy $u(x)$ is considered admissible with respect to the cost function (1.2) in $\bar{\Omega}$, denoted by $u(x) \in \tilde{\Psi}(\bar{\Omega})$, if $u(x)$ is continuous over $\bar{\Omega}$, $u(0) = 0$, $u(x)$ stabilizes (1.1) over $\bar{\Omega}$, and $J(x)$ is finite for all $x \in \bar{\Omega}$ [8].

Define the Hamiltonian of (1.1) as

$$H(x, u(x), \nabla J(x)) = U(x, u(x)) + (\nabla J(x))^\top(f(x) + g(x)u(x)). \tag{1.4}$$

The optimal cost function is given as

$$J^*(x) = \min_{u\in\tilde{\Psi}(\bar{\Omega})} \int_0^\infty \{U(x(\tau), u(x(\tau)))\}\mathrm{d}\tau. \tag{1.5}$$

Considering the cost function to be continuously differentiable, Bellman's principle of optimality can be utilized to obtain the following optimality condition [9]

$$0 = \min_{u \in \tilde{\Psi}(\bar{\Omega})} H(x, u(x), \nabla J^*(x)), \tag{1.6}$$

which is a nonlinear partial differential equation (PDE), also called as the HJB equation. The HJB equation provides a means to obtain the optimal control $u^*(x)$ in feedback form. The optimal control law for the given problem is derived as

$$u^*(x) = -\frac{1}{2}R^{-1}g^\top(x)\nabla J^*(x). \tag{1.7}$$

By replacing the optimal control policy (1.7) into the nonlinear Lyapunov equation (1.3), the HJB equation can be expressed in terms of $\nabla J^*(x)$ as follows

$$x^\top Qx + (\nabla J^*(x))^\top f(x) - \frac{1}{4}(\nabla J^*(x))^\top g(x)R^{-1}g^\top(x)\nabla J^*(x) = 0 \tag{1.8}$$

with $J^*(0) = 0$.

To obtain the optimal controller (1.7), $J^*(x)$ must be calculated first. This is difficult to achieve because it requires the solution to the HJB equation (1.8). For the case of linear systems, the HJB equation (1.8) becomes the algebraic Riccati equation (ARE). Obtaining the solution of the ARE is easy. However, since the HJB equation is nonlinear PDE, it is generally difficult to solve and may not have an analytical solution. Moreover, the traditional dynamic programming approach for solving the optimal control problem suffers from the "curse of dimensionality" issue, which refers to the exponential increase in the requirement of computational resources with the increase in the dimension of the state space. Therefore, within the framework of adaptive dynamic programming (ADP), an approximate solution of the HJB equation is sought. ADP leverages the universal function approximation property of neural networks to approximate the cost function, which represents the solution to the HJB equation. The following subsection elaborates on how neural networks, inspired by the architecture of human neurons, enable this approximation.

1.1.2 Function Approximation Property of Neural Network

The architecture and functioning of human neurons provide the foundation for artificial neural networks (ANNs). An ANN, also known as a neural network (NN), is simply a collection of artificial neurons with a huge information processing capability. Usually, these neurons are linked together and arranged in layers. An ANN consists of an input layer, an output layer, and one or more hidden layers. In a two layered network, the input layer, serving as the initial layer, receives input from external sources and transmits it to the second layer, known as the hidden layer. Within the hidden layer, each neuron processes input signals from neurons in the preceding layer, calculates a weighted sum, and transmits the result to neurons in the output layer. The schematic of such an ANN is shown in Figure 1.1. In the ADP framework, the ability of the NN

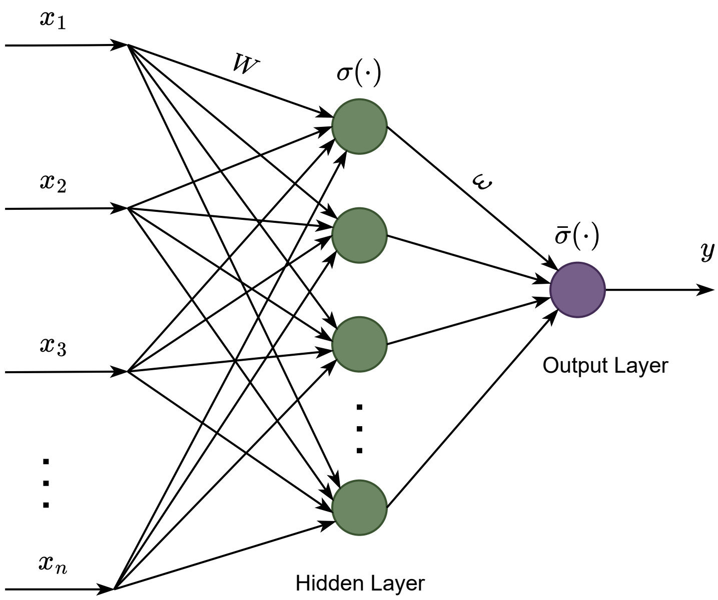

Figure 1.1: Schematic of a two layered ANN

to approximate and adapt to different functions is utilized to approximate the cost function of the optimal control problem. In Figure 1.1, $x_1, x_2, \ldots, x_n$ are the inputs, the matrix W contains the synaptic weights from the input layer to the hidden layer, the hidden layer's activation function is represented by $\sigma(\cdot)$, the vector ω holds the synaptic weights from the hidden layer to the output layer, the output layer's activation function is $\bar{\sigma}(\cdot)$, and the output of the ANN is denoted by y. Let the vector x represent the inputs, and let the reconstruction error be denoted by $\epsilon(x)$. Then, the output of the ANN is given by

$$y = \bar{\sigma}\left(\omega^\top \sigma\left(W^\top x\right) + \epsilon(x)\right). \tag{1.9}$$

By selecting the activation function $\bar{\sigma}(\cdot)$ of the output layer as a linear function, the output in (1.9) can be expressed as

$$y = \omega^\top \sigma\left(W^\top x\right) + \epsilon(x). \tag{1.10}$$

When W is fixed, the only parameter to design is ω, simplifying the neural network to a single-layer function link network. This simplification makes tuning easier. If W is initially selected randomly and kept unchanged with a sufficiently large number of hidden layer neurons, the reconstruction error $\epsilon(x)$ can be significantly reduced because the activation function vector forms a basis and the term $\sigma(W^\top x)$ in (1.10) can be replaced by $\sigma(x)$ [10].

1.1.3 Adaptive Dynamic Programming

Reinforcement learning (RL) is a branch of artificial intelligence focused on teaching an agent to make better decisions by learning from its interactions with the environment. In this context, the agent is the system or entity that makes decisions. The environment, which includes everything other than the agent, interacts with the agent, which serves as both a learner and a decision maker. The primary objective of RL is to guide the agent in taking actions that either maximize cumulative rewards or minimize penalties, emphasizing the concept of optimization. A category of reinforcement learning approaches involves a structure known as actor-critic (or adaptive critic). In this structure, the actor is responsible for applying actions or control laws to the system. The critic, on the other hand, evaluates the actions taken by the actor, estimating their long-term value. The feedback from the critic helps the actor refine its actions, gradually improving its performance. The actor-critic mechanism is shown in Figure 1.2.

The concept of the actor-critic approach was introduced by Werbos as adaptive critic designs (ACDs). Later, the term ACD was interchangeably used with adaptive/approximate dynamic programming (ADP) [11]. The ADP framework is particularly powerful for solving optimal control problems. Optimal control involves determining the best possible actions that an agent should take to achieve specific goals while operating within certain constraints. ADP helps eliminate the "curse of dimensionality" issue associated with the dynamic programming approach traditionally used to solve the optimal control problem. Moreover, it aids in designing control strategies that optimize performance and adapt to changing conditions, making it a versatile tool for managing complex systems.

In real-world applications, researchers have focused on streamlining ADP methods to make

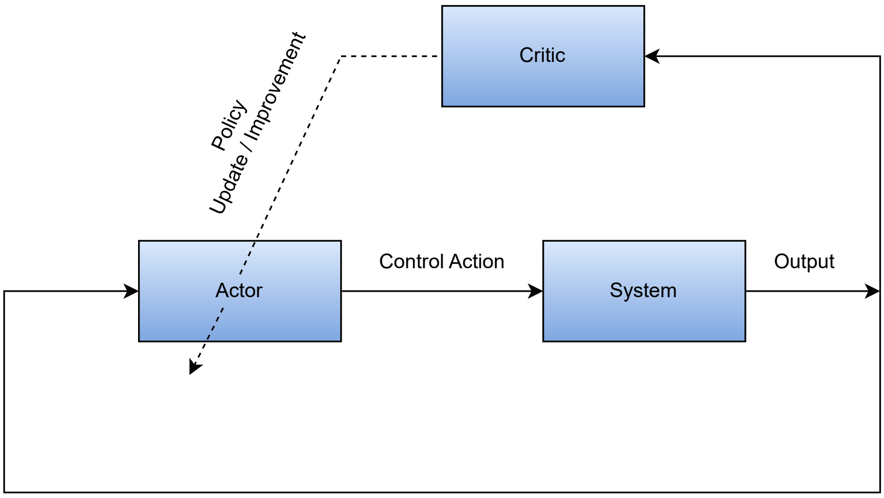

Figure 1.2: Actor-critic mechanism

them more efficient and less complex. One popular approach is single-network adaptive critic design, introduced in [12]. This method uses a single critic network to approximate the optimal cost function, allowing for the derivation of the optimal control law without requiring an actor network. Single network adaptive critic reduces the structural complexity of actor-critic architecture by eliminating the need for an actor network. Moreover, it significantly reduces the computational cost by eliminating the iterative training loops between the actor and critic networks.

A basic block diagram of how a single critic neural network under the ADP framework can be used to solve the optimal control problem is shown in Figure 1.3. Using the universal function approximation property of a neural network, explained in the above subsection, the cost function (1.5) of the optimal control problem can be approximated as

$$J^*(x) = \omega^\top \sigma(x) + \epsilon(x), \tag{1.11}$$

where $\omega \in \mathbb{R}^l$ is the ideal weight vector, $\sigma(x) \in \mathbb{R}^l$ is the activation function, l is the number of neurons in the hidden layer, and $\epsilon(x)$ represents the approximation error of the neural network. Since the ideal weight vector, ω, is not available, a critic network under the ADP framework is constructed to approximate the cost function as

$$\hat{J}^*(x) = \hat{\omega}^\top \sigma(x), \tag{1.12}$$

where $\hat{\omega}$ is the approximate weight of the critic network. The approximate value of the optimal control input (1.7) is given as

$$\begin{aligned}\hat{u}^*(x) &= -\frac{1}{2}R^{-1}g^\top(x)\nabla\hat{J}^*(x)\\ &= -\frac{1}{2}R^{-1}g^\top(x)(\nabla\sigma(x))^\top\hat{\omega}.\end{aligned} \tag{1.13}$$

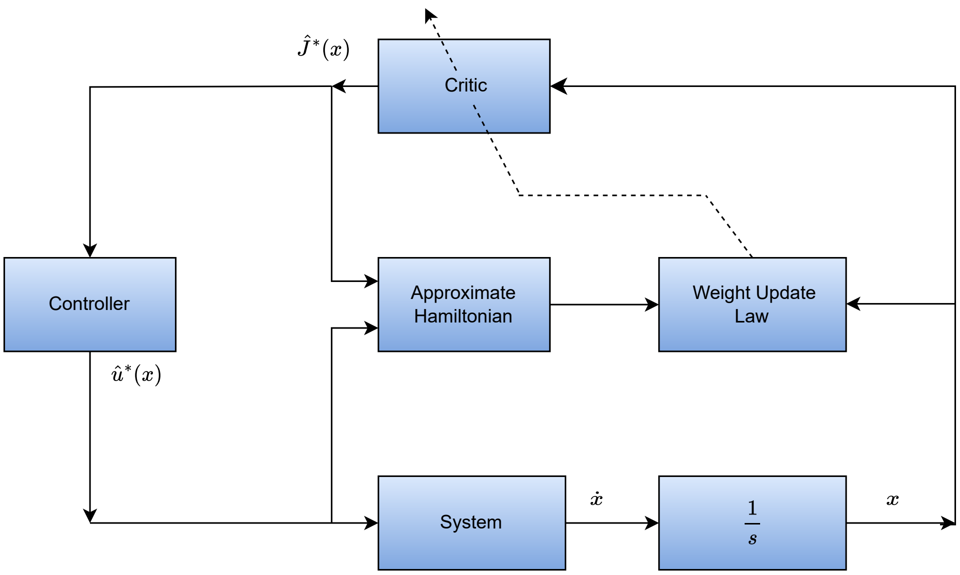

Figure 1.3: Application of single critic network to solve optimal control problem under ADP framework.

A weight update law is designed, typically using a method like gradient descent, to accurately approximate the critic network's weight vector.

In literature, several types of activation functions exist, such as sigmoid (which outputs between 0 and 1), tanh (which outputs between -1 and 1), and ReLU (which returns the input value if it is positive; otherwise, it returns zero). Choosing the proper activation function is often based on heuristic and specific needs. This thesis uses quadratic polynomial and tanh as the activation function. These functions are selected primarily based on the trial and error approach.

1.1.4 Event-Triggered Control

In the classical time-triggered control scheme, the control tasks are scheduled to occur at fixed intervals. For example, depending on the sampling time, a controller may be set to update every ten milliseconds irrespective of the instantaneous system need or status. Although this method simplifies the design process, it can cause inefficient resource utilization since the system may function optimally without continuous updates.

On the other hand, irregular sampling intervals are used in the event-triggered control approach. This means the control input is updated only when a condition is met or a particular event occurs. These conditions or events might include a significant deviation from a desired state, a change in system dynamics, or crossing a predefined threshold. When such an event is detected, the controller computes and applies a new control action. This aperiodic control update approach leads to efficient use of resources. The event-triggered approach is suitable for systems where efficient use of computational and communicational resources is crucial. The event-triggering mechanism is shown in Figure 1.4.

Let $\{t_j\}_{j=0}^{\infty}$ be a monotonically increasing sequence of sampled instants, where $j \in \mathbb{N}$. Here, t_j is the j th sampled instant. Let the value of state $x(t)$ at j th sampled instant be x_j, i.e., $x(t_j) = x_j$. The triggering error, which is defined as the difference between the sampled state x_j and the current state $x(t)$, is expressed as

$$e_{trigg}(t) = x_j - x(t), \quad \forall t \in [t_j, t_{j+1}), j \in \mathbb{N}. \tag{1.14}$$

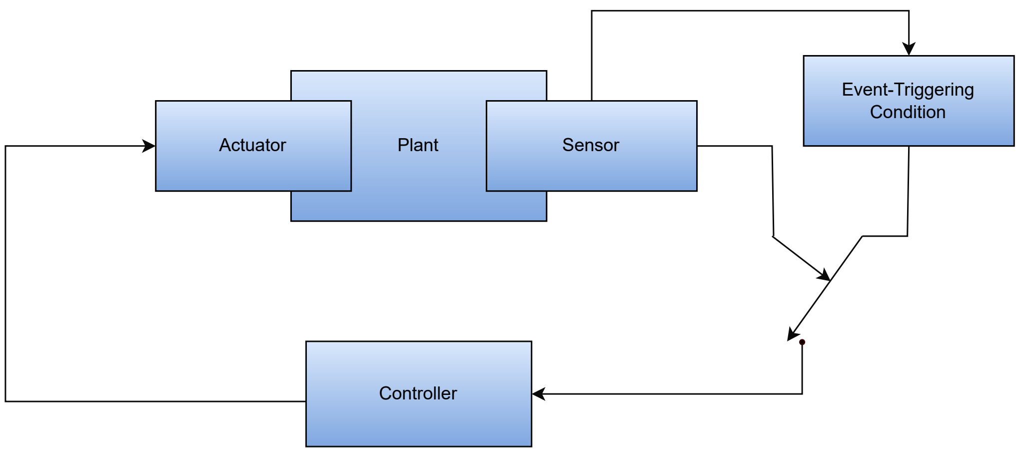

Figure 1.4: Event-triggering mechanism

The triggering depends on $e_{trigg}(t)$. When $e_{trigg}(t)$ violates the predefined triggering threshold, an event is triggered, and the controller is updated. At the triggering instant, the error $e_{trigg}(t)$ is reset to zero. When $e_{trigg}(t)$ does not violate the triggering condition, then the controller is held constant at its previous value. This technique is commonly referred to as the zero-order hold (ZOH) technique. Thus, using the ZOH technique, the event-triggered controller can be described as

$$u(x(t)) = u(x_j), \quad \forall t \in [t_j, t_{j+1}), j \in \mathbb{N}. \tag{1.15}$$

In literature, several approaches are used to design the event triggering rule based on the triggering threshold [13]. The primary methods of determining the triggering threshold are mentioned below.

- **Fixed threshold:** In this approach, a constant value is set as the event-triggering threshold. If the norm of the triggering error crosses this value, an event will occur, and the controller will be updated. This approach provides a simple event-based control design scheme. However, the primary drawback of this approach is its lack of adaptability to varying system conditions [14].

- **Relative threshold:** In this approach, the triggering threshold is determined as a function of the system state, causing its magnitude to vary accordingly. This method enhances resource efficiency while maintaining system performance [15].

- **Switching threshold:** The triggering rule designed based on this approach consists of both the fixed and relative threshold. The triggering threshold switches between the fixed and the relative threshold according to the requirements of certain system performances [13].

- **Lyapunov approach-based threshold:** In this method, the triggering threshold is determined based on the Lyapunov stability criteria. Here, the threshold is mainly a function of the system states, control input, and other design parameters. In the ADP-based event-triggered control design, the Lyapunov-based approach is primarily used to design the triggering rule due to its direct relation with the system's stability [16].

While the event-triggered control method offers advantages over the time-triggered approach, it may require compromising certain control performance to ensure reasonable resource allocation. Thus, the primary challenge in the event-triggered approach lies in co-designing the control law and event-triggering criteria to strike a balance between system performance and the judicious use of limited resources. An additional challenge in designing event-triggered control systems is avoiding setting the minimum inter-event time too low, as this could result in excessive system sampling. This undesirable phenomenon is known as Zeno-Sampling. Therefore, careful consideration and optimization are necessary to establish an effective event-triggered mechanism that optimally utilizes resources while maintaining adequate control performance.

1.1.5 Why Event-Triggered ADP?

The combination of the event-triggered technique with the ADP methodology provides multiple advantages in control system design. Under the event-triggered ADP mechanism, the controller is only updated when an event is triggered, and hence, the computational burden of learning and updating can be greatly reduced. In distributed systems, the event-triggered ADP reduces communication resources between the controller and other components by exchanging data only when necessary. The reduction in computational and communication requirements can translate to reduced energy consumption, particularly relevant for battery-powered devices or environmentally conscious applications. Furthermore, the joint approach reduces actuator attrition, contributing to the robustness and extended longevity of the control system.

1.2 Literature Survey

Reinforcement learning (RL) draws inspiration from natural learning processes observed in animals, where behaviors are adjusted based on rewards and punishments received from the environment. In essence, RL addresses how an agent should adapt its actions to effectively interact with an unfamiliar environment, ultimately aiming to achieve a long-term objective. This concept, born in the 1960s as part of machine learning, has become a powerful tool in computer science and control systems [17]. Subsequently, considerable advancements in RL have been made, particularly from a control perspective [18, 19].

In the realm of control theory, mathematical realizations of RL have been facilitated by ADP. This method helps find the best control actions by focusing on desired performance and learning from collected data, without needing a perfect model of the system. Both RL and ADP are fundamentally influenced by the principles of dynamic programming (DP). The DP, which was introduced by Bellman [20], provides a systematic approach for solving sequential decision problems in an optimal manner. However, the DP faces inherent computational complexity, often referred to as the “curse of dimensionality” [21]. Hence, the necessity for approximate techniques has been acknowledged since the late 1950s [22]. Strategies like ADP and RL are consequently devised to address the challenges and constraints inherent in the DP approach. Initially termed as adaptive critic designs (ACDs) by Werbos, these methods generally consist of actor neural network (NN) and critic NN [23]. The critic NN is used for cost function approximation and the actor NN is used for approximation of the control policy. The ADP, ACDs, RL, and neural (or neuro) dynamic programming (NDP) shares similar principles and are often considered synonymous [24–26]. In this literature survey, ACDs, RL, and NDP are considered as different types of ADP approaches.

Various methodologies exist for estimating the cost function in the ADP framework, with notable approaches including heuristic dynamic programming (HDP), dual heuristic programming (DHP), and globalized DHP (GDHP) as outlined by Werbos [27] and Prokhorov [28]. In HDP, the critic network is designed to estimate the cost function, representing the cost-to-go or strategic utility function, within the Bellman equation of dynamic programming. Conversely, DHP introduces an alternative method where the critic network approximates the derivatives of future costs concerning the state variable, a technique shown to produce smoother derivatives and enhanced performance compared to HDP [29]. The concept of GDHP was initially introduced by Werbos, which involves training the critic network using an error measure that combines elements from both HDP and DHP methodologies [30]. The single-network adaptive critic design introduced in [12] uses a single estimator to approximate the optimal cost function, eliminating the need for an actor network. This approach simplifies the structure and reduces computational costs by removing iterative training loops.

The success of ADP promoted major research in the field of both discrete-time optimal control [24, 31, 32] and continuous-time optimal control [33–37]. In recent years, ADP has been extensively applied to study robust stabilization of nonlinear control systems. Researchers have transformed the robust stabilization problem as optimal control problem and studied it under the framework of ADP [38–41]. In [39], an offline optimal control approach for robust stabilization of nonlinear systems is developed utilizing the HJB equation. Subsequently, in [40], an online approach is formulated to address the nonlinear robust stabilization issue utilizing the policy iteration algorithm under the framework of ADP. A robust actor-critic learning framework is proposed for constrained input nonlinear systems in [41].

In most practical applications, the system states need to track the desired trajectories rather than converge to zero merely [42–44]. In the past several years, significant work has been done on robust tracking control by converting the robust tracking control problem into an optimal control problem and using the ADP framework [45–50]. In [45], single critic network is used to design optimal tracking controller for nonlinear systems without taking into account any uncertainties.

In [46], tracking controller is designed for nonlinear systems with fully unknown dynamics using an identifier-critic based ADP framework. In [47], tracking controller for nonlinear matched uncertain systems is designed using actor-critic dual network within the framework of the ADP. In [48], Zhao proposed an ADP-based optimal tracking control scheme for strict-feedback nonlinear systems. In [49, 50], single critic network is utilized to design tracking controller for nonlinear systems with matched uncertainty. Unmatched uncertainty is considered in [51] while using ADP framework to design tracking controller for nonlinear systems.

When controlling a real system, it is essential to design a controller that not only achieves system stability but also ensures a satisfactory level of performance. The guaranteed cost control approach provides an upper bound to the system cost and ensures the system performance degradation is within that bound. Using the ADP framework the guaranteed cost tracking controller is studied for nonlinear systems considering matched uncertainty in [52, 53] .

The works mentioned above are developed in the conventional time-triggered framework. However, in the time-triggered framework, the controller is updated every sampling instant, leading to inappropriate use of computation and communication resources. In contrast, the event-triggered framework updates the controller only when a predefined triggering condition occurs, resulting in efficient use of resources [15, 43, 54]. The preliminary ideas of event-triggered control were proposed in [55, 56]. Åström's work in [55] provided a crucial theoretical foundation for event-based control. He designed both event-based and periodic controllers for a first-order stochastic system aiming to keep the state near the origin. His analysis showed that for the same average sampling rate, the event-based controller significantly reduced output variance compared to the periodic one. This breakthrough sparked widespread research interest, marking the beginning of a vibrant field. The work by Arzen [56] demonstrated the potential of event-triggered scheme by converting a standard PID controller to an event-driven form. Their comparison through simulations and lab experiments using a double-tank process validated the potential of event-based mechanisms. In [15], Tabuada investigated the asymptotic stability of event-based systems using the Lyapunov approach. He introduced a general framework for designing event-triggering mechanisms for nonlinear systems using an input-to-state stable Lyapunov function. Since the event-triggered mechanism can use energy efficiently, it has been extensively used in networked control systems [57] and multiagent systems [58]. The earlier works on event-triggered control were based on accurate system models [15, 59, 60]. However, in many cases, it is impossible to obtain the system model accurately. To overcome this limitation, the event-triggered strategy was introduced with the adaptive critic designs [16].

The combination of the ADP method with the event-triggered approach can achieve a balance between control performance and resource efficiency, making it a promising solution for a wide range of control applications [61–66]. In the case of discrete-time nonlinear control systems, Sahoo *et al.* [67] designed an event-based adaptive critic while partially relaxing the knowledge of systems dynamics by using an event-based neural network (NN) approximator. However, Sahoo *et al.* [67] focused solely on ensuring stability without optimizing any performance index. In [68], they further achieved near optimal performance index. Most recently, Ha *et al.* [69] studied the problem of nonlinear discrete-time constrained input systems. They used a nonquadratic performance index to tackle the problem of control constraints.

In continuous-time nonlinear control systems, the event-triggered adaptive critic design method is being used in robust control of systems with unknown dynamics [70], systems with uncertainties [71–74] and systems with constrained inputs [75, 76]. Yang *et al.* [70] considered a robust control problem with unknown dynamics. They proposed a unique critic network which is updated by using simultaneously historical and instantaneous state data. An advantage of this type of update law is that it can relax the persistence of excitation (PE) condition. Wang *et al.* [71] designed a robust state feedback considering matched uncertainties. In [72–74] the unmatched uncertainties are considered. Wang *et al.* [72] used a single critic neural network with three layer structure to approximate the cost function but was not able to define a meaningful cost function with respect to the original uncertain system and also the PE condition should satisfy. Zhang *et al.* [74] proposed an event-based ADP algorithm which can relax the PE condition. Compared with the work of Wang *et al.* [72], Yang *et al.* [73] provides more general value function which reduces the computational complexity.

The robust control of constrained input systems is considered in [75–78]. In Dong *et al.* [75] the knowledge of systems dynamics is relaxed. They used two neural networks, i.e., actor and critic. The critic network approximates the cost function and the action network learns the event-triggered constrained control law. Zhu *et al.* [76] considered partially unknown constrained input systems. They employed the identifier network, the critic network and the actor network to approximate the unknown drift dynamics, optimal value and the optimal policy, respectively. The identifier is tuned based on online data, which further trains the critic and actor at triggering instants. In [77, 78] constrained input systems with perturbations are considered. Wang *et al.* in [78] considered the case of matched perturbation. Yang *et al.* in [77] considered the case of mismatched perturbations used an single network adaptive critic to solve the event-triggered HJB equation. They updated the critic using the gradient descent method.

Most recently, in continuous-time nonlinear systems, the event-based adaptive critic design is used in systems with unknown internal states [79] and to study the guaranteed cost control problem [80]. In Zhong *et al*. [79], first they designed an event-triggered regulator based on the system input/output data. Then a neural network based observer is established to recover the entire states from the measurable feedback. Wang *et al*. [80] developed guaranteed cost control strategy of nonlinear systems considering the matched uncertainties. They combine the event-based formulation with the adaptive critic learning strategy under uncertain environment, so as to obtain the nonlinear guaranteed cost control law with adaptivity and self learning properties. The tracking controller for nonlinear systems is developed utilising the event-based ADP approach in [81–83]. In [81], actor-critic framework is used to obtain event-triggered tracking controller for nonlinear systems without considering uncertainty. In [82], a single critic NN is used to obtain tracking controller for nonlinear systems without considering uncertainty and in [83].

Control inputs in many real-world applications may have a bound due to the physical limitation of the actuator or safety constraints. So, it is necessary to consider input constraints while designing a controller for those systems. Otherwise, the controller may attempt to create control inputs that exceed the physical limitations of the actuators, resulting in system instability or even damage. The event-based ADP approach is employed in [84, 85] for the stabilization problem of constrained input nonlinear systems. The tracking control problem of constrained input nonlinear systems without considering uncertainty is investigated in [86]. In [87], matched uncertainty is considered while developing a tracking controller for constrained input partially unknown nonlinear systems via the event-based ADP approach. In safety-critical systems, maintaining states within a designated safety set is crucial for system safety. As systems grow more complex, ensuring this becomes challenging. Control barrier functions (CBFs) have emerged as effective tools for enhancing system safety [88, 89]. In [90], the event-based ADP approach is used to address the regulation problem of state constraint nonlinear systems without any uncertainty.

In many practical scenarios, obtaining exact knowledge of system dynamics is difficult or impossible. To acquire the necessary understanding of the system dynamics, [91] identified a plant model and subsequently synthesized an RL-based optimal tracking controller using this model. In [92], a novel actor-critic-identifier was developed to address the optimal control problem for continuous-time nonlinear systems without needing knowledge of the system's drift dynamics. Modares *et al.* in [93] used online measured data to create an RL-based optimal tracking controller for partially unknown nonlinear systems. In the area of event-triggered control, [94] proposed an identifier network within the ADP framework to approximate drift dynamics. Xue *et al.* in [87] presented an event-triggered tracking controller for partially unknown systems with constraint input using the integral reinforcement learning technique. Based on the discussion in this section, the research motivation is drawn and discussed below.

1.3 Research Motivation

To operate a real plant effectively, it is often necessary to design a controller that not only accurately follows the reference trajectory but also guarantees satisfactory performance, where performance is defined by the cost function. The guaranteed cost tracking control strategy sets an upper bound on a given cost function and promises that any uncertainty-related deterioration of system performance would be less severe than this bound. Notably, the application of the event-triggered ADP approach to address the guaranteed cost tracking control problem in uncertain nonlinear systems remains unexplored. The unmatched uncertainties are more general in nature and can be widely seen in most of the practical systems. Therefore, it is vital to consider unmatched uncertainty while designing a controller for nonlinear systems. However, the application of the event-based ADP approach to tackle the tracking control problem in unmatched uncertain nonlinear systems remains an unexplored domain.

Control inputs in many real-world applications may have a bound due to the physical limitation of the actuator or safety constraints. Thus, it is necessary to consider input constraints while designing a controller for those systems. Otherwise, the controller may attempt to create control inputs that exceed the physical limitations of the actuators, resulting in system instability or even damage. The event-based ADP approach has not been utilized to solve the tracking control problem of unmatched uncertain constrained input nonlinear systems.

In many practical systems, states are restricted by a bound. Deviating from this bound, even briefly, can harm performance or cause permanent damage. Moreover, obtaining precise knowledge of the system dynamics is often impractical due to factors such as modeling errors, varying parameters, and external disturbances. Therefore, it is crucial to consider partially unknown dynamics when developing controllers. The issue of tracking control for such systems, particularly those with input and state constraints, has not been examined using the event-triggered adaptive dynamic programming approach. The discussion in this section forms the basis for the contributions of the thesis, which are detailed in the following section.

1.4 Contributions of the Thesis

The principal objective of the thesis is to design tracking controllers for uncertain nonlinear systems using event-triggered adaptive dynamic programming. Furthermore, constraints in input and states and partially unknown dynamics are also considered while designing the tracking controllers for uncertain nonlinear systems. The primary contributions of the thesis are as follows.

- **Event-triggered guaranteed cost tracking controller for nonlinear systems with matched uncertainty using ADP.**
  By creating an augmented system and utilizing a discounted cost function, the problem of guaranteed cost tracking control is converted into an optimal control problem for the nominal augmented system. The ADP framework is employed to approximate the solution of the HJB equation associated with the optimal control problem. In parallel, a new event-triggering rule is developed to ensure that the obtained optimal controller can be applied to the original system. The work also demonstrates the connection between event-triggered guaranteed cost and time-triggered guaranteed cost. The Lyapunov approach is utilized to demonstrate the uniform ultimate boundedness of all the signals associated with the closed-loop system.

- **Robust tracking control of nonlinear unmatched uncertain systems via the event-triggered ADP.**
  An augmented system is initially constructed based on the nonlinear system and the reference trajectory. Then, by forming an auxiliary system and introducing a discounted cost function, the event-based robust tracking control problem is transformed into the event-based optimal control problem of the auxiliary system. The event-based HJB equation associated with the event-based optimal control problem is solved using a single critic NN under the ADP framework. A novel weight tuning rule for the critic network is formulated to avoid the necessity of an initial admissible control at the beginning of the weight tuning process. Meanwhile, it is demonstrated that the obtained event-based controller can guarantee the tracking error's uniform ultimate boundedness. Furthermore, using the Lyapunov method, the designed novel event-triggering rule is guaranteed to ensure uniform ultimate boundedness of all signals associated with the closed-loop auxiliary system.

- **Guaranteed cost tracking control of constrained input nonlinear uncertain systems via event-triggered ADP.**
  A robust tracking controller is designed to ensure guaranteed cost for nonlinear systems under input constraints and unmatched uncertainties. The event-based ADP approach is utilized to address this problem. First, the tracking error and reference trajectory are combined to form an augmented uncertain system. Then, by decomposing the uncertainty into the matched and unmatched parts, the original tracking problem is converted into the optimal regulation problem of an auxiliary system. The cost function for the auxiliary system is defined, and the associated HJB equation is solved using a single critic NN. Moreover, a novel event-triggering rule is formulated, and it is shown that the designed event-based controller guarantees that the tracking error is uniformly ultimately bounded (UUB). The derivation of event-based guaranteed cost and its relation with the time-based counterpart is presented.

- **Event-triggered ADP-based tracking controller for partially unknown nonlinear uncertain systems with input and state constraints.**
  The event-based ADP approach is used to design a robust tracking controller for partially unknown, unmatched uncertain nonlinear systems with input and state constraints. The process begins with the design of an identifier neural network to approximate the system's unknown dynamics. Following this, an augmented uncertain system is constructed, and the original tracking problem is then transformed into an optimal regulation problem for an auxiliary system. To ensure safety, a novel safe HJB equation is formulated by incorporating a control barrier function (CBF) and a non-quadratic term into the cost function, penalizing any violations of safety regulations. The solution to this safe HJB equation is approximated using a critic neural network. The Lyapunov stability theory is applied to prove that, despite state constraints and uncertain disturbances, the system's states and the critic neural network parameters remain UUB.

1.5 Organization of the Thesis

The remaining chapters of the thesis are organized as follows.

- **Chapter 2:** This chapter presents the design of a guaranteed cost tracking controller for uncertain nonlinear systems. The approach begins with formulating an augmented system and a discounted cost function. An event-triggered HJB equation is then derived, along with an event-triggering rule for the controller's implementation. The UUB of the tracking error is shown using the Lyapunov approach. The solution to the event-triggered HJB equation is obtained through a single critic network. Additionally, a separate triggering rule is formulated for the weight-learning process, and UUB of the weight approximation error and stability of closed-loop augmented systems is analyzed. This chapter includes two simulation examples to validate the theoretical findings.

- **Chapter 3:** This chapter addresses the tracking control problem for unmatched uncertain nonlinear systems using an event-triggered ADP approach. The problem is converted into an optimal control problem for an auxiliary system, and the event-triggered HJB equation is derived and solved using ADP. The UUB of the tracking error and all signals of the closed-loop auxiliary system are established, along with the event-triggering and weight tuning rules. Two simulation examples are included to demonstrate the effectiveness of the developed strategy.

- **Chapter 4:** This chapter presents a robust guaranteed cost tracking controller for constrained input nonlinear systems with unmatched uncertainty using the event-based ADP. The chapter begins by reformulating the control problem into an optimal regulation problem for an auxiliary system. Next, a single critic neural network is used to solve the HJB equation, ensuring the tracking error is UUB. The event-based guaranteed cost is proven to be upper bound. The Lyapunov method then confirms the UUB of the weight estimation error. Finally, two simulation examples demonstrate the effectiveness and reliability of the proposed approach.

- **Chapter 5:** In this chapter, the design of an event-triggered robust tracking controller for unmatched uncertain nonlinear systems with state and input constraints is presented. A neural network-based identifier is employed to approximate the system's unknown drift dynamics. The robust tracking control problem is then converted into an optimal control problem for an augmented auxiliary system. A critic neural network is used to solve the optimal control problem, and an event-triggering rule is developed to update the controller only when necessary. The chapter also demonstrates that the identifier, critic weight approximation error, identification error, and tracking error are all UUB. The effectiveness of the proposed controller is validated through a simulation study.

- **Chapter 6:** This chapter concludes the thesis by reviewing and discussing the main ideas, contributions, and limitations of the research. Furthermore, it indicates potential directions for future research, paving the way for ongoing advancements in the field.

2

Event-Triggered Guaranteed Cost Tracking Controller for Nonlinear Systems with Matched Uncertainty using ADP

Contents

2.1 Introduction

In practical applications, uncertainties from sources such as modeling errors, system aging, and external disturbances inevitably arise. The uncertainties can be classified as matched and unmatched. The matched uncertainties are those where the uncertainty enters the system through the same channel as the control input. These uncertainties degrade control system performance and pose a risk of instability. While existing literature predominantly focuses on designing stable controllers for uncertain nonlinear systems, it is essential to acknowledge that stability is the minimum requirement in system design. Beyond stability, there is a pressing need to ensure that controllers not only maintain system stability but also guarantee a satisfactory level of performance. This challenge is addressed through guaranteed cost control methods, which provide an upper limit on a predefined cost, ensuring the closed-loop system remains stable and achieves a certain performance level.

In this chapter, the robust guaranteed cost tracking control problem of nonlinear matched uncertain systems is studied using the event-based adaptive dynamic programming (ADP). By constructing an augmented system and using a discounted cost function, the guaranteed cost control problem is transformed into an optimal control problem of the nominal augmented system. The ADP framework is utilized to approximate the solution of the Hamilton-Jacobi-Bellman (HJB) equation associated with the optimal control problem. The event-based guaranteed cost is derived, and its relation with the time-based one is discussed. Furthermore, it is proved that the derived event-based controller can make the tracking error uniformly ultimately bounded (UUB). The applicability of the suggested technique is exhibited using a simulation study.

The rest of the chapter is structured in the following manner. In Section 2.2, the problem formulation is presented briefly. In Section 2.3, the event-triggering rule is formulated, and using the Lyapunov method, it is shown that the tracking error is uniformly ultimately bounded. Additionally, the event-based guaranteed cost is derived. In Section 2.4, the ADP framework is utilized to solve the event-based HJB equation. Uniform ultimate boundedness of the weight approximation error is shown in Section 2.5. In Section 2.6, two simulation examples are shown to display the effectiveness of the proposed method. Finally, the findings are summarized in Section 2.7.

2.2 Problem Description

Consider the following continuous-time nonlinear system

$$\dot{x}(t) = f(x(t)) + g(x(t))u(t) + \Delta f(x(t)), \tag{2.1}$$

where $x(t) \in \mathbb{R}^n$ is the state vector and $u(t) \in \mathbb{R}^m$ is the control input. The nonlinear functions $f(\cdot)$ and $g(\cdot)$ are known and differentiable in their arguments with $f(0) = 0$. The uncertainty $\Delta f(x)$ is considered as matched uncertainty, and it is given by $\Delta f(x) = g(x)d_1(x)$. Let $d_1(x) \in \mathbb{R}^m$ be a bounded function with $d_1(0) = 0$. Let the upper bound of $d_1(x)$ be $d_M(x)$. The dynamics of the reference trajectory is

$$\dot{x}_r(t) = Z(x_r(t)), \tag{2.2}$$

where $x_r(t) \in \mathbb{R}^n$ and $Z(x_r)$ is Lipschitz continuous and it satisfies $Z(0) = 0$. Define the tracking error as $e_r(t) = x(t) - x_r(t)$. Using (2.1) and (2.2), the tracking error dynamics is obtained as

$$\dot{e}_r(t) = f(e_r(t) + x_r(t)) + g(e_r(t) + x_r(t))u(t) + \Delta f(e_r(t) + x_r(t)) - Z(x_r(t)). \tag{2.3}$$

In standard optimal tracking control, both a steady-state and feedback controller are used. However, under event-triggering, determining triggering instants for the steady-state part is difficult. By defining an augmented system that captures the tracking error dynamics along with the reference model, the original optimal tracking control problem is converted into the optimal regulation problem of the augmented system. The augmented state is defined as $\zeta(t) = [e_r^\top(t), x_r^\top(t)]^\top \in \mathbb{R}^{2n}$. Using (2.2) and (2.3) the augmented system is derived as

$$\dot{\zeta}(t) = F(\zeta(t)) + G(\zeta(t))u(t) + \Delta F(\zeta(t)), \tag{2.4}$$

where

$$F(\zeta(t)) = \begin{bmatrix} f(e_r(t) + x_r(t)) - Z(x_r(t)) \\ Z(x_r(t)) \end{bmatrix}, \tag{2.5}$$

$$G(\zeta(t)) = \begin{bmatrix} g(e_r(t) + x_r(t)) \\ 0 \end{bmatrix}, \tag{2.6}$$

and $\Delta F(\zeta(t)) = G(\zeta(t))d(\zeta(t))$ with $d(\zeta) = d_1(e_r(t) + x_r(t))$. The upper bound of $d(\zeta)$ can be derived as

$$\|d(\zeta)\| = \|d_1(e_r + x_r)\| = \|d_1(x)\| \leq d_M(x) = d_M(e_r + x_r) \triangleq d_M(\zeta). \tag{2.7}$$

For the augmented system (2.4), a discounted cost function is defined as

$$\bar{J}(\zeta(t), u) = \int_t^\infty e^{-\gamma(\tau - t)}\{U(\zeta(\tau), u(\tau))\}\mathrm{d}\tau, \tag{2.8}$$

where $\gamma > 0$ is the discount factor $U(\zeta, u) = \zeta^\top \bar{Q}\zeta + u^\top Ru$. The matrix $\bar{Q} = diag\{Q, 0_{n\times n}\}$, where $0_{n\times n}$ is an $n \times n$ null matrix, and $Q \in \mathbb{R}^{n\times n}$, $R \in \mathbb{R}^{m\times m}$ are positive definite matrices.

The goal of this study is to derive a robust controller u using the event-based ADP approach such that the trajectory of the uncertain system (2.1) follows the reference trajectory (2.2). Additionally, the study aims to ensure that the cost function (2.8) remains within a specified upper bound.

Remark 2.1. The control input may become unbounded if the reference trajectory does not converge to zero since it is dependent on the reference trajectory [52]. The cost function may become unbounded as a result of this. To make the cost function $\bar{J}(\zeta, u) < \infty$, the discount term $e^{-\gamma(\tau - t)}$ is incorporated.

2.3 Event-Triggered Guaranteed Cost Tracking Controller

The guaranteed cost robust tracking control problem of nonlinear uncertain system can be obtained by designing an optimal controller for nominal augmented system. The nominal part of the augmented system is written as

$$\dot{\zeta}(t) = F(\zeta(t)) + G(\zeta(t))u(t). \tag{2.9}$$

The cost function associated with the nominal augmented system (2.9) is expressed as

$$J(\zeta(t), u) = \int_t^{\infty} e^{-\gamma(\tau - t)} \{U(\zeta(\tau), u(\tau)) + \beta d_M^2(\zeta(\tau))\} \mathrm{d}\tau, \tag{2.10}$$

where β is a positive constant and $\beta d_M^2(\zeta)$ is included to counter the presence of the uncertainty in the original system. Moreover, it is considered that $\beta d_M^2(\zeta) \geq \lambda_M(R) d_M^2(\zeta)$, where $\lambda_M(R)$ represents the maximum eigenvalue value of R.

Let Ω be a compact subset of $\mathbb{R}^{2n}$. Let $\Psi(\Omega)$ be the set of admissible controls on Ω, and let the proposed optimal controller be admissible. If the relevant cost function is continuously differentiable then the infinitesimal variant of (2.10) is derived as

$$\zeta^\top \bar{Q} \zeta + u^\top R u + \beta d_M^2(\zeta) + \dot{J}(\zeta) - \gamma J(\zeta) = 0 \tag{2.11}$$

with $J(0) = 0$. The associated Hamiltonian is expressed as

$$H(\zeta, u, \nabla J(\zeta)) = (\nabla J(\zeta))^\top (F(\zeta) + G(\zeta) u) + \zeta^\top \bar{Q} \zeta + u^\top R u + \beta d_M^2(\zeta) - \gamma J(\zeta), \tag{2.12}$$

where ∇ represents the gradient operator. From this chapter onwards, ∇ signifies gradient with respect to ζ. The optimal value of the cost function is given as

$$J^*(\zeta(t), u) = \min_{u \in \Psi(\Omega)} \int_t^{\infty} e^{-\gamma(\tau - t)} \{U(\zeta(\tau), u(\tau)) + \beta d_M^2(\zeta(\tau))\} \mathrm{d}\tau \tag{2.13}$$

and it fulfills

$$\min_{u \in \Psi(\Omega)} H(\zeta, u, \nabla J^*(\zeta)) = 0. \tag{2.14}$$

The optimal value of the control input is expressed as

$$\begin{aligned} u^*(\zeta) &= arg \min_{u \in \Psi(\Omega)} H(\zeta, u, \nabla J^*(\zeta)) \\ &= -\frac{1}{2} R^{-1} G^\top(\zeta) \nabla J^*(\zeta). \end{aligned} \tag{2.15}$$

The time-triggered HJB equation is obtained by substituting $u^*(\zeta)$ for u in the (2.12)

$$(\nabla J^*(\zeta))^\top (F(\zeta) + G(\zeta) u^*(\zeta)) + \zeta^\top \bar{Q} \zeta + u^{*\top}(\zeta) R u^*(\zeta) + \beta d_M^2(\zeta) - \gamma J^*(\zeta) = 0 \tag{2.16}$$

with $J^*(0) = 0$.

2.3.1 Event-Based Tracking Controller Design

In this study, the event-based method is employed rather than the conventional time-triggered one. The event-based approach helps to conserve computing and communication resources by updating the controller only when a predefined triggering condition occurs. Based on the event-triggering mechanism explained in Chapter 1, for the remaining part of the thesis, let the triggering error be denoted by $e_j(t)$ and given as

$$e_j(t) = \zeta_j - \zeta(t), \quad \forall t \in [t_j, t_{j+1}), j \in \mathbb{N}.$$

The control input $u(\zeta(t))$ under the event-triggered scenario is expressed as

$$u(\zeta(t)) = u(\zeta_j) \triangleq \mu(\zeta_j), \quad \forall t \in [t_j, t_{j+1}), j \in \mathbb{N}. \tag{2.17}$$

Now, the time-triggered control input (2.15) under event-triggered mechanism is written as

$$\mu^*(\zeta_j) = -\frac{1}{2}R^{-1}G^\top(\zeta_j)\nabla J^*(\zeta_j), \quad \forall t \in [t_j, t_{j+1}), j \in \mathbb{N}. \tag{2.18}$$

Using the event-based control input (2.18) in (2.16), the event-based HJB equation is expressed as

$$\begin{aligned} H(\zeta, \mu^*(\zeta_j), \nabla J^*(\zeta)) = (\nabla J^*(\zeta))^\top F(\zeta) - \frac{1}{2}G(\zeta)R^{-1}G^\top(\zeta_j)\nabla J^*(\zeta_j) - \gamma J^*(\zeta) \\ + \frac{1}{4}(\nabla J^*(\zeta_j))^\top G(\zeta_j)R^{-1}G^\top(\zeta_j)\nabla J^*(\zeta_j) + \beta d_M^2. \end{aligned} \tag{2.19}$$

Before deriving the event-triggering condition by using the Lyapunov approach, the following assumption is made. This assumption holds in numerous applications where the controller is affine in relation to the event-triggering error [16, 95].

Assumption 2.1. The control law $u^*(\zeta)$ is Lipschitz continuous on Ω with a positive Lipschitz constant $\mathcal{L}$ such that

$$\left\|u^*(\zeta(t)) - \mu^*(\zeta_j)\right\| \leq \mathcal{L}\left\|e_j(t)\right\|. \tag{2.20}$$

Theorem 2.1. For the augmented system (2.4), if Assumption 2.1 holds, $J^*(\zeta)$ is the solution to the event-based HJB equation (2.19), then the event-based control input (2.18) can ensure that the closed loop system is asymptotically stable for $\gamma = 0$ and the tracking error is uniformly ultimately bounded for $\gamma \neq 0$, provided the event-triggering rule is given by

$$\left\|e_j(t)\right\|^2 \leq \frac{(1-\eta_1^2)\lambda_m(Q)\left\|e_r\right\|^2 + d_M^2(\zeta)(\beta - 2\lambda_M(R))}{2\lambda_M(R)\mathcal{L}^2} \triangleq \|e_T\|^2, \tag{2.21}$$

where $\eta_1 \in (0,1)$ is a design parameter and $\lambda_m(Q)$ represents the minimum eigenvalue of Q.

Proof: Since $J^*(\zeta)$ is positive definite, it is considered as a candidate Lyapunov function. Now, taking the time differentiation of $J^*(\zeta)$ along the path of $\dot{\zeta}(t) = F(\zeta(t)) + G(\zeta(t))(\mu^*(\zeta_j) + d(\zeta(t)))$ yields

$$\dot{J}^*(\zeta) = (\nabla J^*(\zeta))^\top (F(\zeta) + G(\zeta)(\mu^*(\zeta_j) + d(\zeta))). \tag{2.22}$$

Using (2.16), $(\nabla J^*(\zeta))^\top F(\zeta)$ is expressed as

$$(\nabla J^*(\zeta))^\top F(\zeta) = -(\nabla J^*(\zeta))^\top G(\zeta)u^*(\zeta) - \zeta^\top \bar{Q}\zeta - u^{*\top}(\zeta)Ru^*(\zeta) - \beta d_M^2(\zeta) + \gamma J^*(\zeta) \tag{2.23}$$

and from (2.15), one can write

$$(\nabla J^*(\zeta))^\top G(\zeta) = -2u^{*\top}(\zeta)R. \tag{2.24}$$

With the help of (2.23) and (2.24), (2.22) is expressed as

$$\dot{J}^*(\zeta) = -\zeta^\top \bar{Q}\zeta - \beta d_M^2(\zeta) + u^{*\top}(\zeta)Ru^*(\zeta) - 2u^{*\top}(\zeta)R(\mu^*(\zeta_j) + d(\zeta)) + \gamma J^*(\zeta). \tag{2.25}$$

One can write

$$\begin{aligned} & u^{*\top}(\zeta)Ru^*(\zeta) - 2u^{*\top}(\zeta)R(\mu^*(\zeta_j) + d(\zeta)) \\ & = (u^*(\zeta) - (\mu^*(\zeta_j) + d(\zeta)))^\top R(u^*(\zeta) - (\mu^*(\zeta_j) + d(\zeta))) \\ & \quad - (\mu^*(\zeta_j) + d(\zeta))^\top R(\mu^*(\zeta_j) + d(\zeta)). \end{aligned} \tag{2.26}$$

Now,

$$\begin{aligned}&(u^*(\zeta) - (\mu^*(\zeta_j) + d(\zeta)))^\top R(u^*(\zeta) - (\mu^*(\zeta_j) + d(\zeta)))\\ &\leq 2\lambda_M(R)(\left\|(u^*(\zeta) - \mu^*(\zeta_j)) - d(\zeta)\right\|^2)\\ &\leq 2\lambda_M(R)(\mathcal{L}^2 \left\|e_j(t)\right\|^2 + d_M^2(\zeta)).\end{aligned} \tag{2.27}$$

The expression $\zeta^\top \bar{Q}\zeta$ is equal to $e_r^\top Q e_r$. Utilising (2.26), (2.27) and Assumption 2.1, (2.25) can be rewritten as

$$\begin{aligned}\dot{J}^*(\zeta) \leq -\eta_1^2\lambda_m(Q)\left\|e_r(t))\right\|^2 + (\eta_1^2 - 1)\lambda_m(Q)\left\|e_r(t))\right\|^2\\ - \beta d_M^2(\zeta) + \gamma J^*(\zeta) + 2\lambda_M(R)(\mathcal{L}^2\left\|e_j(t)\right\|^2 + d_M^2(\zeta)).\end{aligned} \tag{2.28}$$

Since, $J^*(\zeta)$ is positive definite and bounded on Ω, let J^*_{max} be the maximum value of $J^*(\zeta)$. So, from (2.28), $\dot{J}^*(\zeta) \leq 0$ only if e_r lies outside of the set

$$\Omega_{e_r} = \left\{ e_r : \|e_r\| \leq \frac{1}{\eta_1}\sqrt{\frac{\gamma J^*_{max}}{\lambda_m(Q)}}\right\}. \tag{2.29}$$

Thus, it is concluded that for $\gamma \neq 0$, the tracking error $e_r(t)$ is uniformly ultimately bounded and the ultimate bound is $\frac{1}{\eta_1}\sqrt{\frac{\gamma J^*_{max}}{\lambda_m(Q)}}$. When $\gamma = 0$, then from (2.28) it is clear that $\dot{J}^*(\zeta) \leq -\eta_1^2\lambda_m(Q)\left\|e_r(t))\right\|^2$. In other words, the closed loop system is asymptotically stable for $\gamma = 0$.

Theorem 2.2. The event-based guaranteed cost can be expressed as

$$\begin{aligned}\bar{J}(\zeta, \mu^*(\zeta_j)) \leq \int_t^\infty e^{-\gamma(\tau - t)}\{(\mu^*(\zeta_j) - u^*(\zeta))^\top R(\mu^*(\zeta_j) - u^*(\zeta))\}\mathrm{d}\tau\\ + \int_t^\infty e^{-\gamma(\tau-t)}\{u^{*\top}(\zeta)Ru^*(\zeta)\}\mathrm{d}\tau + J^*(\zeta).\end{aligned} \tag{2.30}$$

Proof: The original cost function

$$\bar{J}(\zeta(t), u) \leq \int_t^\infty e^{-\gamma(\tau-t)}\{U(\zeta(\tau), u(\tau)) + \dot{J}^*(\zeta) - \gamma J^*(\zeta)\}\mathrm{d}\tau + J^*(\zeta). \tag{2.31}$$

Now,

$$\begin{aligned}U(\zeta, u) + \dot{J}^*(\zeta) - \gamma J^*(\zeta) = \zeta^\top\bar{Q}\zeta + u^\top Ru - \gamma J^*(\zeta)\\ + (\nabla J^*(\zeta))^\top(F(\zeta) + G(\zeta)(u + d(\zeta))).\end{aligned} \tag{2.32}$$

Using (2.15) and (2.16), it can be deduced that

$$U(\zeta,u)+\dot{J}^*(\zeta)-\gamma J^*(\zeta)=u^\top Ru+u^{*\top}(\zeta)Ru^*(\zeta)-2u^{*\top}(\zeta)Ru \\ -2u^{*\top}(\zeta)Rd(\zeta)-\beta d_M^2(\zeta). \tag{2.33}$$

Since $d^\top(\zeta)Rd(\zeta)\le\lambda_M(R)\|d(\zeta)\|^2\le\beta d_M^2(\zeta)$, it follows that

$$\begin{aligned}U(\zeta,u)+\dot{J}^*(\zeta)-\gamma J^*(\zeta)&\le(u-u^*(\zeta))^\top R(u-u^*(\zeta))+u^{*\top}(\zeta)Ru^*(\zeta)\\&\quad-(u^*(\zeta)+d(\zeta))^\top R(u^*(\zeta)+d(\zeta))\\&\le(u-u^*(\zeta))^\top R(u-u^*(\zeta))+u^{*\top}(\zeta)Ru^*(\zeta).\end{aligned}\tag{2.34}$$

Now using (2.34) and (2.31), one can write

$$\begin{aligned}\bar{J}(\zeta(t),u)=&\int_t^\infty e^{-\gamma(\tau-t)}\{(u-u^*(\zeta))^\top R(u-u^*(\zeta))\}\\&+\int_t^\infty e^{-\gamma(\tau-t)}\{u^{*\top}(\zeta)Ru^*(\zeta)\}\mathrm{d}\tau+J^*(\zeta).\end{aligned}\tag{2.35}$$

Replace u by $\mu^*(\zeta_j)$ to obtain the event-triggered guaranteed cost as given in (2.30). This concludes the proof.

Remark 2.2. From (2.35), it is clear that the event-triggered guaranteed cost is greater than the time-triggered guaranteed cost. However, the main objective of the event-triggered guaranteed cost control approach is to balance the system performance degradation and the computational and communicational resources used.

2.3.2 Zeno-Behavior Analysis

Zeno-behavior refers to the phenomenon where an infinite number of events occur within a finite time. This phenomenon can make the controlled system unstable. The avoidance of Zeno-behavior can be guaranteed by guaranteeing that the inter-event time is nonzero. Therefore, it is essential to do the Zeno-behaviour analysis while designing an event-triggered control. Before proceeding further, the following assumption is made.

Assumption 2.2. The function $F(\zeta)+G(\zeta)\mu^*(\zeta_j)$ satisfies the Lipschitz condition on the set Ω.

That is, there exist positive constants $F_M > 0$ and $A > 0$ such that

$$\|F(\zeta) + G(\zeta)\mu^*(\zeta_j)\| \leq F_M\|\zeta\| + A\|e_j\|, \tag{2.36}$$

where e_j represents the triggering error.

Theorem 2.3. Let Assumption 2.2 be valid. Consider the system (2.4) and let the optimal event-triggered control input $\mu^*(\zeta_j)$ given in (2.18) be applied to it, and the events are triggered according to the triggering law (2.21), then the minimum inter-event time $(\Delta t_j)_{\min} = \min\limits_{j\in\mathbb{N}}\{t_{j+1} - t_j\}$ is guaranteed to have a lower bound determined by

$$(\Delta t_j)_{\min} \geq \frac{1}{F_M + A}\ln(1 + \alpha_{\min}) > 0, \tag{2.37}$$

where $\alpha_{\min} = \min\limits_{j\in\mathbb{N}}(\alpha_j)$ is a positive value and α_j is defined in (2.43).

Proof: By Assumption 2.2, consider the augmented system (2.4) with the event-triggered control $\mu^*(\zeta_j)$. One can write

$$\|\dot{\zeta}\| \leq \|F(\zeta)\| + \|G(\zeta)\mu^*(\zeta_j)\| + \|G(\zeta)d(\zeta)\|. \tag{2.38}$$

Since, $G(\zeta)$ and $d(\zeta)$ both are bounded, considering $\|G(\zeta)d(\zeta)\| = K_{Gd}$, (2.38) implies

$$\|\dot{\zeta}\| \leq F_M\|\zeta\| + A\|e_j\| + K_{Gd}. \tag{2.39}$$

Given that $e_j(t) = \zeta_j - \zeta(t)$ for $t \in [t_j, t_{j+1})$, thus $\dot{\zeta} = -\dot{e}_j$. Hence, one can write

$$\|\dot{e}_j\| \leq (F_M + A)\|e_j\| + F_M\|\zeta_j\| + K_{Gd}. \tag{2.40}$$

At the triggering instant t_j, the triggering error is 0, i.e., $e_j(t_j) = 0$. Using the comparison lemma from [96], mentioned in Appendix A.4, the solution to (2.40) is obtained as

$$\|e_j\| \leq \frac{F_M\|\zeta_j\| + K_{Gd}}{(F_M + A)}(e^{(F_M+A)(t-t_j)} - 1). \tag{2.41}$$

The next triggering instant t_{j+1} occurs when the right-hand side of (2.41) exceeds the triggering threshold $\|e_T\|$ given by (2.21), leading to the inequality

$$\frac{F_M\|\zeta_j\| + K_{Gd}}{(F_M + A)}(e^{(F_M+A)(t_{j+1}-t_j)} - 1) > \|e_T^-(t_{j+1})\|, \tag{2.42}$$

with $e_T^-(t_{j+1}) = \lim_{\bar{q}\to 0^+} e_T(t_{j+1} - \bar{q})$. Define

$$\alpha_j = \frac{(F_M + A)\|e_T^-(t_{j+1})\|}{F_M\|\zeta_j\| + K_{Gd}}, \tag{2.43}$$

so, (2.42) becomes

$$e^{(F_M+A)(t_{j+1}-t_j)} - 1 > \alpha_j. \tag{2.44}$$

Substituting $\Delta t_j = t_{j+1} - t_j$, one can write

$$\Delta t_j > \frac{1}{(F_M + A)} \ln(1 + \alpha_j), \quad j \in \mathbb{N}. \tag{2.45}$$

Let $\alpha_{\min} = \min_{j\in\mathbb{N}}(\alpha_j)$, where $\alpha_{\min} > 0$. Taking the minimum over Δt_j, the minimum inter-event time is expressed as

$$(\Delta t_j)_{\min} > \frac{1}{(F_M + A)} \ln(1 + \alpha_{\min}) > 0. \tag{2.46}$$

Therefore, the Zeno-behavior is avoided.

2.4 Event-Based ADP Implementation

A single critic NN is employed under ADP framework to approximate the cost function as $J^*(\zeta) = \omega_c^\top \sigma_c(\zeta) + \epsilon_c(\zeta)$, where the terms $\omega_c \in \mathbb{R}^q$, $\sigma_c(\zeta) \in \mathbb{R}^q$, q, and $\epsilon_c(\zeta)$ represent the ideal weight, the activation function, the number of neurons in the hidden layer, and the NN reconstruction error, respectively. Then,

$$\nabla J^*(\zeta) = (\nabla\sigma_c(\zeta))^\top \omega_c + \nabla\epsilon_c(\zeta). \tag{2.47}$$

Due to the inaccessibility of the exact weight ω_c, the estimated value $\hat{\omega}_c$ is applied to estimate the cost function $J^*(\zeta)$ as $\hat{J}^*(\zeta) = \hat{\omega}_c^\top \sigma_c(\zeta)$. Thus, one can write

$$\nabla \hat{J}^*(\zeta) = (\nabla \sigma_c(\zeta))^\top \hat{\omega}_c. \tag{2.48}$$

Using (2.47) in (2.18) , it can be written that

$$\mu^*(\zeta_j) = -\frac{1}{2} R^{-1} G^\top(\zeta_j)(\nabla \sigma_c(\zeta_j))^\top \omega_c + \epsilon_u^*, \tag{2.49}$$

where $\epsilon_u^* = -\frac{1}{2} R^{-1} G^\top(\zeta_j) \nabla \epsilon_c(\zeta_j)$. Similarly, using (2.48) in (2.18), the approximate value of event-based control is obtained as

$$\hat{\mu}^*(\zeta_j) = -\frac{1}{2} R^{-1} G^\top(\zeta_j)(\nabla \sigma_c(\zeta_j))^\top \hat{\omega}_c. \tag{2.50}$$

Using (2.49), the Hamiltonian (2.12) can be expressed as

$$\begin{aligned} H(\zeta, \mu^*(\zeta_j), \omega_c) &= \omega_c^\top \nabla \sigma_c(\zeta)(F(\zeta) + G(\zeta)\mu^*(\zeta_j)) - \gamma \omega_c^\top \sigma_c(\zeta) \\ &\quad + \zeta^\top \bar{Q} \zeta + u^{*^\top}(\zeta_j) R \mu^*(\zeta_j) + \beta d_M^2(\zeta) \\ &\triangleq e_{cH}, \end{aligned} \tag{2.51}$$

where $e_{cH} = -(\nabla \epsilon_c(\zeta))^\top (F(\zeta) + G(\zeta)\mu^*(\zeta_j)) + \gamma \epsilon_c(\zeta)$ denotes the residual error resulting from NN approximation. Utilising (2.50), the approximate Hamiltonian is expressed as

$$\begin{aligned} \hat{H}(\zeta, \hat{\mu}^*(\zeta_j), \hat{\omega}_c) &= \hat{\omega}_c^\top \nabla \sigma_c(\zeta)(F(\zeta) + G(\zeta)\hat{\mu}^*(\zeta_j)) - \gamma \hat{\omega}_c^\top \sigma_c(\zeta) \\ &\quad + \zeta^\top \bar{Q} \zeta + \hat{\mu}^*(\zeta_j) R \hat{\mu}^*(\zeta_j) + \beta d_M^2(\zeta). \end{aligned} \tag{2.52}$$

From the HJB equation (2.19), it can be inferred that $H(\zeta, \mu^*(\zeta_j), \omega_c) = 0$. Hence, the approximation error of Hamiltonian $\hat{H}(\zeta, \hat{\mu}^*(\zeta_j), \hat{\omega}_c) - H(\zeta, \mu^*(\zeta_j), \omega_c)$ is written as

$$e_c = \hat{\omega}_c^\top \nabla \sigma_c(\zeta)(F(\zeta) + G(\zeta)\hat{\mu}^*(\zeta_j)) + \zeta^\top \bar{Q} \zeta + \hat{\mu}^*(\zeta_j) R \hat{\mu}^*(\zeta_j) + \beta d_M^2(\zeta) - \gamma \hat{\omega}_c^\top \sigma_c(\zeta). \tag{2.53}$$

The gradient descent approach is now used to optimize the quadratic function $E = (1/2) e_c^\top e_c$ in order to sufficiently reduce the approximation error of the Hamiltonian. The critic weight tuning rule $\dot{\hat{\omega}}_c = -l_c(\partial E/\partial \hat{\omega}_c)$ is obtained as

$$\dot{\hat{\omega}}_c = \frac{-l_c \phi}{(1+\phi^\top \phi)^2}(\hat{\omega}_c^\top \phi + \zeta^\top \bar{Q}\zeta + \hat{\mu}^*(\zeta_j) R \hat{\mu}^*(\zeta_j) + \beta d_M^2(\zeta)), \tag{2.54}$$

where $l_c > 0$ is the critic learning rate, $\phi = \nabla\sigma_c(\zeta)(F(\zeta) + G(\zeta)\hat{\mu}^*(\zeta_j)) - \gamma\hat{\omega}_c^\top \sigma_c(\zeta)$ and the term $1/(1+\phi^\top\phi)^2$ is employed to normalise ϕ. The weight estimation error of the critic network is given as $\tilde{\omega}_c = \omega_c - \hat{\omega}_c$. Now considering (2.51) and (2.53), it is derived that

$$e_c = -\tilde{\omega}_c^\top \phi + e_{cH}. \tag{2.55}$$

By using (2.54) and (2.55), error dynamics is presented as

$$\dot{\tilde{\omega}}_c = \frac{-l_c \phi}{(1+\phi^\top \phi)^2}(\tilde{\omega}_c^\top \phi - e_{cH}). \tag{2.56}$$

Given the continuous nature of the system dynamics and the abrupt shifts in the controller's value when an event is triggered, the closed-loop system is best represented as an impulsive dynamical system [97]. This system is characterized by flow dynamics for $t \in [t_j, t_{j+1})$ and jump dynamics at $t = t_{j+1}$. Let $\psi = [\zeta^\top, \zeta_j^\top, \tilde{\omega}_c^\top]^\top$ be an augmented state vector. The impulsive dynamical representation is given as

$$\dot{\psi}(t) = \begin{bmatrix} F(\zeta) + G(\zeta)\hat{\mu}^*(\zeta_j) \\ 0 \\ \frac{-l_c\phi}{(1+\phi^\top\phi)^2}(\tilde{\omega}_c^\top \phi - e_{cH}) \end{bmatrix}, \quad t \in [t_j, t_{j+1}) \tag{2.57}$$

$$\psi(t^+) = \psi(t) + \begin{bmatrix} 0 \\ \zeta_j - \zeta(t) \\ 0 \end{bmatrix}, \quad t \in t_{j+1}, \tag{2.58}$$

where $\psi(t^+) = \lim_{\iota \to 0^+} \psi(t+\iota)$ and $\iota \in (0, t_{j+1} - t_j)$.

2.5 Stability Analysis

In this section, the stability of the impulsive dynamical representation of the closed-loop system, described by (2.57) and (2.58), is analyzed. Before proceeding, some commonly assumed conditions from the literature are presented [70].

Assumption 2.3. Let $\nabla\sigma_c(\zeta)$ be Lipschitz continuous satisfying

$$\left\|\nabla\sigma_c(\zeta) - \nabla\sigma_c(\zeta_j)\right\| \leq B\left\|e_j(t)\right\|,$$

where B is a positive constant.

Assumption 2.4. Let $G(\zeta)$, $\nabla\sigma_c(\zeta)$, $\nabla\epsilon_c(\zeta)$, and the ideal weight vector ω_c are upper bounded by positive constants G_M, $\nabla\sigma_{cM}$, $\nabla\epsilon_{cM}$, and ω_{cM}, respectively.

Theorem 2.4. Let the Assumptions 2.1 to 2.4 hold. Consider the nominal augmented system (2.9) with the control input (2.50). Let the critic weights be learned using the tuning rule (2.54). Then the closed-loop system is asymptotically stable, and the weight approximation error is UUB if

$$\begin{aligned}\left\|e_j(t)\right\|^2 &\leq \frac{(1-\eta_2^2)\lambda_m(Q)\left\|e_r(t)\right\|^2 + \beta d_M^2(\zeta) + \lambda_m(R)\left\|\hat{\mu}^*(\zeta_j)\right\|^2}{2\lambda_M(R)\left\|R^{-1}\right\|^2\left(A^2\nabla\sigma_{cM}^2 + B^2G_M^2\right)\left\|\hat{\omega}_c\right\|^2} \\ &\triangleq \left\|\hat{e}_T\right\|^2 \end{aligned} \tag{2.59}$$

and

$$\|\tilde{\omega}_c\| > \sqrt{\frac{2\lambda_1\lambda_M(R)\|R^{-1}\|^2 G_M^2\nabla\varepsilon_{cM}^2 + l_c e_{cHM}^2 + \lambda_1\gamma J_{max}^*}{\lambda_1(l_c\lambda_{\varphi m} - 2\lambda_M(R)\|R^{-1}\|^2 G_M^2\nabla\sigma_{cM}^2) - l_c\lambda_{\varphi M}}} \tag{2.60}$$

where $\eta_2 \in (0,1)$ and $\lambda_1 = 2(1+\phi^\top\phi)$.

Proof: Considering the impulsive dynamical representation given in (2.57) and (2.58), $\Upsilon(t) = \Upsilon_1(t) + \Upsilon_2(t) + \Upsilon_3(t)$ is considered as Lyapunov function candidate, where $\Upsilon_1(t) = J^*(\zeta)$, $\Upsilon_2(t) = J^*(\zeta_j)$ and $\Upsilon_3(t) = \frac{1}{2}\tilde{\omega}_c^\top\tilde{\omega}_c$. The proof is divided into two cases stated below.

Case 1. Events are not triggered, i.e., $t \in [t_j, t_{j+1})$, $j \in \mathbb{N}$. Differentiating $\Upsilon(t)$ with respect to t, it is obtained that $\dot{\Upsilon}(t) = \dot{\Upsilon}_1(t) + \dot{\Upsilon}_2(t) + \dot{\Upsilon}_3(t)$. Now, for $t \in [t_j, t_{j+1})$, $\dot{\Upsilon}_2(t) = 0$. Computing the first derivative of $\Upsilon_1(t)$ along the trajectory generated from $\dot{\zeta}(t) = F(\zeta) + G(\zeta)\hat{\mu}^*(\zeta_j)$,

$$\begin{aligned}\dot{\Upsilon}_1(t) &= -\zeta^\top \bar{Q}\zeta - \beta d_M^2(\zeta) + u^{*\top}(\zeta)Ru^*(\zeta) - 2u^{*\top}(\zeta)R\hat{\mu}^*(\zeta_j) + \gamma J^*(\zeta) \\ &= -\zeta^\top \bar{Q}\zeta - \beta d_M^2(\zeta) - \lambda_m(R)\left\|\hat{\mu}^*(\zeta_j)\right\|^2 + \lambda_M(R)\left\|u^*(\zeta) - \hat{\mu}^*(\zeta_j)\right\|^2 + \gamma J^*(\zeta).\end{aligned} \tag{2.61}$$

One can write

$$\begin{aligned}\left\|u^*(\zeta) - \hat{\mu}^*(\zeta_j)\right\|^2 \leq &\left\|R^{-1}(G^\top(\zeta_j)(\nabla\sigma_c(\zeta_j))^\top - G^\top(\zeta)(\nabla\sigma_c(\zeta))^\top)\hat{\omega}_c\right\|^2 \\ &+ \left\|R^{-1}G^\top(\zeta)((\nabla\sigma_c(\zeta))^\top\tilde{\omega}_c + \nabla\epsilon_c(\zeta))\right\|^2.\end{aligned} \tag{2.62}$$

Now, using Assumption 2.3 and Assumption 2.4, it follows that

$$\begin{aligned}&\left\|G^\top(\zeta_j)(\nabla\sigma_c(\zeta_j))^\top - G^\top(\zeta)(\nabla\sigma_c(\zeta))^\top\right\|^2 \\ &= \left\|(\nabla\sigma_c(\zeta_j) - \nabla\sigma_c(\zeta))G(\zeta_j) + \nabla\sigma_c(\zeta)(G(\zeta_j) - G(\zeta))\right\|^2 \\ &\leq 2(A^2\nabla\sigma_{cM}^2 + B^2G_M^2)\left\|e_j(t)\right\|^2.\end{aligned} \tag{2.63}$$

Considering (2.62) and (2.63), the derivative of $\Upsilon_1(t)$ given in (2.61) can be rewritten as

$$\begin{aligned}\dot{\Upsilon}_1(t) \leq &-\zeta^\top \bar{Q}\zeta - \beta d_M^2(\zeta) - \lambda_m(R)\left\|\hat{\mu}^*(\zeta_j)\right\|^2 + \gamma J^*(\zeta) \\ &+ 2\lambda_M(R)\left\|R^{-1}\right\|^2(A^2\nabla\sigma_{cM}^2 + B^2G_M^2)\left\|e_j(t)\right\|^2\left\|\hat{\omega}_c\right\|^2 \\ &+ 2\lambda_M(R)\left\|R^{-1}\right\|^2 G_M^2\nabla\sigma_{cM}^2\left\|\tilde{\omega}_c\right\|^2 + \nabla\epsilon_{cM}^2.\end{aligned} \tag{2.64}$$

It can stated that $\omega_c^\top\phi = \phi^\top\omega_c$ and $\omega_c^\top\sigma_c(\zeta) = \sigma_c^\top(\zeta)\omega_c$. Letting $\varphi = \phi/(1+\phi^\top\phi)$ and using (2.56), the time derivative of $\Upsilon_3(t)$ is derived as

$$\dot{\Upsilon}_3(t) = -l_c\tilde{\omega}_c^\top\varphi\varphi^\top\tilde{\omega}_c + \frac{l_c}{(1+\phi^\top\phi)}\tilde{\omega}_c^\top\varphi e_{cH}. \tag{2.65}$$

Let $\lambda_M(\varphi\varphi^\top) = \lambda_{\varphi M}$, $\lambda_m(\varphi\varphi^\top) = \lambda_{\varphi m}$, $\lambda_M(\sigma_c(\zeta)\sigma_c^\top(\zeta)) = \lambda_{\sigma M}$ and $\lambda_m(\sigma_c(\zeta)\sigma_c^\top(\zeta)) = \lambda_{\sigma m}$. Now, considering Young's inequality $2a^\top b \leq a^\top a + b^\top b$ and Assumption 2.4, (2.65) can be written as

$$\dot{\Upsilon}_3(t) \leq -l_c\lambda_{\varphi m}\left\|\tilde{\omega}_c\right\|^2 + \frac{l_c}{2(1+\phi^\top\phi)}(\lambda_{\varphi M}\left\|\tilde{\omega}_c\right\|^2 + e_{cHM}^2). \tag{2.66}$$

Combining (2.64) and (2.66), one can write

$$\begin{aligned}\dot{\Upsilon}(t) \leq & -\zeta^\top \bar{Q}\zeta - \beta d_M^2(\zeta) - \lambda_m(R)\left\|\hat{\mu}^*(\zeta_j)\right\|^2 + \gamma J^*_{max} \\ & + 2\lambda_M(R)\left\|R^{-1}\right\|^2 (A^2\nabla\sigma_{cM}^2 + B^2G_M^2)\left\|e_j(t)\right\|^2\left\|\hat{\omega}_c\right\|^2 \\ & + 2\lambda_M(R)\left\|R^{-1}\right\|^2 G_M^2(\nabla\sigma_{cM}^2\left\|\tilde{\omega}_c\right\|^2 + \nabla\epsilon_{cM}^2) \\ & - l_c\lambda_{\varphi m}\left\|\tilde{\omega}_c\right\|^2 + \frac{l_c}{2(1+\phi^\top\phi)}(\lambda_{\varphi M}\left\|\tilde{\omega}_c\right\|^2 + e_{cHM}^2).\end{aligned} \tag{2.67}$$

Since, $\bar{Q} = diag\{Q, 0_{n\times n}\}$, one can write $\zeta^\top(t)\bar{Q}\zeta(t) = e_r^\top(t)Qe_r(t)$. Now, introducing the design parameter η_2 and considering the fact

$$e_r^\top(t)Qe_r(t) \leq \eta_2^2\lambda_m(Q)\left\|e_r(t)\right\|^2 - (\eta_2^2 - 1)\lambda_m(Q)\left\|e_r(t)\right\|^2,$$

if the conditions stated in Theorem 2.4 satisfy then (46) becomes

$$\dot{\Upsilon}(t) \leq -\eta_2^2\lambda_m(Q)\left\|e_r(t)\right\|^2 < 0,$$

which indicates that the derivative of proposed Lyapunov function for $t \in [t_j, t_{j+1})$, $j \in \mathbb{N}$, is negative.

Case 2. Events are triggered, i.e., $t \in t_{j+1}$. Now, the difference of the Lyapunov function candidate is written as

$$\begin{aligned}\Delta\Upsilon(t_j) = & J^*(\zeta(t_j^+)) - J^*(\zeta(t_j)) + \frac{1}{2}\tilde{\omega}_c^\top(t_j^+)\tilde{\omega}_c(t_j^+) \\ & - \frac{1}{2}\tilde{\omega}_c^\top(t_j)\tilde{\omega}_c(t_j)) + J^*(\zeta_{j+1}) - J^*(\zeta_j),\end{aligned} \tag{2.68}$$

where $\zeta(t_j^+) = \lim_{\iota\to 0^+}\zeta(t_j + \iota)$ and $\iota \in (0, t_{j+1} - t_j)$. Since, the derivative of $\Upsilon(t)$ is negative for $t \in [t_j, t_{j+1})$,

$$\Upsilon(t_j) \geq \lim_{\iota\to 0^+}\Upsilon(t_j + \iota) = \Upsilon(t_j^+)\forall\iota \in (0, t_{j+1} - t_j). \tag{2.69}$$

$$J^*(\zeta(t_j^+)) + \frac{1}{2}\tilde{\omega}_c^\top(t_j^+)\tilde{\omega}_c(t_j^+) - J^*(\zeta(t_j)) - \frac{1}{2}\tilde{\omega}_c^\top(t_j)\tilde{\omega}_c(t_j)) \leq 0. \tag{2.70}$$

Let ϑ be a class $\mathcal{K}$ function. If $e_{j+1}(t_j) = \zeta_{j+1} - \zeta_j$, then one can obtain

$$(J^*(\zeta_{j+1}) - J^*(\zeta_j)) \leq -\vartheta \left\| e_{j+1}(t_j) \right\|. \tag{2.71}$$

Thus from (2.70) and (2.71), it is clear that for $t \in t_{j+1}$ the Lyapunov function candidate is monotonically decreasing.

The two aforementioned cases demonstrate that the closed-loop system is asymptotically stable, and the critic weight approximation error is UUB.

The core methodology of the presented work in this chapter is outlined in the flowchart presented in Figure 2.1. The proposed methodology can be divided into learning and implementation phases. During the learning phase, the critic weights are iteratively converged using the weight update rule (2.54) and the event-triggering rule (2.59). These converged weights are then utilized in the implementation phase to approximate the optimal control policy $\mu^*(\zeta_j)$ as $\hat{\mu}^*(\zeta_j)$. The event-triggering rule (2.21) is employed during the implementation phase.

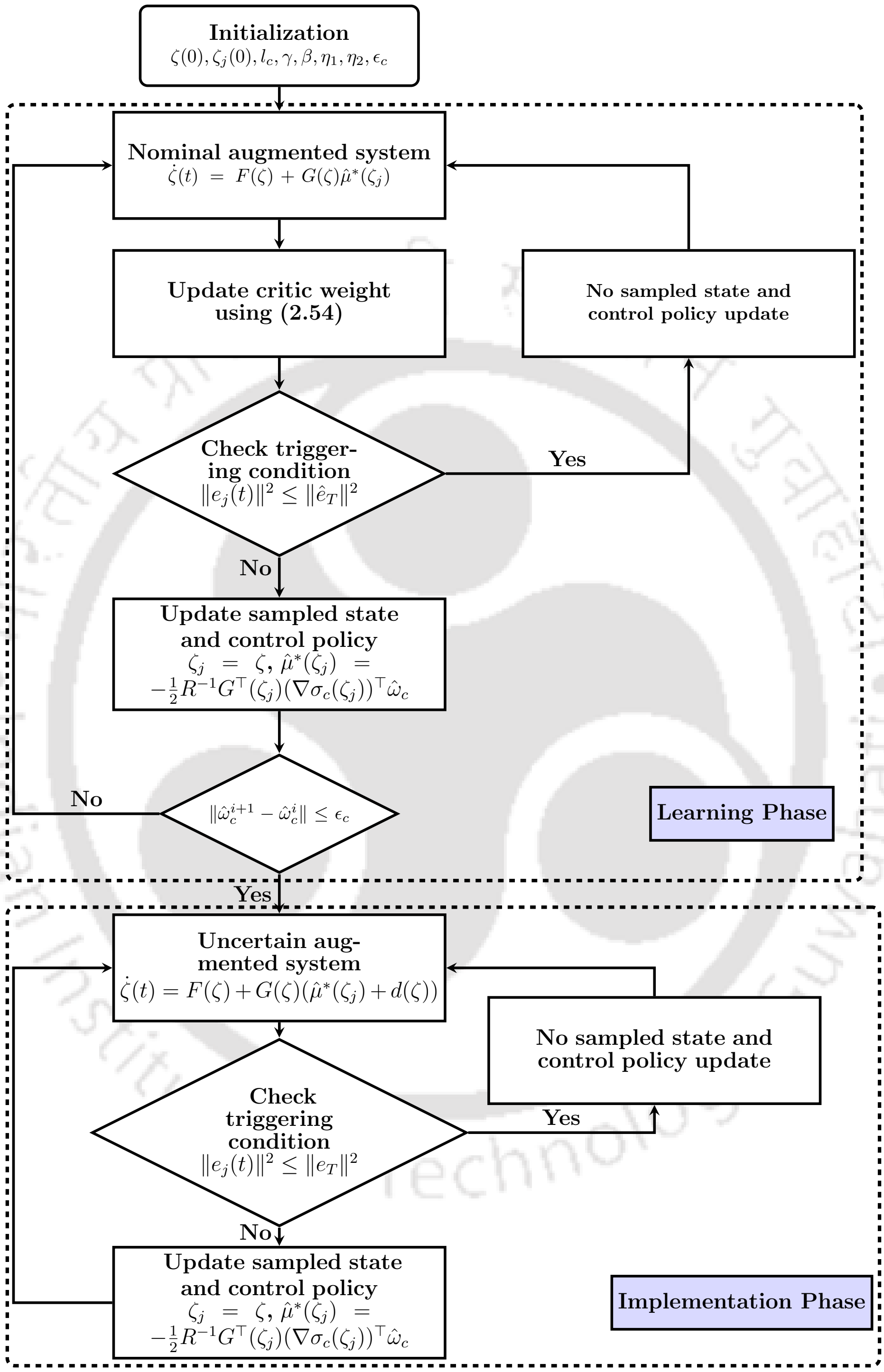

Figure 2.1: Flowchart of the proposed control strategy.

2.6 Simulation Examples

In this section, two simulation examples are presented to show the effectiveness of the proposed event-triggered tracking control strategy.

2.6.1 Example 1

Consider the following continues-time nonlinear system with matched uncertainty

$$\dot{x}(t) = \begin{bmatrix} x_2 \\ -0.5(x_1 + x_2) + 0.5x_1^2 x_2 \end{bmatrix} + \begin{bmatrix} 0 \\ 1 \end{bmatrix} (u(t) + d_1(x)), \tag{2.72}$$

where $x = [x_1, x_2]^\top$ is the state vector, $u(t) \in \mathbb{R}$ is the control input, and $d_1(x)$ is the matched uncertainty given by $d_1(x) = 0.5\theta_1 x_1 x_2 \cos(x_1)\sin(x_2+\theta_2)$, with $\theta_1, \theta_2 \in (-5, 5)$. Let the upper bound of uncertainty $d_1(x)$ be $2.5|x_1||x_2|$. The initial state of the system is $x_0 = [0.7, -0.5]^\top$. The reference trajectory $x_r(t) = [x_{r1}, x_{r2}]^\top$ with the initial state $x_{r0} = [0.2, 0.4]^\top$ is generated

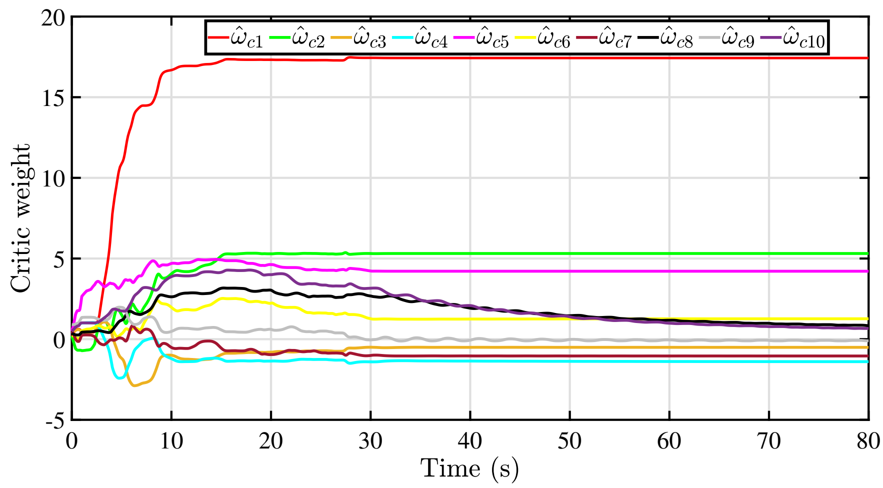

Figure 2.2: Critic weight convergence.

from

$$\dot{x}_r(t) = \begin{bmatrix} x_{r2} \\ -x_{r1} \end{bmatrix}. \tag{2.73}$$

The tracking error is given as $e_r(t) = x(t) - x_r(t)$.The augmented state is now formed using the tracking error and the reference trajectory as $\zeta = [e_r^\top, x_r^\top]^\top \in \mathbb{R}^4$ and then the following augmented system is formulated

$$\dot{\zeta} = \begin{bmatrix} \zeta_2 \\ 0.5(-\zeta_1 - \zeta_2 + \zeta_3 - \zeta_4 + (\zeta_1 + \zeta_3)^2(\zeta_2 + \zeta_4)) \\ \zeta_4 \\ -\zeta_3 \end{bmatrix} + \begin{bmatrix} 0 \\ 1 \\ 0 \\ 0 \end{bmatrix} (u + d(\zeta)), \tag{2.74}$$

where $d(\zeta) = 0.5\theta_1(\zeta_1+\zeta_3)(\zeta_2+\zeta_4)cos(\zeta_1+\zeta_3)sin(\zeta_2+\zeta_4+\theta_2)$, $d_M(\zeta) = 2.5|\zeta_1+\zeta_3||\zeta_2+\zeta_4|$, and $\zeta(0) = [0.5, -0.9, 0.2, 0.4]^\top$. The cost function for the nominal part of augmented system

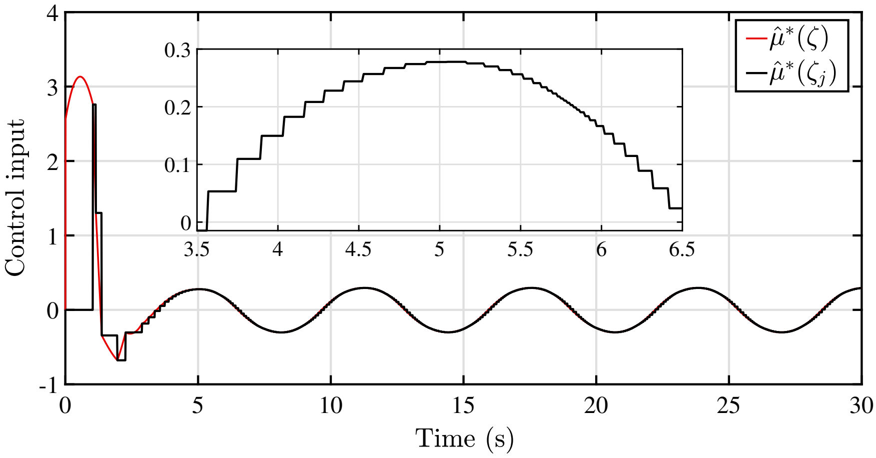

Figure 2.3: Event-triggered and time-triggered control inputs.

(2.74) is given as

$$J(\zeta(t), u) = \int_t^\infty e^{-\gamma(\tau - t)}\{U(\zeta(\tau), u(\tau)) + \beta d_M^2(\zeta(\tau))\}\mathrm{d}\tau, \tag{2.75}$$

where $U(\zeta, u) = \zeta^\top \bar{Q}\zeta + u^\top Ru$, $\bar{Q} = diag\{Q, 0_{2\times2}\}$, $Q = 40I_2$ and $R = I_1$, $\beta = 2.5$, and $\gamma = 1.2$. Under the ADP framework, a critic network with 10 neurons in the hidden layer is utilized to approximate the cost function (2.75). The weight vector is chosen as $\hat{\omega}_c = [\hat{\omega}_{c1}, ..., \hat{\omega}_{c10}]^\top$ and the activation function is selected as $\sigma_c(\zeta) = [\zeta_1^2, \zeta_1\zeta_2, \zeta_1\zeta_3, \zeta_1\zeta_4, \zeta_2^2, \zeta_2\zeta_3, \zeta_2\zeta_4, \zeta_3^2, \zeta_3\zeta_4, \zeta_4^2]^\top$. During the training process, critic learning rate l_c, the design parameters η_2 and $A^2\nabla\sigma_{cM}^2 + B^2G_M^2$ are heuristically considered as 2.2, 0.8, and 4, respectively. The initial weights of the critic NN are taken randomly between 0 and 1. A probing noise satisfying the persistence of excitation

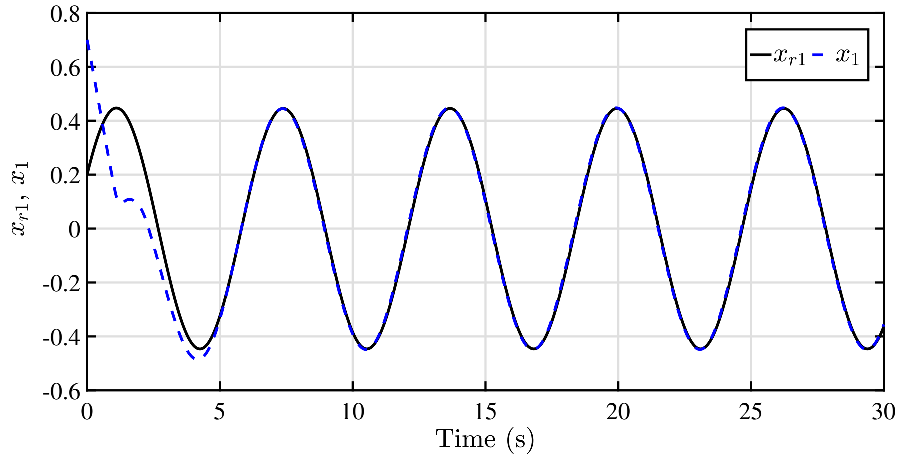

Figure 2.4: Tracking performance of x_1 for $\theta_1 = 0.5$ and $\theta_2 = -0.5$.

(PE) condition is applied during the initial 30 seconds of the learning phase. After 80 seconds, the critic weight vector converges to

$$\hat{\omega}_c == [17.43, 5.31, -0.51, -1.39, 4.21, 1.26, -1.04, 0.84, -0.10, 0.67]^\top$$

as shown in Figure 2.2. During the learning process, the event-based controller updates only 2205 times, whereas the conventional time-triggered controller updates 8000 times. This significantly reduces the number of times the controller updates during the neural network learning phase.

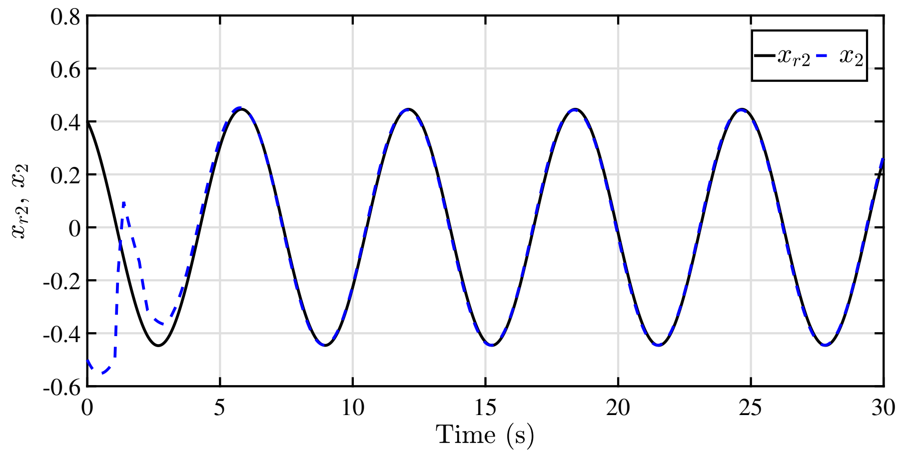

Figure 2.5: Tracking performance of x_2 for $\theta_1 = 0.5$ and $\theta_2 = -0.5$.

Remark 2.3. The number of neurons in the hidden layer is determined through trial and error. In simulations, using 10 neurons in the hidden layer of the critic network produced satisfactory results. Similarly, the choice of activation function is also based on trial and error, as there is no established rule for selecting the best activation function.

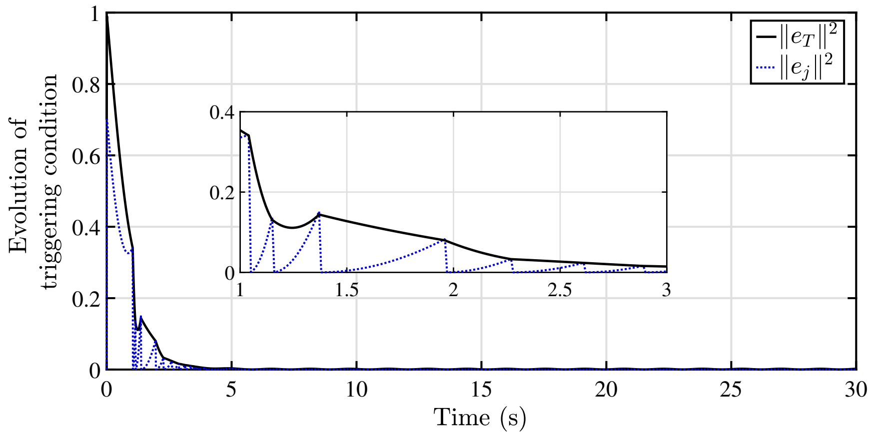

Figure 2.6: Evolution of the triggering condition with $\|e_T\|^2$ and $\|e_j\|^2$.

The converged critic weights are now used in the implementation phase to obtain the event-triggered guaranteed cost tracking controller (2.50). The Lipschitz constant $\mathcal{L}$ and the design parameter η_1 are chosen as 2.8 and 0.8, respectively. The parameters of the uncertain term are taken as $\theta_1 = 0.5$ and $\theta_2 = -0.5$. The tracking performance of x_1 and x_2 are exhibited in Figure 2.4 and Figure 2.5, respectively. The obtained event-based guaranteed cost control input is shown in Figure 2.3. The evolution of the triggering condition with $\|e_T\|^2$ and $\|e_j\|^2$ is illustrated in

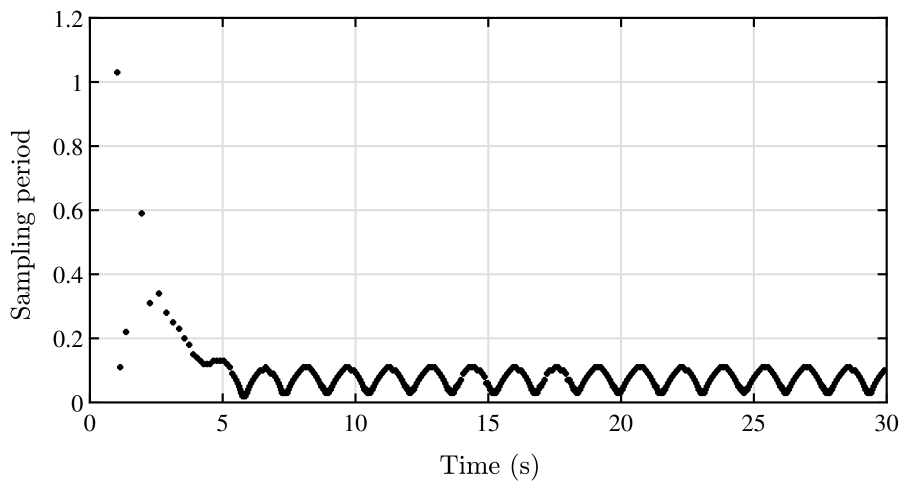

Figure 2.7: Triggering instants during the tracking process.

Figure 2.6. The sampling period is depicted in Figure 2.7. During the simulation process, it

is observed that the minimum intersample time is 0.01 second, which means the occurrence of the problematic Zeno-behavior is avoided. The event-based controller updates 417 times, whereas the time-triggered controller updates 3000 times. The time-triggered guaranteed cost is calculated as 5.3295 and the event-based guaranteed cost is more than 5.3295. Even though the guaranteed cost cannot be reduced using the event-based approach, the decrease in the number of control updates offers the most significant benefit.

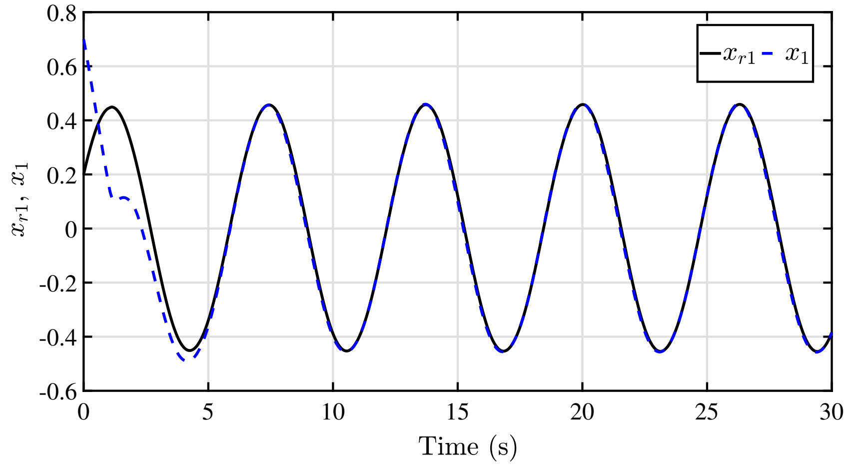

Figure 2.8: Tracking performance of x_1 for $\theta_1 = -2.5$ and $\theta_2 = 4$.

The sampling frequency η_1 is considered within the interval $(0, 1)$. Table 2.1 demonstrates the relationship between η_1 and the number of event-triggering instants, denoted as N_s. It is evident from the table that an increase in the sampling frequency η_1 corresponds to an increase in the number of triggering instants N_s.

Table 2.1: Effect of η_1 on number of triggering instants.

Parameter	**Case 1**	**Case 2**	**Case 3**	**Case 4**
η_1	0.7	0.75	0.8	0.85
N_s	405	409	417	441

The parameters of the uncertain term are changed to $\theta_1 = -2.5$ and $\theta_2 = 4$ to exhibit the robust tracking performance of the obtained event-based guaranteed cost controller. The tracking performance of x_1 and x_2 while using the changed values of θ_1 and θ_2 are shown in Figures 2.8 and 2.9, respectively. Since the tracking performance remains satisfactory even with varying levels of uncertainty, it can be concluded that the designed tracking controller demonstrates robust performance.

Remark 2.4. In the simulation examples, the sampling frequencies η_1 and η_2 are deliberately chosen to ensure positive values for $\|e_T\|^2$ and $\|\hat{e}_T\|^2$, respectively. Increasing η_1 and η_2 enhances the sampling frequency and the number of event-triggering instants, which improves tracking performance. However, it is essential to balance the number of triggering instants with tracking performance. In line with the literature [86], other parameters are heuristically chosen to optimize the convergence time of the critic weights and the number of triggering instants while ensuring satisfactory tracking performance.

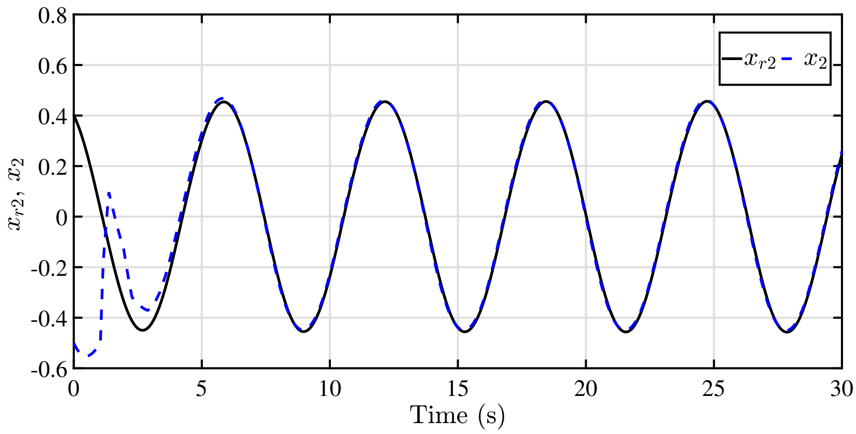

Figure 2.9: Tracking performance of x_2 for $\theta_1 = -2.5$ and $\theta_2 = 4$.

To test the impact of sensor noise, zero-mean Gaussian sensor noise has been added along with matched uncertainty. The following plots demonstrate that the proposed event-triggered ADP controller retains satisfactory tracking performance, indicating robustness to both noise and matched disturbances.

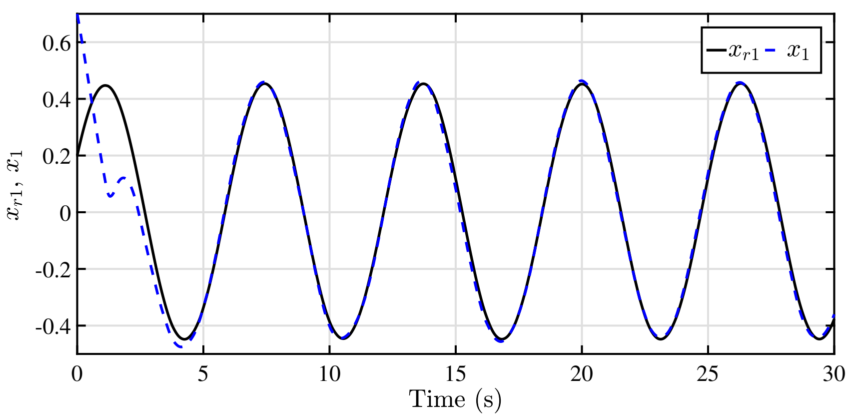

Figure 2.10: Tracking performance of x_1 under sensor noise.

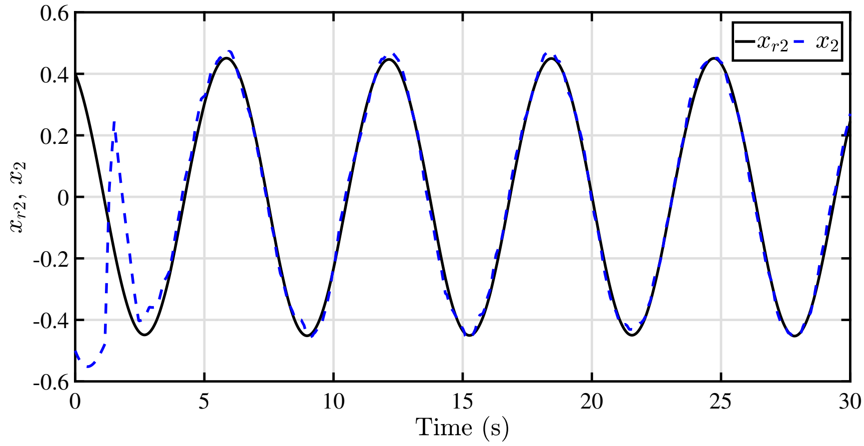

Figure 2.11: Tracking performance of x_2 under sensor noise.

2.6.2 Example 2

Consider the schematic of a single link robotic manipulator shown in Figure 2.12. The dynamical equation of the robotic manipulator can be written as

$$\frac{1}{2}\bar{I}\ddot{\bar{\theta}} + \bar{m}\bar{g}l_1 \sin\bar{\theta} = \bar{\tau} + d_1, \tag{2.76}$$

where $\bar{\theta}$ is the angle, $\bar{\tau}$ is the input torque, $\bar{I}$ is the moment of inertia of the link, $\bar{g}$ is the gravitational constant, $\bar{m}$ and l_1 are the mass and the length of the link, respectively. d_1 models the system's matched uncertainty and it is added to the input torque. By defining $x_1 = \bar{\theta}$, $x_2 = \dot{\bar{\theta}}$, and $\bar{\tau} = u(t)$, 2.76 can be rewritten in the following form

$$\dot{x}(t) = \begin{bmatrix} x_2 \\ -\frac{\bar{m}\bar{g}l_1}{2\bar{I}} sin(x_1) \end{bmatrix} + \begin{bmatrix} 0 \\ 1 \end{bmatrix} (u(t) + d_1(x)). \tag{2.77}$$

After considering the values of the robot's parameters given in Table 2.2, the equation 2.77 can be written as

$$\dot{x}(t) = \begin{bmatrix} x_2 \\ -4.9sin(x_1) \end{bmatrix} + \begin{bmatrix} 0 \\ 1 \end{bmatrix} (u(t) + d_1(x)). \tag{2.78}$$

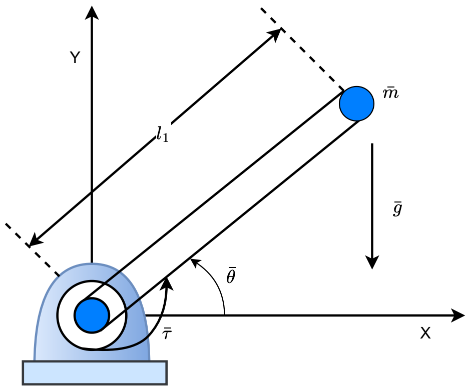

Figure 2.12: Schematic of a robotic manipulator

Table 2.2: Parameters of the manipulator

Parameter	Value
l_1	1 m
$\bar{I}$	1 kg.m^2
$\bar{m}$	1 kg
$\bar{g}$	9.8 m/s²

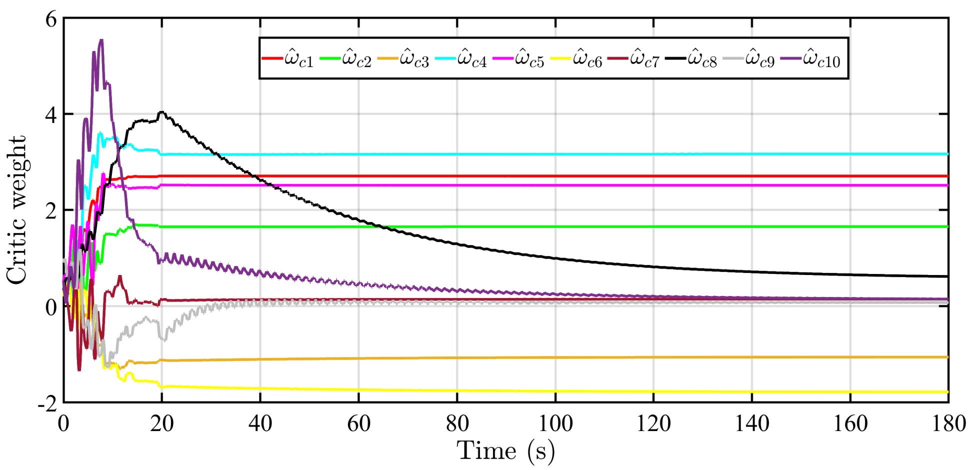

Figure 2.13: Critic weight convergence.

Let the initial state be $x_0 = [0.5, 0.1]^\top$ and the uncertainty be given by

$$d_1(x) = 0.5\theta_1 x_1 x_2 \cos(x_1)\sin(x_2 + \theta_2),$$

where θ_1 and θ_2 are within the range $(-1, 1)$. The upper bound of $d_1(x)$ is $0.5|x_1||x_2|$. The reference trajectory $x_r = [x_{r1}, x_{r2}]^\top \in \mathbb{R}^2$ is obtained from

$$\dot{x}_r(t) = \begin{bmatrix} x_{r2} \\ -4x_{r1} \end{bmatrix}, \tag{2.79}$$

where the initial condition is $x_{r0} = [0.4, -0.2]^\top$.

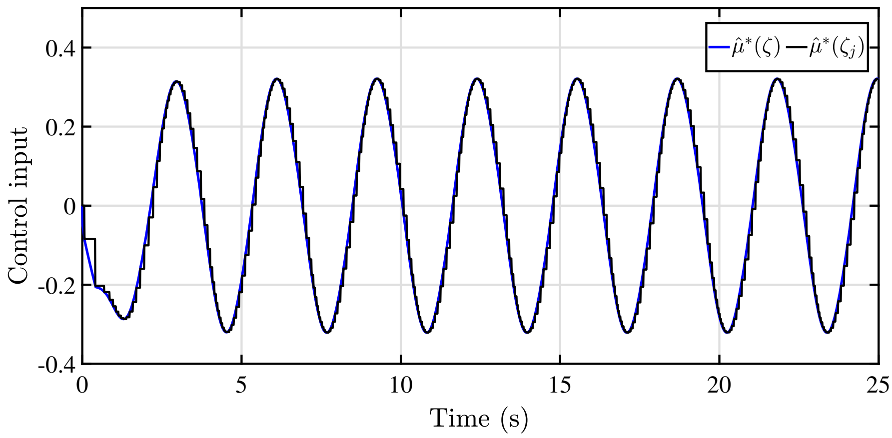

Figure 2.14: Comparison between event-triggered and time-triggered control inputs.

The augmented system is derived as

$$\dot{\zeta} = \begin{bmatrix} \zeta_2 \\ -4.9sin(\zeta_1 + \zeta_3) + 4\zeta_3 \\ \zeta_4 \\ -4\zeta_3 \end{bmatrix} + \begin{bmatrix} 0 \\ 1 \\ 0 \\ 0 \end{bmatrix} (u(\zeta) + d(\zeta)), \tag{2.80}$$

with the initial condition $\zeta(0) = [0.1, 0.3, 0.4, -0.2]^\top$. The upper bound of the uncertainty term is given by $d_M(\zeta) = 0.5|\zeta_1 + \zeta_3||\zeta_2 + \zeta_4|$.

The cost function for the nominal part of augmented system (2.80) is given as

$$J(\zeta(t), u) = \int_t^\infty e^{-\gamma(\tau - t)}\{U(\zeta(\tau), u(\tau)) + \beta d_M^2(\zeta(\tau))\}\mathrm{d}\tau, \tag{2.81}$$

where $\bar{Q} = \mathrm{diag}\{Q, 0_{2\times 2}\}$, $Q = 70I_2$, $R = I$, and $\beta = 1.4$.

A critic network under the ADP framework is employed to obtain the optimal control for the nominal part of the augmented system (2.80) using the cost function (2.81). The activation function is chosen as $\sigma_c(\zeta) = [\zeta_1^2, \zeta_1\zeta_2, \zeta_1\zeta_3, \zeta_1\zeta_4, \zeta_2^2, \zeta_2\zeta_3, \zeta_2\zeta_4, \zeta_3^2, \zeta_3\zeta_4, \zeta_4^2]^\top$, and the critic weight vector is chosen as $\hat{\omega}_c = [\hat{\omega}_{c1}, \ldots, \hat{\omega}_{c10}]^\top$.

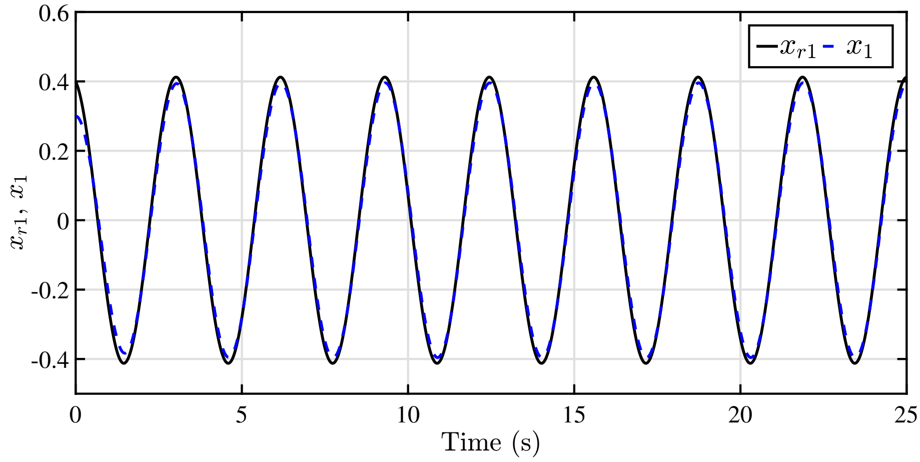

Figure 2.15: Tracking performance of x_1 for $\theta_1 = -0.9$ and $\theta_2 = -0.5$.

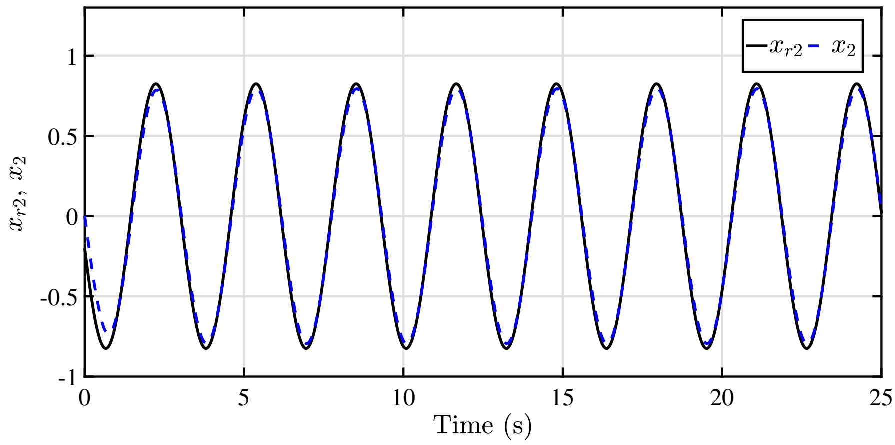

Figure 2.16: Tracking performance of x_2 for $\theta_1 = -0.9$ and $\theta_2 = -0.5$.

During the learning phase of the critic network, the parameters are experimentally set as $\eta_2 = 0.8$, the critic learning rate $l_c = 2.8$, and $A^2\nabla\sigma_{cM}^2 + B^2G_M^2 = 7$. The elements of the weight vector are initialized randomly within the interval $(0, 1)$. To satisfy the persistence of excitation condition, a probing noise is added during the initial 20 seconds of the learning phase. The critic weight vector converges to

$$\hat{\omega}_c = [2.70, 1.65, -1.05, 3.17, 2.50, -1.78, 0.14, 0.61, 0.08, 0.15]^\top,$$

as illustrated in Figure 2.13.

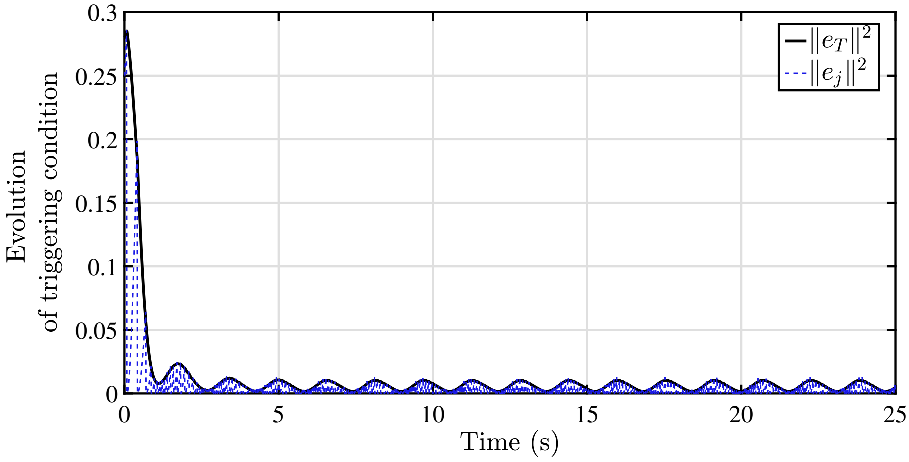

Figure 2.17: The evolution of $\|e_T\|^2$ and $\|e_j\|^2$

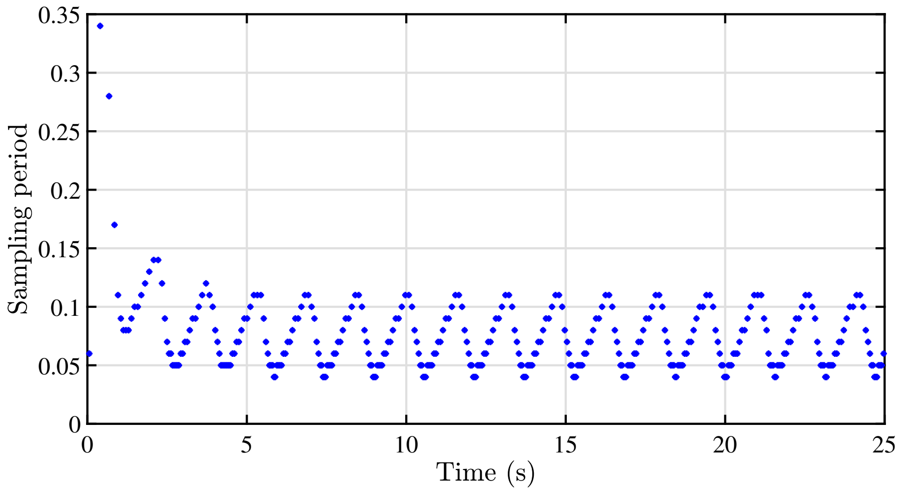

Figure 2.18: Sampling period.

The value of θ_1 and θ_2 are considered as -0.9 and -0.5, respectively to evaluate the trajectory tracking performance using $\hat{\mu}^*(\zeta_j)$ and the triggering condition defined in (2.21). The design parameters are selected as $\eta_1 = 0.8$ and $\mathcal{L} = 1.5$. In Figure 2.14, the event-triggered controller is compared with the time-triggered controller. The event-triggered controller updates only 419 times, whereas the time-triggered controller updates 2500 times. The tracking performance of x_1 and x_2 are shown in Figures 2.15 and 2.15, respectively. The evolution of the triggering condition with $\|e_T\|^2$ and $\|e_j\|^2$ is shown in Figure 2.17. The sampling period is depicted in Figure 2.18. The minimum intersample time is 0.01 seconds, effectively ruling out the possibility of the Zeno-phenomenon.

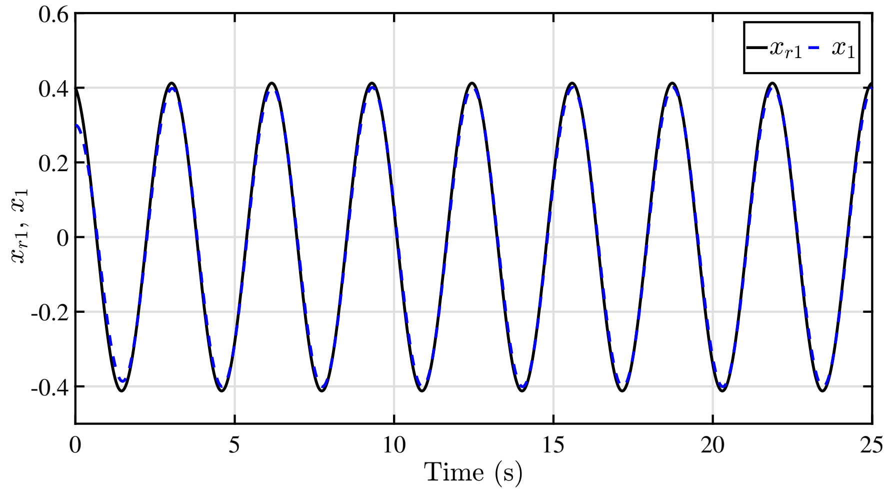

Figure 2.19: Tracking performance of x_1 for $\theta_1 = 0.8$ and $\theta_2 = -0.2$.

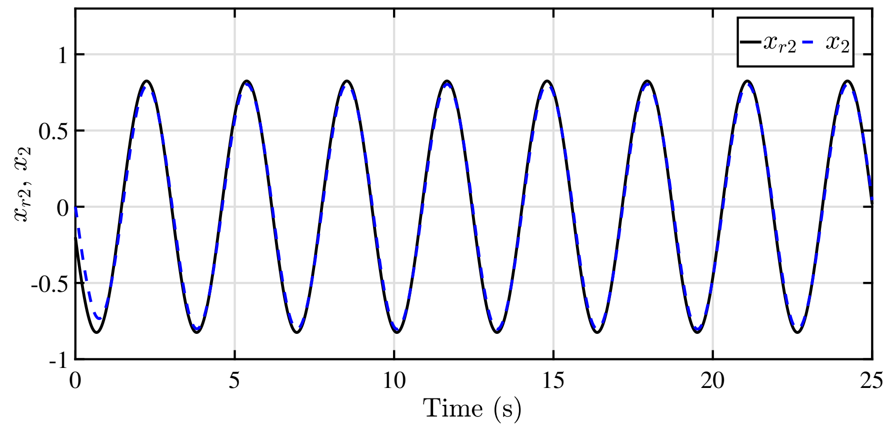

Figure 2.20: Tracking performance of x_2 for $\theta_1 = 0.8$ and $\theta_2 = -0.2$.

The guaranteed cost for the time-triggered method is calculated as 0.1497, while the event-triggered method results in a slightly higher guaranteed cost. Despite the increase in cost with the event-triggered approach, this work prioritizes the reduction in computational burden.

In order to show the robustness of the proposed controller, the values of θ_1 and θ_2 are changed to 0.8 and -0.2, respectively. Figures 2.19 and 2.20 show the tracking performance while considering the new uncertainty. As seen in Figures 2.19 and 2.20, the controller provides satisfactory tracking performance even in the change of uncertainty, which shows the robust nature of the proposed controller.

2.7 Summary

In this chapter, the robust guaranteed cost tracking control problem of the nonlinear systems with matched uncertainty is addressed by applying the event-based ADP methodology. The original control problem is transformed into the optimal control problem of the nominal augmented system. The event-based guaranteed cost is established, and convergence of the tracking error within an adjustable neighbourhood of the origin is demonstrated using the Lyapunov technique. Two simulation examples are provided to validate the proposed approach. The event-triggered guaranteed cost is found to be more than the time-triggered guaranteed cost. However, the event-triggered control input updates much fewer times than the time-triggered control input. The tracking controller provides satisfactory tracking performance even in the presence of uncertainties, indicating the robustness of the controller.

3

Robust Tracking Control of Nonlinear Unmatched Uncertain Systems via Event-Triggered ADP

Contents

3.1 Introduction

Unlike the matched uncertainty, which enters the system through the same channel as the control input, the unmatched uncertainty enters the system through a different channel than the control input. Unmatched uncertainties are more general and can be widely seen in most practical systems. For example, consider a car with uncertain wind resistance. The wind affects the car's speed (system behavior) but is not directly influenced by how much the accelerator is pressed. Considering unmatched uncertainty while designing a controller for nonlinear systems is vital.

In this chapter, a novel robust tracking control strategy for nonlinear unmatched uncertain systems is proposed using the event-based ADP approach. First, an augmented system is constructed based on the original system dynamics and the tracking error dynamics. Then, by forming an auxiliary system and introducing a discounted cost function, the event-based robust tracking control problem is transformed into the event-based optimal control problem of the auxiliary system. The event-based HJB equation associated with the optimal control problem is solved using a single critic NN under the ADP framework. A novel weight tuning rule for the critic network is formulated to avoid the necessity of an initial admissible control at the beginning of the weights tuning process. The obtained event-based controller is updated only at the triggering instants decided by the designed triggering condition, which helped in a significant reduction of resources used in computation and communication. Meanwhile, it is demonstrated that the obtained event-based controller can guarantee the tracking error's uniform ultimate boundedness. Furthermore, using the Lyapunov method, it is guaranteed that the established novel event-triggering rule ensures uniform ultimate boundedness of all signals associated with the closed-loop auxiliary system. Finally, the applicability of the proposed control scheme is demonstrated by providing two simulation examples.

The remaining part of this chapter is organized in the following manner. In Section 3.2, the original tracking control problem is transformed into the optimal control problem of an auxiliary system. The event-based HJB equation is formulated, and the event-triggering rule is derived in Section 3.3. In Section 3.4, the HJB equation is solved via the ADP approach. In Section 3.5, the Lyapunov approach is used to show that all the signals associated with the closed-loop auxiliary system are uniformly ultimately bounded. In Section 3.6, two simulation examples are presented. Finally, a brief summary of the chapter is given in Section 3.7.

3.2 Problem Formulation

Consider the continuous-time nonlinear uncertain system given in the form

$$\dot{x}(t) = f(x(t)) + g(x(t))u(t) + \Delta f(x(t)), \tag{3.1}$$

where $x(t) \in \mathbb{R}^n$ and $u(t) \in \mathbb{R}^m$ are the state vector and control input, respectively. Let $x(0) = x_0$ be the initial state. $f(\cdot)$ and $g(\cdot)$ are smooth functions in their arguments with $f(0) = 0$ and $f + gu$ satisfies the Lipschitz continuity. The unmatched uncertainty is given by $\Delta f(x) = k(x)d_1(x)$, where $k(x) \in \mathbb{R}^{n\times p}$, $d_1(x) \in \mathbb{R}^p$ and if $m = p$ then $k(x) \neq g(x)$. Let $d_1(x)$ be bounded by a known function $d_M(x)$, i.e., $\|d_1(x)\| \leq d_M(x)$. Furthermore, $d_M(0) = 0$ and $d(0) = 0$. In addition, there exist a non-negative function $g_M(x)$ satisfying

$$\|g^+(x)\Delta f(x)\| \leq g_M(x),$$

where $g^+(x)$ is the pseudoinverse of $g(x)$. Let the desired trajectory $x_r(t) \in \mathbb{R}^n$ be generated from

$$\dot{x}_r(t) = Z(x_r(t)), \tag{3.2}$$

where $Z(x_r)$ satisfies the Lipschitz continuity and $Z(0) = 0$. Let $x_r(0) = x_{r0}$ be the initial condition.

The objective of this chapter is to derive an event-based robust controller for system (3.1) so that the system state $x(t)$ follow the desired trajectory $x_r(t)$. Define the tracking error as $e_r(t) = x(t) - x_r(t)$. From (3.1) and (3.2), the tracking error dynamics can be presented as

$$\dot{e}_r(t) = f(e_r(t) + x_r(t)) + g(e_r(t) + x_r(t))u(t) + \Delta f(e_r(t) + x_r(t)) - Z(x_r(t)). \tag{3.3}$$

Now, based on the tracking error and the desired trajectory, an augmented state vector $\zeta(t) = [e_r^\top(t), x_r^\top(t)]^\top \in \mathbb{R}^{2n}$ is formed. Then, using (3.2) and (3.3), the augmented system dynamics is formulated as

$$\dot{\zeta}(t) = F(\zeta(t)) + G(\zeta(t))u(\zeta(t)) + \Delta F(\zeta(t)), \tag{3.4}$$

where $F : \mathbb{R}^{2n} \to \mathbb{R}^{2n}$ and $G : \mathbb{R}^{2n} \to \mathbb{R}^{2n\times m}$ are new system matrices while $\Delta F(\zeta(t)) \in \mathbb{R}^{2n}$

is the new uncertain term. They can be expressed as

$$F(\zeta(t)) = \begin{bmatrix} f(e_r(t) + x_r(t)) - Z(x_r(t)) \\ Z(x_r(t)) \end{bmatrix},$$

$$G(\zeta(t)) = \begin{bmatrix} g(e_r(t) + x_r(t)) \\ 0 \end{bmatrix},$$

and

$$\Delta F(\zeta(t)) = \begin{bmatrix} \Delta f(e_r(t) + x_r(t)) \\ 0 \end{bmatrix} = K(\zeta(t))d(\zeta(t)).$$

The terms $d(\zeta)$ and $G^+(\zeta)\Delta F(\zeta)$ are still upper bounded and the bound can be derived as

$$\|d(\zeta)\| = \|d_1(e_r + x_r)\| = \|d_1(x)\| \leq d_M(x) = d_M(e_r + x_r) \triangleq d_M(\zeta). \tag{3.5}$$

and

$$\left\|G^+(\zeta)\Delta F(\zeta)\right\| = \left\|g^+(x)\Delta f(x)\right\| \leq g_M(x) = g_M(e_r + x_r) \triangleq g_M(\zeta), \tag{3.6}$$

respectively. Next, the uncertain term $K(\zeta)d(\zeta)$ is projected onto the range of matrix $G(\zeta)$ and decomposed into sum of matched and unmatched component, that is

$$K(\zeta)d(\zeta) = G(\zeta)G^+(\zeta)K(\zeta)d(\zeta) + (I_{2n} - G(\zeta)G^+(\zeta))K(\zeta)d(\zeta).$$

Then following auxiliary system is formed

$$\dot{\zeta} = F(\zeta) + G(\zeta)u(\zeta) + (I_{2n} - G(\zeta)G^+(\zeta))K(\zeta)v(\zeta), \tag{3.7}$$

where $v(\zeta) \in \mathbb{R}^p$ is an auxiliary control that handles the unmatched component.

3.3 Event-Based Robust Tracking Control Strategy

In this section, the event-based HJB equation is developed for the auxiliary system (3.7). Moreover, the event-triggering rule is also obtained using Lyapunov approach. The cost function associated with the auxiliary system (3.7) is defined as

$$J(\zeta(t)) = \int_t^\infty \mathrm{e}^{-\gamma(\tau - t)}\{U(\zeta(\tau), u(\zeta(\tau)), v(\zeta(\tau))) + \beta^2\|m^\top\|^2 d_M^2(\zeta) + \|r^\top\|^2 g_M^2(\zeta)\}\mathrm{d}\tau, \tag{3.8}$$

where γ and β are positive constant, $U(\zeta, u(\zeta), v(\zeta)) = \zeta^\top \bar{Q}\zeta + u^\top(\zeta)Ru(\zeta) + \beta^2 v^\top(\zeta)Mv(\zeta)$ and $\bar{Q} = diag\{Q, 0_{n\times n}\}$. Q, M, and R are positive definite matrices with appropriate dimension. The term $\beta^2\|m^\top\|^2 d_M^2(\zeta) + \|r^\top\|^2 g_M^2(\zeta)$ is included in the cost function to incorporate the unmatched uncertainty present in the system. Let r and m be lower triangular matrices with appropriate dimension. Then, using Cholesky decomposition one can write $R = rr^\top$ and $M = mm^\top$.

Let $\Psi(\Omega)$ be the set of admissible controls on Ω. Assume that the optimal control policy pair is admissible. If the cost function $J(\zeta)$ is continuously differentiable then one can write

$$\|r^\top\|^2 g_M^2(\zeta) + \beta^2\|m^\top\|^2 d_M^2(\zeta) + U(\zeta, u(\zeta), v(\zeta)) - \gamma J(\zeta) + \dot{J}(\zeta) = 0 \tag{3.9}$$

with $J(0) = 0$. Here (3.9) is called the infinitesimal version of (3.8) [8]. The Hamiltonian for the auxiliary system (3.7) is given as

$$\begin{aligned} H(\zeta, u(\zeta), v(\zeta), \nabla J(\zeta)) = {} & (\nabla J(\zeta))^\top (F(\zeta) + G(\zeta)u(\zeta) + (I_{2n} - G(\zeta)G^+(\zeta))K(\zeta)v(\zeta)) \\ & + \|r^\top\|^2 g_M^2(\zeta) + \beta^2\|m^\top\|^2 d_M^2(\zeta) + U(\zeta, u(\zeta), v(\zeta)) - \gamma J(\zeta). \end{aligned} \tag{3.10}$$

The optimal cost function is given by

$$\begin{aligned} J^*(\zeta(t)) = \min_{u,v\in\Psi(\Omega)} \int_t^\infty & \mathrm{e}^{-\gamma(\tau - t)}\{U(\zeta(\tau), u(\zeta(\tau)), v(\zeta(\tau))) \\ & + \beta^2\|m^\top\|^2 d_M^2(\zeta) + \|r^\top\|^2 g_M^2(\zeta)\}\mathrm{d}\tau. \end{aligned} \tag{3.11}$$

By the Bellman's principle, $J^*(\zeta(t))$ holds the HJB equation

$$\min_{u,v\in\Psi(\Omega)} H(\zeta, u(\zeta), v(\zeta), \nabla J^*(\zeta)) = 0 \tag{3.12}$$

with $J^*(0) = 0$. Define $(I_{2n} - G(\zeta)G^+(\zeta))K(\zeta) = L(\zeta)$. The optimal control policies are obtained as

$$u^*(\zeta) = -\frac{1}{2}R^{-1}G^\top(\zeta)\nabla J^*(\zeta) \tag{3.13}$$

and

$$v^*(\zeta) = -\frac{1}{2\beta^2}M^{-1}L^\top(\zeta)\nabla J^*(\zeta). \tag{3.14}$$

Substituting (3.13) and (3.14) into (3.12), the HJB equation is presented as

$$\begin{aligned}&(\nabla J^*(\zeta))^\top F(\zeta) + \zeta^\top \bar{Q}\zeta + \beta^2\|m^\top\|^2 d_M^2(\zeta) + \|r^\top\|^2 g_M^2(\zeta) - \gamma J^*(\zeta)\\ &- \frac{1}{4}\nabla(J^*(\zeta))^\top G(\zeta)R^{-1}G^\top(\zeta)\nabla J^*(\zeta) - \frac{1}{4\beta^2}\nabla(J^*(\zeta))^\top L(\zeta)M^{-1}L^\top(\zeta)\nabla J^*(\zeta) = 0.\end{aligned} \tag{3.15}$$

3.3.1 The Event-Based HJB Equation Formulation

Here, the HJB equation (3.15) is expresses in the event-based form. Using the event-triggering mechanism, as described in Chapter 1, the sampled version of auxiliary system (3.7) is obtained as

$$\dot{\zeta} = F(\zeta) + G(\zeta)\mu(\zeta(t) + e_j(t)) + L(\zeta)v(\zeta). \tag{3.16}$$

The optimal control (3.13), under event-triggered mechanism, can be expressed as

$$\mu^*(\zeta_j) = -\frac{1}{2}R^{-1}G^\top(\zeta_j)\nabla J^*(\zeta_j). \tag{3.17}$$

Now, using (3.17), the HJB equation under event-based framework is formulated as

$$H(\zeta, \mu^*(\zeta_j), v^*(\zeta), \nabla J^*(\zeta)) = 0,$$

that is,

$$\begin{aligned}&(\nabla J^*(\zeta))^\top F(\zeta) + \zeta^\top \bar{Q}\zeta + \beta^2\|m^\top\|^2 d_M^2(\zeta) + \|r^\top\|^2 g_M^2(\zeta) - \gamma J^*(\zeta)\\ &- \frac{1}{2}\nabla(J^*(\zeta))^\top G(\zeta)R^{-1}G^\top(\zeta_j)\nabla J^*(\zeta_j) + \frac{1}{4}\nabla(J^*(\zeta_j))^\top G(\zeta_j)R^{-1}G^\top(\zeta_j)\nabla J^*(\zeta_j)\\ &- \frac{1}{4\beta^2}\nabla(J^*(\zeta))^\top L(\zeta)M^{-1}L^\top(\zeta)\nabla J^*(\zeta) = 0,\end{aligned} \tag{3.18}$$

where $J^*(0) = 0$.

3.3.2 Event-Triggering Condition

In this subsection, the event-triggering condition is obtained using the Lyapunov approach.

Theorem 3.1. Let Assumption 2.1 in Chapter 2 be true, $J^*(\zeta)$ satisfy the HJB equation (3.12), the control policies be described by (3.14) and (3.17), and the event-triggering law be formulated as

$$\begin{aligned}\|e_j(t)\|^2 &\leq \frac{(1-\eta_1^2)\lambda_m(Q)\|e_r\|^2 - 2\beta^2\|m^\top v^*(\zeta)\|^2}{2\|r^\top\|^2\mathcal{L}^2} \\ &\triangleq \|e_T\|^2, \end{aligned} \tag{3.19}$$

then for $\eta_1 \in (0,1)$ and $\gamma = 0$, the closed-loop augmented system (3.4) is asymptotically stable under $\mu^*(\zeta_j)$ and for $\gamma \neq 0$ the tracking error e_r is uniformly ultimately bounded.

Proof: Consider $J^*(\zeta)$ be the Lyapunov function candidate. Differentiating $J^*(\zeta)$ along the trajectory of $\dot{\zeta}(t) = F(\zeta(t)) + G(\zeta(t))\mu^*(\zeta_j) + \Delta F(\zeta(t))$, one can write

$$\begin{aligned}\dot{J}^*(\zeta) &= (\nabla J^*(\zeta))^\top(F(\zeta) + G(\zeta)\mu^*(\zeta_j) + \Delta F(\zeta(t)) \\ &= (\nabla J^*(\zeta))^\top F(\zeta) + (\nabla J^*(\zeta))^\top G(\zeta)\mu^*(\zeta_j) \\ &\quad + (\nabla J^*(\zeta))^\top(G(\zeta)G^+(\zeta)K(\zeta) + L(\zeta))d(\zeta).\end{aligned} \tag{3.20}$$

From (3.12), the following expression is obtained

$$\begin{aligned}(\nabla J^*(\zeta))^\top F(\zeta) &= -\zeta^\top\bar{Q}\zeta - \beta^2\|m^\top\|^2 d_M^2(\zeta) - \|r^\top\|^2 g_M^2(\zeta) + \gamma J^*(\zeta) \\ &\quad + \frac{1}{4}\nabla(J^*(\zeta))^\top G(\zeta)R^{-1}G^\top(\zeta)\nabla J^*(\zeta) \\ &\quad + \frac{1}{4\beta^2}\nabla(J^*(\zeta))^\top L(\zeta)M^{-1}L^\top(\zeta)\nabla J^*(\zeta).\end{aligned} \tag{3.21}$$

From (3.13), one can write

$$G^\top(\zeta)\nabla J^*(\zeta) = -2Ru^*(\zeta) \tag{3.22}$$

and from (3.14)

$$L^{\top}(\zeta)\nabla J^{*}(\zeta) = -2\beta^{2} M v^{*}(\zeta). \tag{3.23}$$

Using (3.21), (3.22) and (3.23), $\dot{J}^{*}(\zeta)$ is derived as

$$\begin{aligned}\dot{J}^{*}(\zeta) = &-\zeta^{\top}\bar{Q}\zeta - \beta^{2}\|m^{\top}\|^{2}d_{M}^{2}(\zeta) - \|r^{\top}\|^{2}g_{M}^{2}(\zeta)\\ &+ \gamma J^{*}(\zeta) + u^{*\top}(\zeta)Ru^{*}(\zeta) + \beta^{2}v^{*\top}(\zeta)Mv^{*}(\zeta)\\ &- 2u^{*\top}(\zeta)R\mu^{*}(\zeta_{j}) - 2u^{*\top}(\zeta)RG^{+}(\zeta)K(\zeta)d(\zeta) - 2\beta^{2}v^{*\top}(\zeta)Md(\zeta).\end{aligned} \tag{3.24}$$

Now,

$$\begin{aligned}&u^{*\top}(\zeta)Ru^{*}(\zeta) - 2u^{*\top}(\zeta)R\mu^{*}(\zeta_{j}) - 2u^{*\top}(\zeta)RG^{+}(\zeta)K(\zeta)d(\zeta)\\ &= \|r^{\top}(u^{*}(\zeta) - u^{*}(\zeta_{j}) - G^{+}(\zeta)K(\zeta)d(\zeta))\|^{2} - \|r^{\top}(u^{*}(\zeta_{j}) + G^{+}(\zeta)K(\zeta)d(\zeta))\|^{2}\\ &\leq 2\|r^{\top}\|^{2} + 2\|r^{\top}G^{+}(\zeta)K(\zeta)d(\zeta)\|^{2} - \|r^{\top}(u^{*}(\zeta_{j}) + G^{+}(\zeta)K(\zeta)d(\zeta))\|^{2}\\ &\leq 2\|r^{\top}\|^{2}\mathcal{L}^{2}\|e_{j}\|^{2} + 2\|r^{\top}G^{+}(\zeta)K(\zeta)d(\zeta)\|^{2} - \|r^{\top}(u^{*}(\zeta_{j}) + G^{+}(\zeta)K(\zeta)d(\zeta))\|^{2}\end{aligned} \tag{3.25}$$

and

$$-2\beta^{2}v^{*\top}(\zeta)Md(\zeta) \leq \beta^{2}(\|m^{\top}v^{*}(\zeta)\|^{2} + \|m^{\top}d(\zeta)\|^{2}). \tag{3.26}$$

Since, $\bar{Q} = diag\{Q, 0_{n\times n}\}$, one can write $\zeta^{\top}\bar{Q}\zeta = e_{r}^{\top}Qe_{r}$. Now, following expression is obtained using (3.25), (3.26), and Assumption 2.1

$$\begin{aligned}\dot{J}^{*}(\zeta) \leq &-\lambda_{m}(Q)\|e_{r}\|^{2} - \beta^{2}\|m^{\top}\|^{2}d_{M}^{2}(\zeta) - \|r^{\top}\|^{2}g_{M}^{2}(\zeta) + 2\beta^{2}v^{*\top}(\zeta)Mv^{*}(\zeta)\\ &+ \gamma J^{*}(\zeta) + \beta^{2}\|m^{\top}d(\zeta)\|^{2} + 2\|r^{\top}\|^{2}\mathcal{L}^{2}\|e_{j}\|^{2} + 2\|r^{\top}G^{+}(\zeta)K(\zeta)d(\zeta)\|^{2}\\ &- \|r^{\top}(u^{*}(\zeta_{j}) + G^{+}(\zeta)K(\zeta)d(\zeta))\|^{2}\\ \leq &-\lambda_{m}(Q)\|e_{r}\|^{2} - \|r^{\top}\|^{2}(g_{M}^{2}(\zeta) - 2\|G^{+}(\zeta)K(\zeta)d(\zeta)\|^{2}) + 2\|r^{\top}\|^{2}\mathcal{L}^{2}\|e_{j}\|^{2}\\ &- \beta^{2}\|m^{\top}\|^{2}(d_{M}^{2}(\zeta) - \|d(\zeta)\|^{2}) + 2\beta^{2}v^{*\top}(\zeta)Mv^{*}(\zeta) + \gamma J^{*}(\zeta)\\ &- \|r^{\top}(u^{*}(\zeta_{j}) + G^{+}(\zeta)K(\zeta)d(\zeta))\|^{2}\\ \leq &-\eta_{1}^{2}\lambda_{m}(Q)\|e_{r}\|^{2} + (\eta_{1}^{2} - 1)\lambda_{m}(Q)\|e_{r}\|^{2} + 2\|r^{\top}\|^{2}\mathcal{L}^{2}\|e_{j}\|^{2}\\ &+ 2\beta^{2}\|m^{\top}v^{*}(\zeta)\|^{2} + \gamma J^{*}(\zeta).\end{aligned} \tag{3.27}$$

Hence, when the triggering rule stated in Theorem 3.1 is satisfied and $\gamma = 0$, then using (3.27) one can write

$$\dot{J}^*(\zeta) \leq -\eta_1^2 \lambda_m(Q) \|e_r(t))\|^2. \tag{3.28}$$

Thus, the system is asymptotically stable for $\gamma = 0$. When $\gamma \neq 0$, then

$$\dot{J}^*(\zeta) \leq \gamma J^*(\zeta) - \eta_1^2 \lambda_m(Q) \|e_r(t))\|^2. \tag{3.29}$$

Since, $J^*(\zeta)$ is positive definite and bounded on Ω, let J^*_{max} be the maximum value of $J^*(\zeta)$. So, from (3.29), $\dot{J}^*(\zeta) \leq 0$ only if e_r lies outside the set

$$\Omega_{e_r} = \left\{ e_r : \|e_r\| \leq \frac{1}{\eta_1} \sqrt{\frac{\gamma J^*_{max}}{\lambda_m(Q)}} \right\}. \tag{3.30}$$

Thus for $\gamma \neq 0$, the tracking error $e_r(t)$ is uniformly ultimately bounded and the ultimate bound is $\frac{1}{\eta_1} \sqrt{\frac{\gamma J^*_{max}}{\lambda_m(Q)}}$.

Remark 3.1. In this work, the control policy $\mu^*(\zeta_j)$ is formulated under the event-triggered framework, but the augmented control policy $v^*(\zeta)$ is formulated under the time-triggered framework. There are two reasons behind this. First, the control policy to be used in the uncertain system is $\mu^*(\zeta_j)$ not the augmented control $v^*(\zeta)$. Second, if the augmented control is also considered in the event-triggering framework, then it becomes very difficult to obtain the event-triggering rule (3.19).

Remark 3.2. The lower bound of the minimum inter-event time $(\Delta t_j)_{\min} = \min\limits_{j \in \mathbb{N}} \{t_{j+1} - t_j\}$ can be expressed as

$$(\Delta t_j)_{\min} \geq \frac{1}{\mathcal{P}} \ln(1 + \alpha_{\min}),$$

where

$$\alpha_{\min} = \min_{j \in \mathbb{N}} \left\{ \frac{\|e_T^-(t_{j+1})\|}{\|\zeta_j\| + \pi} \right\} > 0,$$

with $e_T^-(t_{j+1}) = \lim\limits_{\bar{q} \to 0^+} e_T(t_{j+1} - \bar{q})$, and $\mathcal{P}$ and π are positive constants satisfying $F(\zeta) + G(\zeta)u(\zeta) + \Delta F(\zeta) \leq \mathcal{P}\|\zeta\| + \pi$. Note that the positive constants $\mathcal{P}$ and π exist because $F(\zeta) + G(\zeta)u$ is Lipscitz continuous and the terms $d(\zeta)$ and $G^+(\zeta)\Delta F(\zeta)$ are upper bounded. In the simulation result, it is presented that the intersample time indeed has a lower limit which is larger than zero. As a result, the infamous Zeno-behavior is avoided.

3.4 ADP for Solving Event-Based HJB Equation

In this section, a single critic network is employed to approximate the optimal value of the cost function under the ADP framework. Considering (2.47) from Chapter 2, the augmented control law (3.14) and the event-based control law (3.17) are presented as

$$v^*(\zeta) = -\frac{1}{2\beta^2} M^{-1} L^\top(\zeta)((\nabla\sigma_c(\zeta))^\top \omega_c + \nabla\epsilon_c(\zeta)) \tag{3.31}$$

and

$$\mu^*(\zeta_j) = -\frac{1}{2} R^{-1} G^\top(\zeta_j)((\nabla\sigma_c(\zeta_j))^\top \omega_c + \nabla\epsilon_c(\zeta_j)), \tag{3.32}$$

respectively. Then by using (2.48) from Chapter 2, the approximate value of $v^*(\zeta)$ and $\mu^*(\zeta_j)$ can be obtained as

$$\hat{v}^*(\zeta) = -\frac{1}{2\beta^2} M^{-1} L^\top(\zeta)(\nabla\sigma_c(\zeta))^\top \hat{\omega}_c \tag{3.33}$$

and

$$\hat{\mu}^*(\zeta_j) = -\frac{1}{2} R^{-1} G^\top(\zeta_j)(\nabla\sigma_c(\zeta_j))^\top \hat{\omega}_c, \tag{3.34}$$

respectively. Next, the Hamiltonian is expressed as

$$\begin{aligned} H(\zeta, \omega_c, \mu^*(\zeta_j), v^*(\zeta)) &= \omega_c^\top \nabla\sigma_c(\zeta)(F(\zeta) + G(\zeta)\mu^*(\zeta_j) + L(\zeta)v^*(\zeta)) + \|r^\top\|^2 g_M^2(\zeta) \\ &\quad + \beta^2\|m^\top\|^2 d_M^2(\zeta) + U(\zeta, \mu^*(\zeta_j), v^*(\zeta)) - \gamma\omega_c^\top \sigma_c(\zeta) \\ &\triangleq e_{cH}, \end{aligned} \tag{3.35}$$

where $e_{cH} = -(\nabla\epsilon_c(\zeta))^\top(F(\zeta) + G(\zeta)\mu^*(\zeta_j) + L(\zeta)v^*(\zeta)) + \gamma\epsilon_c(\zeta)$ is the residual because of the reconstruction error associated with the NN approximation. Now, the Hamiltonian (3.10) is approximated as

$$\hat{H}(\zeta, \hat{\omega}_c, \hat{\mu}^*(\zeta_j), \hat{v}^*(\zeta)) = \hat{\omega}_c^\top \nabla\sigma_c(\zeta)(F(\zeta) + G(\zeta)\hat{\mu}^*(\zeta_j) + L(\zeta)\hat{v}^*(\zeta)) + \|r^\top\|^2 g_M^2(\zeta) + \beta^2\|m^\top\|^2 d_M^2(\zeta) + U(\zeta, \hat{\mu}^*(\zeta_j), \hat{v}^*(\zeta)) - \gamma\hat{\omega}_c^\top\sigma_c(\zeta). \quad (3.36)$$

From the HJB equation it is evident that $H(\zeta, \omega_c, \mu^*(\zeta_j), v^*(\zeta)) = 0$. So, the approximation error of the Hamiltonian is given by

$$\begin{aligned} e_c &= \hat{H}(\zeta, \hat{\omega}_c, \hat{\mu}^*(\zeta_j), \hat{v}^*(\zeta)) - H(\zeta, \omega_c, \mu^*(\zeta_j), v^*(\zeta)) \\ &= \hat{\omega}_c^\top \nabla\sigma_c(\zeta)(F(\zeta) + G(\zeta)\hat{\mu}^*(\zeta_j) + L(\zeta)\hat{v}^*(\zeta)) \\ &\quad + \|r^\top\|^2 g_M^2(\zeta) + \beta^2\|m^\top\|^2 d_M^2(\zeta) + U(\zeta, \hat{\mu}^*(\zeta_j), \hat{v}^*(\zeta)) - \gamma\hat{\omega}_c^\top\sigma_c(\zeta) \\ &= \|r^\top\|^2 g_M^2(\zeta) + \beta^2\|m^\top\|^2 d_M^2(\zeta) + U(\zeta, \hat{\mu}^*(\zeta_j), \hat{v}^*(\zeta)) + \hat{\omega}_c^\top\phi, \end{aligned} \quad (3.37)$$

where $\phi = \nabla\sigma_c(\zeta)(F(\zeta) + G(\zeta)\hat{\mu}^*(\zeta_j) + L(\zeta)\hat{v}^*(\zeta)) - \gamma\sigma_c(\zeta)$.

To ensure that the error e_c defined in (3.37) is kept sufficiently small, it is necessary to train the critic network to find the right weights. This involves minimizing the objective function $E = \frac{1}{2}e_c^\top e_c$. Here, the minimization is performed using the gradient descent method. Based on this method, the tuning rule for adjusting the critic weights is given as

$$\begin{aligned} \dot{\hat{\omega}}_{c1} &= \frac{-l_c}{(1+\phi^\top\phi)^2}\frac{\partial E}{\partial\hat{\omega}_c} \\ &= \frac{-l_c\phi}{(1+\phi^\top\phi)^2}(\hat{\omega}_c^\top\phi + \|r^\top\|^2 g_M^2(\zeta) + \beta^2\|m^\top\|^2 d_M^2(\zeta) + U(\zeta, \hat{\mu}^*(\zeta_j), \hat{v}^*(\zeta)), \end{aligned} \quad (3.38)$$

where $l_c > 0$ is a design parameter which is also known as the critic network's learning rate and $1/(1+\phi^\top\phi)^2$ is introduced to normalize ϕ.

An initial stabilising control is needed at the beginning of the critic weight vector learning process while using the tuning rule provided in (3.38). However, determining the initial admissible control can be difficult in some practical applications. To overcome the drawback, the tuning rule (3.38) is modified via the Lyapunov approach. Before continuing further, the following assumption, which is similar to [49], is presented.

Assumption 3.1. Let $V(\zeta)$ be a continuously differentiable Lyapunov function candidate for the system (3.7) under the action of control policies given by (3.31) and (3.32), and satisfy

$$\begin{aligned}\dot{V}(\zeta) &= (\nabla V(\zeta))^{\top}(F(\zeta) + G(\zeta)\mu^*(\zeta_j) + L(\zeta)v^*(\zeta)) \\ &< 0.\end{aligned} \tag{3.39}$$

Moreover, there exists a symmetric positive definite matrix $T \in \mathbb{R}^{2n}$ defined on Ω ensuring

$$\begin{aligned}(\nabla V(\zeta))^{\top}(F(\zeta) + G(\zeta)\mu^*(\zeta_j) + L(\zeta)v^*(\zeta)) &= -(\nabla V(\zeta))^{\top} T \nabla V(\zeta) \\ &\leq -\lambda_m(T)\|V(\zeta)\|^2.\end{aligned} \tag{3.40}$$

Remark 3.3. $F(\zeta)+G(\zeta)\mu^*(\zeta_j)+L(\zeta)v^*(\zeta)$ is frequently considered to be bounded by a positive constant on a compact set Ω [98]. In other words, there exists a constant z_1 such that $\|F(\zeta) + G(\zeta)\mu^*(\zeta_j)+L(\zeta)v^*(\zeta)\| \leq z_1$. Here, $F(\zeta)+G(\zeta)\mu^*(\zeta_j)+L(\zeta)v^*(\zeta)$ is assumed to be bounded by a function with respect to ζ, which is less stringent than the constant upper bound assumption. Without loss of generality, consider that $\|(F(\zeta) + G(\zeta)\mu^*(\zeta_j) + L(\zeta)v^*(\zeta))\| \leq z_2\|\nabla V(\zeta)\|$, where z_2 is a positive constant. In this regard, one can write $\|(\nabla V(\zeta))^{\top}(F(\zeta) + G(\zeta)\mu^*(\zeta_j) + L(\zeta)v^*(\zeta))\| \leq z_2\|\nabla V(\zeta)\|^2$. Observing (3.39), one can find that (3.40) is reasonable. In simulation, a polynomial with respect to ζ is chosen as $V(\zeta)$.

When applying the approximated control policies (3.33) and (3.34) to the auxiliary system (3.7), it is crucial to avoid the following condition to prevent instability

$$(\nabla V(\zeta))^{\top}(F(\zeta) + G(\zeta)\hat{\mu}^*(\zeta_j) + L(\zeta)\hat{v}^*(\zeta)) > 0. \tag{3.41}$$

To avoid (3.41), the training process is enhanced by introducing an additional term which is obtained using the steepest descent method as given below

$$\begin{aligned}\dot{\hat{\omega}}_{c2} &= l_s \frac{\partial((\nabla V(\zeta))^{\top}(F(\zeta) + G(\zeta)\hat{\mu}^*(\zeta_j) + L(\zeta)\hat{v}^*(\zeta)))}{\partial \hat{\omega}_c} \\ &= \frac{l_s}{2}\left(\nabla\sigma_c(\zeta_j)G(\zeta_j)R^{-1}G^{\top}(\zeta)\nabla V(\zeta) + \frac{1}{\beta^2}\nabla\sigma_c(\zeta)L(\zeta)M^{-1}L^{\top}(\zeta)\nabla V(\zeta)\right),\end{aligned} \tag{3.42}$$

where $l_s > 0$ is a design parameter. Now, the modified critic weights tuning rule is obtained by adding the stabilising term (3.42) to the traditional tuning rule (3.38) as

$$
\begin{aligned}
\dot{\hat{\omega}}_c &= \dot{\hat{\omega}}_{c1} + \dot{\hat{\omega}}_{c2} \\
&= \frac{-l_c\phi}{(1+\phi^\top\phi)^2}\Big(\hat{\omega}_c^\top\phi + \|r^\top\|^2 g_M^2(\zeta) + \beta^2\|m^\top\|^2 d_M^2(\zeta) + U(\zeta,\hat{\mu}^*(\zeta_j),\hat{\upsilon}^*(\zeta))\Big) \\
&\quad + \frac{l_s}{2}\bigg(\nabla\sigma_c(\zeta_j)G(\zeta_j)R^{-1}G^\top(\zeta)\nabla V(\zeta) + \frac{1}{\beta^2}\nabla\sigma_c(\zeta)L(\zeta)M^{-1}L^\top(\zeta)\nabla V(\zeta)\bigg). \qquad (3.43)
\end{aligned}
$$

Remark 3.4. The new tuning rule (3.43) can eliminate the need of initial admissible control. Hence, the critic weight vector can be initialized to zero while learning the appropriate critic weights.

The critic weights approximation error $\tilde{\omega}_c$ is defined as the difference between the ideal and the approximate weight vector, i.e., $\tilde{\omega}_c = \omega_c - \hat{\omega}_c$. From (3.35) and (3.37) one can write

$$e_c = -\tilde{\omega}_c^\top\phi + e_{cH}. \qquad (3.44)$$

Then, using (3.43) and (3.44), the critic weights approximation error dynamics is presented as

$$
\begin{aligned}
\dot{\tilde{\omega}}_c &= \frac{-l_c\phi}{(1+\phi^\top\phi)^2}(\tilde{\omega}_c^\top\phi - e_{cH}) - \frac{l_s}{2}(\nabla\sigma_c(\zeta_j)G(\zeta_j)R^{-1}G^\top(\zeta)\nabla V(\zeta) \\
&\quad + \frac{1}{\beta^2}\nabla\sigma_c(\zeta)L(\zeta)M^{-1}L^\top(\zeta)\nabla V(\zeta)). \qquad (3.45)
\end{aligned}
$$

The closed-loop system functions as an impulsive dynamical system consisting of flow dynamics and jump dynamics under the event-based control law. Let $\psi = [\zeta^\top, \zeta_j^\top, \tilde{\omega}_c^\top]^\top$ be an augmented state vector. Then, the flow dynamics of the closed-loop system, which occurs for all $t \in [t_j, t_{j+1})$, can be presented as

$$
\dot{\psi}(t) = \begin{bmatrix} F(\zeta) + G(\zeta)\hat{\mu}^*(\zeta_j) + L(\zeta)\hat{\upsilon}^*(\zeta) \\ \hline 0 \\ \hline \frac{-l_c\phi}{(1+\phi^\top\phi)^2}(\tilde{\omega}_c^\top\phi - e_{cH}) \\ -\frac{l_s}{2}(\nabla\sigma_c(\zeta_j)G(\zeta_j)R^{-1}G^\top(\zeta)\nabla V(\zeta) \\ +\frac{1}{\beta^2}\nabla\sigma_c(\zeta)L(\zeta)M^{-1}L^\top(\zeta)\nabla V(\zeta)) \end{bmatrix}, \quad \forall t \in [t_j, t_{j+1}), j \in \mathbb{N} \qquad (3.46)
$$

and the jump dynamics of the closed-loop system, which occurs for all $t \in t_{j+1}$, can be presented as

$$\psi(t^+) = \psi(t) + \begin{bmatrix} 0 \\ \zeta_j - \zeta(t) \\ 0 \end{bmatrix}, \quad \forall t \in t_{j+1}, j \in \mathbb{N}, \tag{3.47}$$

where $\psi(t^+) = \lim_{\varsigma \to 0^+} \psi(t + \varsigma)$ and $\varsigma \in (0, t_{j+1} - t_j)$.

3.5 Stability Analysis

In this section, the stability of impulsive dynamical representation of the closed-loop system, given by (3.46) and (3.47) is studied. Prior to proceeding further, the following assumption, which is common in literature, is stated below [70].

Assumption 3.2. The dynamics $L(\zeta)$ is upper bounded by a positive constant L_M.

Theorem 3.2. Let Assumptions 2.1 to 2.4, along with Assumptions 3.1 and 3.2, hold true. Then, under the control policies (3.33) and (3.34), the closed-loop auxiliary system (3.7) is asymptotically stable, and the weight approximation error is uniformly ultimately bounded, provided that the inequalities (3.48) and (3.49) hold. Here, $\eta_2 \in (0, 1)$ is a design parameter, and the values of $\varGamma_1$ and $\varGamma_2$ are given by (3.57) and (3.63), respectively.

$$\|e_j(t)\|^2 \leq \frac{(1-\eta_2^2)\lambda_m(Q)\|e_r(t)\|^2 + \|r^\top \hat{\mu}^*(\zeta_j)\|^2 - \beta^2\|m^\top\|^2\|\hat{v}^*(\zeta)\|^2}{\|R^{-1}\|^2\|r^\top\|^2(A^2\nabla\sigma_{cM}^2 + B^2G_M^2)\|\hat{\omega}_c\|^2} \triangleq \|\hat{e}_T\|^2 \tag{3.48}$$

$$\|\tilde{\omega}_c\| > \sqrt{\frac{2\|R\|^2(1+\phi^\top\phi)(\varGamma_1 + \varGamma_2 + \gamma J^*_{max})}{2(1+\phi^\top\phi)(l_c\|R\|^2\lambda_{\varphi m} - G_M^2\nabla\sigma_{cM}^2) - l_c\|R\|^2\lambda_{\varphi M}}} \tag{3.49}$$

Proof: In light of the flow dynamics (3.46) and the jump dynamics (3.47), the Lyapunov function candidate is considered as

$$\Upsilon(t) = \Upsilon_1(t) + \Upsilon_2(t) + \Upsilon_3(t) + \Upsilon_4(t), \tag{3.50}$$

where $\Upsilon_1(t) = J^*(\zeta)$, $\Upsilon_2(t) = J^*(\zeta_j)$, $\Upsilon_3(t) = \frac{1}{2}\tilde{\omega}_c^\top\tilde{\omega}_c$ and $\Upsilon_4(t) = l_s V(\zeta)$. Now, the analysis is separated into two cases.

Case 1. Events are not triggered, i.e., $t \in [t_j, t_{j+1})$. Taking the differentiation of (3.50) one can write

$$\dot{\Upsilon}(t) = \dot{\Upsilon}_1(t) + \dot{\Upsilon}_2(t) + \dot{\Upsilon}_3(t) + \dot{\Upsilon}_4(t). \tag{3.51}$$

It is evident that for $t \in [t_j, t_{j+1})$, $\dot{\Upsilon}_2(t) = 0$. Now, differentiating $\Upsilon_1(t)$ along the trajectory of $\dot{\zeta}(t) = F(\zeta) + G(\zeta)\hat{\mu}^*(\zeta_j) + L(\zeta)\hat{v}^*(\zeta)$ yields

$$\dot{\Upsilon}_1(t) = (\nabla J^*(\zeta))^\top \left(F(\zeta) + G(\zeta)\hat{\mu}^*(\zeta_j) + L(\zeta)\hat{v}^*(\zeta)\right).$$

Using equation (3.21) and (3.22), the following expression is obtained

$$\begin{aligned}\dot{\Upsilon}_1(t) = & -\zeta^\top \bar{Q}\zeta - \beta^2\|m^\top\|^2 d_M^2(\zeta) - \|r^\top\|^2 g_M^2(\zeta) + \gamma J^*(\zeta) + u^{*\top}(\zeta)Ru^*(\zeta) \\ & - 2u^{*\top}(\zeta)R\hat{\mu}^*(\zeta_j) + \beta^2 v^{*\top}(\zeta)Mv^*(\zeta) - 2\beta^2 v^{*\top}(\zeta)M\hat{v}^*(\zeta).\end{aligned} \tag{3.52}$$

Now

$$\begin{aligned}& u^{*\top}(\zeta)Ru^*(\zeta) - 2u^{*\top}(\zeta)R\hat{\mu}^*(\zeta_j) \\ & \leq \|r^\top(u^*(\zeta) - \hat{\mu}^*(\zeta_j))\|^2 - \|r^\top\hat{\mu}^*(\zeta_j)\|^2 \\ & \leq \|r^\top\|^2\|\frac{1}{2}R^{-1}G^\top(\zeta)(\nabla\sigma_c(\zeta))^\top\hat{\omega}_c - \frac{1}{2}R^{-1}G^\top(\zeta_j)(\nabla\sigma_c(\zeta_j))^\top\hat{\omega}_c \\ & \quad + \frac{1}{2}R^{-1}G^\top(\zeta)(\nabla\sigma_c(\zeta))^\top(\tilde{\omega}_c + \nabla\epsilon_c(\zeta))\|^2 - \|r^\top\hat{\mu}^*(\zeta_j)\|^2 \\ & \leq \frac{\|r^\top\|^2}{2}\|R^{-1}(G^\top(\zeta)(\nabla\sigma_c(\zeta))^\top - G^\top(\zeta_j)(\nabla\sigma_c(\zeta_j))^\top)\hat{\omega}_c\|^2 \\ & \quad - \|r^\top\hat{\mu}^*(\zeta_j)\|^2 + \frac{1}{2}\|R^{-1}G^\top(\zeta)((\nabla\sigma_c(\zeta))^\top\tilde{\omega}_c + \nabla\epsilon_c(\zeta))\|^2 \\ & \leq \|r^\top\|^2\|R^{-1}\|^2(A^2\nabla\sigma_{cM}^2 + B^2G_M^2)\|e_j\|^2\|\hat{\omega}_c\|^2 \\ & \quad + \frac{1}{\|R\|^2}G_M^2\nabla\sigma_{cM}^2\|\tilde{\omega}_c\|^2 + \frac{1}{\|R\|^2}G_M^2\nabla\epsilon_{cM} - \|r^\top\hat{\mu}^*(\zeta_j)\|^2,\end{aligned} \tag{3.53}$$

$$-2\beta^2 v^{*\top}(\zeta)M\hat{v}^*(\zeta) \leq \beta^2 v^{*\top}(\zeta)Mv^*(\zeta) + \beta^2\hat{v}^{*\top}(\zeta)M\hat{v}^*(\zeta) \tag{3.54}$$

and

$$\begin{aligned}2\beta^2 v^{*\top}(\zeta)Mv^*(\zeta) & \leq \frac{1}{2\beta^2\|M\|}\|L^\top(\zeta)(\nabla\sigma_c(\zeta))^\top(\omega_c + \nabla\epsilon_c)\|^2 \\ & \leq \frac{1}{2\beta^2\|M\|}L_M^2\nabla\sigma_{cM}^2(\omega_{cM}^2 + \nabla\epsilon_{cM}).\end{aligned} \tag{3.55}$$

Based on the above inequalities, (3.52) can be expressed as

$$\dot{\Upsilon}_1(t) \leq -\zeta^\top \bar{Q}\zeta - \beta^2\|m^\top\|^2 d_M^2(\zeta) - \|r^\top\|^2 g_M^2(\zeta) + \gamma J^*(\zeta) \\ + \beta^2\|m^\top\|^2\|\hat{v}^*(\zeta)\|^2 - \|r^\top\hat{\mu}^*(\zeta_j)\|^2 + \|r^\top\|^2\|R^{-1}\|^2(A^2\nabla\sigma_{cM}^2 + B^2G_M^2)\|e_j\|^2\|\hat{\omega}_c\|^2 \\ + \frac{1}{\|R\|^2}G_M^2\nabla\sigma_{cM}^2\|\tilde{\omega}_c\|^2 + \mathit{\Gamma}_1, \tag{3.56}$$

where $\mathit{\Gamma}_1$ is a positive constant and it is expressed as

$$\mathit{\Gamma}_1 = \frac{G_M^2}{\|R\|^2}\nabla\epsilon_{cM}^2 + \frac{L_M^2\nabla\sigma_{cM}^2}{2\beta^2\|M\|}(\omega_{cM}^2 + \nabla\epsilon_{cM}^2). \tag{3.57}$$

$\omega_c^\top\phi = \phi^\top\omega_c$ holds. Let $\varphi = \phi/(1+\phi^\top\phi)$. Now, using (3.45), the time derivative of $\Upsilon_3(t)$ is found as

$$\dot{\Upsilon}_3(t) = -l_c\tilde{\omega}_c^\top\varphi\varphi^\top\tilde{\omega}_c + \frac{l_c}{(1+\phi^\top\phi)}\tilde{\omega}_c^\top\varphi e_{cH} - \frac{l_s}{2}\tilde{\omega}_c^\top\nabla\sigma_c(\zeta_j)G(\zeta_j)R^{-1}G^\top(\zeta)\nabla V(\zeta) \\ - \frac{l_s}{2\beta^2}\tilde{\omega}_c^\top\nabla\sigma_c(\zeta)L(\zeta)M^{-1}L^\top(\zeta)\nabla V(\zeta). \tag{3.58}$$

Let $\lambda_M(\varphi\varphi^\top) = \lambda_{\varphi M}$ and $\lambda_m(\varphi\varphi^\top) = \lambda_{\varphi m}$. Then, considering Young's inequality $2c^\top d \leq c^\top c + d^\top d$ and Assumption 3.1, (3.58) can be expressed as

$$\dot{\Upsilon}_3(t) \leq -l_c\lambda_{\varphi m}\|\tilde{\omega}_c\|^2 + \frac{l_c}{2(1+\phi^\top\phi)}(\lambda_{\varphi M}\|\tilde{\omega}_c\|^2 + e_{cHM}^2) \\ - \frac{l_s}{2}\tilde{\omega}_c^\top\nabla\sigma_c(\zeta_j)G(\zeta_j)R^{-1}G^\top(\zeta)\nabla V(\zeta) \\ - \frac{l_s}{2\beta^2}\tilde{\omega}_c^\top\nabla\sigma_c(\zeta)L(\zeta)M^{-1}L^\top(\zeta)\nabla V(\zeta). \tag{3.59}$$

Now, substituting $\tilde{\omega}_c = \omega_c - \hat{\omega}_c$ in last two terms of (3.59) and considering the control policies (3.33) and (3.34), one can write

$$\dot{\Upsilon}_3(t) \leq -l_c\lambda_{\varphi m}\|\tilde{\omega}_c\|^2 + \frac{l_c}{2(1+\phi^\top\phi)}(\lambda_{\varphi M}\|\tilde{\omega}_c\|^2 + e_{cHM}^2) \\ - \frac{l_s}{2}(\nabla V(\zeta))^\top G(\zeta)R^{-1}G^\top(\zeta_j)\nabla\sigma_c(\zeta_j)\omega_c - l_s(\nabla V(\zeta))^\top G(\zeta)\hat{\mu}^*(\zeta_j) \\ - \frac{l_s}{2\beta^2}(\nabla V(\zeta))^\top L(\zeta)M^{-1}L^\top(\zeta)\nabla\sigma_c(\zeta)\omega_c - l_s(\nabla V(\zeta))^\top L(\zeta)\hat{v}^*(\zeta). \tag{3.60}$$

The derivative of $\Upsilon_4(t)$ is

$$\dot{\Upsilon}_4(t) = l_s \nabla V(\zeta)(F(\zeta) + G(\zeta)\hat{\mu}^*(\zeta_j) + L(\zeta)\hat{v}^*(\zeta)). \tag{3.61}$$

Now, combining (3.60) and (3.61) and using the control policies (3.31) and (3.32), one can write

$$\begin{aligned}\dot{\Upsilon}_3(t) + \dot{\Upsilon}_4(t) \leq & -l_c\lambda_{\varphi m}\|\tilde{\omega}_c\|^2 + \frac{l_c}{2(1+\phi^\top\phi)}(\lambda_{\varphi M}\|\tilde{\omega}_c\|^2 + e_{cHM}^2) \\ & + l_s(\nabla V(\zeta))^\top(F(\zeta) + G(\zeta)\mu^*(\zeta_j) + L(\zeta)v^*(\zeta)) \\ & + \frac{l_s}{2}(\nabla V(\zeta))^\top G(\zeta)R^{-1}G^\top(\zeta_j)\nabla\epsilon_c(\zeta_j) \\ & + \frac{l_s}{2\beta^2}(\nabla V(\zeta))^\top L(\zeta)M^{-1}L^\top(\zeta)\nabla\epsilon_c(\zeta).\end{aligned}$$

Utilizing Assumptions 2.1 to 2.4, along with Assumptions 3.1 and 3.2, one can write

$$\begin{aligned}\dot{\Upsilon}_3(t) + \dot{\Upsilon}_4(t) \leq & -l_c\lambda_{\varphi m}\|\tilde{\omega}_c\|^2 + \frac{l_c}{2(1+\phi^\top\phi)}(\lambda_{\varphi M}\|\tilde{\omega}_c\|^2 + e_{cHM}^2) \\ & - l_s\lambda_m(T)\|V(\zeta)\|^2 + l_s\kappa\|\nabla V(\zeta)\| \\ \leq & -l_c\lambda_{\varphi m}\|\tilde{\omega}_c\|^2 + \frac{l_c}{2(1+\phi^\top\phi)}\lambda_{\varphi M}\|\tilde{\omega}_c\|^2 + \frac{l_c}{2(1+\phi^\top\phi)}e_{cHM}^2 \\ & - l_s\lambda_m(T)\left(\|V(\zeta)\| - \frac{\kappa}{2\lambda_m(T)}\right)^2 + \frac{l_s\kappa^2}{4\lambda_m(T)} \\ \leq & -l_c\lambda_{\varphi m}\|\tilde{\omega}_c\|^2 + \frac{l_c\lambda_{\varphi M}}{2(1+\phi^\top\phi)}\|\tilde{\omega}_c\|^2 + \mathit{\Gamma}_2,\end{aligned} \tag{3.62}$$

where $\kappa = \frac{1}{2}\nabla\epsilon_{cM}(G_M^2\|R^{-1}\| + \frac{1}{\beta^2}L_M^2\|M^{-1}\|)$ and the positive constant $\mathit{\Gamma}_2$ is given by

$$\mathit{\Gamma}_2 = \frac{l_c e_{cHM}^2}{2(1+\phi^\top\phi)} + \frac{l_s\kappa^2}{4\lambda_m(T)}. \tag{3.63}$$

Substituting (3.56) and (3.62) into (3.51) yields

$$\begin{aligned}\dot{\Upsilon}(t) \leq & -\zeta^\top\bar{Q}\zeta - \beta^2\|m^\top\|^2 d_M^2(\zeta) - \|r^\top\|^2 g_M^2(\zeta) + \gamma J^*(\zeta) + \beta^2\|m^\top\|^2\|\hat{v}^*(\zeta)\|^2 \\ & + \|r^\top\|^2\|R^{-1}\|^2(A^2\nabla\sigma_{cM}^2 + B^2G_M^2)\|e_j\|^2\|\hat{\omega}_c\|^2 - \|r^\top\hat{\mu}^*(\zeta_j)\|^2 \\ & + \frac{1}{\|R\|^2}G_M^2\nabla\sigma_{cM}^2\|\tilde{\omega}_c\|^2 - l_c\lambda_{\varphi m}\|\tilde{\omega}_c\|^2 + \frac{l_c\lambda_{\varphi M}}{2(1+\phi^\top\phi)}\|\tilde{\omega}_c\|^2 + \mathit{\Gamma}_1 + \mathit{\Gamma}_2.\end{aligned} \tag{3.64}$$

Since, $\bar{Q} = diag\{Q, 0_{n\times n}\}$, one can write $\zeta^\top(t)\bar{Q}\zeta(t) = e_r^\top(t)Qe_r(t)$. Now, introducing the design parameter η_2, (3.64) can be presented as

$$\dot{\Upsilon}(t) \leq -\eta_2^2 \lambda_m(Q)\|e_r(t)\|^2 - (1-\eta_2^2)\lambda_m(Q)\|e_r(t)\|^2 - \beta^2\|m^\top\|^2 d_M^2(\zeta) - \|r^\top\|^2 g_M^2(\zeta) + \beta^2\|m^\top\|^2\|\hat{v}^*(\zeta)\|^2 - \|r^\top\hat{\mu}^*(\zeta_j)\|^2 + \|r^\top\|^2\|R^{-1}\|^2(A^2\nabla\sigma_{cM}^2 + B^2G_M^2)\|e_j\|^2\|\hat{\omega}_c\|^2 + \frac{G_M^2}{\|R\|^2}\nabla\sigma_{cM}^2\|\tilde{\omega}_c\|^2 - l_c\lambda_{\varphi m}\|\tilde{\omega}_c\|^2 + \frac{l_c\lambda_{\varphi M}}{2(1+\phi^\top\phi)}\|\tilde{\omega}_c\|^2 + \gamma J_{max}^* + \mathit{\Gamma}_1 + \mathit{\Gamma}_2. \quad (3.65)$$

If the inequalities (3.48) and (3.49) mentioned in Theorem 3.2 hold then (3.65) implies

$$\dot{\Upsilon}(t) \leq -\eta_2^2\lambda_m(Q)\|e_r(t)\|^2 - \beta^2\|m^\top\|^2 d_M^2(\zeta) - \|r^\top\|^2 g_M^2(\zeta) < 0,$$

i.e., the proposed Lyapunov function candidate has negative time derivative for all $t \in [t_j, t_{j+1})$.
Case 2. Events are triggered, i.e., $t \in t_{j+1}$. The difference of the Lyapunov function candidate is derived as

$$\Delta\Upsilon(t_j) = J^*(\zeta(t_j^+)) - J^*(\zeta(t_j)) + \frac{1}{2}\tilde{\omega}_c^\top(t_j^+)\tilde{\omega}_c(t_j^+) - \frac{1}{2}\tilde{\omega}_c^\top(t_j)\tilde{\omega}_c(t_j)) + J^*(\zeta_{j+1}) - J^*(\zeta_j) + l_s(V(t_j^+) - V(t_j)), \quad (3.66)$$

where $\zeta(t_j^+) = \lim_{\varsigma\to 0^+}\zeta(t_j+\varsigma)$ and $\varsigma \in (0, t_{j+1}-t_j)$. In Case 1, $\dot{\Upsilon}(t) < 0$ for all $t \in [t_j, t_{j+1})$ was derived, so

$$\Upsilon(t_j) \geq \lim_{\varsigma\to 0^+}\Upsilon(t_j+\varsigma) \quad \forall\varsigma \in (0, t_{j+1}-t_j), j \in \mathbb{N} \triangleq \Upsilon(t_j^+). \quad (3.67)$$

Thus, one can write

$$J^*(\zeta(t_j^+)) + \frac{1}{2}\tilde{\omega}_c^\top(t_j^+)\tilde{\omega}_c(t_j^+) + l_sV(t_j^+) - J^*(\zeta_j) - \frac{1}{2}\tilde{\omega}_c^\top(t_j)\tilde{\omega}_c(t_j)) - l_sV(t_j^+) \leq 0. \quad (3.68)$$

Hence, it can be further expressed as

$$(J^*(\zeta_{j+1}) - J^*(\zeta_j)) \leq -\vartheta\|e_{j+1}(t_j)\|, \quad (3.69)$$

where ϑ is a class $\mathcal{K}$ function and $e_{j+1}(t_j) = \zeta_{j+1} - \zeta_j$. The inequalities (3.68) and (3.69) imply the monotonically decreasing property of the proposed Lyapunov function candidate for all

$t \in t_{j+1}$.

Thus, from the two cases presented above, it is concluded that the closed-loop system is asymptotically stable and the critic weights approximation error is uniformly ultimately bounded.

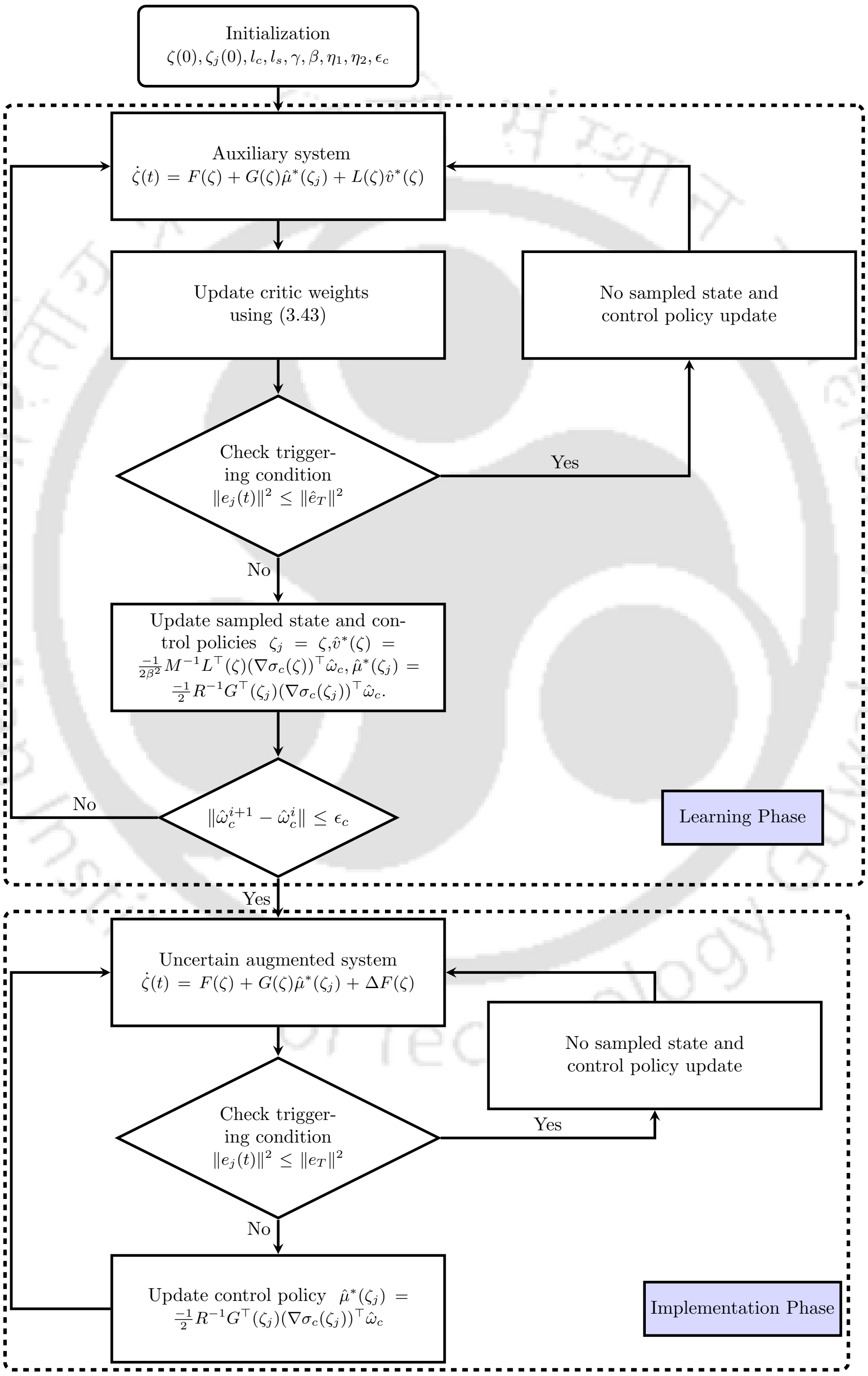

Figure 3.1: Flowchart of the proposed method.

A flowchart is given in Figure 3.1 to explain the fundamental methodology of the proposed work, which comprises the learning and implementation phases. In the learning phase, the converged critic weights are obtained after sufficient iterations while using the event-triggering rule (3.48). Then the converged weights are passed to the implementation phase to obtain the approximate values of the optimal control policies $\mu^*(\zeta_j)$ and $v^*(\zeta)$ as $\hat{\mu}^*(\zeta_j)$ and $\hat{v}^*(\zeta)$, respectively. The approximated event-based control policy $\hat{\mu}^*(\zeta_j)$ is applied to the uncertain nonlinear system while using the event-triggering rule (3.19) to track the desired trajectory.

Remark 3.5. The values of the sampling frequencies η_1 and η_2 are chosen such that the terms $\|e_T\|^2$ and $\|\hat{e}_T\|^2$ become positive, respectively. The increase in η_1 and η_2 will increase the sampling frequency and the number of the event-triggering instants. Furthermore, it improves tracking performance. However, the sampling frequency should be selected in such a way that there is a trade-off between the number of triggering instants and the tracking performance. Similar to relevant literature [83], other parameters are chosen heuristically such that the convergence time of the critic weights and the number of triggering instants are minimum with acceptable tracking performance.

Remark 3.6. The convergence time of the critic weights is influenced by several factors, including the learning rate, the event-triggering frequency, and the complexity of the value function being approximated. These factors are jointly tuned to strike a balance between convergence speed, reliable tracking performance, and a reduced number of triggering instants. Retuning of the critic weights is not required during normal operation as long as the system operates within the region for which the value function has been adequately learned. However, weight retraining may be needed if the desired trajectory changes.

3.6 Simulation Illustration

In this section, two simulation examples are presented to exhibit the efficacy of the proposed event-based robust trajectory tracking scheme. In Example 1, a linear system with unmatched uncertainty is considered, and in Example 2, the spring-mass-damper system with nonlinear spring constant and unmatched uncertainty is considered.

3.6.1 Example 1

Consider the following linear unmatched uncertain system [52]

$$\dot{x} = \begin{bmatrix} x_2 \\ -100x_1 - 2x_2 \end{bmatrix} + \begin{bmatrix} 0 \\ 1 \end{bmatrix} u + \Delta f(x), \tag{3.70}$$

where $x = [x_1, x_2]^\top \in \mathbb{R}^2$ is the state vector, $u \in \mathbb{R}$ denotes the control input, $\Delta f(x) = k(x)d_1(x)$ and $k(x) = [1, 0]^\top$. The perturbation is given as $d_1(x) = 0.5\theta_1 x_1 sin(x_2 + \theta_2)$, where the parameters θ_1 and θ_2 are unknown. Let $\theta_1 \in [-1, 1]$, $\theta_2 \in [-5, 5]$ and the upper bound of the perturbation $d_1(x)$ is $d_M(x) = |x_1|$. Let $x_0 = [0.6, -0.5]^\top$ be the initial state. The desired trajectory $x_r(t)$ is generated from

$$\dot{x}_r(t) = \begin{bmatrix} x_{r2} \\ -100x_{r1} \end{bmatrix}, \tag{3.71}$$

where $x_r = [x_{r1}, x_{r2}]^\top \in \mathbb{R}^2$ with the initial condition $x_{r0} = [0.3, -0.3]^\top$.

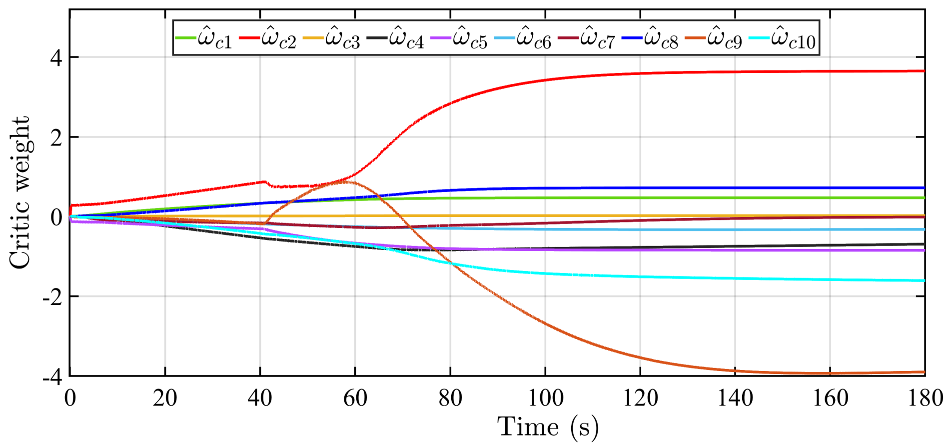

Figure 3.2: Convergence process of critic weights.

The tracking error e_r is defined as $e_r = x - x_r$, where $e_r = [e_{r1}, e_{r2}]^\top \in \mathbb{R}^2$, and initial condition $e_{r0} = x_0 - x_{r0}$. Then an augmented state vector $\zeta = [\zeta_1, \zeta_2, \zeta_3, \zeta_4]^\top \in \mathbb{R}^4$ is defined and following augmented system is formed

$$\dot{\zeta} = \begin{bmatrix} \zeta_2 \\ -100\zeta_1 - 2(\zeta_2 + \zeta_4) \\ \zeta_4 \\ -100\zeta_3 \end{bmatrix} + \begin{bmatrix} 0 \\ 1 \\ 0 \\ 0 \end{bmatrix} u(\zeta) + K(\zeta)d(\zeta), \tag{3.72}$$

where $K(\zeta) = [1, 0, 0, 0]^\top$ and $d(\zeta) = 0.5\theta_1(\zeta_1 + \zeta_3)sin((\zeta_2 + \zeta_4) + \theta_2)$. The initial condition is given by $\zeta_0 = [e_{r0}, x_{r0}]^\top = [0.3, -0.2, 0.3, -0.3]^\top$. The upper bound for $d_M(\zeta)$ is derived as $d_M(\zeta) = |\zeta_1 + \zeta_3|$. It is obtained that $G^+(\zeta) = [0, 1, 0, 0]$ so $(I_4 - G(\zeta)G^+(\zeta))K(\zeta) = [1, 0, 0, 0]^\top$. As in (3.7), the auxiliary system is formulated as

$$\dot{\zeta} = \begin{bmatrix} \zeta_2 \\ -100\zeta_1 - 2(\zeta_2 + \zeta_4) \\ \zeta_4 \\ -100\zeta_3 \end{bmatrix} + \begin{bmatrix} 0 \\ 1 \\ 0 \\ 0 \end{bmatrix} u(\zeta) + \begin{bmatrix} 1 \\ 0 \\ 0 \\ 0 \end{bmatrix} v(\zeta). \tag{3.73}$$

Since, $\|G^+(\zeta)K(\zeta)d(\zeta)\| = 0$, it is considered that $g_M(\zeta) = 0$. Let $R = I_1$, $M = I_1$ and $Q = 500I_2$. For the simulation purpose, consider $\gamma = 0.5$ and $\beta = 0.85$.

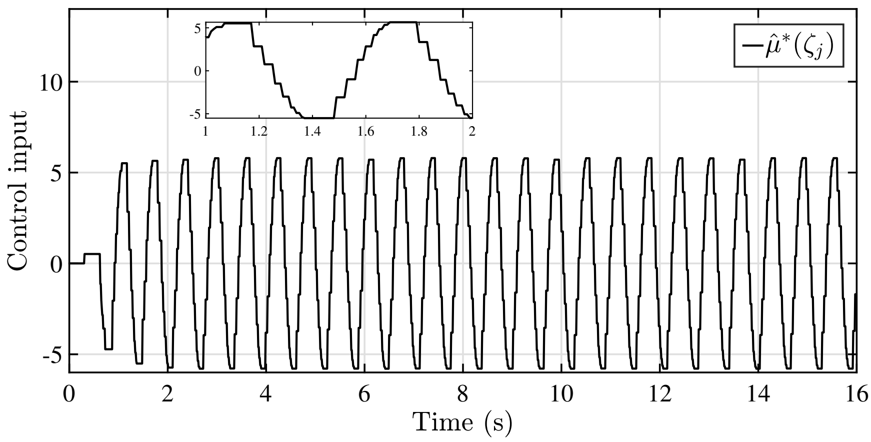

Figure 3.3: Event-based control input.

The aim is to develop an event-based robust controller for the system (3.70) to track the reference trajectory generated by (3.71). As described in the theoretical analysis, to achieve this design criteria, the augmented system (3.72) is formed and then the original control problem is transformed to designing an event-based optimal controller for auxiliary system (3.73). Based on (3.8), the cost function for (3.73) can be presented as

$$J(\zeta(t)) = \int_t^\infty \mathrm{e}^{-0.5(\tau-t)}\{500\|e_r\|^2 + \|u(\zeta)\|^2 + 0.72\|v(\zeta)\|^2 + 0.72|\zeta_1+\zeta_3|^2\}\mathrm{d}\tau. \quad (3.74)$$

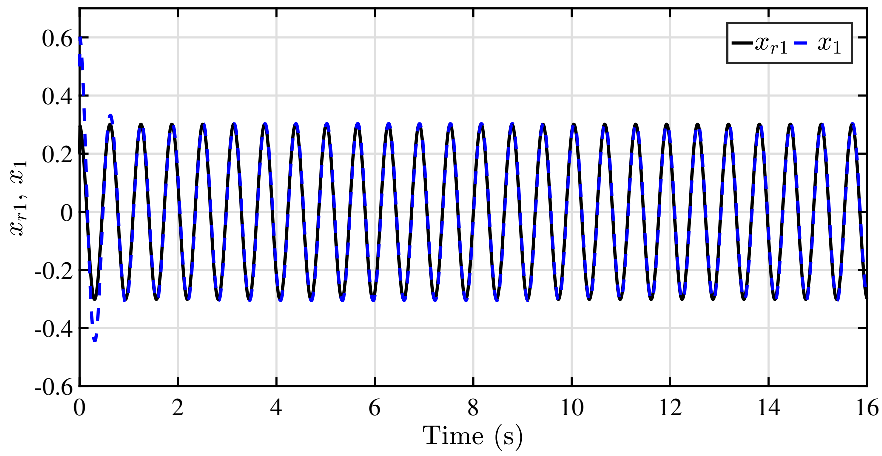

Figure 3.4: Tracking performance of x_1 for $\theta_1 = -0.3$ and $\theta_2 = 5$.

A single critic network is employed to find the solution of the event-based optimal control problem approximately. In the hidden layer of the critic network, $l = 10$ numbers of neurons are taken and the weight vector of the critic network is represented as $\hat{\omega}_c = [\hat{\omega}_{c1}, ..., \hat{\omega}_{c10}]^\top$. The activation function for the critic network is selected as

$$\sigma_c(\zeta) = [\zeta_1^2, \zeta_2^2, \zeta_3^2, , \zeta_4^2, \zeta_1\zeta_2, \zeta_1\zeta_3, \zeta_1\zeta_4, \zeta_2\zeta_3, \zeta_2\zeta_4, \zeta_3\zeta_4]^\top.$$

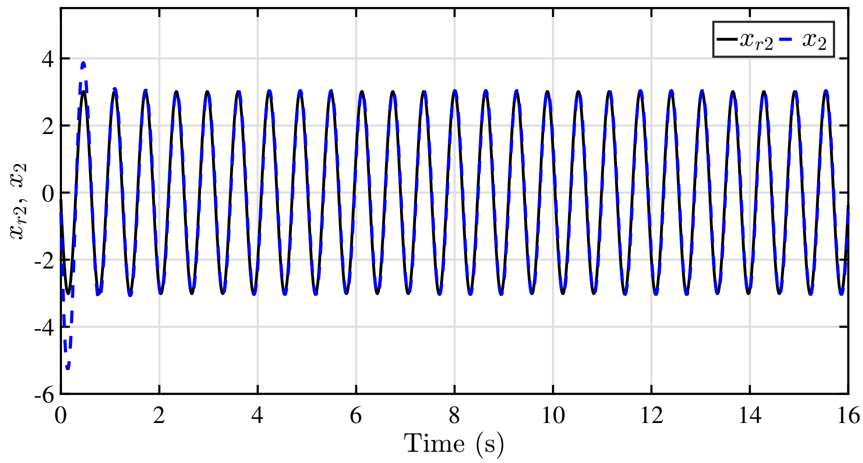

Figure 3.5: Tracking performance of x_2 for $\theta_1 = -0.3$ and $\theta_2 = 5$.

The weights are trained using the tuning rule (3.43) and the triggering condition (3.48) is used during the training process. The parameters used during the tuning process are $l_c = 3$, $l_s = 0.1$, $(A^2 \nabla \sigma_{cM}^2 + B^2 G_M^2) = 8$, and $\eta_2 = 0.7$.

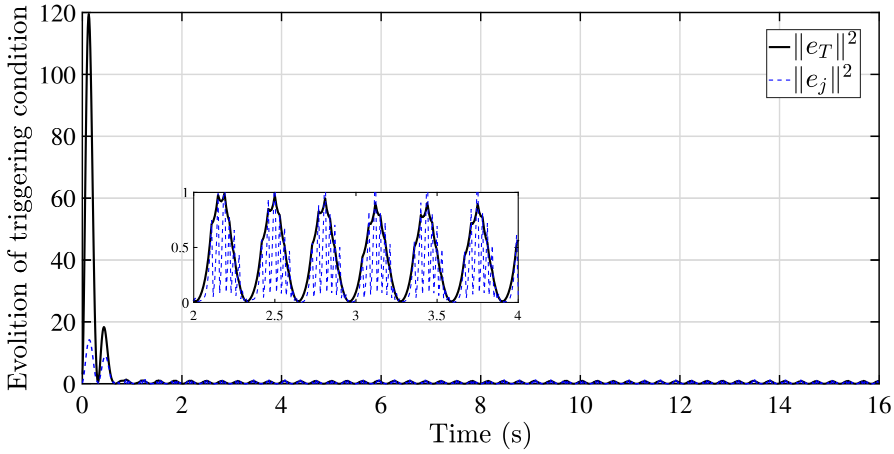

Figure 3.6: Evolution of the triggering condition with $\|e_T\|^2$ and $\|e_j\|^2$.

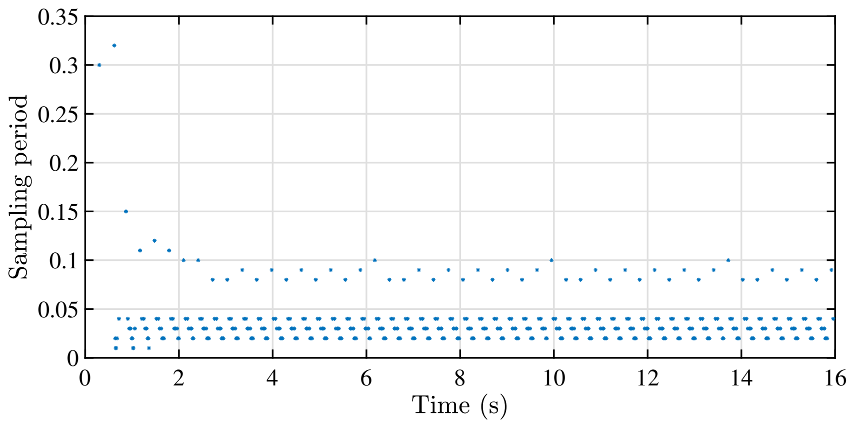

Figure 3.7: Triggering instants during the tracking process.

To satisfy the PE condition, a small exponentially decreasing probing noise is applied to the control input for the initial 10 seconds of the training process. All the elements of the weight vector are initialized to zero. As shown in Figure 3.2, the critic weight vector converges to

$$\hat{\omega}_c = [0.46, 3.64, 0.01, -0.69, -0.85, -0.32, -0.02, 0.71, -3.89, -1.60]^\top.$$

During the training process the event-based controller updates 5714 times. On the contrary, under the same design criteria, the time-based controller updates 18000 times.

Then, the converged weights are used to obtain the approximate values of control polices (3.33) and (3.34). Now, $\theta_1 = -0.3$ and $\theta_2 = 5$ are selected to demonstrate the trajectory tracking ability of the designed control policy $\hat{\mu}^*(\zeta_j)$ and the triggering rule described in (3.19). For this analysis, $\eta_1 = 0.65$ and $\mathcal{L} = 2.5$ are considered. The sampling period is taken as 0.01 second. The tracking performance of the designed controller is displayed in Figures 3.4 and 3.5. The obtained event-based control policy $\hat{\mu}^*(\zeta_j)$ is shown in Figure 3.3.

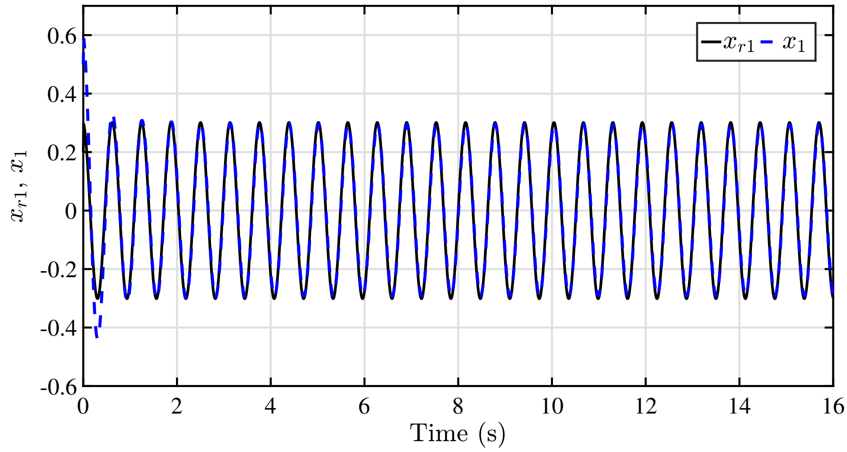

Figure 3.8: Tracking performance of x_1 for $\theta_1 = 0.4$ and $\theta_2 = -1$.

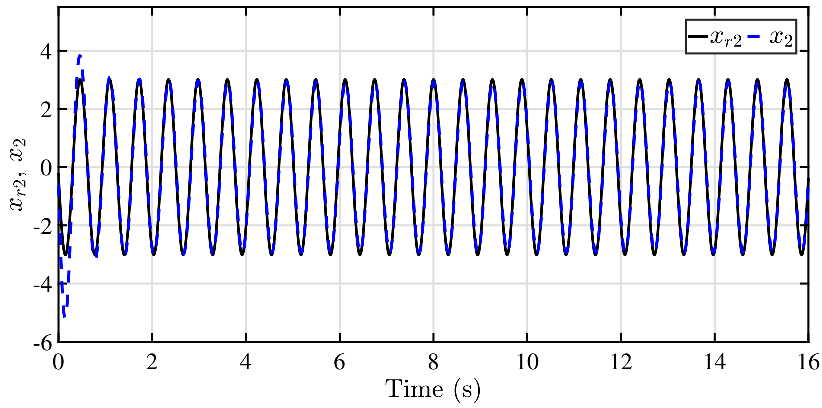

Figure 3.9: Tracking performance of x_2 for $\theta_1 = 0.4$ and $\theta_2 = -1$.

Table 3.1: Effect of η_1 on number of triggering instants.

Parameters	**Case 1**	**Case 2**	**Case 3**
η_1	0.65	0.75	0.8
N_s	435	777	906

The range of the sampling frequency η_1 is considered as $\eta_1 \in (0, 1)$. Table 3.1 illustrates the relationship between η_1 and the number of triggering instants N_s. From the table it is clear that as η_1 increases the number of event-triggering instants N_s increases.

The evolution of the triggering condition with $\|e_T\|^2$ and $\|e_j\|^2$ is displayed in Figure 3.6. The sampling period is shown in Figure 3.7. In the simulation, the minimal intersample time is observed to be 0.01 second. That means the infamous Zeno-behavior is excluded. Furthermore, Figure 3.7 also conveys that only 435 state samples are used during the tracking process. So, the controller is updated only 435 times. Nonetheless, if the time-triggering method under the same condition is used then 1600 samples are required. So, the developed event-based tracking control strategy reduces the resources used significantly.

Next, to show that the derived controller is robust, let $\theta_1 = 0.4$ and $\theta_2 = -1$. The tracking performance for new values of θ_1 and θ_2 is shown in Figures 3.8 and 3.9. In this scenario, the event-based controller updates 468 times only. On the contrary, the conventional time-triggered controller updates 1600 times under the same design criteria.

The proposed controller primarily addresses external disturbance $d(x)$, modelled as a function of the system state x. To investigate the applicability of the proposed controller in the case of disturbance related to the time, the value of $d(x)$ is changed to $d(t) = 0.1\big(sin^2(t)cos(t) + 0.1sin^2(2t)cos(0.1t)\big)$, while keeping all other parameters same. The tracking performance of x_1 and x_2 when the system is subjected to the above time-dependent disturbance is shown below.

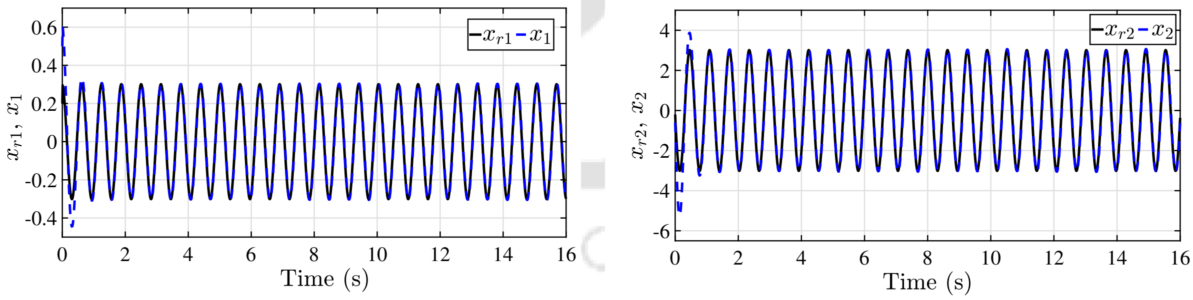

(a) Performance of x_1 **(b)** Performance of x_2

Figure 3.10: Tracking performance for $d(t) = 0.1\big(sin^2(t)cos(t) + 0.1sin^2(2t)cos(0.1t)\big)$.

Next, to check the influence of the parametric errors in the proposed approach, the original system dynamics $f(x) = \begin{bmatrix} x_2 \\ -100x_1 - 2x_2 \end{bmatrix}$ is used while tuning the critic weights, and during the implementation phase $f(x)$ is changed to $f\prime(x) = \begin{bmatrix} 0.5x_2 \\ -105x_1 - 2x_2 \end{bmatrix}$ while keeping all other parameters unchanged. It is observed that the number of triggering instants increased to 654 from 435 and there was a overshoot for a short duration. The tracking performance of x_1 and x_2 are shown below.

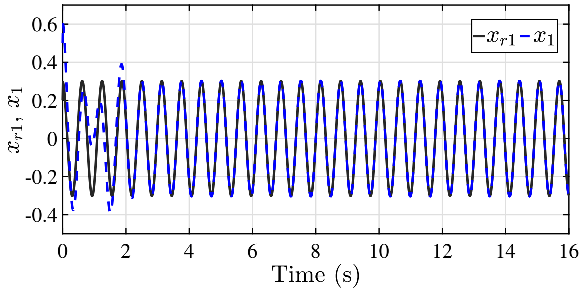

(a) Performance of x_1

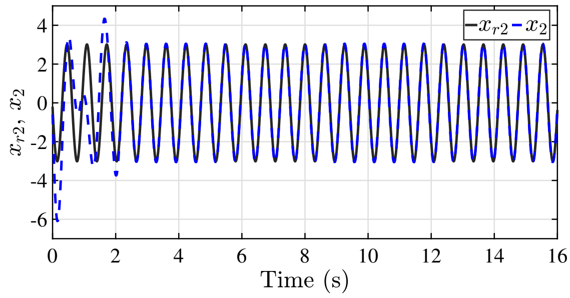

(b) Performance of x_2

Figure 3.11: Tracking performance for $f\prime(x)$.

3.6.2 Example 2

Consider the spring-mass-damper system [82]

$$\dot{x} = \begin{bmatrix} 0 & 1 \\ -\frac{\bar{k}}{m} & -\frac{c}{m} \end{bmatrix} x + \begin{bmatrix} 0 \\ \frac{1}{m} \end{bmatrix} u, \tag{3.75}$$

where $x = [x_1, x_2]^\top$, x_1 is the position and x_2 is the velocity, m represents the mass of the object, $\bar{k}$ denotes the spring constant and c is the damping coefficient. Let $m = 1Kg$, $c = 0.5N.s/m$ and the spring is nonlinear with the nonlinearity $\bar{k}(x) = -5x^3 N/m$. After adding an unmatched uncertainty $\Delta f(x)$, the system dynamics is obtained as

$$\dot{x} = \begin{bmatrix} x_2 \\ -5x_1^3 - 0.5x_2 \end{bmatrix} + \begin{bmatrix} 0 \\ 1 \end{bmatrix} u + \Delta f(x), \tag{3.76}$$

where $\Delta f(x) = k(x)d_1(x)$ with $k(x) = [1, 0]^\top$ and $d_1(x) = 0.5\theta_1 x_1 x_2 sin(x_1)cos(x_2 + \theta_2)$, where the parameters θ_1 and θ_2 are unknown. Let $\theta_1 \in [-1, 1]$, $\theta_2 \in [-5, 5]$ and the upper bound of the perturbation $d_1(x)$ is $d_M(x) = |x_2|$. Let $x_0 = [0.5, 0.2]^\top$ be the initial state.

The desired trajectory $x_r(t)$ is generated from

$$\dot{x}_r(t) = \begin{bmatrix} x_{r2} \\ -5x_{r1} \end{bmatrix}, \tag{3.77}$$

where $x_r = [x_{r1}, x_{r2}]^\top \in \mathbb{R}^2$ with the initial condition $x_{r0} = [0.2, -0.2]^\top$.

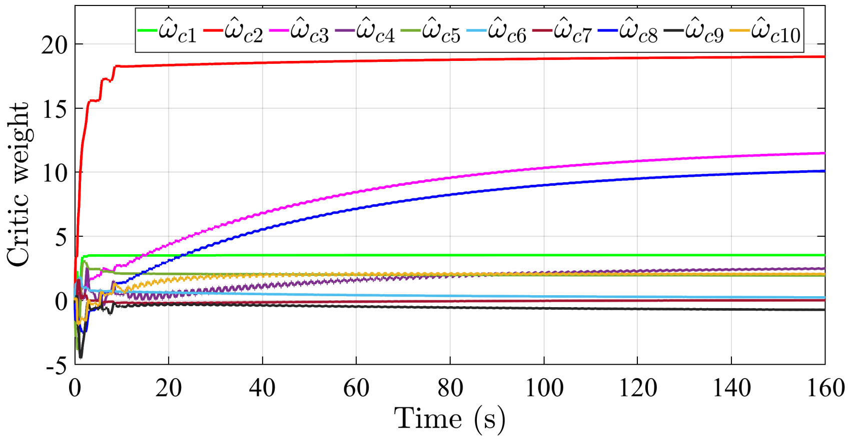

Figure 3.12: Convergence process of critic weights.

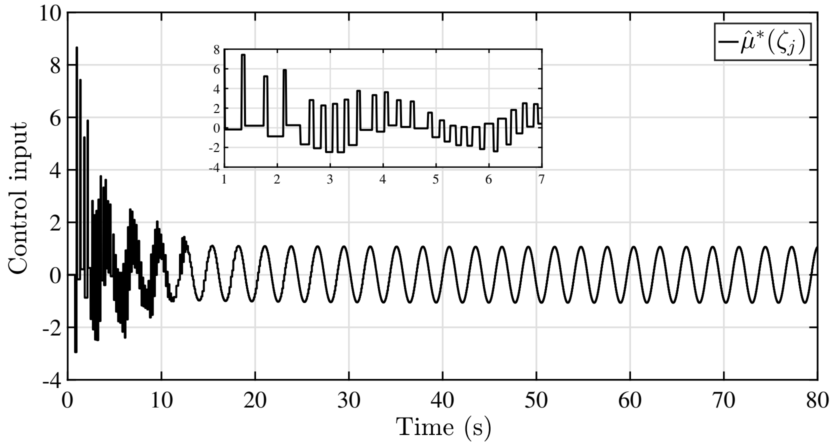

Figure 3.13: Event-based control input.

Then an augmented state vector $\zeta = [\zeta_1, \zeta_2, \zeta_3, \zeta_4]^\top \in \mathbb{R}^4$ is defined and following augmented system is formed

$$\dot{\zeta} = \begin{bmatrix} \zeta_2 \\ -5(\zeta_1+\zeta_3)^3 - 0.5(\zeta_2+\zeta_4) + 5\zeta_3 \\ \zeta_4 \\ -5\zeta_3 \end{bmatrix} + \begin{bmatrix} 0 \\ 1 \\ 0 \\ 0 \end{bmatrix} u(\zeta) + K(\zeta)d(\zeta), \tag{3.78}$$

where $K(\zeta) = [1, 0, 0, 0]^\top$ and $d(\zeta) = 0.5\theta_1(\zeta_1+\zeta_3)(\zeta_2+\zeta_4)sin(\zeta_1+\zeta_3)cos((\zeta_2+\zeta_4)+\theta_2)$. The initial condition is obtained as $\zeta_0 = [0.3, 0.4, 0.2, -0.2]^\top$. The upper bound for $d_M(\zeta)$ is derived as $d_M(\zeta) = |\zeta_2+\zeta_4|$.

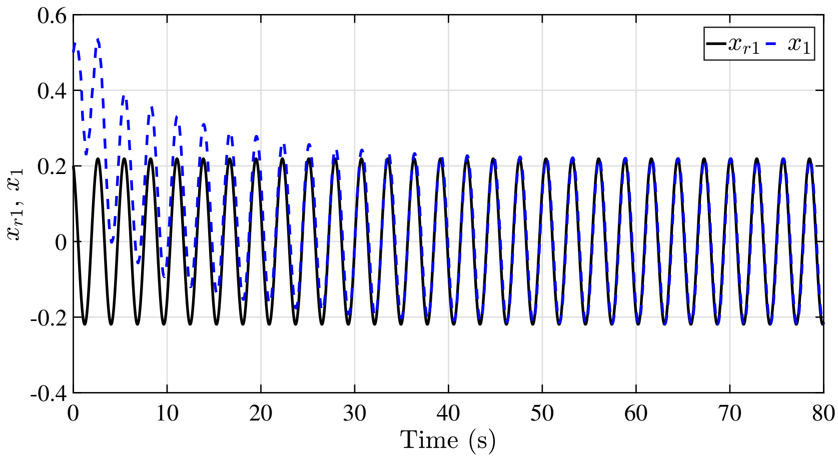

Figure 3.14: Tracking performance of x_1 for $\theta_1 = 0.2$ and $\theta_2 = -5$.

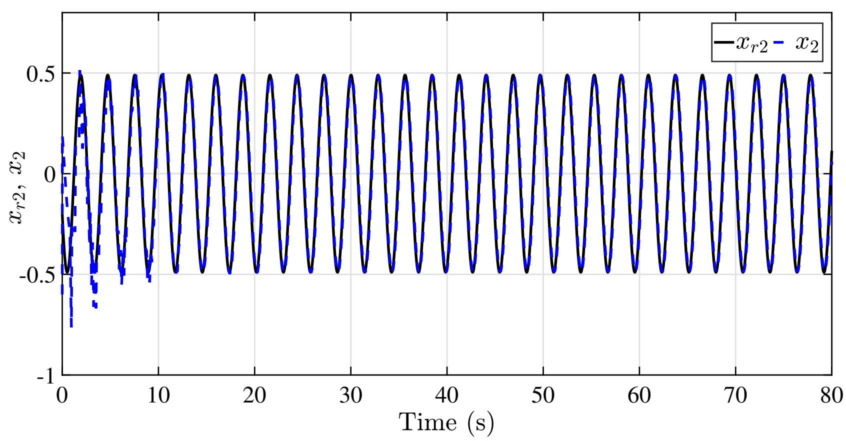

Figure 3.15: Tracking performance of x_2 for $\theta_1 = 0.2$ and $\theta_2 = -5$.

The auxiliary system is formulated as

$$\dot{\zeta} = \begin{bmatrix} \zeta_2 \\ -5(\zeta_1+\zeta_3)^3 - 0.5(\zeta_2+\zeta_4) + 5\zeta_3 \\ \zeta_4 \\ -5\zeta_3 \end{bmatrix} + \begin{bmatrix} 0 \\ 1 \\ 0 \\ 0 \end{bmatrix} u(\zeta) + \begin{bmatrix} 1 \\ 0 \\ 0 \\ 0 \end{bmatrix} v(\zeta). \tag{3.79}$$

Since, $\|G^{+}(\zeta)K(\zeta)d(\zeta)\| = 0$, it is considered that $g_M(\zeta) = 0$. Let $R = I_1$, $M = I_1$ and $Q = 300I_2$. For the simulation purpose, consider $\gamma = 1.2$ and $\beta = 0.9$. Based on (3.8), the cost function for (3.79) can be presented as

$$J(\zeta(t)) = \int_t^{\infty} \mathrm{e}^{-1.2(\tau-t)}\{300\|e_r\|^2 + \|u(\zeta)\|^2 + 0.81\|v(\zeta)\|^2 + 0.81|\zeta_2+\zeta_4|^2\}\mathrm{d}\tau. \tag{3.80}$$

In the hidden layer, 10 numbers of neurons are considered, i.e., $l = 10$ and the activation function is chosen as $\sigma_c(\zeta) = [\zeta_1^2, \zeta_1\zeta_2, \zeta_1\zeta_3, \zeta_1\zeta_4, \zeta_2^2, \zeta_2\zeta_3, \zeta_2\zeta_4, \zeta_3^2, \zeta_3\zeta_4, \zeta_4^2]^{\top}$. The parameters used during the tuning process are $l_c = 4$, $l_s = 0.5$, $(A^2\nabla\sigma_{cM}^2 + B^2G_M^2) = 8$ and $\eta_2 = 0.7$. To fulfil the PE criteria, a small exponentially decreasing probing noise is applied to the control input for the initial 10 seconds of the training process. All the elements of the weight vector are initialized to zero. The critic weight vector $\hat{\omega}_c$ converges to

$$[3.53, 19, 11.46, 2.49, 1.93, 0.23, 0.01, 10.07, -0.73, 2.05]^{\top}$$

as shown in Figure 3.12. During the training process the event-based controller updates 8947 times. on the contrary, under the same design criteria, the time-based controller updates 16000 times.

Then, the converged weights are used to obtain the control polices (3.33) and (3.34). Now, let us consider $\theta_1 = 0.2$ and $\theta_2 = -5$ to check the trajectory tracking performance of the designed control policy $\hat{\mu}^*(\zeta_j)$ and the triggering rule described in (3.19). The values of η_1 and $\mathcal{L}$ are considered as 0.7 and 10, respectively. The sampling period is taken as 0.01 second. The performance of the designed tracking controller is displayed in Figure 3.14 and Figure 3.15. The obtained event-based control policy $\hat{\mu}^*(\zeta_j)$ is displayed in Figure 3.13.

The evolution of the triggering condition with respect to $\|e_T\|^2$ and $\|e_j\|^2$ is illustrated in Figure 3.16, while Figure 3.17 depicts the corresponding sampling periods. The minimum inter-sample time is observed to be 0.01 seconds, effectively eliminating the possibility of Zeno-behavior. Additionally, Figure 3.17 shows that only 1440 state samples were used during the tracking process, meaning the controller was updated 1440 times. In contrast, a time-triggered control method under the same conditions would require 8000 samples. Therefore, the developed event-based tracking control strategy significantly reduces resource consumption.

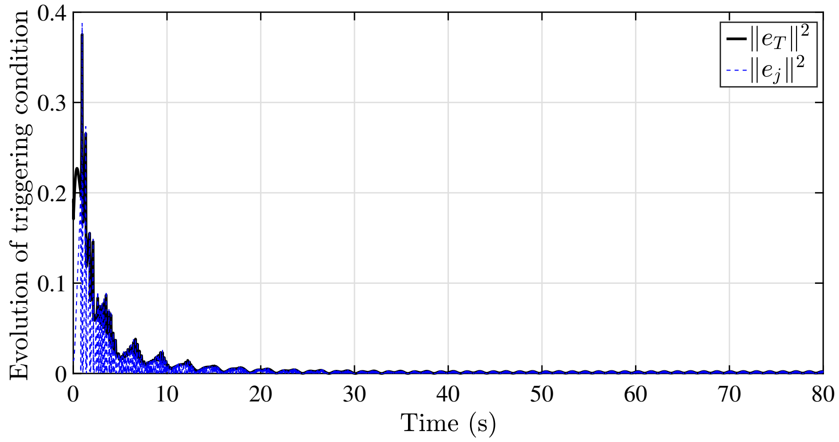

Figure 3.16: Evolution of the triggering condition with $\|e_T\|^2$ and $\|e_j\|^2$.

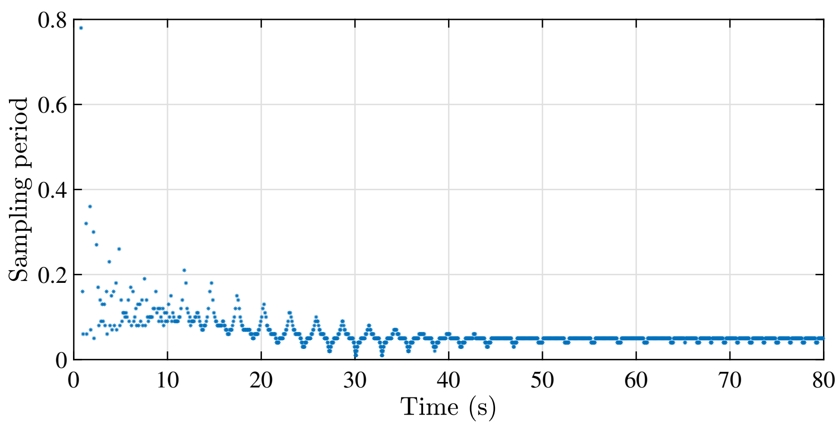

Figure 3.17: Triggering instants during the tracking process.

Next, in order to show that the derived controller is robust, the values of θ_1 and θ_2 are changed to -0.9 and 4, respectively. The tracking performance for new value of θ_1 and θ_2 is shown in Figure 3.18 and Figure 3.19. Here, only 1420 state samples are used during the tracking process. In other words, the event-based controller updates 1420 times only. On the other hand, the conventional time-triggered controller updates 8000 times under the same design criteria.

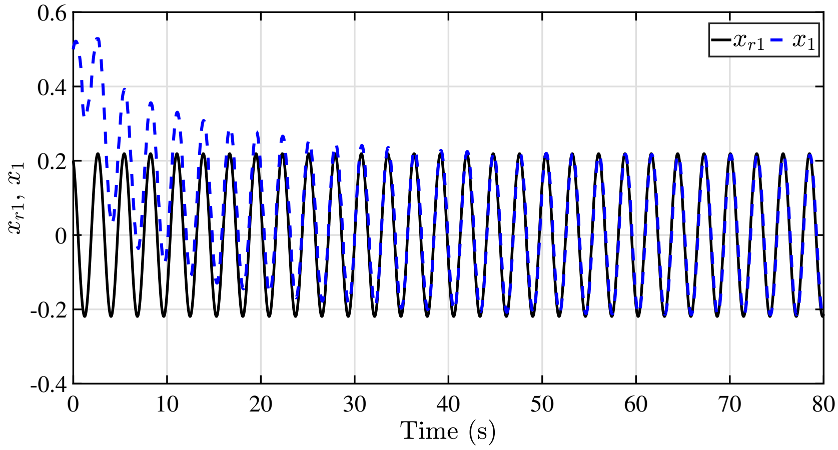

Figure 3.18: Tracking performance of x_1 for $\theta_1 = -0.9$ and $\theta_2 = 4$.

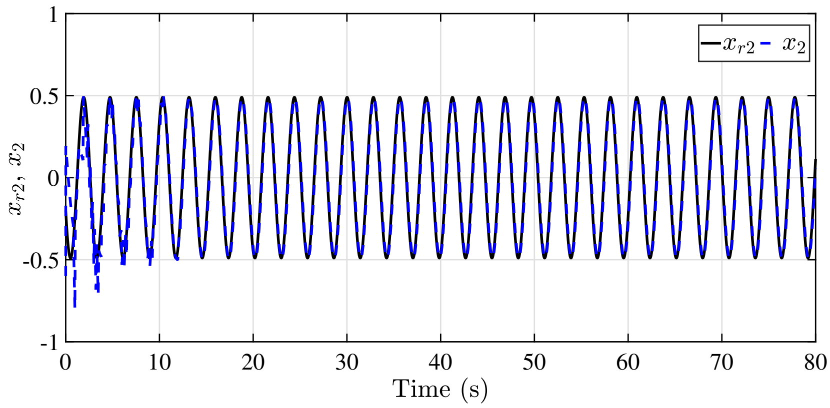

Figure 3.19: Tracking performance of x_2 for $\theta_1 = -0.9$ and $\theta_2 = 4$.

3.7 Summary

In this chapter, an event-based robust tracking strategy for an unmatched uncertain system is developed. The original control problem is transformed into obtaining an optimal controller for an auxiliary system by decomposing the unmatched uncertainty and forming an auxiliary system. The event-based HJB equation associated with the optimal control problem is solved using a single critic NN within the ADP framework. The critic weights tuning law is modified to eliminate the need for initial stabilizing control at the beginning of the tuning process, enhancing the control system's efficiency. Simultaneously, a novel event-triggering law is developed, and the uniform ultimate boundedness of the tracking error is verified using the Lyapunov method.

Furthermore, using the Lyapunov method, it is ensured that the established event-triggering rule ensures the uniform ultimate boundedness of all signals associated with the closed-loop auxiliary system. Finally, the proposed control scheme's applicability is validated through two simulation examples. The simulation studies revealed that the resulting event-based controller updates only at the triggering instants determined by the designed triggering condition, which significantly reduces the computational and communication resources, illustrating its effectiveness in real-world scenarios.

4

Guaranteed Cost Tracking Control of Constrained Input Nonlinear Uncertain Systems via Event-Triggered ADP

Contents

4.1 Introduction

In many real-world applications, control inputs are often bounded due to the physical limitations of actuators or safety constraints. Consequently, it becomes imperative to consider these input constraints when designing controllers for such systems. Failure to account for these constraints may lead the controller to generate control inputs that surpass the actuators' physical limitations, potentially causing system instability or damage. Therefore, integrating input constraints into the controller design process is essential for ensuring reliable and effective control performance, particularly in complex and uncertain environments.

In this chapter, the event-based ADP approach is utilized to address the guaranteed cost robust tracking control problem of nonlinear systems subjected to input constraint and unmatched uncertainty. First, the tracking error and reference trajectory are combined to form an augmented uncertain system. Then, by decomposing the uncertainty into the matched and unmatched parts, the original tracking problem is converted into the optimal regulation problem of an auxiliary system. The cost function for the auxiliary system is defined, and the associated HJB equation is solved using a single critic NN. Moreover, a novel event-triggering rule is formulated, and it is shown that the designed event-based controller guarantees that the tracking error is uniformly ultimately bounded. The derivation of event-based guaranteed cost and its relation with the time-based counterpart is presented. The exclusion of the infamous Zeno-behavior is guaranteed. The uniform ultimate boundedness of the critic weight estimation error is shown. Finally, the effectiveness of the proposed event-triggered ADP method is illustrated through simulations of the spring-mass-damper system and Van der Pol's oscillator with unmatched uncertainty.

The rest of this chapter is structured in the following manner. In Section 4.2, the problem formulation is presented briefly. In Section 4.3, the event-triggering rule is formulated and using the Lyapunov method it is shown that the tracking error is uniformly ultimately bounded. Additionally, the event-based guaranteed cost is derived. In Section 4.4, the ADP framework is utilized to solve the event-based HJB equation. Uniform ultimate boundedness of the weight approximation error is shown in Section 4.5. In Section 4.6, two simulation studies are shown to display the effectiveness of the proposed method. Finally, in Section 4.7, a brief summary of the chapter is given.

4.2 Problem Formulation

Consider the following continuous-time unmatched uncertain nonlinear system

$$\dot{x}(t) = f(x(t)) + g(x(t))u(x) + k(x(t))d_1(x(t)), \tag{4.1}$$

where $x = x(t) \in \mathbb{R}^n$ is the state vector, $u = u(x) \in \mathbb{R}^m$ is the control input. The elements of $u(x)$ are defined by $u_i(x)$, $i = 1, ..., m$ and each element is bounded by λ, where $\lambda \in \mathbb{R}^+$ is the saturating bound. $f(x) \in \mathbb{R}^n$, $g(x) \in \mathbb{R}^{n\times m}$, and $k(x) \in \mathbb{R}^{n\times p}$ are the system's drift dynamics, input gain matrix, and disturbance matrix, respectively. $d_1(x) \in \mathbb{R}^p$ denotes the unknown external disturbance which is considered to be bounded by $d_M(x)$ satisfying $\|d_1(x)\| \leq d_M(x)$. Furthermore, there exists a non-negative function $g_M(x)$ such that $\|g^+(x)k(x)d_1(x)\| \leq g_M(x)$, where $g^+(x)$ is the Moore-Penrose pseudo inverse of $g(x)$.

The reference trajectory to be tracked is obtained from the following system

$$\dot{x}_r(t) = Z(x_r(t)), \tag{4.2}$$

where $x_r = x_r(t) \in \mathbb{R}^n$ with the initial condition $x_r(0) = 0$. Moreover, $x_r(t)$ is assumed to be Lipschitz continuous. The tracking error $e_r(t)$ is defined as the difference between the system trajectory and the reference trajectory, i.e., $e_r(t) = x(t) - x_r(t)$. The tracking error dynamics is expressed as

$$\begin{aligned}\dot{e}_r(t) = {} & f(e_r(t) + x_r(t)) + g(e_r(t) + x_r(t))u(e_r(t) + x_r(t)) \\ & + k(e_r(t) + x_r(t))d(e_r(t) + x_r(t)) - Z(x_r(t)).\end{aligned} \tag{4.3}$$

Using the tracking error and the reference trajectory an augmented state $\zeta(t) \in \mathbb{R}^{2n}$, as given below, is formed

$$\zeta(t) = [e_r^\top(t), x_r^\top(t)]^\top,$$

where $\zeta(0) = [e_r^\top(0), x_r^\top(0)]^\top$. Now, using $\zeta(t)$, an augmented system is formed as given below

$$\dot{\zeta}(t) = F(\zeta) + G(\zeta)u(\zeta) + K(\zeta)d(\zeta), \tag{4.4}$$

where

$$F(\zeta) = \begin{bmatrix} f(e_r(t) + x_r(t)) - Z(x_r(t)) \\ Z(x_r(t)) \end{bmatrix}$$

and

$$G(\zeta) = \begin{bmatrix} g(e_r(t) + x_r(t)) \\ 0 \end{bmatrix}.$$

The terms $d_M(x)$ and $g_M(x)$ will remain upper bounded and they can be expressed as

$$\|d(\zeta)\| = \|d_1(e_r + x_r)\| = \|d_1(x)\| \leq d_M(x) = d_M(e_r + x_r) \triangleq d_M(\zeta). \tag{4.5}$$

and

$$\left\|G^+(\zeta)K(\zeta)d(\zeta)\right\| = \left\|g^+(x)k(x)d_1(x)\right\| \leq g_M(x) = g_M(e_r(t) + x_r(t)) \triangleq g_M(\zeta), \tag{4.6}$$

respectively. Now, the uncertain term is divided into sum of matched and unmatched parts by projecting into the range of matrix $G(\zeta)$ as given below

$$K(\zeta)d(\zeta) = G(\zeta)G^+(\zeta)K(\zeta)d(\zeta) + (I_{2n} - G(\zeta)G^+(\zeta))K(\zeta)d(\zeta),$$

where $G^+(\zeta)$ is the Moore-Penrose pseudo inverse of $G(\zeta)$. Then the following auxiliary system is formed

$$\dot{\zeta} = F(\zeta) + G(\zeta)u(\zeta) + (I_{2n} - G(\zeta)G^+(\zeta))K(\zeta)v(\zeta), \tag{4.7}$$

where the auxiliary control $v(\zeta) \in \mathbb{R}^p$ is introduced to deal with the unmatched part.

Next in order to design the optimal controller for the uncertain augmented system, a discounted cost function is formulated as

$$\bar{J}(\zeta, u) = \int_t^\infty \mathrm{e}^{-\gamma(\tau - t)}\{\zeta^\top \bar{Q}\zeta + W(u(\zeta))\}\mathrm{d}\tau, \tag{4.8}$$

where γ is a positive constant, known as the discount factor, $\bar{Q} = diag\{Q, 0_{n\times n}\}$, and $Q \in \mathbb{R}^{n\times n}$ is a positive definite matrix. The cost associated with the control input is $W(u(\zeta))$. The quadratic form of the control variable $u(\zeta)$ is often a popular selection for $W(u(\zeta))$ when the control is not subjected to constraints. However, when the control input is constrained, the quadratic cost function fails to incorporate these constraints. Therefore, following the approach in the literature [99, 100], the following non-quadratic function is considered

$$W(u(\zeta)) = 2\lambda \int_0^{u(\zeta)} (\varpi^{-1}(\tau/\lambda))^\top R \, \mathrm{d}\tau, \tag{4.9}$$

where $\varpi(\cdot)$ is a monotonic odd function whose first derivative is bounded. This nonquadratic term addresses the input constraint problem by effectively incorporating the constraint into the cost function. Without loss of generality, $\varpi(\cdot) = \tanh(\cdot)$ is considered in this work. R is a positive definite matrix. For simplicity, let $R = I_1$.

The objective of this chapter is to obtain a robust controller $u(\zeta)$ with $\|u(\zeta)\| \leq \lambda$ under the framework of event-based ADP such that the system trajectory $x(t)$ follow the reference trajectory $x_r(t)$ in presence of uncertainty. Moreover, the cost function (4.8) is guaranteed to be within a finite upper bound, that is, $\bar{J}(\zeta, u) \leq \bar{P}(\zeta, u)$, where $\bar{P}(\zeta, u)$ is called as the guaranteed cost.

The cost function for the auxiliary system (4.7) is formulated as

$$J(\zeta) = \int_t^\infty \mathrm{e}^{-\gamma(\tau - t)} \{\zeta^\top \bar{Q}\zeta + W(u(\zeta)) + \beta d_M^2(\zeta) + 2g_M^2(\zeta) + \beta v^\top(\zeta)v(\zeta)\} \mathrm{d}\tau, \tag{4.10}$$

where β is a positive constant.

Let $\Psi(\Omega)$ be the set of admissible control on Ω, where $\Omega \subset \mathbb{R}^{2n}$. Then the infinitesimal version of (4.10), which is also known as the Lyapunov equation of (4.10), is obtained as

$$\zeta^\top \bar{Q}\zeta + W(u(\zeta)) + \beta\|v(\zeta)\|^2 + 2g_M^2(\zeta) + \beta d_M^2 - \gamma J(\zeta) + \dot{J}(\zeta) = 0 \tag{4.11}$$

with $J(0) = 0$. Next, the Hamiltonian associated with the auxiliary system (4.7) is derived as

$$\begin{aligned} H(\zeta, u(\zeta), v(\zeta), \nabla J(\zeta)) = {} & (\nabla J(\zeta))^\top (F(\zeta) + G(\zeta)u(\zeta) + (I_{2n} - G(\zeta)G^+(\zeta))K(\zeta)v(\zeta)) \\ & + \zeta^\top \bar{Q}\zeta + W(u(\zeta)) + \beta\|v(\zeta)\|^2 + 2g_M^2(\zeta) + \beta d_M^2 - \gamma J(\zeta). \end{aligned} \tag{4.12}$$

The optimal value of the cost function is expressed as

$$J^*(\zeta) = \min_{u,v\in\Psi(\Omega)} \int_t^{\infty} \mathrm{e}^{-\gamma(\tau-t)}\{\zeta^\top \bar{Q}\zeta + W(u(\zeta)) + \beta d_M^2(\zeta) + 2g_M^2(\zeta) + \beta v^\top(\zeta)v(\zeta)\}\mathrm{d}\tau. \tag{4.13}$$

From the Bellman's theorem, $J^*(\zeta)$ satisfy the HJB equation

$$\min_{u,v\in\Psi(\Omega)} H(\zeta, u(\zeta), v(\zeta), \nabla J^*(\zeta)) = 0 \tag{4.14}$$

with $J^*(0) = 0$. Define $(I_{2n} - G(\zeta)G^+(\zeta))K(\zeta) = L(\zeta)$. the optimal control policies are obtained as

$$u^*(\zeta) = -\lambda \tanh\left(\frac{1}{2\lambda}G^\top(\zeta)\nabla J^*(\zeta)\right) \tag{4.15}$$

and

$$v^*(\zeta) = -\frac{1}{2\beta}L^\top(\zeta)\nabla J^*(\zeta). \tag{4.16}$$

Using above two equations in (4.14), the HJB equation is derived as

$$\begin{aligned}&(\nabla J^*(\zeta))^\top \left(F(\zeta) + G(\zeta)u^*(\zeta) + L(\zeta)v^*(\zeta)\right) + \zeta^\top \bar{Q}\zeta \\ &+ W(u^*(\zeta)) + \beta\|v^*(\zeta)\|^2 + 2g_M^2(\zeta) + \beta d_M^2 - \gamma J^*(\zeta) = 0.\end{aligned} \tag{4.17}$$

4.3 Guaranteed Cost Tracking Controller Design via Event-Based ADP

4.3.1 Event-Based Guaranteed Cost Controller Design

In this subsection, the time-triggered HJB equation (4.17) is converted to event-based HJB equation.

The auxiliary system (4.7) under event-triggered controller can be written as

$$\begin{aligned}\dot{\zeta} &= F(\zeta) + G(\zeta)\mu(\zeta_j) + (I_{2n} - G(\zeta)G^+(\zeta))K(\zeta)v(\zeta) \\ &= F(\zeta) + G(\zeta)\mu(e_j(t) + \zeta(t)) + (I_{2n} - G(\zeta)G^+(\zeta))K(\zeta)v(\zeta)\end{aligned} \tag{4.18}$$

The optimal control policy (4.15) under the event-triggered scheme is presented as

$$\mu^*(\zeta_j) = -\lambda \tanh\left(\frac{1}{2\lambda} G^\top(\zeta_j) \nabla J^*(\zeta_j)\right). \tag{4.19}$$

Now, using (4.19) in (4.17), the event-triggered HJB equation is derived as

$$\begin{aligned}
&(\nabla J^*(\zeta))^\top \big(F(\zeta) + G(\zeta)\mu^*(\zeta_j) + L(\zeta)v^*(\zeta)\big) + \zeta^\top \bar{Q}\zeta \\
&+ W(\mu^*(\zeta_j)) + \beta\|v^*(\zeta)\|^2 + 2g_M^2(\zeta) + \beta d_M^2 - \gamma J^*(\zeta) = 0
\end{aligned} \tag{4.20}$$

with $J^*(0) = 0$.

Theorem 4.1. Let Assumption 2.1 from Chapter 2 hold, $J^*(\zeta)$ satisfy the HJB equation (4.17), the control policies be given by (4.16) and (4.19). If $v^*(\zeta)$ satisfies

$$\|v^*(\zeta)\|^2 \leq \lambda_m(Q)\|e_r\|^2 \tag{4.21}$$

and the event-triggering law is formulated as

$$\begin{aligned}
\|e_j(t)\|^2 &\leq \frac{(1-2\beta)\lambda_m(Q)\|e_r\|^2}{2\mathcal{L}^2} \\
&\triangleq \|e_T\|^2,
\end{aligned} \tag{4.22}$$

then for $\beta \in (0, 0.5)$ the tracking error e_r is guaranteed to be uniformly ultimately bounded.

Proof: Since $J^*(\zeta)$ is positive definite, it is considered to be the Lyapunov function candidate. Taking the time derivative of $J^*(\zeta)$ along the trajectory of (4.4) yields

$$\begin{aligned}
\dot{J}^*(\zeta) &= (\nabla J^*(\zeta))^\top \big(F(\zeta) + G(\zeta)\mu^*(\zeta_j) + K(\zeta)d(\zeta)\big) \\
&= (\nabla J^*(\zeta))^\top F(\zeta) + (\nabla J^*(\zeta))^\top G(\zeta)\mu^*(\zeta_j) + (\nabla J^*(\zeta))^\top \big(G(\zeta)G^+(\zeta)K(\zeta) + L(\zeta)\big)d(\zeta).
\end{aligned} \tag{4.23}$$

From (4.17), one can derive

$$\begin{aligned}
(\nabla J^*(\zeta))^\top F(\zeta) &= -\zeta^\top \bar{Q}\zeta - W(u^*(\zeta)) - \beta\|v^*(\zeta)\|^2 - 2g_M^2(\zeta) - \beta d_M^2(\zeta) \\
&\quad + \gamma J^*(\zeta) - (\nabla J^*(\zeta))^\top \big(G(\zeta)u^*(\zeta) + L(\zeta)v^*(\zeta)\big),
\end{aligned} \tag{4.24}$$

from (4.15), the following expression is obtained

$$(\nabla J^*(\zeta))^\top G(\zeta) = -2\lambda \left(\tanh^{-1}\left(\frac{u^*(\zeta)}{\lambda}\right)\right)^\top \tag{4.25}$$

and from (4.16), one can derive

$$(\nabla J^*(\zeta))^\top L(\zeta) = -2\beta v^{*\top}(\zeta) \tag{4.26}$$

Using (4.24), (4.25) and (4.26) in (4.23) following expression is derived

$$\begin{aligned}
\dot{J}^*(\zeta) &= -\zeta^\top \bar{Q}\zeta - W(u^*(\zeta)) - \beta\|v^*(\zeta)\|^2 - 2g_M^2(\zeta) - \beta d_M^2(\zeta) + \gamma J^*(\zeta) \\
&\quad - (\nabla J^*(\zeta))^\top G(\zeta)\left(u^*(\zeta) - \mu^*(\zeta_j)\right) + (\nabla J^*(\zeta))^\top G(\zeta)G^+(\zeta)K(\zeta)d(\zeta) \\
&\quad - (\nabla J^*(\zeta))^\top L(\zeta)v^*(\zeta) + (\nabla J^*(\zeta))^\top L(\zeta)d(\zeta) \\
&= -\zeta^\top \bar{Q}\zeta - W(u^*(\zeta)) + \beta\|v^*(\zeta)\|^2 - 2g_M^2(\zeta) - \beta d_M^2(\zeta) + \gamma J^*(\zeta) \\
&\quad \underbrace{+ 2\lambda\left(\tanh^{-1}\left(\frac{u^*(\zeta)}{\lambda}\right)\right)^\top \left(u^*(\zeta) - \mu^*(\zeta_j)\right)}_{\pi_1} \\
&\quad \underbrace{+ 2\lambda\left(\tanh^{-1}\left(\frac{u^*(\zeta)}{\lambda}\right)\right)^\top G^+(\zeta)K(\zeta)d(\zeta)}_{\pi_2} \underbrace{-2\beta v^{*\top}(\zeta)d(\zeta)}_{\pi_3}
\end{aligned} \tag{4.27}$$

Utilizing Assumption 2.1 along with Young's inequality, the expression can be formulated as follows

$$\begin{aligned}
\pi_1 &\leq \frac{\lambda^2}{2}\|\tanh^{-1}\left(\frac{u^*(\zeta)}{\lambda}\right)\|^2 + 2\|u^*(\zeta) - \mu^*(\zeta_j)\|^2 \\
&\leq \frac{\lambda^2}{2}\sum_{i=1}^{m}\left(\tanh^{-1}\left(\frac{u_i^*(\zeta)}{\lambda}\right)\right)^2 + 2\mathcal{L}^2\|e_j(t)\|^2,
\end{aligned} \tag{4.28}$$

$$\begin{aligned}
\pi_2 &\leq \frac{\lambda^2}{2}\|\tanh^{-1}\left(\frac{u^*(\zeta)}{\lambda}\right)\|^2 + 2\|G^+(\zeta)K(\zeta)d(\zeta)\|^2 \\
&\leq \frac{\lambda^2}{2}\sum_{i=1}^{m}\left(\tanh^{-1}\left(\frac{u_i^*(\zeta)}{\lambda}\right)\right)^2 + 2g_M^2(\zeta)
\end{aligned} \tag{4.29}$$

and

$$\pi_3 \leq \beta \|v^*(\zeta)\|^2 + \beta \|d(\zeta)\|^2 \\ \leq \beta \|v^*(\zeta)\|^2 + \beta d_M^2(\zeta). \tag{4.30}$$

The function $W(u^*(\zeta))$ of (4.9) can be rewritten as

$$W(u^*(\zeta)) = \lambda^2 \sum_{i=1}^{m} \left(\tanh^{-1}\left(\frac{u_i^*(\zeta)}{\lambda} \right) \right)^2 - 2\lambda^2 \sum_{i=1}^{m} \left(\int_0^{\tanh(\frac{u_i^*(\zeta)}{\lambda})} z_i \tanh^2(z_i) dz_i \right) \tag{4.31}$$

So, (4.27) can be rewritten as

$$\dot{J}^*(\zeta) \leq -\zeta^\top \bar{Q} \zeta + 2\beta \|v^*(\zeta)\|^2 + \gamma J^*(\zeta) + 2\mathcal{L}^2 \|e_j(t)\|^2 \\ \underbrace{+ 2\lambda^2 \sum_{i=1}^{m} \left(\int_0^{\tanh(\frac{u_i(\zeta)}{\lambda})} z_i \tanh^2(z_i) dz_i \right)}_{\pi_4} \tag{4.32}$$

The term π_4 in (4.32) is bounded. To make further discussion easier to follow, consider the condition $\|\pi_4\| \leq K_m$, where $K_m \geq 0$ is a constant. Since, $\bar{Q} = diag\{Q, 0_{n\times n}\}$, it is possible to express $\zeta^\top \bar{Q} \zeta = e_r^\top Q e_r$. Hence, (4.32) can be rewritten as

$$\dot{J}^*(\zeta) \leq -\lambda_m(Q)\|e_r\|^2 + 2\beta \|v^*(\zeta)\|^2 + \gamma J^*(\zeta) + 2\mathcal{L}^2 \|e_j(t)\|^2 + K_m \\ \leq -2\beta(\lambda_m(Q)\|e_r\|^2 - \|v^*(\zeta)\|^2) - (1-2\beta)\lambda_m(Q)\|e_r\|^2 \\ + 2\mathcal{L}^2 \|e_j(t)\|^2 + \gamma J^*(\zeta) + K_m. \tag{4.33}$$

Hence, when the conditions (4.21) and (4.22), stated in Theorem 4.1, are satisfied then using (4.33) one can write

$$\dot{J}^*(\zeta) \leq -(1-2\beta)\lambda_m(Q)\|e_r\|^2 + \gamma J^*(\zeta) + K_m. \tag{4.34}$$

Given that $J^*(\zeta)$ is both positive definite and bounded on Ω, let J^*_{max} represent the maximum value of $J^*(\zeta)$. Thus, based on (4.34), $\dot{J}^*(\zeta) \leq 0$ only if e_r is located outside the set

$$\Omega_{e_r} = \left\{ e_r : \|e_r\| \leq \sqrt{\frac{\gamma J^*_{max} + K_m}{(1-2\beta)\lambda_m(Q)}} \right\}. \tag{4.35}$$

Hence, it can be inferred that when $\gamma \neq 0$, the tracking error $e_r(t)$ is uniformly ultimately bounded.

Theorem 4.2. Suppose that the optimal cost function $J^*(\zeta)$ is the solution of the HJB equation (4.17) and the event-triggered optimal controller is given by $\mu^*(\zeta_j)$. Then, the event-based optimal guaranteed cost function (4.8) satisfies the following inequality

$$\begin{aligned}\bar{J}(\zeta, \mu^*(\zeta_j)) \leq 2\int_t^\infty \mathrm{e}^{-\gamma(\tau-t)} \left(\int_{u^*(\zeta)}^{\mu^*(\zeta_j)} \Phi^{-1}(\mu^*(\zeta_j))\mathrm{d}\mu^*(\zeta_j) - \Phi^{-1}(u^*(\zeta))(\mu^*(\zeta_j) - u^*(\zeta)) \right) \mathrm{d}\tau \\ + \int_t^\infty \mathrm{e}^{-\gamma(\tau-t)} \left(\frac{\lambda^2}{2} \| \tanh^{-1}\left(\frac{u^*(\zeta)}{\lambda}\right) \|^2 + 2\beta\|v^*(\zeta)\|^2 \right) \mathrm{d}\tau + J^*(\zeta),\end{aligned} \tag{4.36}$$

where $\Phi^{-1}(\cdot) = \lambda \tanh^{-\top}(\frac{\cdot}{\lambda})$.

Proof: For an admissible controller $u(\zeta)$, the cost function (4.8) can be rewritten as

$$\bar{J}(\zeta, u(\zeta)) = \int_t^\infty \mathrm{e}^{-\gamma(\tau-t)} \{\dot{J}^*(\zeta) - \gamma J^*(\zeta) + \zeta^\top \bar{Q}\zeta + W(u(\zeta))\}\mathrm{d}\tau + J^*(\zeta), \tag{4.37}$$

where $\dot{J}^*(\zeta)$ is the time derivative of cost function (4.10) along the trajectory of the augmented system (4.4). Now, using (4.24) the term $\dot{J}^*(\zeta) - \gamma J^*(\zeta) + \zeta^\top \bar{Q}\zeta + W(u(\zeta))$ can be written as

$$\begin{aligned}&\dot{J}^*(\zeta) - \gamma J^*(\zeta) + \zeta^\top \bar{Q}\zeta + W(u(\zeta)) \\ &= W(u(\zeta)) - W(u^*(\zeta)) - \beta\|v^*(\zeta)\|^2 - 2g_M^2(\zeta) - (\nabla J^*(\zeta))^\top G(\zeta)(u^*(\zeta) - u(\zeta)) \\ &\quad - \beta d_M^2(\zeta) - (\nabla J^*(\zeta))^\top L(\zeta)v^*(\zeta) + (\nabla J^*(\zeta))^\top (G(\zeta)G^+(\zeta)K(\zeta) + L(\zeta))d(\zeta) \\ &= W(u(\zeta)) - W(u^*(\zeta)) - \beta\|v^*(\zeta)\|^2 - 2g_M^2(\zeta) - \beta d_M^2(\zeta) \\ &\quad + 2\beta v^{*\top}(\zeta)v^*(\zeta) + 2\lambda \left(\tanh^{-1}\left(\frac{u^*(\zeta)}{\lambda}\right)\right)^\top (u^*(\zeta) - u(\zeta)) \\ &\quad \underbrace{-2\lambda \left(\tanh^{-1}\left(\frac{u^*(\zeta)}{\lambda}\right)\right)^\top G^+(\zeta)K(\zeta)d(\zeta)}_{k_1} \underbrace{-2\beta v^{*\top}(\zeta)d(\zeta)}_{k_2}.\end{aligned} \tag{4.38}$$

Now using Young's inequality, the following expression is obtained

$$k_1 \leq \frac{\lambda^2}{2} \| \tanh^{-1}\left(\frac{u^*(\zeta)}{\lambda}\right) \|^2 + 2g_M^2(\zeta) \tag{4.39}$$

and

$$k_2 \leq \beta \|v^*(\zeta)\|^2 + \beta d_M^2(\zeta). \tag{4.40}$$

Using above two inequalities (4.38) can be expressed as

$$\begin{aligned}
&\dot{J}^*(\zeta) - \gamma J^*(\zeta) + \zeta^\top \bar{Q}\zeta + W(u(\zeta)) \\
&= W(u(\zeta)) - W(u^*(\zeta)) + 2\beta\|v^*(\zeta)\|^2 \\
&\quad + 2\lambda\left(\tanh^{-1}\left(\frac{u^*(\zeta)}{\lambda}\right)\right)^\top (u^*(\zeta) - u(\zeta)) + \frac{\lambda^2}{2}\| \tanh^{-1}\left(\frac{u^*(\zeta)}{\lambda}\right) \|^2 \\
&= 2\left(\int_{u^*(\zeta)}^{u(\zeta)} \Phi^{-1}(u)\mathrm{d}u - \Phi^{-1}(u^*(\zeta))(u(\zeta) - u^*(\zeta))\right) \\
&\quad + 2\beta\|v^*(\zeta)\|^2 + \frac{\lambda^2}{2}\| \tanh^{-1}\left(\frac{u^*(\zeta)}{\lambda}\right) \|^2.
\end{aligned} \tag{4.41}$$

Now, substituting (4.41) in (4.37), one can write

$$\begin{aligned}
\bar{J}(\zeta, u(\zeta)) \leq 2\int_t^\infty \mathrm{e}^{-\gamma(\tau-t)}\left(\int_{u^*(\zeta)}^{u(\zeta)} \Phi^{-1}(u)\mathrm{d}u - \Phi^{-1}(u^*(\zeta))(u(\zeta) - u^*(\zeta))\right)\mathrm{d}\tau \\
+ \int_t^\infty \mathrm{e}^{-\gamma(\tau-t)}\left(\frac{\lambda^2}{2}\| \tanh^{-1}\left(\frac{u^*(\zeta)}{\lambda}\right) \|^2 + 2\beta\|v^*(\zeta)\|^2\right)\mathrm{d}\tau + J^*(\zeta).
\end{aligned} \tag{4.42}$$

The term

$$\int_{u^*(\zeta)}^{u(\zeta)} \Phi^{-1}(u)\mathrm{d}u - \Phi^{-1}(u^*(\zeta))(u(\zeta) - u^*(\zeta))$$

can be written as

$$\begin{aligned}
&\int_{u^*(\zeta)}^{u(\zeta)} \Phi^{-1}(u)\mathrm{d}u - \Phi^{-1}(u^*(\zeta))(u(\zeta) - u^*(\zeta)) \\
&= \sum_{i=1}^m \left(\int_{u_i^*(\zeta)}^{u_i(\zeta)} \Phi^{-1}(u_i)\mathrm{d}u_i - \Phi^{-1}(u_i^*(\zeta))(u_i(\zeta) - u_i^*(\zeta))\right),
\end{aligned} \tag{4.43}$$

where $i = 1, \cdots, m$. Define

$$P_i = \int_{u_i^*(\zeta)}^{u_i(\zeta)} \Phi^{-1}(u_i)\mathrm{d}u_i - \Phi^{-1}(u_i^*(\zeta))(u_i(\zeta) - u_i^*(\zeta)).$$

First let us consider that $u_i(\zeta) > u_i^*(\zeta)$. Since $\Phi^{-1}(\cdot)$ is monotonic odd, so $\Phi^{-1}(u_i(\zeta)) > \Phi^{-1}(u_i^*(\zeta))$. Using mean value theorem for the integrals there exists a $\ell_i \in (u_i^*(\zeta), u_i(\zeta))$, such that

$$\begin{aligned}\int_{u_i^*(\zeta)}^{u_i(\zeta)} \Phi^{-1}(u_i)\mathrm{d}u_i &= \Phi^{-1}(\ell_i)(u_i(\zeta) - u_i^*(\zeta)) \\ &> \Phi^{-1}(u_i^*(\zeta))(u_i(\zeta) - u_i^*(\zeta)).\end{aligned} \tag{4.44}$$

Therefore, $P_i > 0$ for $u_i(\zeta) > u_i^*(\zeta)$.

Now consider that $u_i(\zeta) < u_i^*(\zeta)$, $\Phi^{-1}(u_i(\zeta)) < \Phi^{-1}(u_i^*(\zeta))$. Using mean value theorem for the integrals there exists a $\ell_i \in (u_i(\zeta), u_i^*(\zeta))$, such that

$$\begin{aligned}\int_{u_i^*(\zeta)}^{u_i(\zeta)} \Phi^{-1}(u_i)\mathrm{d}u_i &= -\int_{u_i(\zeta)}^{u_i^*(\zeta)} \Phi^{-1}(u_i)\mathrm{d}u_i \\ &= -\Phi^{-1}(\ell_i)(u_i^*(\zeta) - u_i(\zeta)) \\ &> -\Phi^{-1}(u_i^*(\zeta))(u_i^*(\zeta) - u_i(\zeta)) \\ &= \Phi^{-1}(u_i^*(\zeta))(u_i(\zeta) - u_i^*(\zeta)).\end{aligned} \tag{4.45}$$

Therefore, $P_i > 0$ for $u_i(\zeta) < u_i^*(\zeta)$.

From the above analysis it is evident that the first term on the right hand side of (4.42) is greater than 0 for all $u_i(\zeta) \neq u_i^*(\zeta)$ and attain its minimum vale, i.e., 0 at $u_i(\zeta) = u_i^*(\zeta)$. Therefore, it can be expressed that

$$\bar{J}(\zeta, u^*(\zeta)) \leq \int_t^\infty \mathrm{e}^{-\gamma(\tau - t)} \left(\frac{\lambda^2}{2} \| \tanh^{-1}\left(\frac{u^*(\zeta)}{\lambda}\right) \|^2 + 2\beta \|v^*(\zeta)\|^2 \right) \mathrm{d}\tau + J^*(\zeta). \tag{4.46}$$

When $u(\zeta) = \mu^*(\zeta_j)$, from (4.42), the event-based guaranteed cost (4.36) can be obtained as

$$\bar{J}(\zeta, \mu^*(\zeta_j))$$
$$\leq 2\int_t^\infty \mathrm{e}^{-\gamma(\tau-t)}\left(\int_{u^*(\zeta)}^{\mu^*(\zeta_j)} \Phi^{-1}(\mu^*(\zeta_j))\mathrm{d}\mu^*(\zeta_j) - \Phi^{-1}(u^*(\zeta))(\mu^*(\zeta_j) - u^*(\zeta))\right)\mathrm{d}\tau$$
$$+ \int_t^\infty \mathrm{e}^{-\gamma(\tau-t)}\left(\frac{\lambda^2}{2}\|\tanh^{-1}\left(\frac{u^*(\zeta)}{\lambda}\right)\|^2 + 2\beta\|v^*(\zeta)\|^2\right)\mathrm{d}\tau + J^*(\zeta). \tag{4.47}$$

Remark 4.1. Theorem 4.2 proves the boundedness of the cost function (4.10). Observing (4.46) and (4.47) it is evident that the event-based guaranteed cost is greater than the time-based guaranteed cost. Therefore, under event-based formulation, certain specified control performance has to be sacrificed along with the reduction of resource consumption.

Remark 4.2. The event-triggered framework is used to formulate the control policy $\mu^*(\zeta_j)$. However, the auxiliary control policy $v^*(\zeta)$ is derived via the traditional time-triggered framework because of two reasons. Firstly, the control policy applied to the uncertain system is $\mu^*(\zeta_j)$, not the auxiliary control $v^*(\zeta)$. Secondly, incorporating the auxiliary control in the event-triggered framework can make it challenging to determine the event-triggering rule (4.22).

4.3.2 Zeno-Behavior Analysis

In the context of continuous-time systems with an event-based controller, examining the occurrence of Zeno-behavior is essential. Zeno-behavior in event-triggered control methods refers to a situation where the time between successive events becomes zero, resulting in an infinite number of events occurring in a finite time interval. Theorem 4.3 is provided to ensure a nonzero positive minimum inter-event time. The following assumption, which is common in literature [87], is taken.

Assumption 4.1. $F(\zeta)$ is Lipschitz continuous with Lipschitz constant F_M and $F(0) = 0$. Additionally, $G(\zeta)$ and $K(\zeta)d(\zeta)$ are bounded by positive constants G_M and K_d, respectively.

Theorem 4.3. Given the system (4.4) and employing the event-triggered controller $\mu^*(\zeta_j)$ along with the event-triggering condition (4.22), if Assumption 4.1 holds, there exists a positive minimal inter-event time $(\Delta t_j)_{\min} = \min_{j\in\mathbb{N}}\{t_{j+1} - t_j\}$.

Proof: Considering Assumption 4.1, the augmented system (4.4) with the event-triggered controller $\mu^*(\zeta_j)$ implies

$$\begin{aligned}\left\|\dot{\zeta}\right\| &\leq \left\|F(\zeta)\right\| + \left\|G(\zeta)\mu^*(\zeta_j)\right\| + \left\|K(\zeta)d(\zeta)\right\| \\ &\leq F_M\|\zeta\| + G_M\lambda + K_d. \end{aligned} \tag{4.48}$$

Given that $e_j(t) = \zeta_j - \zeta(t)$, it follows that $\dot{\zeta} = -\dot{e}_j$. Hence, above inequality can be written as

$$\left\|\dot{e}_j\right\| \leq F_M\left\|e_j\right\| + F_M\left\|\zeta_j\right\| + G_M\lambda + K_d. \tag{4.49}$$

At the triggering moment t_j, it holds that $e_j(t_j) = 0$. Now using the comparison lemma [96], the solution of the differential inequality (4.49) is obtained as

$$\left\|e_j\right\| \leq \frac{F_M\left\|\zeta_j\right\| + G_M\lambda + K_d}{F_M}(e^{F_M(t-t_j)} - 1). \tag{4.50}$$

From the event-triggering mechanism, it is evident that the next triggering instant t_{j+1} releases only when the right hand side of (4.50) violates the triggering threshold $\|e_T\|$ given in (4.22). Thus one can write

$$\frac{F_M\left\|\zeta_j\right\| + G_M\lambda + K_d}{F_M}(e^{F_M(t-t_j)} - 1) > \left\|e_T^-(t_{j+1})\right\|. \tag{4.51}$$

with $e_T^-(t_{j+1}) = \lim_{\bar{q}\to 0^+} e_T(t_{j+1} - \bar{q})$. Define

$$\alpha_j = \frac{F_M\|e_T^-(t_{j+1})\|}{F_M\|\zeta_j\| + G_M\lambda + K_d}, \tag{4.52}$$

so the inequality (4.51) becomes

$$e^{F_M(t-t_j)} - 1 > \alpha_j. \tag{4.53}$$

Considering $\Delta t_j = t_{j+1} - t_j$, inequality (4.53) is expressed as

$$\Delta t_j > \frac{1}{F_M}\ln(1+\alpha_j), \quad j \in \mathbb{N}. \tag{4.54}$$

Let the minimum of α_j for all $j \in \mathbb{N}$ be $\alpha_{\min}$, i.e.,

$$\alpha_{\min} = \min_{j\in\mathbb{N}}\{\alpha_j\}. \tag{4.55}$$

Now, from (4.52) and (4.55) one can write $\alpha_{\min} > 0$. Thus, following expression is obtained by taking the minimum on both sides of (4.54)

$$(\Delta t_j)_{\min} > \frac{1}{F_M}\ln(1+\alpha_{\min}) > 0. \tag{4.56}$$

That is, the minimum inter-event time has a positive lower bound. In other words, the infamous Zeno-behavior is omitted.

4.4 Solution of the HJB Equation via ADP

In this section, the solution of the event-triggered HJB equation is obtained using the universal function approximation property of the neural network. Now, using (2.47) from Chapter 2, the optimal control policies (4.16) and (4.19) can be expressed as

$$v^*(\zeta) = -\frac{1}{2\beta}L^\top(\zeta)\left((\nabla\sigma_c(\zeta))^\top\omega_c + \nabla\epsilon_c(\zeta)\right) \tag{4.57}$$

and

$$\mu^*(\zeta_j) = -\lambda\tanh\left(\frac{1}{2\lambda}G^\top(\zeta_j)\left((\nabla\sigma_c(\zeta_j))^\top\omega_c + \nabla\epsilon_c(\zeta_j)\right)\right), \tag{4.58}$$

respectively. Similarly, utilizing (2.48) from Chapter 2, the approximate control policies are expressed as

$$\hat{v}^*(\zeta) = -\frac{1}{2\beta}L^\top(\zeta)(\nabla\sigma_c(\zeta))^\top\hat{\omega}_c \tag{4.59}$$

and

$$\hat{\mu}^*(\zeta_j) = -\lambda\tanh\left(\frac{1}{2\lambda}G^\top(\zeta_j)(\nabla\sigma_c(\zeta_j))^\top\hat{\omega}_c\right). \tag{4.60}$$

While considering the expressions (4.57) and (4.58), the Hamiltonian becomes

$$\begin{aligned} H(\zeta,\omega_c,\mu^*(\zeta_j),v^*(\zeta)) &= \omega_c^\top \nabla\sigma_c(\zeta)(F(\zeta)+G(\zeta)\mu^*(\zeta_j)+L(\zeta)v^*(\zeta)) + \zeta^\top \bar{Q}\zeta \\ &\quad + W(\mu^*(\zeta_j)) + \beta\|v^*(\zeta)\|^2 + 2g_M^2(\zeta) + \beta d_M^2 - \gamma\omega_c^\top\sigma_c(\zeta) \\ &\triangleq e_{cH}, \end{aligned} \tag{4.61}$$

where

$$e_{cH} = -(\nabla\epsilon_c(\zeta))^\top \big(F(\zeta)+G(\zeta)\mu^*(\zeta_j)+L(\zeta)v^*(\zeta)\big) + \gamma\epsilon_c(\zeta)$$

stand for the residual error due to NN approximation. Similarly, substituting (4.59) and (4.60) in (4.12), the approximate Hamiltonian is derived as

$$\begin{aligned} \hat{H}(\zeta,\hat{\omega}_c,\hat{\mu}^*(\zeta_j),\hat{v}^*(\zeta)) &= \hat{\omega}_c^\top \nabla\sigma_c(\zeta)(F(\zeta)+G(\zeta)\hat{\mu}^*(\zeta_j)+L(\zeta)\hat{v}^*(\zeta)) + \zeta^\top \bar{Q}\zeta \\ &\quad + W(\hat{\mu}^*(\zeta_j)) + \beta\|\hat{v}^*(\zeta)\|^2 + 2g_M^2(\zeta) + \beta d_M^2 - \gamma\hat{\omega}_c^\top\sigma_c(\zeta). \end{aligned} \tag{4.62}$$

From (4.14), it can be observed that

$$H(\zeta,\omega_c,\mu^*(\zeta_j),v^*(\zeta)) = 0.$$

Thus the Hamiltonian approximation error e_c can be obtained as

$$\begin{aligned} e_c &= \hat{H}(\zeta,\hat{\omega}_c,\hat{\mu}^*(\zeta_j),\hat{v}^*(\zeta)) - H(\zeta,\omega_c,\mu^*(\zeta_j),v^*(\zeta)) \\ &= \hat{\omega}_c^\top \nabla\sigma_c(\zeta)(F(\zeta)+G(\zeta)\hat{\mu}^*(\zeta_j)+L(\zeta)\hat{v}^*(\zeta)) + \zeta^\top \bar{Q}\zeta \\ &\quad + W(\hat{\mu}^*(\zeta_j)) + \beta\|\hat{v}^*(\zeta)\|^2 + 2g_M^2(\zeta) + \beta d_M^2 - \gamma\hat{\omega}_c^\top\sigma_c(\zeta) \\ &= \zeta^\top \bar{Q}\zeta + W(\hat{\mu}^*(\zeta_j)) + \beta\|\hat{v}^*(\zeta)\|^2 + 2g_M^2(\zeta) + \beta d_M^2 + \hat{\omega}_c^\top\phi, \end{aligned} \tag{4.63}$$

where $\phi = \nabla\sigma_c(\zeta)(F(\zeta)+G(\zeta)\hat{\mu}^*(\zeta_j)+L(\zeta)\hat{v}^*(\zeta)) - \gamma\sigma_c(\zeta)$.

Now, to make the weight approximation error sufficiently small, the gradient descent method is utilised to minimized the target function $E = (1/2)e_c^\top e_c$. Thus the weight tuning rule is obtained as

$$\dot{\hat{\omega}}_{c_t} = \frac{-l_c}{(1+\phi^\top\phi)^2}\frac{\partial E}{\partial \hat{\omega}_c}$$
$$= \frac{-l_c\phi}{(1+\phi^\top\phi)^2}\big(\zeta^\top\bar{Q}\zeta + W(\hat{\mu}^*(\zeta_j)) + \beta\|\hat{v}^*(\zeta)\|^2 + 2g_M^2(\zeta) + \beta d_M^2 + \hat{\omega}_c^\top\phi\big), \tag{4.64}$$

where $\hat{\omega}_{c_t}$ is the critic weight vector, i.e., $\hat{\omega}_{c_t} = \hat{\omega}_c$, $l_c > 0$ denotes learning rate of the critic NN and $1/(1+\phi^\top\phi)^2$ is brought to normalize ϕ.

However, while using the tuning rule (4.64), an initial admissible control is required to guarantee the convergence of the critic weights. But, the initial admissible control is a sub-optimal control, and it is difficult to obtain the sub-optimal control. To avoid this drawback, the tuning rule (4.64) is modified with the help of Assumption 3.1, which is stated in Chapter 3, as below

$$\dot{\hat{\omega}}_c = \frac{-l_c\phi}{(1+\phi^\top\phi)^2}\big(\zeta^\top\bar{Q}\zeta + W(\hat{\mu}^*(\zeta_j)) + \beta\|\hat{v}^*(\zeta)\|^2 + 2g_M^2(\zeta) + \beta d_M^2 + \hat{\omega}_c^\top\phi\big)$$
$$+ \frac{l_s}{2}\big(\nabla\sigma_c(\zeta_j)G(\zeta_j)G^\top(\zeta)\nabla V(\zeta) + \frac{1}{\beta}\nabla\sigma_c(\zeta)L(\zeta)L^\top(\zeta)\nabla V(\zeta)\big), \tag{4.65}$$

where $l_s > 0$ is a design parameter and $V(\zeta)$ is defined in Assumption 3.1.

Remark 4.3. The additional term in the tuning rule (4.65) is introduced to avoid the possibility of the closed loop system becoming unstable while tuning the critic weight. To avoid instability one needs to avoid the possibility

$$(\nabla V(\zeta))^\top(F(\zeta) + G(\zeta)\hat{\mu}^*(\zeta_j) + L(\zeta)\hat{v}^*(\zeta)) > 0. \tag{4.66}$$

To omit the possibility (4.66), the steepest descent method is utilised to obtain the additional term in (4.65) as follow

$$\dot{\hat{\omega}}_{c_s} = l_s\frac{\partial\big((\nabla V(\zeta))^\top(F(\zeta) + G(\zeta)\hat{\mu}^*(\zeta_j) + L(\zeta)\hat{v}^*(\zeta))\big)}{\partial\hat{\omega}_c}$$
$$= \frac{l_s}{2}\big(\nabla\sigma_c(\zeta_j)G(\zeta_j)G^\top(\zeta)\nabla V(\zeta) + \frac{1}{\beta}\nabla\sigma_c(\zeta)L(\zeta)L^\top(\zeta)\nabla V(\zeta)\big). \tag{4.67}$$

Remark 4.4. The newly proposed weight update rule can eliminate the requirement for an initial admissible control. Therefore, the critic weights can be set to zero at the beginning of the learning process to find the suitable critic weights.

Let the critic weight vector estimation error be $\tilde{\omega}_c = \omega_c - \hat{\omega}_c$. Then combining (4.61) and

(4.63), one can write

$$e_c = -\tilde{\omega}_c^\top \phi + e_{cH}. \tag{4.68}$$

Now, the dynamics of the critic weight vector approximation error is derived from (4.65) and (4.68) as

$$\begin{aligned}\dot{\tilde{\omega}}_c = &\frac{-l_c\phi}{(1+\phi^\top\phi)^2}(\tilde{\omega}_c^\top\phi - e_{cH}) - \frac{l_s}{2}\big(\nabla\sigma_c(\zeta_j)G(\zeta_j)G^\top(\zeta)\nabla V(\zeta)\\ &+\frac{1}{\beta}\nabla\sigma_c(\zeta)L(\zeta)L^\top(\zeta)\nabla V(\zeta)\big).\end{aligned} \tag{4.69}$$

Under the event-triggered framework the closed loop system acts as an impulsive dynamical system. The closed loop systems shows flow dynamics for all $t \in [t_j, t_{j+1})$ and jump dynamics for all $t \in t_{j+1}$. The impulsive dynamical representation is given below.

$$\dot{\psi}(t) = \begin{bmatrix} F(\zeta) + G(\zeta)\hat{\mu}^*(\zeta_j) + L(\zeta)\hat{v}^*(\zeta) \\ \hdashline 0 \\ \hdashline \frac{-l_c\phi}{(1+\phi^\top\phi)^2}(\tilde{\omega}_c^\top\phi - e_{cH}) \\ -\frac{l_s}{2}\big(\nabla\sigma_c(\zeta_j)G(\zeta_j)G^\top(\zeta)\nabla V(\zeta) \\ +\frac{1}{\beta}\nabla\sigma_c(\zeta)L(\zeta)L^\top(\zeta)\nabla V(\zeta)\big) \end{bmatrix}, \quad \forall t \in [t_j, t_{j+1}) \tag{4.70}$$

and

$$\psi(t^+) = \psi(t) + \begin{bmatrix} 0 \\ \zeta_j - \zeta(t) \\ 0 \end{bmatrix}, \quad \forall t \in t_{j+1}, \tag{4.71}$$

where $\psi(t^+) = \lim_{\varsigma\to 0^+}\psi(t+\varsigma)$ and $\varsigma \in (0, t_{j+1} - t_j)$.

4.5 Stability Analysis

In this section, the closed loop stability of the control system is analysed.

Theorem 4.4. Consider the auxiliary system (4.7), the control policies (4.59) and (4.60), and the weight tuning rule (4.65). Let the Assumptions 2.1 to 2.4, along with Assumptions 3.1, 3.2, and

4.1 be valid. Then, the closed-loop auxiliary system (4.7) is locally asymptotically stable and the weight approximation error is uniformly ultimately bounded if the inequalities (4.72), (4.73) and (4.74) hold, where $\eta_2 \in (0,1)$ is a design parameter.

$$\begin{aligned} \|e_j(t)\|^2 &\leq \frac{(1-\eta_2^2)\lambda_m(Q)\|e_r(t)\|^2}{2(A^2\nabla\sigma_{cM}^2 + B^2G_M^2)\|\hat{\omega}_c\|^2} \\ &\triangleq \|\hat{e}_T\|^2 \end{aligned} \tag{4.72}$$

$$\|\tilde{\omega}_c\| > \sqrt{\frac{\kappa}{l_c\lambda_{\varphi m} - 2G_M^2\nabla\sigma_{cM}^2 - \frac{1}{2\beta}L_M^2\nabla\sigma_{cM}^2 - \frac{l_c\lambda_{\varphi M}}{2(1+\phi^\top\phi)}}} \tag{4.73}$$

$$\|V(\zeta)\| > \sqrt{\frac{\kappa}{l_s\lambda_m(T)}} + \frac{\kappa_1}{2\lambda_m(T)}. \tag{4.74}$$

Proof: In view of impulsive dynamical representation of the closed loop system, the Lyapunov function candidate is considered as

$$\Upsilon(t) = \Upsilon_1(t) + \Upsilon_2(t) + \Upsilon_3(t) + \Upsilon_4(t), \tag{4.75}$$

where $\Upsilon_1(t) = J^*(\zeta)$, $\Upsilon_2(t) = J^*(\zeta_j)$, $\Upsilon_3(t) = \frac{1}{2}\tilde{\omega}_c^\top\tilde{\omega}_c$, and $\Upsilon_4(t) = l_sV(\zeta)$. The proof is divided into following two cases.

Case 1. When $t \in [t_j, t_{j+1})$, i.e., the events are not triggered. The differentiation of (4.75) is represented as

$$\dot{\Upsilon}(t) = \dot{\Upsilon}_1(t) + \dot{\Upsilon}_2(t) + \dot{\Upsilon}_3(t) + \dot{\Upsilon}_4(t). \tag{4.76}$$

Taking the differentiation of $\Upsilon_1(t)$ along $\dot{\zeta}(t) = F(\zeta) + G(\zeta)\hat{\mu}^*(\zeta_j) + L(\zeta)\hat{v}^*(\zeta)$, following expression is obtained

$$\dot{\Upsilon}_1(t) = (\nabla J^*(\zeta))^\top(F(\zeta) + G(\zeta)\hat{\mu}^*(\zeta_j) + L(\zeta)\hat{v}^*(\zeta)).$$

Considering equation (4.24) and (4.25), above equation can be written as

$$\dot{\Upsilon}_1(t) = -\zeta^\top \bar{Q}\zeta - W(u^*(\zeta)) - \beta\|v^*(\zeta)\|^2 - 2g_M^2(\zeta) - \beta d_M^2(\zeta) + \gamma J^*(\zeta) + \underbrace{2\lambda\left(\tanh^{-1}\left(\frac{u^*(\zeta)}{\lambda}\right)\right)^\top (u^*(\zeta) - \hat{\mu}^*(\zeta_j))}_{L_1} + \underbrace{2\beta v^{*\top}(\zeta)(v^*(\zeta) - \hat{v}^*(\zeta))}_{L_2} \tag{4.77}$$

Using Young's inequality, one can write

$$L_1 \leq \lambda^2 \sum_{i=1}^{m}\left(\tanh^{-1}\left(\frac{u_i^*(\zeta)}{\lambda}\right)\right)^2 + \|\left(u^*(\zeta) - \hat{\mu}^*(\zeta_j)\right)\|^2. \tag{4.78}$$

Now using (4.31) and (4.78), following expression is obtained

$$-W(u^*(\zeta)) + L_1 \leq K_m + \|\left(u^*(\zeta) - \hat{\mu}^*(\zeta_j)\right)\|^2, \tag{4.79}$$

where $\|\pi_4\| \leq K_m$ and π_4 is mentioned in equation (4.32). Next,

$$\begin{aligned}
&\|\left(u^*(\zeta) - \hat{\mu}^*(\zeta_j)\right)\|^2 \\
&= \left\|-\lambda \tanh\left(\frac{1}{2\lambda}G^\top(\zeta)((\nabla\sigma_c(\zeta))^\top\omega_c + \nabla\epsilon_c(\zeta))\right) - \lambda\tanh\left(\frac{1}{2\lambda}G^\top(\zeta_j)(\nabla\sigma_c(\zeta_j))^\top\hat{\omega}_c\right)\right\|^2 \\
&\leq 2(A^2\nabla\sigma_{cM}^2 + B^2G_M^2)\|e_j\|^2\|\hat{\omega}_c\|^2 + 2G_M^2\nabla\sigma_{cM}^2\|\tilde{\omega}_c\|^2 + 2G_M^2\nabla\epsilon_{cM}^2.
\end{aligned} \tag{4.80}$$

Thus

$$\begin{aligned}
-W(u^*(\zeta)) + L_1 \leq K_m &+ 2(A^2\nabla\sigma_{cM}^2 + B^2G_M^2)\|e_j\|^2\|\hat{\omega}_c\|^2 \\
&+ 2G_M^2\nabla\sigma_{cM}^2\|\tilde{\omega}_c\|^2 + 2G_M^2\nabla\epsilon_{cM}^2.
\end{aligned} \tag{4.81}$$

Now, L_2 can be expressed as

$$\begin{aligned}
L_2 &\leq \beta\|v^*(\zeta)\|^2 + \beta\|(v^*(\zeta) - \hat{v}^*(\zeta)\|^2 \\
&\leq \beta\|v^*(\zeta)\|^2 + \beta\left\|-\frac{1}{2\beta}L^\top(\zeta)((\nabla\sigma_c(\zeta))^\top\omega_c + \nabla\epsilon_c(\zeta)) + \frac{1}{2\beta}L^\top(\zeta)(\nabla\sigma_c(\zeta))^\top\hat{\omega}_c\right\|^2 \\
&\leq \beta\|v^*(\zeta)\|^2 + \frac{1}{2\beta}L_M^2\nabla\sigma_{cM}^2(\|\tilde{\omega}_c\|^2 + \nabla\epsilon_{cM}^2).
\end{aligned} \tag{4.82}$$

Using (4.81) and (4.82) in (4.77), the following expression is deduced

$$\dot{\Upsilon}_1(t) \leq -\zeta^\top \bar{Q}\zeta - 2g_M^2(\zeta) - \beta d_M^2(\zeta) + \gamma J^*(\zeta) + K_m + 2(A^2\nabla\sigma_{cM}^2 + B^2G_M^2)\|e_j\|^2\|\hat{\omega}_c\|^2 + 2G_M^2\nabla\sigma_{cM}^2\|\tilde{\omega}_c\|^2 + 2G_M^2\nabla\epsilon_{cM}^2 + \frac{1}{2\beta}L_M^2\nabla\sigma_{cM}^2(\|\tilde{\omega}_c\|^2 + \nabla\epsilon_{cM}^2). \quad (4.83)$$

One can write $\omega_c^\top\phi = \phi^\top\omega_c$. Let us consider $\varphi = \phi/(1+\phi^\top\phi)$. In view of (4.69), the following expression is obtained

$$\dot{\Upsilon}_3(t) = -l_c\tilde{\omega}_c^\top\varphi\varphi^\top\tilde{\omega}_c + \frac{l_c}{(1+\phi^\top\phi)}\tilde{\omega}_c^\top\varphi e_{cH} - \frac{l_s}{2}\tilde{\omega}_c^\top\nabla\sigma_c(\zeta_j)G(\zeta_j)G^\top(\zeta)\nabla V(\zeta) - \frac{l_s}{2\beta}\tilde{\omega}_c^\top\nabla\sigma_c(\zeta)L(\zeta)L^\top(\zeta)\nabla V(\zeta). \quad (4.84)$$

Let $\lambda_M(\varphi\varphi^\top) = \lambda_{\varphi M}$ and $\lambda_m(\varphi\varphi^\top) = \lambda_{\varphi m}$. Now, utilising Young's inequality $2a_1^\top a_2 \leq a_1^\top a_1 + a_2^\top a_2$ and Assumption 3.1, (4.84) is written as

$$\dot{\Upsilon}_3(t) \leq -l_c\lambda_{\varphi m}\|\tilde{\omega}_c\|^2 + \frac{l_c}{2(1+\phi^\top\phi)}(\lambda_{\varphi M}\|\tilde{\omega}_c\|^2 + e_{cHM}^2) - \frac{l_s}{2}\tilde{\omega}_c^\top\nabla\sigma_c(\zeta_j)G(\zeta_j)G^\top(\zeta)\nabla V(\zeta) - \frac{l_s}{2\beta}\tilde{\omega}_c^\top\nabla\sigma_c(\zeta)L(\zeta)L^\top(\zeta)\nabla V(\zeta). \quad (4.85)$$

Similarly, taking the derivative of $\Upsilon_4(t)$, one can write

$$\begin{aligned}\dot{\Upsilon}_4(t) &= l_s(\nabla V(\zeta))^\top(F(\zeta) + G(\zeta)\hat{\mu}^*(\zeta_j) + L(\zeta)\hat{v}^*(\zeta)) \\ &= l_s(\nabla V(\zeta))^\top(F(\zeta) + G(\zeta)u^*(\zeta) + L(\zeta)v^*(\zeta)) \\ &\quad - l_s(\nabla V(\zeta))^\top G(\zeta)(u^*(\zeta) - \hat{\mu}^*(\zeta_j)) - l_s(\nabla V(\zeta))^\top L(\zeta)(v^*(\zeta) - \hat{v}^*(\zeta)) \end{aligned} \quad (4.86)$$

Simplifying the term $(u^*(\zeta) - \hat{\mu}^*(\zeta_j))$, the following expression is obtained

$$\begin{aligned}(u^*(\zeta) - \hat{\mu}^*(\zeta_j)) &= -(1-\tanh^2(\zeta))\left(\frac{1}{2}(G^\top(\zeta)(\nabla\sigma_c(\zeta))^\top - G^\top(\zeta_j)(\nabla\sigma_c(\zeta_j))^\top)\omega_c\right) \\ &\quad - (1-\tanh^2(\zeta))\left(\frac{1}{2}G^\top(\zeta)\nabla\epsilon_c(\zeta) + G^\top(\zeta_j)(\nabla\sigma_c(\zeta_j))^\top\tilde{\omega}_c\right). \end{aligned} \quad (4.87)$$

Thus, it follows that

$$
\begin{aligned}
&- l_s(\nabla V(\zeta))^\top (u^*(\zeta) - \hat{\mu}^*(\zeta_j)) \\
&\leq \frac{1}{2} l_s(\nabla V(\zeta))^\top G(\zeta) G^\top(\zeta_j)(\nabla \sigma_c(\zeta_j))^\top \tilde{\omega}_c + l_s \|V(\zeta)\| (2G_M^2 \nabla \sigma_{cM} \omega_{CM} + \frac{1}{2} G_M^2 \nabla \epsilon_{CM}).
\end{aligned} \tag{4.88}
$$

Similarly,

$$
(v^*(\zeta) - \hat{v}^*(\zeta)) = -\frac{1}{2\beta} L^\top(\zeta)(\nabla \sigma_c(\zeta))^\top \omega_c + \nabla \epsilon_c(\zeta)) + \frac{1}{2\beta} L^\top(\zeta)(\nabla \sigma_c(\zeta))^\top \hat{\omega}_c. \tag{4.89}
$$

Therefore

$$
-l_s(\nabla V(\zeta))^\top (v^*(\zeta) - \hat{v}^*(\zeta)) \leq \frac{l_s}{2\beta} \|V(\zeta)\| L_M^2 \nabla \epsilon_{CM} + \frac{l_s}{2\beta} (\nabla V(\zeta))^\top L(\zeta) L^\top(\zeta) \nabla \sigma_c^\top(\zeta) \tilde{\omega}_c. \tag{4.90}
$$

Using Assumption 3.1 and substituting (4.88) and (4.90) in (4.86), the following expression is deduced

$$
\begin{aligned}
\dot{\Upsilon}_4(t) \leq & -l_s \lambda_m(T) \|V(\zeta)\|^2 + \frac{1}{2} l_s (\nabla V(\zeta))^\top G(\zeta) G^\top(\zeta_j)(\nabla \sigma_c(\zeta_j))^\top \tilde{\omega}_c \\
& + l_s \|V(\zeta)\| (2G_M^2 \nabla \sigma_{cM} \omega_{CM} + \frac{1}{2} G_M^2 \nabla \epsilon_{CM}) \\
& + \frac{l_s}{2\beta} \|V(\zeta)\| L_M^2 \nabla \epsilon_{CM} + \frac{l_s}{2\beta} (\nabla V(\zeta))^\top L(\zeta) L^\top(\zeta) \nabla \sigma_c^\top(\zeta) \tilde{\omega}_c.
\end{aligned} \tag{4.91}
$$

Now, utilising Assumptions 2.1 to 2.4, along with Assumptions 3.1, 3.2, and 4.1, one can write

$$
\begin{aligned}
&\dot{\Upsilon}_3(t) + \dot{\Upsilon}_4(t) \\
&\leq -l_c \lambda_{\varphi m} \|\tilde{\omega}_c\|^2 + \frac{l_c}{2(1+\phi^\top \phi)} (\lambda_{\varphi M} \|\tilde{\omega}_c\|^2 + e_{cHM}^2) - l_s \lambda_m(T) \|V(\zeta)\|^2 \\
&\quad + l_s \|V(\zeta)\| \left(2G_M^2 \nabla \sigma_{cM} \omega_{CM} + \frac{1}{2} G_M^2 \nabla \epsilon_{CM} + \frac{1}{2\beta} L_M^2 \nabla \epsilon_{CM} \right) \\
&\leq -l_c \lambda_{\varphi m} \|\tilde{\omega}_c\|^2 + \frac{l_c}{2(1+\phi^\top \phi)} (\lambda_{\varphi M} \|\tilde{\omega}_c\|^2 + e_{cHM}^2) \\
&\quad - l_s \lambda_m(T) \left(\|V(\zeta)\| - \frac{\kappa_1}{2\lambda_m(T)} \right)^2 + \frac{l_s \kappa_1^2}{4\lambda_m(T)} \\
&\leq -l_c \lambda_{\varphi m} \|\tilde{\omega}_c\|^2 + \frac{l_c \lambda_{\varphi M}}{2(1+\phi^\top \phi)} \|\tilde{\omega}_c\|^2 - l_s \lambda_m(T) \left(\|V(\zeta)\| - \frac{\kappa_1}{2\lambda_m(T)} \right)^2 + \kappa_2,
\end{aligned} \tag{4.92}
$$

where $\kappa_1 = \left(2G_M^2 \nabla\sigma_{cM}\omega_{CM} + \frac{1}{2}G_M^2\nabla\epsilon_{CM} + \frac{1}{2\beta}L_M^2\nabla\epsilon_{CM}\right)$ and $\kappa_2 = \frac{l_s\kappa_1^2}{4\lambda_m(T)} + \frac{l_c e_{cHM}^2}{2(1+\phi^\top\phi)}$. Now substituting (4.83) and (4.92) into (4.76), the time derivative of the Lyapunov function can be expressed as

$$\begin{aligned}\dot{\Upsilon}(t) \leq & -\zeta^\top\bar{Q}\zeta - 2g_M^2(\zeta) - \beta d_M^2(\zeta) + 2(A^2\nabla\sigma_{cM}^2 + B^2G_M^2)\|e_j\|^2\|\hat{\omega}_c\|^2 \\ & - \left(-2G_M^2\nabla\sigma_{cM}^2 - \frac{1}{2\beta}L_M^2\nabla\sigma_{cM}^2 + l_c\lambda_{\varphi m} - \frac{l_c\lambda_{\varphi M}}{2(1+\phi^\top\phi)}\right)\|\tilde{\omega}_c\|^2 \\ & - l_s\lambda_m(T)\left(\|V(\zeta)\| - \frac{\kappa_1}{2\lambda_m(T)}\right)^2 + \kappa, \end{aligned} \tag{4.93}$$

where $\kappa = 2G_M^2\nabla\epsilon_{cM}^2 + \frac{1}{2\beta}L_M^2\nabla\sigma_{cM}^2\nabla\epsilon_{cM}^2 + \gamma J_{max}^* + K_m + \kappa_2$. Considering the fact $\zeta^\top(t)\bar{Q}\zeta(t) = e_r^\top(t)Qe_r(t)$ and introducing the design parameter η_2, (4.93) can be rewritten as

$$\begin{aligned}\dot{\Upsilon}(t) \leq & -\eta_2^2\lambda_m(Q)\|e_r(t)\|^2 - (1-\eta_2^2)\lambda_m(Q)\|e_r(t)\|^2 - 2g_M^2(\zeta) - \beta d_M^2(\zeta) \\ & + 2(A^2\nabla\sigma_{cM}^2 + B^2G_M^2)\|e_j\|^2\|\hat{\omega}_c\|^2 \\ & - \left(l_c\lambda_{\varphi m} - 2G_M^2\nabla\sigma_{cM}^2 - \frac{1}{2\beta}L_M^2\nabla\sigma_{cM}^2 - \frac{l_c\lambda_{\varphi M}}{2(1+\phi^\top\phi)}\right)\|\tilde{\omega}_c\|^2 \\ & - l_s\lambda_m(T)\left(\|V(\zeta)\| - \frac{\kappa_1}{2\lambda_m(T)}\right)^2 + \kappa, \end{aligned} \tag{4.94}$$

If the inequalities (4.72), (4.73) and (4.74) stated in Theorem 4.4 satisfied then (4.94) indicates that $\dot{\Upsilon}(t) < 0$, i.e., the proposed Lyapunov function candidate has negative time derivative for all $t \in [t_j, t_{j+1})$.

Case 2. When $t \in t_{j+1}$, i.e., the events are triggered. The difference of the Lyapunov function candidate is expressed as

$$\begin{aligned}\Delta\Upsilon(t_j) = & J^*(\zeta(t_j^+)) - J^*(\zeta(t_j)) + \frac{1}{2}\tilde{\omega}_c^\top(t_j^+)\tilde{\omega}_c(t_j^+) - \frac{1}{2}\tilde{\omega}_c^\top(t_j)\tilde{\omega}_c(t_j)) \\ & + J^*(\zeta_{j+1}) - J^*(\zeta_j) + l_s(V(t_j^+) - V(t_j)), \end{aligned} \tag{4.95}$$

where $\zeta(t_j^+) = \lim_{\varsigma\to 0^+}\zeta(t_j+\varsigma)$ and $\varsigma \in (0, t_{j+1} - t_j)$. In Case 1, it was determined that $\dot{\Upsilon}(t) < 0 \quad \forall t \in [t_j, t_{j+1})$, hence

$$\begin{aligned}\Upsilon(t_j) \geq & \lim_{\varsigma\to 0^+}\Upsilon(t_j+\varsigma) \quad \forall\varsigma \in (0, t_{j+1} - t_j), j \in \mathbb{N} \\ \triangleq & \Upsilon(t_j^+). \end{aligned} \tag{4.96}$$

Hence, one can express

$$J^*(\zeta(t_j^+)) + \frac{1}{2}\tilde{\omega}_c^\top(t_j^+)\tilde{\omega}_c(t_j^+) + l_s V(t_j^+) - J^*(\zeta_j) - \frac{1}{2}\tilde{\omega}_c^\top(t_j)\tilde{\omega}_c(t_j)) - l_s V(t_j) \le 0. \quad (4.97)$$

It can be further written as

$$(J^*(\zeta_{j+1}) - J^*(\zeta_j)) \le -\vartheta\|e_{j+1}(t_j)\|, \quad (4.98)$$

where ϑ is a class $\mathcal{K}$ function and $e_{j+1}(t_j) = \zeta_{j+1} - \zeta_j$. From the above two inequalities, it can be inferred that the proposed Lyapunov function candidate is monotonically decreasing for all $t \in t_{j+1}$.

The above two cases prove that the closed loop system is locally asymptotically stable and the weights approximation error is uniformly ultimately bounded.

Considering the aforementioned analyses, the block diagram of the event-based ADP control algorithm utilized to obtain the optimal tracking controller is shown in Figure 4.1.

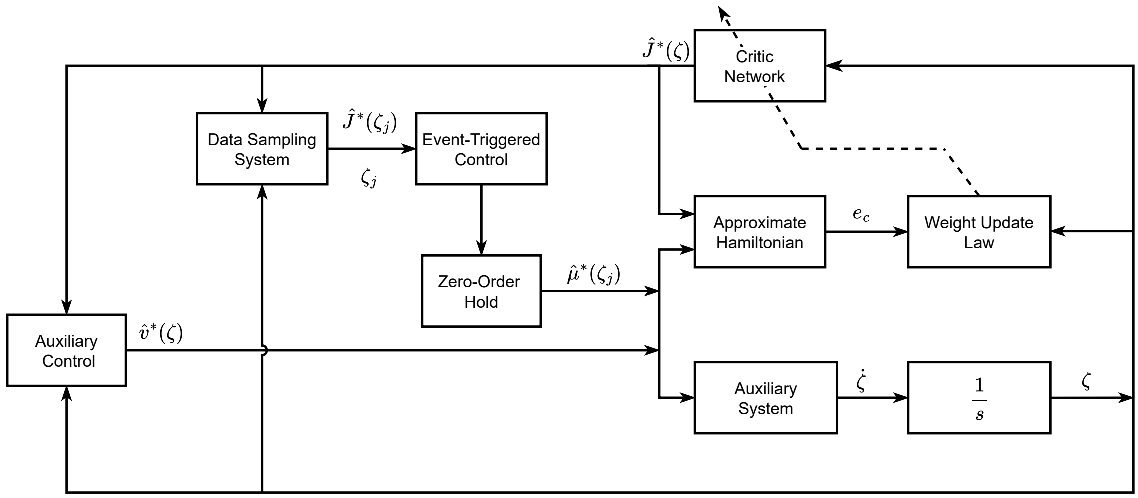

Figure 4.1: Block diagram of the proposed scheme.

4.6 Simulation Study

This section presents two simulation examples to show the developed methodology's effectiveness. In the first example, the spring-mass-damper system is considered where the spring is considered to be linear. In the second example, Vander Pol's oscillator is considered which is a nonlinear system.

4.6.1 Example 1

The dynamics of the spring-mass-damper system can be presented as

$$\dot{x} = \begin{bmatrix} x_2 \\ -\frac{\bar{k}}{m}x_1 - \frac{c}{m}x_2 \end{bmatrix} + \begin{bmatrix} 0 \\ \frac{1}{m} \end{bmatrix} u, \tag{4.99}$$

where x_1 is the position, x_2 is the velocity, $u \in \{u \in \mathbb{R} : |u| \leq 1\}$ is the control input i.e., $\lambda = 1$, m is the mass, c is the damping coefficient and $\bar{k}$ is the stiffness of the spring. Now considering unmatched uncertainty and taking $c = 5$N, $m = 1$Kg, and $\bar{k} = 0.5$, the linear spring-mass-damper system with nonlinear unmatched uncertainty is represented as

$$\dot{x} = \begin{bmatrix} x_2 \\ -5x_1 - 0.5x_2 \end{bmatrix} + \begin{bmatrix} 0 \\ 1 \end{bmatrix} u + \begin{bmatrix} 1 \\ 0 \end{bmatrix} d_1(x), \tag{4.100}$$

where $d_1(x) = 0.5\theta_1 x_1 x_2 cos(x_1) sin(x_2 + \theta_2)$ with $\theta_1, \theta_2 \in (-1, 1)$. The upper bound of $d_1(x)$ is considered as $d_M(x) = |x_1||x_2|$. Let the initial state $x(0) = [1, -1]^\top$.

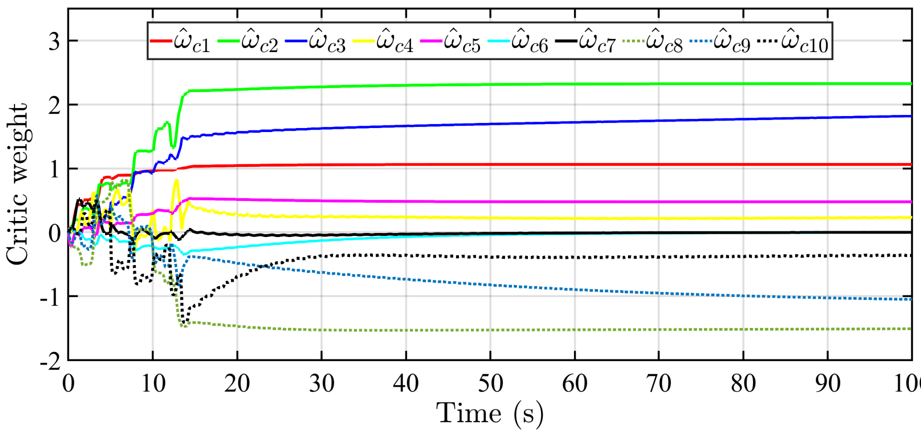

Figure 4.2: Convergence process of critic weights.

The reference trajectory $x_r(t)$ is generated from

$$\dot{x}_r(t) = \begin{bmatrix} x_{r2} \\ -5x_{r1} \end{bmatrix}, \tag{4.101}$$

with the initial condition $x_r(0) = [0.5, 0.5]^\top$. The tracking error, defined as the difference between the system state and the reference trajectory, is given as $e_r(t) = x(t) - x_r(t)$.

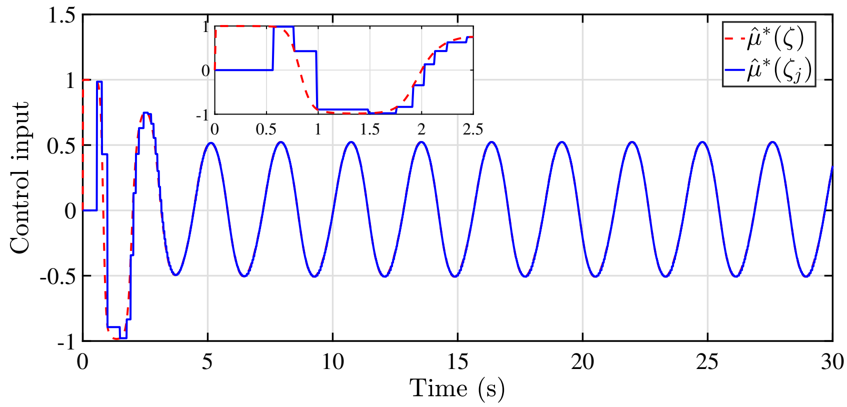

Figure 4.3: Control input.

The augmented state is constructed using the reference trajectory and the tracking error as $\zeta = [e_r^\top, x_r^\top]^\top \in \mathbb{R}^4$ and then the resulting augmented system is formulated as follows

$$\dot{\zeta} = \begin{bmatrix} \zeta_2 \\ -5\zeta_1 - 0.5(\zeta_2 + \zeta_4) \\ \zeta_4 \\ -5\zeta_3 \end{bmatrix} + \begin{bmatrix} 0 \\ 1 \\ 0 \\ 0 \end{bmatrix} u(\zeta) + \begin{bmatrix} 1 \\ 0 \\ 0 \\ 0 \end{bmatrix} d(\zeta), \tag{4.102}$$

where $d(\zeta) = 0.5\theta_1(\zeta_1 + \zeta_3)(\zeta_2 + \zeta_4)cos(\zeta_1 + \zeta_3)sin((\zeta_2 + \zeta_4) + \theta_2)$. The initial condition is derived as $\zeta(0) = [0.5, -1.5, 0.5, 0.5]^\top$. The upper-bound of $d(\zeta)$ is considered as $d_M(\zeta) = |\zeta_1 + \zeta_3||\zeta_2 + \zeta_4|$. Since $\|G^+(\zeta)K(\zeta)d(\zeta)\| = 0$, $g_M(\zeta)$ is considered as 0.

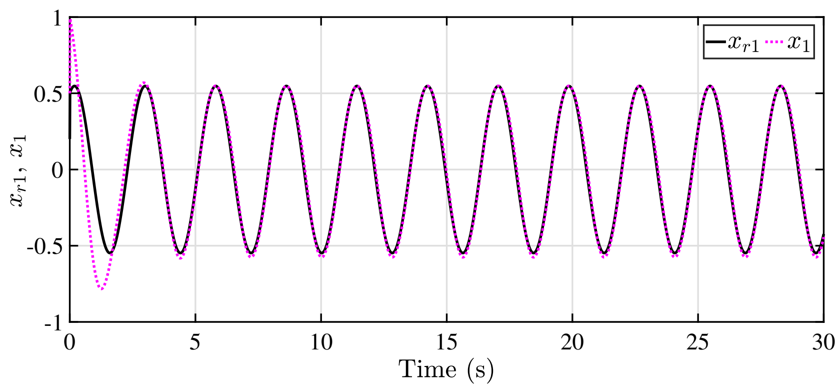

Figure 4.4: Tracking performance of x_1 for $\theta_1 = 0.7$ and $\theta_2 = -0.7$.

The auxiliary system is formed as

$$\dot{\zeta} = \begin{bmatrix} \zeta_2 \\ -5\zeta_1 - 0.5(\zeta_2 + \zeta_4) \\ \zeta_4 \\ -5\zeta_3 \end{bmatrix} + \begin{bmatrix} 0 \\ 1 \\ 0 \\ 0 \end{bmatrix} u(\zeta) + \begin{bmatrix} 1 \\ 0 \\ 0 \\ 0 \end{bmatrix} v(\zeta), \tag{4.103}$$

where $v(\zeta) \in \mathbb{R}$ is the auxiliary controller. The parameters in the corresponding modified cost function (4.10) are chosen as $\gamma = 0.9$, $\bar{Q} = diag\{100I_2, 0_{2\times2}\}$ and $\beta = 0.4$. A critic network with 10 neurons in the hidden layer is employed to approximate the modified cost function. The activation function is taken as $\sigma_c(\zeta) = [\zeta_1^2, \zeta_2^2, \zeta_3^2, \zeta_4^2, \zeta_1\zeta_2, \zeta_1\zeta_3, \zeta_1\zeta_4, \zeta_2\zeta_3, \zeta_2\zeta_4, \zeta_3\zeta_4]^\top$ and the parameters in weight update law (4.65) are chosen as $l_c = 2.5$, $l_s = 0.45$, $(A^2\nabla\sigma_{cM}^2 + B^2G_M^2) = 2$, and $\eta_2 = 0.7$.

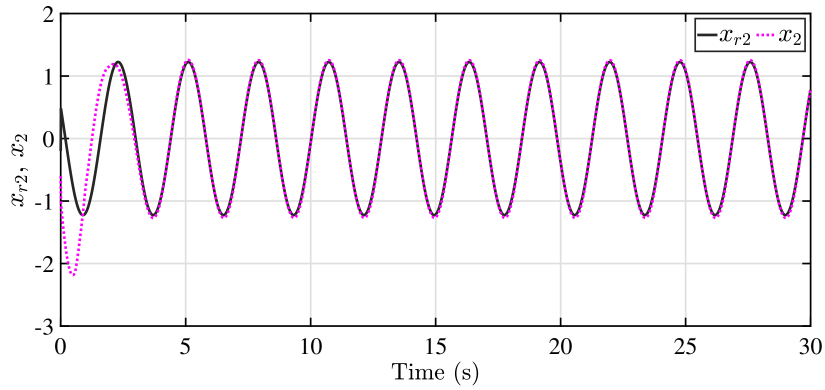

Figure 4.5: Tracking performance of x_2 for $\theta_1 = 0.7$ and $\theta_2 = -0.7$.

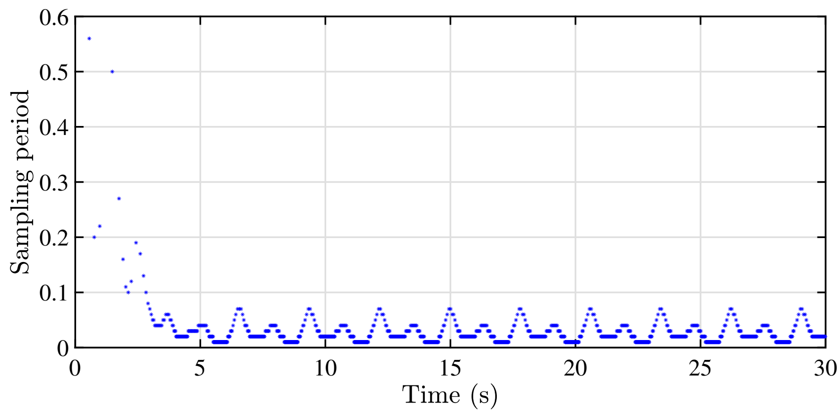

Figure 4.6: Triggering instants during the tracking process.

During the weight update process triggering rule (4.72) is employed. All the 10 elements of the weight vector are chosen as 0 at the beginning of the weight update process, and a probing noise is added during the initial few seconds of the weight update. The convergence process of critic weight vector is shown in Figure 4.2 and the converged value is $\hat{\omega}_c = [1.06, 2.33, 1.82, 0.23, 0.47, 0, 0, -1.51, -1.05, -0.36]^\top$. During the training process, the event-triggered controller updates only 5748 times while the time triggered controller updates 10000 times.

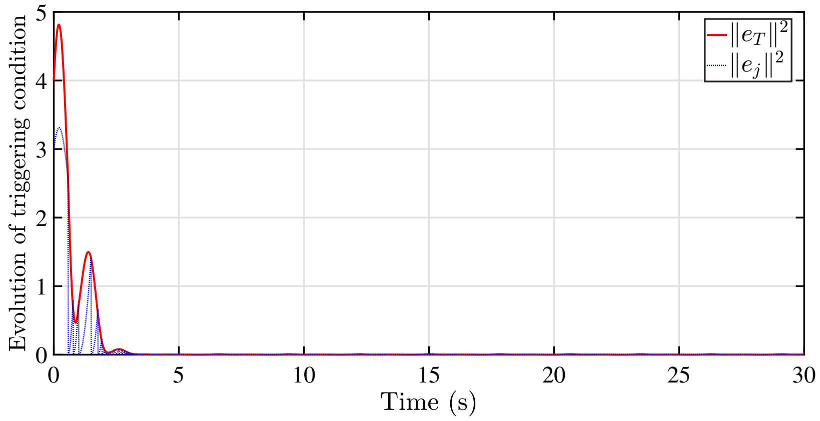

Figure 4.7: Evolution of the triggering condition with $\|e_T\|^2$ and $\|e_j\|^2$.

Remark 4.5. During the simulation, in both the examples, the sampling frequency η_2 and the design parameter β, are intentionally chosen to make the terms $\|e_T\|^2$ and $\|\hat{e}_T\|^2$ positive, respectively. Increasing η_2 and β increases the sampling frequency and the number of event-triggered instants, leading to improved tracking performance. However, balancing the number of triggering instants and the tracking performance is crucial. Following the approach in relevant literature [86], other parameters are heuristically selected to minimize the convergence time of the critic weights and the number of triggering instants while maintaining an acceptable level of tracking performance.

The converged weights are used to derive the auxiliary controller (4.59) and the event-triggered controller (4.60). The obtained event-triggered controller (4.60) is within its constraint value $\lambda = 1$ as shown in Figure 4.3. In Figure 4.3, $\hat{\mu}^*(\zeta)$ represents the time-triggered control input. During the implementation phase, the event-triggering rule (4.22) is used, where the Lipschitz constant $\mathcal{L}$ is chosen as 2.5. To evaluate the tracking performance, θ_1 is chosen as 0.7 and θ_2 as -0.7. The tracking performance is shown in Figure 4.4 and Figure 4.5. These figures show the system's ability to accurately follow the reference trajectory.

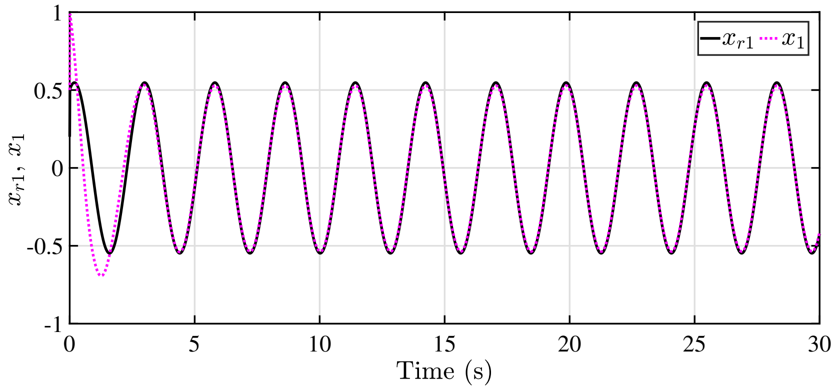

Figure 4.8: Tracking performance of x_1 for $\theta_1 = -0.3$ and $\theta_2 = 0.5$.

Figure 4.7 shows the two norm square of the event-triggering threshold e_T and the event-triggering error e_j. This plot shows how the triggering threshold and the triggering gap or error evolve over time. From Figure 4.6, it can be seen that the Zeno-behavior is avoided. The minimum sampling instant is found to be 0.01. During the implementation phase, using the event-triggered controller, 1290 samples are used, and while using the time-triggered controller $\hat{\mu}^*(\zeta)$, 3000 samples are used.

The time-triggered guaranteed cost is calculated as $\hat{\omega}_c^\top \sigma(\zeta(0))$, and from equation (4.36), it is clear that the event-triggered guaranteed is greater than the time-triggered one. Although the cost is more in the event-triggered scheme, the benefit is the significant reduction in the state samples.

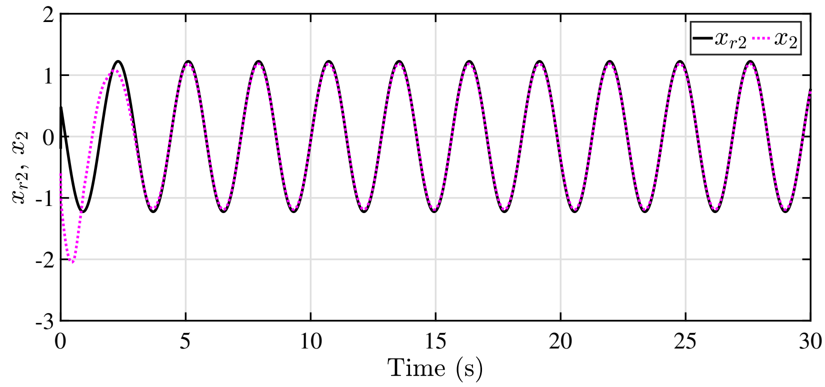

Figure 4.9: Tracking performance of x_2 for $\theta_1 = -0.3$ and $\theta_2 = 0.5$.

During the learning phase, the triggering rule (4.72) is applied with the sampling frequency η_2 in the range $(0, 1)$. During the implementation phase, the trigger rule (4.22) is utilized with the design parameter β in the range $(0, 0.5)$. Let $\nu\%$ represent the percentage by which the number of triggering instants is reduced compared to the time-based case. The table below demonstrates the correlation between η_2 and $\nu\%$, and β and $\nu\%$. It is evident from the table that an increase in the value of η_2 and β correspond to a higher number of event-triggering instants.

Table 4.1: Effect of η_2 and β on number of triggering instants.

Case no.	Learning phase		Implementation phase	
	η_2	$\nu\%$	β	$\nu\%$
1	0.6	44.38	0.3	86.1
2	0.7	42.52	0.35	61.67
3	0.8	38.87	0.4	57
4	0.9	30.28	0.45	45.2

Now to demonstrate the robust tracking performance, let us change the values of θ_1 and θ_2 to -0.3 and 0.5, respectively. The tracking performance of the proposed controller after changing the value of θ_1 and θ_2 are shown in Figure 4.8 and Figure 4.9. In this case, the event-triggered controller updates 1445 times whereas the conventional time-triggered controller updates 3000 times.

4.6.2 Example 2

Consider the dynamical model of the controlled Vander Pol's oscillator with unmatched uncertainty as given below

$$\dot{x} = \begin{bmatrix} x_2 \\ -x_1 - x_2(x_1^2 - 1) \end{bmatrix} + \begin{bmatrix} 0 \\ 1 \end{bmatrix} u + \begin{bmatrix} 1 \\ 0 \end{bmatrix} d_1(x), \tag{4.104}$$

where $d_1(x) = 0.5\theta_1 x_1 x_2 sin(x_1) cos(x_2 + \theta_2)$ with $\theta_1, \theta_2 \in (-1, 1)$ and $|u| \leq 2$ i.e., $\lambda = 2$. Let the initial state $x(0) = [0.4, 0.2]^\top$. The reference trajectory $x_r(t)$ is obtained from the following system

$$\dot{x}_r(t) = \begin{bmatrix} x_{r2} \\ -x_{r1} \end{bmatrix}, \tag{4.105}$$

where $x_r(0) = [0.1, 0.5]^\top$. Next, as in example 1, the tracking error $e_r(t) = x(t) - x_r(t)$ is defined and the augmented state $\zeta = [e_r^\top, x_r^\top]^\top \in \mathbb{R}^4$ is formed. After that the following augmented system is formed

$$\dot{\zeta} = \begin{bmatrix} \zeta_2 \\ -\zeta_1 - (\zeta_2 + \zeta_4)((\zeta_1 + \zeta_3)^2 - 1) \\ \zeta_4 \\ -\zeta_3 \end{bmatrix} + \begin{bmatrix} 0 \\ 1 \\ 0 \\ 0 \end{bmatrix} u(\zeta) + \begin{bmatrix} 1 \\ 0 \\ 0 \\ 0 \end{bmatrix} d(\zeta). \tag{4.106}$$

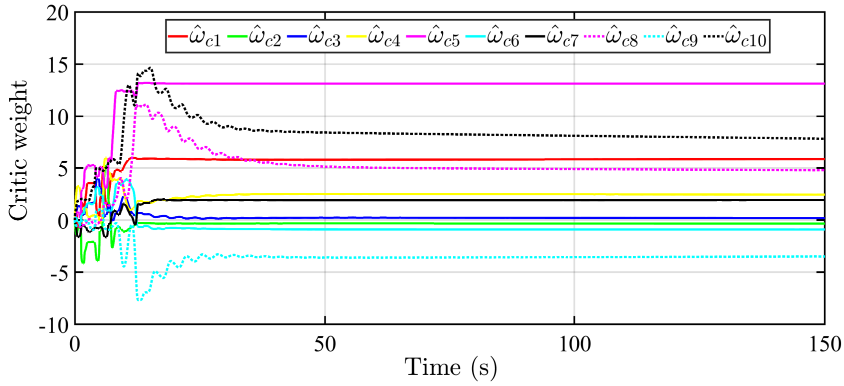

Figure 4.10: Convergence process of critic weights.

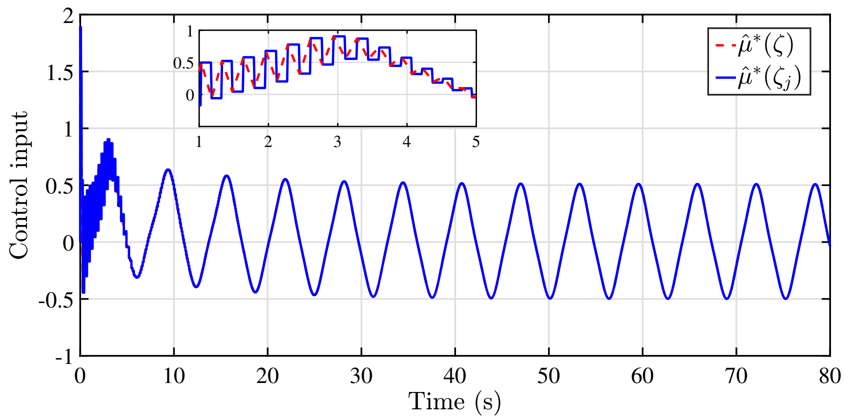

Figure 4.11: Control input.

Now, an auxiliary control $v(\zeta)$ is introduced and an auxiliary system is formed as given below

$$\dot{\zeta} = \begin{bmatrix} \zeta_2 \\ -\zeta_1 - (\zeta_2 + \zeta_4)((\zeta_1 + \zeta_3)^2 - 1) \\ \zeta_4 \\ -\zeta_3 \end{bmatrix} + \begin{bmatrix} 0 \\ 1 \\ 0 \\ 0 \end{bmatrix} u(\zeta) + \begin{bmatrix} 1 \\ 0 \\ 0 \\ 0 \end{bmatrix} v(\zeta). \tag{4.107}$$

The parameters of the cost function, as specified in (4.10), are set as $\bar{Q} = diag\{200I_2, 0_{2\times 2}\}$, $\gamma = 0.9$, and $\beta = 0.4$. Additionally, 10 neurons are chosen for the hidden layer of the critic network and the activation function is chosen as

$$\sigma_c(\zeta) = [\zeta_1^2, \zeta_1\zeta_2, \zeta_1\zeta_3, \zeta_1\zeta_4, \zeta_2^2, \zeta_2\zeta_3, \zeta_2\zeta_4, \zeta_3^2, \zeta_3\zeta_4, \zeta_4^2]^\top.$$

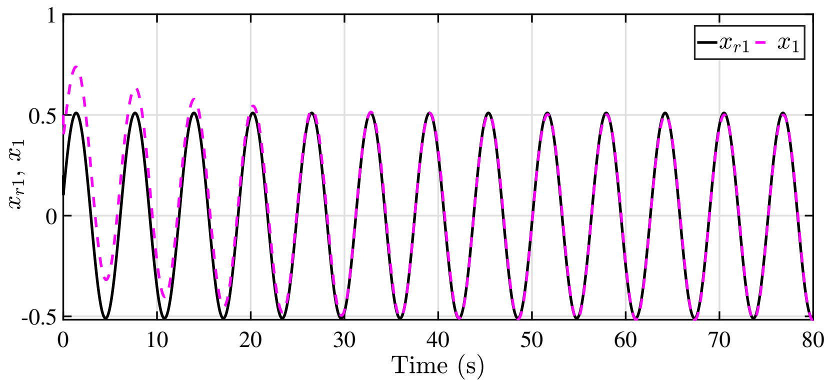

Figure 4.12: Tracking performance of x_1 for $\theta_1 = -0.4$ and $\theta_2 = 0.6$.

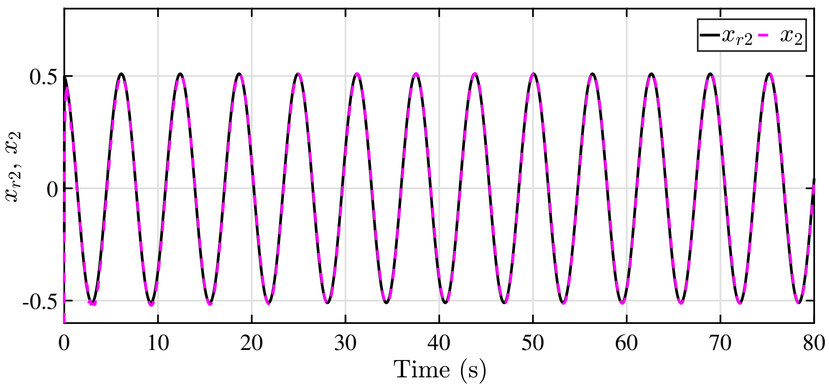

Figure 4.13: Tracking performance of x_2 for $\theta_1 = -.4$ and $\theta_2 = 0.6$.

The parameters of the critic weight update rule (4.65) are selected as $l_c = 3.5$ and $l_s = 0.1$. During the training phase, the event-triggering rule (4.72) is used and the parameters are selected as $(A^2\nabla\sigma_{cM}^2 + B^2G_M^2) = 8$ and $\eta_2 = 0.6$. The critic weight vector is initialized at zero, and a probing noise is added at the beginning for a few seconds of the weight update process. After 150 seconds, the critic weight vector $\hat{\omega}_c$ converges to

$$[5.8520, -0.3239, 0.1992, 2.4425, 13.1373, 0.9042, 1.9143, 4.7839, -3.4844, 7.8547]^\top$$

as shown in Figure 4.10. During the weight tuning phase, the event-based controller updates 6546 whereas the time-triggered controller updates 15000 times. It shows that using the event-based controller, significant amount of computational resources can be saved.

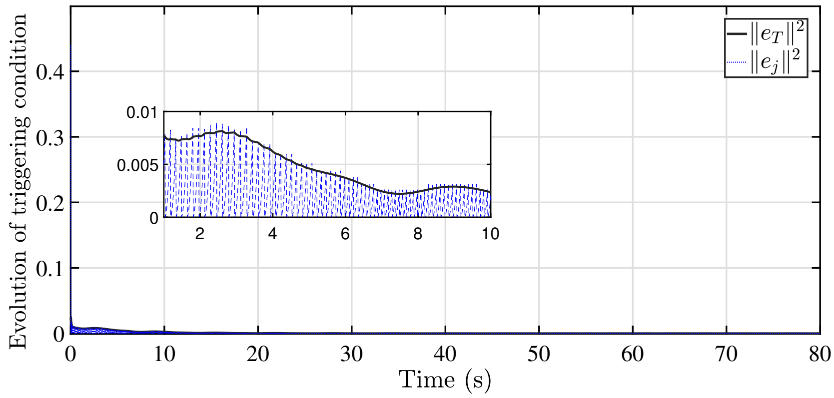

Figure 4.14: Evolution of the triggering condition with $\|e_T\|^2$ and $\|e_j\|^2$.

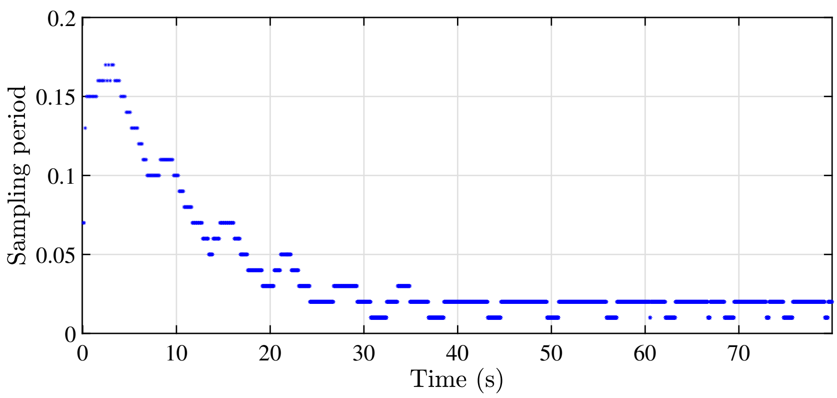

Figure 4.15: Triggering instants during the tracking process.

Next, the converged weights are used in implementation phase where the triggering rule given by equation (4.22) is utilised. $\mathcal{L}$ is set to 12, while θ_1 is chosen as -0.4 and θ_2 as 0.6.

From Figure 4.11, it can be seen that the event-based tracking controller is within its constraint value. The tracking performance are shown in Figure 4.12 and Figure 4.13.

Figure 4.14 shows the norm square of triggering error e_j and the triggering threshold e_T. In Figure 4.15, the sampling period is shown and the minimum sampling period is found to be 0.01. From Figure 4.15, it is found that only 3650 state samples are used while implementing the developed event-triggered tracking controller. Nonetheless, while using the conventional time-triggered method 8000 samples are needed.

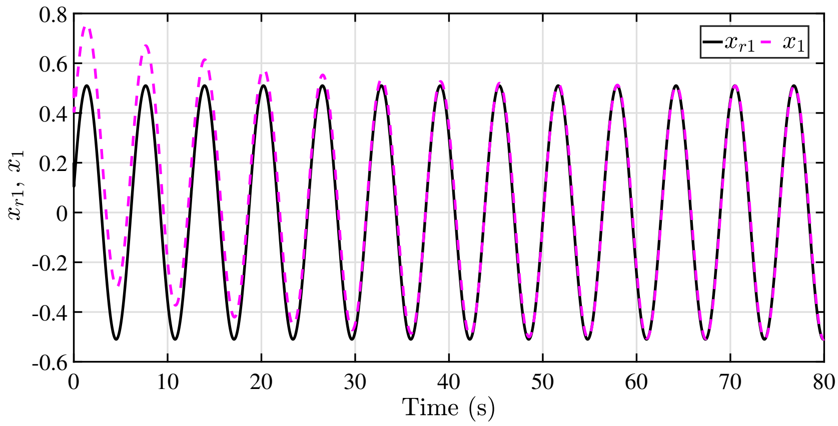

Figure 4.16: Tracking performance of x_1 for $\theta_1 = 0.1$ and $\theta_2 = -0.9$.

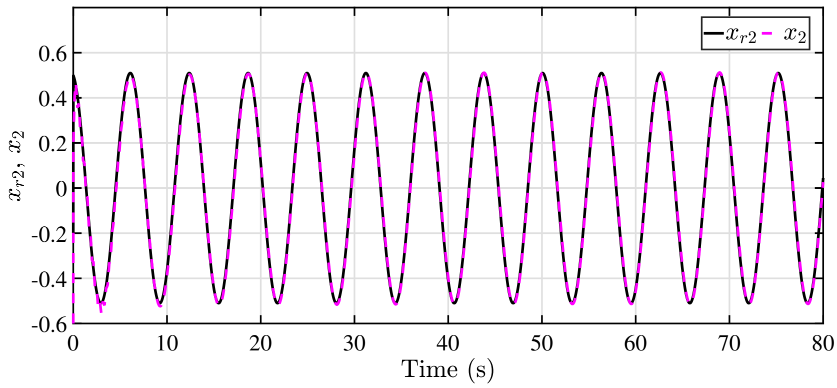

Figure 4.17: Tracking performance of x_2 for $\theta_1 = 0.1$ and $\theta_2 = -0.9$.

The time-triggered guaranteed cost is calculated as 3.6 and the event-triggered guaranteed cost is more than 3.6. Although the guaranteed cost is higher in the event-triggered method, this work considers a reduction in computational burden as the primary factor.

Now the values of θ_1 and θ_2 are changed to 0.1 and -0.9, respectively. The tracking performance for the new value of θ_1 and θ_2 are found to be satisfactory and shown in Figure 4.16 and Figure 4.17. In this case, the event-triggered controller updates 3075 times.

4.7 Summary

This event-based ADP technique is employed in this chapter to investigate and develop a guaranteed cost robust tracking controller for constrained input nonlinear systems with unmatched uncertainty. Initially, the control problem is reformulated into an optimal regulation problem for an auxiliary system, streamlining the controller design process. Utilizing a single critic NN, the solution to the associated HJB equation is obtained, highlighting the efficacy of ADP methods in handling complex control scenarios. Meanwhile, it is shown that while using the derived event-triggered controller, the tracking error is uniformly ultimately bounded. The event-based guaranteed cost is ensured to be upper bounded, confirming the designed controller's robustness in the face of uncertainties. Additionally, utilizing the Lyapunov approach, the UUB of the weight estimation error is established, further confirming the stability and performance characteristics of the proposed control scheme. Finally, through simulation validation with two examples, the effectiveness and robustness of the methodology are successfully demonstrated.

5

Event-Triggered ADP-Based Tracking Controller for Partially Unknown Nonlinear Uncertain Systems with Input and State Constraints

Contents

5.1 Introduction

In addition to control input constraints, state constraints must also be considered while designing a controller to ensure both optimal performance and system safety. Control input constraints, such as actuator limits, are vital for preventing commands that exceed the physical capabilities of the system components. However, state constraints such as position, velocity, and acceleration restrictions are equally crucial for maintaining the system within safe and efficient operational boundaries. These constraints work together to guide the design of tracking controllers, ensuring that the system achieves its performance objectives and remains stable and secure under various operating conditions. Neglecting these constraints can lead to sub-optimal performance, potential damage, or even catastrophic failure, underscoring the importance of a comprehensive approach that integrates input and state considerations in controller design.

In the earlier chapters, the control design is developed assuming that the system dynamics are fully known. While this assumption is common in theoretical analysis, it often fails to hold in practical systems due to modeling inaccuracies, parameter uncertainties, and external disturbances. Therefore, addressing control design for partially unknown nonlinear systems becomes essential. In particular, the problem of tracking control for such systems, subjected to both input and state constraints, using an event-triggered ADP framework remains unexplored in the existing literature.

This chapter explores the problem of robust tracking control of partially unknown unmatched uncertain nonlinear systems with input and state constraints. The event-based ADP approach is employed to address this challenge. Initially, an identifier neural network is designed to approximate the unknown dynamics. Then, the augmented uncertain system is created by merging the tracking error and reference trajectory. Subsequently, decomposing the uncertainty into matched and unmatched components transforms the original tracking problem into the optimal regulation problem of an auxiliary system. The unknown part of the system dynamics is approximated using a neural network. A novel safe HJB equation is formulated by incorporating a control barrier function (CBF) and a nonquadratic term into the cost function to penalize violations of safety regulations. Solving the new safe HJB equation involves employing a critic NN to approximate the solution. The Lyapunov stability theory is applied to demonstrate that, under state constraints and uncertain disturbances, the system states and parameters of the critic neural network are assured to be UUB. The developed theoretical work is verified by simulation study.

The remainder of this chapter is structured as follows. In Section 5.2, the problem formulation is introduced. Section 5.3 presents the design of a neural network-based data-driven identifier to approximate the unknown drift dynamics of the system. The properties of the control barrier function are discussed in Section 5.4. Section 5.5 develops the event-triggered safe HJB equation along with the design of the event-triggering mechanism. In Section 5.6, a critic network is constructed within the ADP framework to approximate the cost function. A Lyapunov-based stability analysis is carried out in Section 5.7, ensuring that all signals in the closed-loop auxiliary system remain uniformly ultimately bounded. Section 5.8 presents a simulation example to verify the theoretical findings. Finally, Section 5.9 concludes the chapter with a summary.

5.2 Problem Description

Consider the continuous-time nonlinear uncertain system given in the form

$$\dot{x}(t) = f(x(t)) + g(x(t))u(t) + \Delta f(x(t)), \tag{5.1}$$

where $x(t) \in \mathcal{D} \subset \mathbb{R}^n$ and $u(t) \in \mathbb{R}^m$ are the state vector and control input, respectively, $\mathcal{D}$ represents the set of safe feasible states. The control input $u(t) \in \mathbb{R}^m$ is defined such that its elements are denoted by $u_i(t)$, $i = 1, \ldots, m$, and each element is constrained by a saturating bound $\lambda \in \mathbb{R}^+$. Let $x(0) = x_0$ be the initial state. The drift dynamics $f(x)$ is considered unknown with $f(0) = 0$. The unmatched uncertainty $\Delta f(x) = k(x)d_1(x)$, where $k(x) \in \mathbb{R}^{n \times p}$, $d_1(x) \in \mathbb{R}^p$ and if $m = p$ then $k(x) \neq g(x)$. Let $d_1(x)$ be bounded by a known function $d_M(x)$, i.e., $\|d_1(x)\| \leq d_M(x)$. Furthermore, $d_M(0) = 0$ and $d(0) = 0$. In addition, there exists a non-negative function $g_M(x)$ satisfying

$$\|g^+(x)\Delta f(x)\| \leq g_M(x),$$

where $g^+(x)$ is the pseudoinverse of $g(x)$. Let the desired trajectory $x_r(t) \in \mathbb{R}^n$ be generated from

$$\dot{x}_r(t) = Z(x_r(t)), \tag{5.2}$$

where $Z(x_r)$ satisfies the Lipschitz continuity and $Z(0) = 0$. Let $x_r(0) = x_{ro}$ be the initial condition.

This chapter aims to design an event-based robust optimal controller for the system (5.1). The designed controller ensures that the system state $x(t)$ accurately follows the desired trajectory $x_r(t)$. Additionally, the design must incorporate safety constraints, ensuring that the system states $x(t)$ remain within the safe set $\mathcal{D}$ and that each component of the control input stays within its specified bound λ. Moreover, the drift dynamics $f(x)$ is considered to be unknown and it is approximated using an identifier network.

5.3 Data-Based Identifier Design

Since the drift dynamics $f(x)$ is unknown, a data-based identifier is designed using a neural network in this section to approximate $f(x)$. First, the uncertain term $k(x)d_1(x)$ is divided into matched and unmatched components within the range space of $g(x)$, resulting in the expression

$$k(x)d_1(x) = g(x)g^+(x)k(x)d_1(x) + (I_n - g(x)g^+(x))k(x)d_1(x).$$

Then, the following auxiliary system is formed

$$\dot{x} = f(x) + g(x)u(t) + l(x)v(t), \tag{5.3}$$

where $l(x) = (I_n - g(x)g^+(x))k(x)$ and $v(t)$ is an auxiliary control introduced to handle the unmatched uncertainty component.

To address the issue of partially unknown dynamics, an identifier neural network is constructed and the auxiliary system (5.3) can be written as

$$\dot{x} = Sx + \omega_f^\top \sigma_f(x) + g(x)u(t) + l(x)v(t) + \epsilon_f, \tag{5.4}$$

where S, ω_f, $\sigma_f(x)$, and ϵ_f are the Hurwitz matrix, the ideal weight, the activation function, and the reconstruction error, respectively. The identifier dynamics can be rewritten as

$$\dot{\hat{x}} = S\hat{x} + \hat{\omega}_f^\top \sigma_f(\hat{x}) + g(x)u(t) + l(x)v(t) + \delta\tilde{x}, \tag{5.5}$$

where $\hat{x}$ and $\hat{\omega}_f$ are the estimates of x and the weight matrix ω_f, respectively. The state estimation error is $\tilde{x} = x - \hat{x}$. The state estimation error dynamics is obtained as

$$\begin{aligned}\dot{\tilde{x}} &= S\tilde{x} + \omega^\top \sigma_f(x) - \hat{\omega}^\top \sigma_f(\hat{x}) + \epsilon_f(x) - \delta\tilde{x} \\ &= S\tilde{x} + \tilde{\omega}^\top \sigma_f(\hat{x}) + \omega^\top \tilde{\sigma}_f + \epsilon_f(x) - \delta\tilde{x},\end{aligned} \tag{5.6}$$

where $\tilde{\sigma}_f = \sigma_f(x) - \sigma_f(\hat{x})$.

Assumption 5.1. The Hurwitz matrix S meets the condition

$$S^\top C + CS = -l_f I_n, \tag{5.7}$$

where $C > 0$ is a symmetric matrix and $l_f > 0$ is a constant.

Assumption 5.2. The identifier weight matrix ω_f, the approximation error $\epsilon_f(x)$, and the activation function $\sigma_f(x)$ are upper bounded by positive constants ω_{fM}, ϵ_{fM}, and σ_{fM}, respectively.

Theorem 5.1. For the system described by (5.3), employing the identifier given in (5.4) and adjusting the identifier weight according to the update law

$$\dot{\hat{\omega}}_f = -n_1 \sigma_f(\hat{x})\tilde{x}^\top (S - \delta I_n)^{-1} - n_2 \|\tilde{x}\| \hat{\omega}_f, \tag{5.8}$$

where n_1 and n_2 are tuning parameters, guarantees that both the state estimation error $\tilde{x}$ and the identifier weight estimation error $\tilde{\omega}_f$ are uniformly ultimately bounded (UUB).

Proof: Let us consider the following Lyapunov function candidate

$$L_f(t) = L_{f1}(t) + L_{f2}(t) \tag{5.9}$$

where $L_{f1} = \frac{1}{2}\tilde{x}^\top C \tilde{x}$ and $L_{f2} = \frac{1}{2}\,\mathrm{tr}\left(\tilde{\omega}_f^\top n_1^{-1} \tilde{\omega}_f\right)$. Taking the derivative of $L_{f1}(t)$ with respect to t and using equation (5.6), one can write

$$\begin{aligned}\dot{L}_{f1} &= \frac{1}{2}\tilde{x}^\top (S^\top C + CS)\tilde{x} + \tilde{x}^\top C \tilde{\omega}_f^\top \sigma_f(\hat{x}) + \tilde{x}^\top C \omega_f^\top \tilde{\sigma}_f + \tilde{x}^\top C \epsilon_f(x) - \delta \tilde{x}^\top C \tilde{x} \\ &= \frac{1}{2}\tilde{x}^\top (S^\top C + CS)\tilde{x} + \tilde{x}^\top C \tilde{\omega}_f^\top \sigma_f(\hat{x}) - \delta \tilde{x}^\top C \tilde{x} + \tilde{x}^\top C h_f\end{aligned} \tag{5.10}$$

where $h_f = \omega_f^\top \tilde{\sigma}_f + \epsilon_f(x)$. Using Assumption 5.1 and Assumption 5.2, from (5.10) one can write

$$\dot{L}_{f1} \leq -\frac{1}{2}\big(l_f + 2\delta\lambda_m(C)\big)\|\tilde{x}\|^2 + \|\tilde{x}\|\|C\|\left(\sigma_{fM}\|\tilde{\omega}_f\| + h_{fM}\right), \tag{5.11}$$

where h_{fM} is the bound of h_f. Now, taking the derivative of L_{f2} with respect to t, one can obtain

$$\begin{aligned}\dot{L}_{f2} &= \mathrm{tr}\left(\tilde{\omega}_f^\top \sigma_f(\hat{x})\tilde{x}^\top (S-\delta I_n)^{-1} + \frac{n_2}{n_1}\tilde{\omega}_f^\top \|\tilde{x}\|\,\hat{\omega}_f\right)\\ &= \mathrm{tr}\left(\tilde{x}^\top (S-\delta I_n)^{-1}\tilde{\omega}_f^\top \sigma_f(\hat{x}) + \frac{n_2}{n_1}\|\tilde{x}\|\,\tilde{\omega}_f^\top(\omega_f - \tilde{\omega}_f)\right)\\ &\leq \sigma_{fM}\|\tilde{x}\|\|(S-\delta I_n)^{-1}\|\|\tilde{\omega}_f\| + \frac{n_2}{n_1}\|\tilde{x}\|\left(\omega_{fM}\|\tilde{\omega}_f\| - \|\tilde{\omega}_f\|^2\right)\end{aligned} \tag{5.12}$$

Using (5.11) and (5.12), the derivative of the Lyapunov function candidate can be expressed as

$$\begin{aligned}\dot{L}_f(t) &\leq -\frac{1}{2}\big(l_f + 2\delta\lambda_m(C)\big)\|\tilde{x}\|^2 + \|\tilde{x}\|\left(\left(\|C\| + \big\|(S-\delta I_n)^{-1}\big\|\right)\sigma_{fM} + \frac{n_2}{n_1}\omega_{fM}\right)\|\tilde{\omega}_f\|\\ &\quad + \|\tilde{x}\|\|C\|\,h_{fM} - \frac{n_2}{n_1}\|\tilde{x}\|\|\tilde{\omega}_f\|^2\\ &= -\frac{1}{2}\big(l_f + 2\delta\lambda_m(C)\big)\|\tilde{x}\|^2 - \|\tilde{x}\|\left(\frac{n_2}{n_1}\|\tilde{\omega}_f\|^2 - b_1\|\tilde{\omega}_f\| - \|C\|\,h_{fM}\right)\\ &= -\frac{1}{2}\big(l_f + 2\delta\lambda_m(C)\big)\|\tilde{x}\|^2 - \frac{n_2}{n_1}\left(\|\tilde{\omega}_f\| - \frac{b_1 n_1}{2b_2}\right)^2\|\tilde{x}\| + b_2\|\tilde{x}\|\\ &\leq -\frac{1}{2}\big(l_f + 2\delta\lambda_m(C)\big)\|\tilde{x}\|^2 + b_2\|\tilde{x}\|\,,\end{aligned} \tag{5.13}$$

where $b_1 = \left(\|C\| + \big\|(S-\delta I_n)^{-1}\big\|\right)\sigma_{fM} + \frac{n_2}{n_1}\omega_{fM}$ and $b_2 = \frac{n_1}{4n_2}b_1^2 + h_{fM}\|C\|$. Based on equation (5.13), the derivative of the Lyapunov function $L_f(t)$ will be negative only if $\tilde{x}$ stays outside the set

$$\Omega_{\tilde{x}} = \left\{\tilde{x} : \|\tilde{x}\| \leq \frac{2b_2}{l_f + 2\delta\lambda_m(C)}\right\}. \tag{5.14}$$

This confirms that the identification error $\tilde{x}$ converges to the compact set $\Omega_{\tilde{x}}$. By selecting a sufficiently large parameter l_f, the set $\Omega_{\tilde{x}}$ described in (5.14) can be made arbitrarily small. Additionally, using the standard Lyapunov extension theorem, this also shows that the weight estimation error $\tilde{\omega}_f$ is uniformly ultimately bounded (UUB).

Remark 5.1. To be precise, the drift dynamics should be represented as $\hat{f}(\hat{x})$ for the subsequent analysis. However, this can lead to confusion. To maintain consistency and clarity in the discussion, $f(x)$ will be used to represent the drift dynamics, understanding that this denotes the converged value after the identifier network has completed the learning process.

5.4 Control Barrier Function

The control barrier function (CBF) originates from the concept of barrier functions in optimization and is designed to ensure system safety by confining the system states within a predefined safe set. A CBF remains positive within the safety set and increases toward infinity as the state approaches the set boundary. Its derivative is negative near the boundary, which helps push the state back into the safe region. In practice, CBF is incorporated into the optimal control problem by modifying the cost function to include a penalty term that penalizes violations of the safety constraints. This ensures that the optimal control solution not only optimizes the performance but also adheres to the safety constraints, thereby maintaining the system state within the predefined safe set.

The set $\mathcal{D}$, also referred to as the safe set, is typically shaped by external constraints imposed on the system or its inherent physical limitations. It is commonly expressed as

$$\mathcal{D} = \{x \mid q(x) \geq 0\},$$

where $q(x)$ represents a continuously differentiable function of x. Effectively implementing the CBF provides a robust solution to the challenges posed by the constraints within the system. The CBF candidate $\mathcal{B}(x)$ satisfies the following conditions

$$\mathcal{B}(x) \geq 0, \forall x \in \mathcal{D}$$
$$\mathcal{B}(x) \to \infty, \forall x \in \partial\mathcal{D},$$

where $\partial\mathcal{D}$ is the boundary of the set $\mathcal{D}$. Moreover, $\mathcal{B}(x)$ is monotonically decreasing for all $x \in \mathcal{D}$ and has the following property

$$\frac{1}{\alpha_1(q(x))} \leq \mathcal{B}(x) \leq \frac{1}{\alpha_2(q(x))}$$
$$\dot{\mathcal{B}}(x) \leq \alpha_3(q(x)),$$

where $\alpha_1(\cdot)$, $\alpha_2(\cdot)$, and $\alpha_3(\cdot)$ are Lipschitz class $\mathcal{K}$ functions.

Considering the aforementioned characteristics of the CBF, the specific expression for the logarithmic barrier function is defined as

$$\mathcal{B}(x) = -\log\left(\frac{\varrho q(x)}{\varrho q(x)+1}\right) \tag{5.15}$$

In this expression, ϱ is a constant determining the speed at which $\mathcal{B}(x)$ is limited as it approaches the safety barrier.

5.5 Event-Triggered Safe HJB Equation Formulation

Define the tracking error as $e_r(t) = x(t) - x_r(t)$. From (5.1) and (5.2), the tracking error dynamics can be presented as

$$\dot{e}_r(t) = f(e_r(t)+x_r(t)) + g(e_r(t)+x_r(t))u(t) + \Delta f(e_r(t)+x_r(t)) - Z(x_r(t)). \tag{5.16}$$

Now, based on the tracking error and the desired trajectory, an augmented state vector $\zeta(t) = [e_r^\top(t), x_r^\top(t)]^\top \in \mathbb{R}^{2n}$ is formed. Then, using (5.2) and (5.16), the augmented system dynamics is formulated as

$$\dot{\zeta}(t) = F(\zeta(t)) + G(\zeta(t))u(\zeta(t)) + \Delta F(\zeta(t)), \tag{5.17}$$

where $F : \mathbb{R}^{2n} \to \mathbb{R}^{2n}$ and $G : \mathbb{R}^{2n} \to \mathbb{R}^{2n\times m}$ are new system matrices while $\Delta F(\zeta(t)) \in \mathbb{R}^{2n}$ is the new uncertain term. They can be expressed as

$$F(\zeta(t)) = \begin{bmatrix} f(e_r(t)+x_r(t)) - Z(x_r(t)) \\ Z(x_r(t)) \end{bmatrix},$$

$$G(\zeta(t)) = \begin{bmatrix} g(e_r(t)+x_r(t)) \\ 0 \end{bmatrix}$$

and

$$\Delta F(\zeta(t)) = \begin{bmatrix} \Delta f(e_r(t)+x_r(t)) \\ 0 \end{bmatrix} = K(\zeta(t))d(\zeta(t)).$$

The terms $d(\zeta)$ and $G^{+}(\zeta)\Delta F(\zeta)$ are still upper bounded and the bound can be derived as

$$\|d(\zeta)\| = \|d_1(e_r + x_r)\| = \|d_1(x)\| \leq d_M(x) = d_M(e_r + x_r) \triangleq d_M(\zeta). \tag{5.18}$$

and

$$\left\|G^{+}(\zeta)\Delta F(\zeta)\right\| = \left\|g^{+}(x)\Delta f(x)\right\| \leq g_M(x) = g_M(e_r + x_r) \triangleq g_M(\zeta), \tag{5.19}$$

respectively.

Next, the uncertain term $K(\zeta)d(\zeta)$ is projected onto the range of matrix $G(\zeta)$ and decomposed into sum of matched and unmatched component, that is

$$K(\zeta)d(\zeta) = G(\zeta)G^{+}(\zeta)K(\zeta)d(\zeta) + (I_{2n} - G(\zeta)G^{+}(\zeta))K(\zeta)d(\zeta). \tag{5.20}$$

Then the following auxiliary system is formed

$$\dot{\zeta} = F(\zeta) + G(\zeta)u(\zeta) + (I_{2n} - G(\zeta)G^{+}(\zeta))K(\zeta)v(\zeta), \tag{5.21}$$

where $v(\zeta) \in \mathbb{R}^p$ is an auxiliary control that handles the unmatched component.

In this section, the event-based HJB equation is developed for the auxiliary system (5.21). Moreover, the event-triggering rule is also obtained using Lyapunov approach. The cost function associated with the auxiliary system (5.21) is defined as

$$J(\zeta(t)) = \int_t^{\infty} \mathrm{e}^{-\gamma(\tau-t)}\{\zeta^{\top}\bar{Q}\zeta + W(u(\zeta)) + \beta d_M^2(\zeta) + \beta\|v(\zeta)\|^2 + 2g_M^2(\zeta) + \mathcal{B}(\zeta)\}\mathrm{d}\tau, \tag{5.22}$$

where γ and β are positive constant and $\bar{Q} = diag\{Q, 0_{n\times n}\}$. The term $\mathcal{B}(\zeta)$ is added to the cost function to incorporate the state constraint. The nonquadratic function $W(u(\zeta))$ is taken as

$$W(u(\zeta)) = 2\lambda\int_0^{u(\zeta)} (\varpi^{-1}(\tau/\lambda))^{\top}R\mathrm{d}\tau, \tag{5.23}$$

where $\varpi(\cdot)$ denotes a monotonic odd function with a bounded first derivative. For simplicity, $\varpi(\cdot)$ is chosen as $\tanh(\cdot)$. The matrix R is positive definite. For convenience, R is selected as I_1.

Let $\Psi(\Omega)$ be the set of admissible controls on Ω. It is assumed that the optimal control policy pair is admissible. If the cost function $J(\zeta)$ is continuously differentiable, then one can write

$$\zeta^\top \bar{Q}\zeta + W(u(\zeta)) + \beta\|v(\zeta)\|^2 + 2g_M^2(\zeta) + \beta d_M^2 + \mathcal{B}(\zeta) - \gamma J(\zeta) + \dot{J}(\zeta) = 0 \tag{5.24}$$

with $J(0) = 0$. Here (5.24) is called the infinitesimal version of (5.22). Next, the Hamiltonian associated with the auxiliary system (5.21) is derived as

$$\begin{aligned} &H(\zeta, u(\zeta), v(\zeta), \nabla J(\zeta)) \\ &= (\nabla J(\zeta))^\top (F(\zeta) + G(\zeta)u(\zeta) + (I_{2n} - G(\zeta)G^+(\zeta))K(\zeta)v(\zeta)) \\ &\quad + \zeta^\top \bar{Q}\zeta + W(u(\zeta)) + \beta\|v(\zeta)\|^2 + 2g_M^2(\zeta) + \beta d_M^2 + \mathcal{B}(\zeta) - \gamma J(\zeta). \end{aligned} \tag{5.25}$$

The optimal value of the cost function is expressed as

$$\begin{aligned} &J^*(\zeta) \\ &= \min_{u,v\in\Psi(\Omega)} \int_t^\infty \mathrm{e}^{-\gamma(\tau-t)}\{\zeta^\top \bar{Q}\zeta + W(u(\zeta)) + \beta d_M^2(\zeta) + \beta\|v(\zeta)\|^2 + 2g_M^2(\zeta) + \mathcal{B}(\zeta)\}\mathrm{d}\tau. \end{aligned} \tag{5.26}$$

By the Bellman's principle, $J^*(\zeta)$ holds the HJB equation

$$\min_{u,v\in\Psi(\Omega)} H(\zeta, u(\zeta), v(\zeta), \nabla J^*(\zeta)) = 0 \tag{5.27}$$

with $J^*(0) = 0$. Define $(I_{2n} - G(\zeta)G^+(\zeta))K(\zeta) = L(\zeta)$. The optimal control policies are derived as follows

$$u^*(\zeta) = -\lambda \tanh\left(\frac{1}{2\lambda}G^\top(\zeta)\nabla J^*(\zeta)\right) \tag{5.28}$$

and

$$v^*(\zeta) = -\frac{1}{2\beta}L^\top(\zeta)\nabla J^*(\zeta). \tag{5.29}$$

Substituting (5.28) and (5.29) into (5.27), the HJB equation can be expressed as

$$(\nabla J^*(\zeta))^\top \big(F(\zeta) + G(\zeta)u^*(\zeta) + L(\zeta)v^*(\zeta)\big) + \zeta^\top \bar{Q}\zeta \\ + W(u^*(\zeta)) + \beta\|v^*(\zeta)\|^2 + 2g_M^2(\zeta) + \beta d_M^2 + \mathcal{B}(\zeta) - \gamma J^*(\zeta) = 0. \tag{5.30}$$

The minimum value of the Hamiltonian (5.25) is given as

$$H(\zeta, u^*(\zeta), v^*(\zeta), \nabla J(\zeta)) = (\nabla J(\zeta))^\top (F(\zeta) + G(\zeta)u^*(\zeta) + L(\zeta)v^*(\zeta)) + \zeta^\top \bar{Q}\zeta \\ + W(u^*(\zeta)) + \beta\|v^*(\zeta)\|^2 + 2g_M^2(\zeta) + \beta d_M^2 - \gamma J(\zeta). \tag{5.31}$$

Considering the event-triggering mechanism discussed in Chapter 1, the sampled version of auxiliary system (5.21) is written as

$$\dot{\zeta} = F(\zeta) + G(\zeta)\mu(\zeta(t) + e_j(t)) + L(\zeta)v(\zeta), \tag{5.32}$$

where $e_j(t)$ is the triggering error and $u(\zeta_j) \triangleq \mu(\zeta_j), \forall t \in [t_j, t_{j+1})$. The optimal control (5.28), under event-triggered mechanism, can be expressed as

$$\mu^*(\zeta_j) = -\lambda \tanh\left(\frac{1}{2\lambda} G^\top(\zeta_j)\nabla J^*(\zeta_j)\right). \tag{5.33}$$

Now, using (5.33), the HJB equation under event-based framework is formulated as

$$H(\zeta, \mu^*(\zeta_j), v^*(\zeta), \nabla J^*(\zeta)) = 0,$$

that is,

$$(\nabla J^*(\zeta))^\top \big(F(\zeta) + G(\zeta)\mu^*(\zeta_j) + L(\zeta)v^*(\zeta)\big) + \zeta^\top \bar{Q}\zeta \\ + W(\mu^*(\zeta_j)) + \beta\|v^*(\zeta)\|^2 + 2g_M^2(\zeta) + \beta d_M^2 + \mathcal{B}(\zeta) - \gamma J^*(\zeta) = 0, \tag{5.34}$$

where $J^*(0) = 0$.

Theorem 5.2. Let Assumption 2.1 from Chapter 2 be true. If $J^*(\zeta)$ satisfies the HJB equation (5.27), the control policies are described by (5.29) and (5.33), and $v^*(\zeta)$ satisfies

$$\|v^*(\zeta)\|^2 \leq \lambda_m(Q)\|e_r\|^2, \tag{5.35}$$

and the event-triggering law is formulated as

$$\begin{aligned}\|e_j(t)\|^2 &\leq \frac{(1-2\beta)\lambda_m(Q)\|e_r\|^2}{2\mathcal{L}^2} \\ &\triangleq \|e_T\|^2, \end{aligned} \tag{5.36}$$

then for $\beta \in (0, 0.5)$ the tracking error e_r is uniformly ultimately bounded.

Proof: Given that $J^*(\zeta)$ is positive definite, it is considered as a Lyapunov function candidate. The time derivative of $J^*(\zeta)$ along the trajectory of (5.17) is given by

$$\begin{aligned}\dot{J}^*(\zeta) &= (\nabla J^*(\zeta))^\top \big(F(\zeta) + G(\zeta)\mu^*(\zeta_j) + K(\zeta)d(\zeta)\big) \\ &= (\nabla J^*(\zeta))^\top F(\zeta) + (\nabla J^*(\zeta))^\top G(\zeta)\mu^*(\zeta_j) \\ &\quad + (\nabla J^*(\zeta))^\top \big(G(\zeta)G^+(\zeta)K(\zeta) + L(\zeta)\big)d(\zeta). \end{aligned} \tag{5.37}$$

From (5.30), it follows that

$$\begin{aligned}(\nabla J^*(\zeta))^\top F(\zeta) = -\zeta^\top \bar{Q}\zeta - W(u^*(\zeta)) - \beta\|v^*(\zeta)\|^2 - 2g_M^2(\zeta) - \mathcal{B}(\zeta) - \beta d_M^2(\zeta) \\ + \gamma J^*(\zeta) - (\nabla J^*(\zeta))^\top \left(G(\zeta)u^*(\zeta) + L(\zeta)v^*(\zeta)\right), \end{aligned} \tag{5.38}$$

from (5.28), the following expression is derived

$$(\nabla J^*(\zeta))^\top G(\zeta) = -2\lambda \left(\tanh^{-1}\left(\frac{u^*(\zeta)}{\lambda}\right)\right)^\top \tag{5.39}$$

and from (5.29), one can write

$$(\nabla J^*(\zeta))^\top L(\zeta) = -2\beta v^{*\top}(\zeta) \tag{5.40}$$

Substituting (5.38), (5.39), and (5.40) into (5.37) yields the following equation

$$\begin{aligned}
\dot{J}^*(\zeta) &= -\zeta^\top \bar{Q}\zeta - W(u^*(\zeta)) - \beta\|v^*(\zeta)\|^2 - 2g_M^2(\zeta) - \mathcal{B}(\zeta) - \beta d_M^2(\zeta) + \gamma J^*(\zeta) \\
&\quad - (\nabla J^*(\zeta))^\top G(\zeta)\left(u^*(\zeta) - \mu^*(\zeta_j)\right) + (\nabla J^*(\zeta))^\top G(\zeta)G^+(\zeta)K(\zeta)d(\zeta) \\
&\quad - (\nabla J^*(\zeta))^\top L(\zeta)v^*(\zeta) + (\nabla J^*(\zeta))^\top L(\zeta)d(\zeta) \\
&= -\zeta^\top \bar{Q}\zeta - W(u^*(\zeta)) + \beta\|v^*(\zeta)\|^2 - 2g_M^2(\zeta) - \mathcal{B}(\zeta) - \beta d_M^2(\zeta) + \gamma J^*(\zeta) \\
&\quad \underbrace{+ 2\lambda\left(\tanh^{-1}\left(\frac{u^*(\zeta)}{\lambda}\right)\right)^\top \left(u^*(\zeta) - \mu^*(\zeta_j)\right)}_{\pi_1} \\
&\quad \underbrace{+ 2\lambda\left(\tanh^{-1}\left(\frac{u^*(\zeta)}{\lambda}\right)\right)^\top G^+(\zeta)K(\zeta)d(\zeta)}_{\pi_2} \underbrace{-2\beta v^{*\top}(\zeta)d(\zeta)}_{\pi_3}
\end{aligned} \tag{5.41}$$

Utilizing Assumption 2.1 along with Young's inequality, one can obtain

$$\begin{aligned}
\pi_1 &\le \frac{\lambda^2}{2}\|\tanh^{-1}\left(\frac{u^*(\zeta)}{\lambda}\right)\|^2 + 2\|u^*(\zeta) - \mu^*(\zeta_j)\|^2 \\
&\le \frac{\lambda^2}{2}\sum_{i=1}^{m}\left(\tanh^{-1}\left(\frac{u_i^*(\zeta)}{\lambda}\right)\right)^2 + 2\mathcal{L}^2\|e_j(t)\|^2,
\end{aligned} \tag{5.42}$$

$$\begin{aligned}
\pi_2 &\le \frac{\lambda^2}{2}\|\tanh^{-1}\left(\frac{u^*(\zeta)}{\lambda}\right)\|^2 + 2\|G^+(\zeta)K(\zeta)d(\zeta)\|^2 \\
&\le \frac{\lambda^2}{2}\sum_{i=1}^{m}\left(\tanh^{-1}\left(\frac{u_i^*(\zeta)}{\lambda}\right)\right)^2 + 2g_M^2(\zeta)
\end{aligned} \tag{5.43}$$

and

$$\begin{aligned}
\pi_3 &\le \beta\|v^*(\zeta)\|^2 + \beta\|d(\zeta)\|^2 \\
&\le \beta\|v^*(\zeta)\|^2 + \beta d_M^2(\zeta).
\end{aligned} \tag{5.44}$$

One can write the function $W(u^*(\zeta))$ as

$$W(u^*(\zeta)) = \lambda^2\sum_{i=1}^{m}\left(\tanh^{-1}\left(\frac{u_i^*(\zeta)}{\lambda}\right)\right)^2 - 2\lambda^2\sum_{i=1}^{m}\left(\int_0^{\tanh(\frac{u_i^*(\zeta)}{\lambda})} z_i\tanh^2(z_i)dz_i\right) \tag{5.45}$$

Thus, (5.41) can be expressed as

$$\dot{J}^*(\zeta) \leq -\zeta^\top \bar{Q}\zeta + 2\beta\|v^*(\zeta)\|^2 + \gamma J^*(\zeta) + 2\mathcal{L}^2\|e_j(t)\|^2 \\ \underbrace{+ 2\lambda^2 \sum_{i=1}^{m} \left(\int_0^{\tanh(\frac{u_i(\zeta)}{\lambda})} z_i \tanh^2(z_i) dz_i \right)}_{\pi_4} \tag{5.46}$$

The term π_4 in (5.46) is bounded. For further analysis, it is assumed that $\|\pi_4\| \leq K_m$, where $K_m \geq 0$ is a constant. Given that $\bar{Q} = \text{diag}\{Q, 0_{n\times n}\}$, it follows that $\zeta^\top \bar{Q}\zeta$ can be written as $e_r^\top Q e_r$. Thus, (5.46) can be expressed as

$$\begin{aligned}\dot{J}^*(\zeta) &\leq -\lambda_m(Q)\|e_r\|^2 + 2\beta\|v^*(\zeta)\|^2 + \gamma J^*(\zeta) + 2\mathcal{L}^2\|e_j(t)\|^2 + K_m \\ &\leq -2\beta(\lambda_m(Q)\|e_r\|^2 - \|v^*(\zeta)\|^2) - (1-2\beta)\lambda_m(Q)\|e_r\|^2 \\ &\quad + 2\mathcal{L}^2\|e_j(t)\|^2 + \gamma J^*(\zeta) + K_m.\end{aligned} \tag{5.47}$$

Thus, if the conditions specified in (5.35) and (5.36) are satisfied, then (5.47) can be used to obtain

$$\dot{J}^*(\zeta) \leq -(1-2\beta)\lambda_m(Q)\|e_r\|^2 + \gamma J^*(\zeta) + K_m. \tag{5.48}$$

Since $J^*(\zeta)$ is positive definite and bounded over Ω, let J^*_{max} denote its maximum value. Consequently, based on (5.48), $\dot{J}^*(\zeta) \leq 0$ holds true only if $\beta \in (0, 0.5)$ and e_r lies outside the region defined by

$$\Omega_{e_r} = \left\{ e_r : \|e_r\| \leq \sqrt{\frac{\gamma J^*_{\text{max}} + K_m}{(1-2\beta)\lambda_m(Q)}} \right\}. \tag{5.49}$$

Therefore, it can be concluded that when $\gamma \neq 0$, the tracking error $e_r(t)$ will be uniformly ultimately bounded.

Remark 5.2. The value of the CBF becomes infinite only at the boundary of the safety set and decreases monotonically within the safety set. Since $J^*(\zeta)$ is positive definite and bounded over Ω, it can be concluded that the CBF is bounded. This ensures that the system state will never reach the boundary of the safety set, thereby guaranteeing the safety of the system.

5.6 Adaptive Critic Design

Considering (2.47) from Chapter 2, the augmented control law (5.29) and the event-based control law (5.33) are presented as

$$v^*(\zeta) = -\frac{1}{2\beta}L^\top(\zeta)\left((\nabla\sigma_c(\zeta))^\top\omega_c + \nabla\epsilon_c(\zeta)\right) \tag{5.50}$$

and

$$\mu^*(\zeta_j) = -\lambda\tanh\left(\frac{1}{2\lambda}G^\top(\zeta_j)\left((\nabla\sigma_c(\zeta_j))^\top\omega_c + \nabla\epsilon_c(\zeta_j)\right)\right), \tag{5.51}$$

respectively. Then by using (2.48) from Chapter 2, the approximate value of $v^*(\zeta)$ and $\mu^*(\zeta_j)$ can be obtained as

$$\hat{v}^*(\zeta) = -\frac{1}{2\beta}L^\top(\zeta)(\nabla\sigma_c(\zeta))^\top\hat{\omega}_c \tag{5.52}$$

and

$$\hat{\mu}^*(\zeta_j) = -\lambda\tanh\left(\frac{1}{2\lambda}G^\top(\zeta_j)(\nabla\sigma_c(\zeta_j))^\top\hat{\omega}_c\right), \tag{5.53}$$

respectively. Substituting $J^*(\zeta)$ into (5.25), the following expression is obtained

$$\begin{aligned} H(\zeta,\omega_c,\mu^*(\zeta_j),v^*(\zeta)) &= \omega_c^\top\nabla\sigma_c(\zeta)(F(\zeta)+G(\zeta)\mu^*(\zeta_j)+L(\zeta)v^*(\zeta))+\zeta^\top\bar{Q}\zeta \\ &\quad + W(\mu^*(\zeta_j))+\beta\|v^*(\zeta)\|^2+2g_M^2(\zeta)+\beta d_M^2+\mathcal{B}(\zeta)-\gamma\omega_c^\top\sigma_c(\zeta) \\ &\triangleq e_{cH}, \end{aligned} \tag{5.54}$$

where $e_{cH} = -(\nabla\epsilon_c(\zeta))^\top(F(\zeta)+G(\zeta)\mu^*(\zeta_j)+L(\zeta)v^*(\zeta))+\gamma\epsilon_c(\zeta)$ is the residual error because of the reconstruction error associated with the NN approximation. Now the Hamiltonian (5.25) is approximated as

$$\begin{aligned} \hat{H}(\zeta,\hat{\omega}_c,\hat{\mu}^*(\zeta_j),\hat{v}^*(\zeta)) &= \hat{\omega}_c^\top\nabla\sigma_c(\zeta)(F(\zeta)+G(\zeta)\hat{\mu}^*(\zeta_j)+L(\zeta)\hat{v}^*(\zeta))+\zeta^\top\bar{Q}\zeta \\ &\quad + W(\hat{\mu}^*(\zeta_j))+\beta\|\hat{v}^*(\zeta)\|^2+2g_M^2(\zeta)+\beta d_M^2+\mathcal{B}(\zeta)-\gamma\hat{\omega}_c^\top\sigma_c(\zeta). \end{aligned} \tag{5.55}$$

From the HJB equation it is evident that $H(\zeta, \omega_c, \mu^*(\zeta_j), v^*(\zeta)) = 0$. So, the approximation error of Hamiltonian is given by

$$\begin{aligned} e_c &= \hat{H}(\zeta, \hat{\omega}_c, \hat{\mu}^*(\zeta_j), \hat{v}^*(\zeta)) - H(\zeta, \omega_c, \mu^*(\zeta_j), v^*(\zeta)) \\ &= \hat{\omega}_c^\top \nabla\sigma_c(\zeta)(F(\zeta) + G(\zeta)\hat{\mu}^*(\zeta_j) + L(\zeta)\hat{v}^*(\zeta)) + \zeta^\top \bar{Q}\zeta \\ &\quad + W(\hat{\mu}^*(\zeta_j)) + \beta\|\hat{v}^*(\zeta)\|^2 + 2g_M^2(\zeta) + \beta d_M^2 + \mathcal{B}(\zeta) - \gamma\hat{\omega}_c^\top \sigma_c(\zeta) \\ &= \zeta^\top \bar{Q}\zeta + W(\hat{\mu}^*(\zeta_j)) + \beta\|\hat{v}^*(\zeta)\|^2 + 2g_M^2(\zeta) + \beta d_M^2 + \mathcal{B}(\zeta) + \hat{\omega}_c^\top \phi, \end{aligned} \tag{5.56}$$

where $\phi = \nabla\sigma_c(\zeta)(F(\zeta) + G(\zeta)\hat{\mu}(\zeta_j) + L(\zeta)\hat{v}(\zeta)) - \gamma\sigma_c(\zeta)$.

To ensure that e_c given in (5.56) remains sufficiently small, it is necessary to train the critic network to find appropriate weight. This involves minimizing the objective function $E = (1/2)e_c^\top e_c$ using the gradient descent method. The tuning rule based on this approach is given by

$$\begin{aligned} \dot{\hat{\omega}}_{c_t} &= \frac{-l_c}{(1+\phi^\top\phi)^2}\frac{\partial E}{\partial \hat{\omega}_c} \\ &= \frac{-l_c\phi}{(1+\phi^\top\phi)^2}\left(\zeta^\top \bar{Q}\zeta + W(\hat{\mu}^*(\zeta_j)) + \beta\|\hat{v}^*(\zeta)\|^2 + 2g_M^2(\zeta) + \beta d_M^2 + \mathcal{B}(\zeta) + \hat{\omega}_c^\top \phi\right), \end{aligned} \tag{5.57}$$

where $l_c > 0$ is a design parameter known as the learning rate of the critic network, and $1/(1+\phi^\top\phi)^2$ is introduced to normalize ϕ. However, the tuning rule (5.57) has the following drawback.

1. An initial stabilizing control is needed at the start of the critic weight vector learning process when using the tuning rule provided in (5.57). In some practical applications, determining the initial admissible control can be challenging.

The tuning rule (5.57) is modified using the Lyapunov approach to address these drawback by following a similar approach as that presented in Chapter 4.

While applying the approximated control policies (5.52) and (5.53) to the auxiliary system (5.21), it is important to avoid following possibility which can make the systems unstable

$$(\nabla V(\zeta))^\top(F(\zeta) + G(\zeta)\hat{\mu}(\zeta_j) + L(\zeta)\hat{v}(\zeta)) > 0. \tag{5.58}$$

To prevent (5.58), the training process is enhanced by introducing an additional term derived using the steepest descent method:

$$\begin{aligned}\dot{\hat{\omega}}_{c2} &= l_s \frac{\partial((\nabla V(\zeta))^\top (F(\zeta) + G(\zeta)\hat{\mu}(\zeta_j) + L(\zeta)\hat{v}(\zeta)))}{\partial \hat{\omega}_c} \\ &= \frac{l_s}{2}\left(\nabla\sigma_c(\zeta_j)G(\zeta_j)R^{-1}G^\top(\zeta)\nabla V(\zeta) + \frac{1}{\beta}\nabla\sigma_c(\zeta)L(\zeta)M^{-1}L^\top(\zeta)\nabla V(\zeta)\right), \end{aligned} \tag{5.59}$$

where $l_s > 0$ is a design parameter. The modified critic weights tuning rule is then obtained by adding the stabilizing term (5.59) to the traditional tuning rule (5.57)

$$\begin{aligned}\dot{\hat{\omega}}_c &= \dot{\hat{\omega}}_{c1} + \dot{\hat{\omega}}_{c2} \\ \dot{\hat{\omega}}_c &= \frac{-l_c\phi}{(1+\phi^\top\phi)^2}\left(\zeta^\top \bar{Q}\zeta + W(\hat{\mu}^*(\zeta_j)) + \beta\|\hat{v}^*(\zeta)\|^2 + 2g_M^2(\zeta) + \beta d_M^2 + \mathcal{B}(\zeta) + \hat{\omega}_c^\top\phi\right) \\ &\quad + \frac{l_s}{2}\left(\nabla\sigma_c(\zeta_j)G(\zeta_j)G^\top(\zeta)\nabla V(\zeta) + \frac{1}{\beta}\nabla\sigma_c(\zeta)L(\zeta)L^\top(\zeta)\nabla V(\zeta)\right), \end{aligned} \tag{5.60}$$

Remark 5.3. The new tuning rule (5.60) eliminates the need for an initial admissible control, allowing the critic weight vector to be initialized to zero while learning the appropriate critic weights.

Define the estimation error of the critic weight vector as $\tilde{\omega}_c = \omega_c - \hat{\omega}_c$. By combining (5.54) and (5.56), one can write

$$e_c = -\tilde{\omega}_c^\top\phi + e_{cH}. \tag{5.61}$$

The dynamics of the critic weight vector approximation error can be obtained from (5.60) and (5.61) as follows

$$\begin{aligned}\dot{\tilde{\omega}}_c &= \frac{-l_c\phi}{(1+\phi^\top\phi)^2}(\tilde{\omega}_c^\top\phi - e_{cH}) \\ &\quad - \frac{l_s}{2}\left(\nabla\sigma_c(\zeta_j)G(\zeta_j)G^\top(\zeta)\nabla V(\zeta) + \frac{1}{\beta}\nabla\sigma_c(\zeta)L(\zeta)L^\top(\zeta)\nabla V(\zeta)\right). \end{aligned} \tag{5.62}$$

Under the event-triggered framework, the closed-loop system behaves as an impulsive dynamical system. It exhibits flow dynamics for $t \in [t_j, t_{j+1})$ and jump dynamics at $t = t_{j+1}$. The impulsive dynamical representation is given by

$$\dot{\psi}(t) = \begin{bmatrix} F(\zeta) + G(\zeta)\hat{\mu}^*(\zeta_j) + L(\zeta)\hat{v}^*(\zeta) \\ \hdashline 0 \\ \hdashline \frac{-l_c\phi}{(1+\phi^\top\phi)^2}(\tilde{\omega}_c^\top \phi - e_{cH}) \\ -\frac{l_s}{2}\Big(\nabla\sigma_c(\zeta_j)G(\zeta_j)G^\top(\zeta)\nabla V(\zeta) + \frac{1}{\beta}\nabla\sigma_c(\zeta)L(\zeta)L^\top(\zeta)\nabla V(\zeta)\Big) \end{bmatrix}, \forall t \in [t_j, t_{j+1}), \tag{5.63}$$

and

$$\psi(t^+) = \psi(t) + \begin{bmatrix} 0 \\ \zeta_j - \zeta(t) \\ 0 \end{bmatrix}, \quad \forall t = t_{j+1}, \tag{5.64}$$

where $\psi(t^+) = \lim_{\varsigma\to 0^+} \psi(t+\varsigma)$ and $\varsigma \in (0, t_{j+1} - t_j)$.

5.7 Stability Analysis

Theorem 5.3. Consider the auxiliary system (5.21), the control policies (5.52) and (5.53), and the weight tuning rule (5.60). Assume that Assumptions 2.1 to 2.4 as well as Assumptions 3.1, 3.2, and 4.1 are satisfied. Then, the closed-loop auxiliary system (5.21) is locally asymptotically stable, and the weight approximation error is uniformly ultimately bounded, provided

$$\begin{aligned} \|e_j(t)\|^2 &\leq \frac{(1-\eta_2^2)\lambda_m(Q)\|e_r(t)\|^2}{2(A^2\nabla\sigma_{cM}^2 + B^2G_M^2)\|\hat{\omega}_c\|^2} \\ &\triangleq \|\hat{e}_T\|^2, \end{aligned} \tag{5.65}$$

$$\|\tilde{\omega}_c\| > \sqrt{\frac{\kappa}{l_c\lambda_{\varphi m} - 2G_M^2\nabla\sigma_{cM}^2 - \frac{1}{2\beta}L_M^2\nabla\sigma_{cM}^2 - \frac{l_c\lambda_{\varphi M}}{2(1+\phi^\top\phi)}}}, \tag{5.66}$$

and

$$\|V(\zeta)\| > \sqrt{\frac{\kappa}{l_s\lambda_m(T)}} + \frac{\kappa_1}{2\lambda_m(T)} \tag{5.67}$$

are satisfied, where $\eta_2 \in (0,1)$ is a design parameter.

Proof: Considering the impulsive dynamical representation of the closed-loop system, the Lyapunov function candidate is defined as

$$\Upsilon(t) = \Upsilon_1(t) + \Upsilon_2(t) + \Upsilon_3(t) + \Upsilon_4(t), \tag{5.68}$$

where $\Upsilon_1(t) = J^*(\zeta)$, $\Upsilon_2(t) = J^*(\zeta_j)$, $\Upsilon_3(t) = \frac{1}{2}\tilde{\omega}_c^\top \tilde{\omega}_c$, and $\Upsilon_4(t) = l_s V(\zeta)$. The proof is structured into following two cases:

Case 1. For $t \in [t_j, t_{j+1})$, i.e., when no events are triggered, the derivative of (5.68) is given by

$$\dot{\Upsilon}(t) = \dot{\Upsilon}_1(t) + \dot{\Upsilon}_2(t) + \dot{\Upsilon}_3(t) + \dot{\Upsilon}_4(t). \tag{5.69}$$

Differentiating $\Upsilon_1(t)$ along $\dot{\zeta}(t) = F(\zeta) + G(\zeta)\hat{\mu}^*(\zeta_j) + L(\zeta)\hat{v}^*(\zeta)$ yields

$$\dot{\Upsilon}_1(t) = (\nabla J^*(\zeta))^\top (F(\zeta) + G(\zeta)\hat{\mu}^*(\zeta_j) + L(\zeta)\hat{v}^*(\zeta)).$$

Utilising equations (5.38) and (5.39), this expression can be rewritten as

$$\begin{aligned} \dot{\Upsilon}_1(t) = &-\zeta^\top \bar{Q}\zeta - W(u^*(\zeta)) - \beta\|v^*(\zeta)\|^2 - 2g_M^2(\zeta) - \mathcal{B}(\zeta) - \beta d_M^2(\zeta) + \gamma J^*(\zeta) \\ &+ \underbrace{2\lambda\left(\tanh^{-1}\left(\frac{u^*(\zeta)}{\lambda}\right)\right)^\top \left(u^*(\zeta) - \hat{\mu}^*(\zeta_j)\right)}_{L_1} + \underbrace{2\beta v^{*\top}(\zeta)(v^*(\zeta) - \hat{v}^*(\zeta))}_{L_2}. \end{aligned} \tag{5.70}$$

Applying Young's inequality yields

$$L_1 \leq \lambda^2 \sum_{i=1}^{m} \left(\tanh^{-1}\left(\frac{u_i^*(\zeta)}{\lambda}\right)\right)^2 + \|\left(u^*(\zeta) - \hat{\mu}^*(\zeta_j)\right)\|^2. \tag{5.71}$$

Combining (5.45) and (5.71), it follows that

$$-W(u^*(\zeta)) + L_1 \leq K_m + \|\left(u^*(\zeta) - \hat{\mu}^*(\zeta_j)\right)\|^2, \tag{5.72}$$

where $\|\pi_4\| \leq K_m$ and π_4 is defined in equation (5.46). Next,

$$\begin{aligned}
&\| \left(u^*(\zeta) - \hat{\mu}^*(\zeta_j)\right) \|^2 \\
&= \| -\lambda \tanh\left(\frac{1}{2\lambda} G^\top(\zeta)((\nabla\sigma_c(\zeta))^\top \omega_c + \nabla\epsilon_c(\zeta))\right) - \lambda \tanh\left(\frac{1}{2\lambda} G^\top(\zeta_j)(\nabla\sigma_c(\zeta_j))^\top \hat{\omega}_c\right) \|^2 \\
&\leq 2(A^2\nabla\sigma_{cM}^2 + B^2G_M^2)\|e_j\|^2\|\hat{\omega}_c\|^2 + 2G_M^2\nabla\sigma_{cM}^2\|\tilde{\omega}_c\|^2 + 2G_M^2\nabla\epsilon_{cM}^2. \qquad (5.73)
\end{aligned}$$

Thus,

$$\begin{aligned}
-W(u^*(\zeta)) + L_1 \leq K_m &+ 2(A^2\nabla\sigma_{cM}^2 + B^2G_M^2)\|e_j\|^2\|\hat{\omega}_c\|^2 \\
&+ 2G_M^2\nabla\sigma_{cM}^2\|\tilde{\omega}_c\|^2 + 2G_M^2\nabla\epsilon_{cM}^2. \qquad (5.74)
\end{aligned}$$

From L_2, one can derive

$$\begin{aligned}
L_2 &\leq \beta\|v^*(\zeta)\|^2 + \beta\|(v^*(\zeta) - \hat{v}^*(\zeta)\|^2 \\
&\leq \beta\|v^*(\zeta)\|^2 + \beta\| -\frac{1}{2\beta}L^\top(\zeta)((\nabla\sigma_c(\zeta))^\top\omega_c + \nabla\epsilon_c(\zeta)) + \frac{1}{2\beta}L^\top(\zeta)(\nabla\sigma_c(\zeta))^\top\hat{\omega}_c\|^2 \\
&\leq \beta\|v^*(\zeta)\|^2 + \frac{1}{2\beta}L_M^2\nabla\sigma_{cM}^2(\|\tilde{\omega}_c\|^2 + \nabla\epsilon_{cM}^2). \qquad (5.75)
\end{aligned}$$

Incorporating (5.74) and (5.75) into (5.70) yields

$$\begin{aligned}
\dot{\Upsilon}_1(t) \leq &-\zeta^\top\bar{Q}\zeta - 2g_M^2(\zeta) - \mathcal{B}(\zeta) - \beta d_M^2(\zeta) + \gamma J^*(\zeta) + K_m \\
&+ 2(A^2\nabla\sigma_{cM}^2 + B^2G_M^2)\|e_j\|^2\|\hat{\omega}_c\|^2 + 2G_M^2\nabla\sigma_{cM}^2\|\tilde{\omega}_c\|^2 + 2G_M^2\nabla\epsilon_{cM}^2 \\
&+ \frac{1}{2\beta}L_M^2\nabla\sigma_{cM}^2(\|\tilde{\omega}_c\|^2 + \nabla\epsilon_{cM}^2). \qquad (5.76)
\end{aligned}$$

Considering $\omega_c^\top\phi = \phi^\top\omega_c$, let $\varphi = \phi/(1+\phi^\top\phi)$. Using (5.62), it follows that

$$\begin{aligned}
\dot{\Upsilon}_3(t) = &-l_c\tilde{\omega}_c^\top\varphi\varphi^\top\tilde{\omega}_c + \frac{l_c}{(1+\phi^\top\phi)}\tilde{\omega}_c^\top\varphi e_{cH} \\
&- \frac{l_s}{2}\tilde{\omega}_c^\top\nabla\sigma_c(\zeta_j)G(\zeta_j)G^\top(\zeta)\nabla V(\zeta) - \frac{l_s}{2\beta}\tilde{\omega}_c^\top\nabla\sigma_c(\zeta)L(\zeta)L^\top(\zeta)\nabla V(\zeta). \qquad (5.77)
\end{aligned}$$

Let $\lambda_M(\varphi\varphi^\top) = \lambda_{\varphi M}$ and $\lambda_m(\varphi\varphi^\top) = \lambda_{\varphi m}$. By applying Young's inequality $2a_1^\top a_2 \leq a_1^\top a_1 +$

$a_2^\top a_2$ and considering Assumption 3.1, (5.77) can be rewritten as

$$\begin{aligned}\dot{\Upsilon}_3(t) \leq & -l_c\lambda_{\varphi m}\|\tilde{\omega}_c\|^2 + \frac{l_c}{2(1+\phi^\top\phi)}(\lambda_{\varphi M}\|\tilde{\omega}_c\|^2 + e_{cHM}^2) \\ & - \frac{l_s}{2}\tilde{\omega}_c^\top\nabla\sigma_c(\zeta_j)G(\zeta_j)G^\top(\zeta)\nabla V(\zeta) - \frac{l_s}{2\beta}\tilde{\omega}_c^\top\nabla\sigma_c(\zeta)L(\zeta)L^\top(\zeta)\nabla V(\zeta). \qquad (5.78)\end{aligned}$$

Similarly, taking the derivative of $\Upsilon_4(t)$, it follows that

$$\begin{aligned}\dot{\Upsilon}_4(t) &= l_s(\nabla V(\zeta))^\top(F(\zeta) + G(\zeta)\hat{\mu}^*(\zeta_j) + L(\zeta)\hat{v}^*(\zeta)) \\ &= l_s(\nabla V(\zeta))^\top(F(\zeta) + G(\zeta)u^*(\zeta) + L(\zeta)v^*(\zeta)) \\ &\quad - l_s(\nabla V(\zeta))^\top G(\zeta)(u^*(\zeta) - \hat{\mu}^*(\zeta_j)) - l_s(\nabla V(\zeta))^\top L(\zeta)(v^*(\zeta) - \hat{v}^*(\zeta)) \qquad (5.79)\end{aligned}$$

Simplifying the term $(u^*(\zeta) - \hat{\mu}^*(\zeta_j))$, the following expression is obtained

$$\begin{aligned}(u^*(\zeta) - \hat{\mu}^*(\zeta_j)) = & -(1-\tanh^2(\zeta))\left(\frac{1}{2}(G^\top(\zeta)(\nabla\sigma_c(\zeta))^\top - G^\top(\zeta_j)(\nabla\sigma_c(\zeta_j))^\top)\omega_c\right) \\ & - (1-\tanh^2(\zeta))\left(\frac{1}{2}G^\top(\zeta)\nabla\epsilon_c(\zeta) + G^\top(\zeta_j)(\nabla\sigma_c(\zeta_j))^\top\tilde{\omega}_c\right). \qquad (5.80)\end{aligned}$$

Thus, it follows that

$$\begin{aligned}-l_s(\nabla V(\zeta))^\top(u^*(\zeta) - \hat{\mu}^*(\zeta_j)) \leq & \frac{1}{2}l_s(\nabla V(\zeta))^\top G(\zeta)G^\top(\zeta_j)(\nabla\sigma_c(\zeta_j))^\top\tilde{\omega}_c \\ & + l_s\|V(\zeta)\|(2G_M^2\nabla\sigma_{cM}\omega_{CM} + \frac{1}{2}G_M^2\nabla\epsilon_{CM}). \qquad (5.81)\end{aligned}$$

Similarly,

$$(v^*(\zeta) - \hat{v}^*(\zeta)) = -\frac{1}{2\beta}L^\top(\zeta)(\nabla\sigma_c(\zeta))^\top\omega_c + \nabla\epsilon_c(\zeta)) + \frac{1}{2\beta}L^\top(\zeta)(\nabla\sigma_c(\zeta))^\top\hat{\omega}_c. \qquad (5.82)$$

Therefore,

$$\begin{aligned}& - l_s(\nabla V(\zeta))^\top(v^*(\zeta) - \hat{v}^*(\zeta)) \\ & \leq \frac{l_s}{2\beta}\|V(\zeta)\|L_M^2\nabla\epsilon_{CM} + \frac{l_s}{2\beta}(\nabla V(\zeta))^\top L(\zeta)L^\top(\zeta)\nabla\sigma_c^\top(\zeta)\tilde{\omega}_c. \qquad (5.83)\end{aligned}$$

Using Assumption 3.1 and substituting (5.81) and (5.83) in (5.79), the following expression is deduced

$$\begin{aligned}\dot{\Upsilon}_4(t) \leq & -l_s\lambda_m(T)\|V(\zeta)\|^2 + \frac{1}{2}l_s(\nabla V(\zeta))^\top G(\zeta)G^\top(\zeta_j)(\nabla\sigma_c(\zeta_j))^\top\tilde{\omega}_c \\ & + l_s\|V(\zeta)\|(2G_M^2\nabla\sigma_{cM}\omega_{CM} + \frac{1}{2}G_M^2\nabla\epsilon_{CM}) \\ & + \frac{l_s}{2\beta}\|V(\zeta)\|L_M^2\nabla\epsilon_{CM} + \frac{l_s}{2\beta}(\nabla V(\zeta))^\top L(\zeta)L^\top(\zeta)\nabla\sigma_c^\top(\zeta)\tilde{\omega}_c. \end{aligned} \tag{5.84}$$

By applying Assumptions 2.1 to 2.4, along with Assumptions 3.1 and 3.2, it follows that

$$\begin{aligned} & \dot{\Upsilon}_3(t) + \dot{\Upsilon}_4(t) \\ & \leq -l_c\lambda_{\varphi m}\|\tilde{\omega}_c\|^2 + \frac{l_c}{2(1+\phi^\top\phi)}(\lambda_{\varphi M}\|\tilde{\omega}_c\|^2 + e_{cHM}^2) - l_s\lambda_m(T)\|V(\zeta)\|^2 \\ & \quad + l_s\|V(\zeta)\|\left(2G_M^2\nabla\sigma_{cM}\omega_{CM} + \frac{1}{2}G_M^2\nabla\epsilon_{CM} + \frac{1}{2\beta}L_M^2\nabla\epsilon_{CM}\right) \\ & \leq -l_c\lambda_{\varphi m}\|\tilde{\omega}_c\|^2 + \frac{l_c}{2(1+\phi^\top\phi)}(\lambda_{\varphi M}\|\tilde{\omega}_c\|^2 + e_{cHM}^2) \\ & \quad - l_s\lambda_m(T)\left(\|V(\zeta)\| - \frac{\kappa_1}{2\lambda_m(T)}\right)^2 + \frac{l_s\kappa_1^2}{4\lambda_m(T)} \\ & \leq -l_c\lambda_{\varphi m}\|\tilde{\omega}_c\|^2 + \frac{l_c\lambda_{\varphi M}}{2(1+\phi^\top\phi)}\|\tilde{\omega}_c\|^2 - l_s\lambda_m(T)\left(\|V(\zeta)\| - \frac{\kappa_1}{2\lambda_m(T)}\right)^2 + \kappa_2, \end{aligned} \tag{5.85}$$

where $\kappa_1 = \left(2G_M^2\nabla\sigma_{cM}\omega_{CM} + \frac{1}{2}G_M^2\nabla\epsilon_{CM} + \frac{1}{2\beta}L_M^2\nabla\epsilon_{CM}\right)$ and $\kappa_2 = \frac{l_c e_{cHM}^2}{2(1+\phi^\top\phi)} + \frac{l_s\kappa_1^2}{4\lambda_m(T)}$. By incorporating (5.76) and (5.85) into (5.69), the time derivative of the Lyapunov function can be represented as

$$\begin{aligned}\dot{\Upsilon}(t) \leq & -\zeta^\top\bar{Q}\zeta - 2g_M^2(\zeta) - \mathcal{B}(\zeta) - \beta d_M^2(\zeta) + 2(A^2\nabla\sigma_{cM}^2 + B^2G_M^2)\|e_j\|^2\|\hat{\omega}_c\|^2 \\ & - \left(-2G_M^2\nabla\sigma_{cM}^2 - \frac{1}{2\beta}L_M^2\nabla\sigma_{cM}^2 + l_c\lambda_{\varphi m} - \frac{l_c\lambda_{\varphi M}}{2(1+\phi^\top\phi)}\right)\|\tilde{\omega}_c\|^2 \\ & - l_s\lambda_m(T)\left(\|V(\zeta)\| - \frac{\kappa_1}{2\lambda_m(T)}\right)^2 + \kappa, \end{aligned} \tag{5.86}$$

where $\kappa = 2G_M^2\nabla\epsilon_{cM}^2 + \frac{1}{2\beta}L_M^2\nabla\sigma_{cM}^2\nabla\epsilon_{cM}^2 + \gamma J_{max}^* + K_m + \kappa_2$. Introducing the design parameter

η_2 and considering the fact $\zeta^\top(t)\bar{Q}\zeta(t) = e_r^\top(t)Qe_r(t)$, (5.86) can be rewritten as

$$\begin{aligned}\dot{\Upsilon}(t) \leq & -\eta_2^2\lambda_m(Q)\|e_r(t)\|^2 - (1-\eta_2^2)\lambda_m(Q)\|e_r(t)\|^2 - 2g_M^2(\zeta) - \mathcal{B}(\zeta) \\ & - \beta d_M^2(\zeta) + 2(A^2\nabla\sigma_{cM}^2 + B^2G_M^2)\|e_j\|^2\|\hat{\omega}_c\|^2 \\ & - \left(l_c\lambda_{\varphi m} - 2G_M^2\nabla\sigma_{cM}^2 - \frac{1}{2\beta}L_M^2\nabla\sigma_{cM}^2 - \frac{l_c\lambda_{\varphi M}}{2(1+\phi^\top\phi)}\right)\|\tilde{\omega}_c\|^2 \\ & - l_s\lambda_m(T)\left(\|V(\zeta)\| - \frac{\kappa_1}{2\lambda_m(T)}\right)^2 + \kappa, \end{aligned} \tag{5.87}$$

If the conditions (5.65), (5.66), and (5.67) from Theorem 5.3 are met, then (5.87) implies that $\dot{\Upsilon}(t) < 0$, meaning the proposed Lyapunov function candidate has a negative time derivative for all $t \in [t_j, t_{j+1})$.

Case 2. When $t = t_{j+1}$, i.e., events are triggered. This case follows a similar approach as presented in Chapter 4, Theorem 4.4, Case 2. Therefore, it is omitted here.

The above two cases establish that the closed-loop system is locally asymptotically stable and the weight approximation error is uniformly ultimately bounded.

5.8 Simulation Results

A simulation example is presented in this section to validate the theoretical findings presented in this chapter.

Consider the spring-mass-damper system

$$\dot{x} = \begin{bmatrix} 0 & 1 \\ -\frac{\bar{k}}{m} & -\frac{c}{m} \end{bmatrix} x + \begin{bmatrix} 0 \\ \frac{1}{m} \end{bmatrix} u, \tag{5.88}$$

where m is the mass, $\bar{k}$ is the spring constant, c is the damping coefficient. The state vector $x = [x_1, x_2]^\top$, where x_1 is the position, and x_2 is the velocity. The control input is constrained by $|u| \leq 4$, i.e., $\lambda = 4$ and the state x_2 is considered to be $-1.1 \leq x_2 \leq 3.3$. Let $m = 1\,\text{kg}$, $c = 0.5\,\text{N}\cdot\text{s/m}$, and the spring exhibits nonlinearity with $\bar{k}(x) = -5x^3\,\text{N/m}$. Introducing an unmatched uncertainty $\Delta f(x)$, the system dynamics can be presented as

$$\dot{x} = f(x) + g(x)u + \Delta f(x), \tag{5.89}$$

where $f(x) = \begin{bmatrix} x_2 \\ -5x_1^3 - 0.5x_2 \end{bmatrix}$, $g(x) = \begin{bmatrix} 0 \\ 1 \end{bmatrix}$, and $\Delta f(x) = k(x)d_1(x)$ with $k(x) = [1, 0]^\top$, and the perturbation $d_1(x) = 0.5\theta_1 x_1 x_2 \sin(x_1)\cos(x_2 + \theta_2)$, where θ_1 and θ_2 are unknown parameters. Let $\theta_1, \theta_2 \in [-1, 1]$ and the upper bound of the perturbation be $d_M(x) = |x_1||x_2|$. The initial state $x_0 = [1, -1]^\top$.

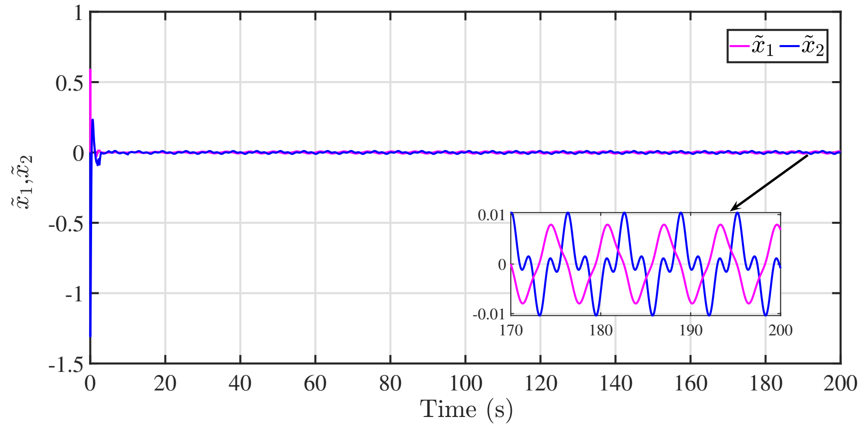

Figure 5.1: Identification error of the identifier network

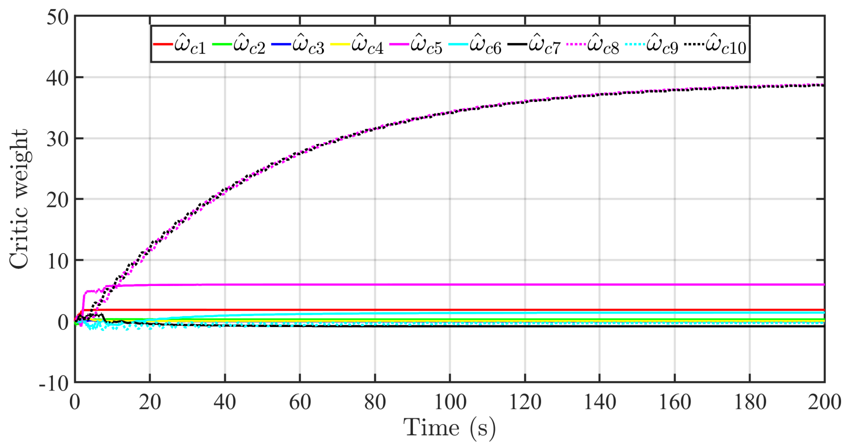

Figure 5.2: Convergence of critic network's weight

This chapter considers the drift dynamics $f(x)$ unknown. A data-based identifier neural network is constructed to approximate the unknown drift dynamics as given in equation (5.5). In

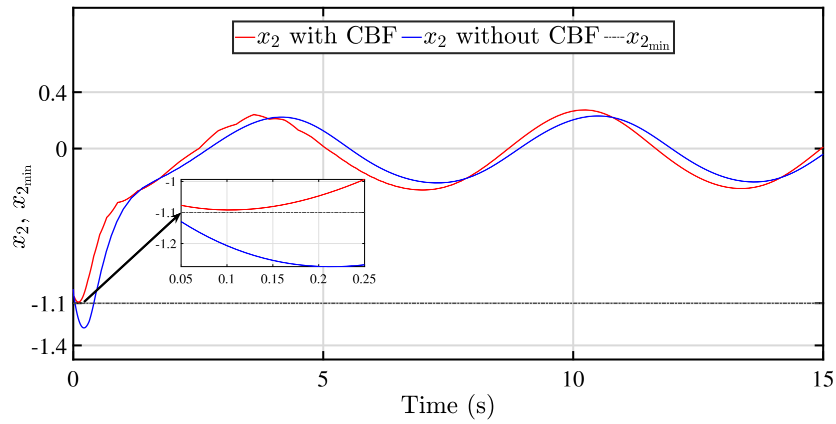

Figure 5.3: State constraint satisfaction

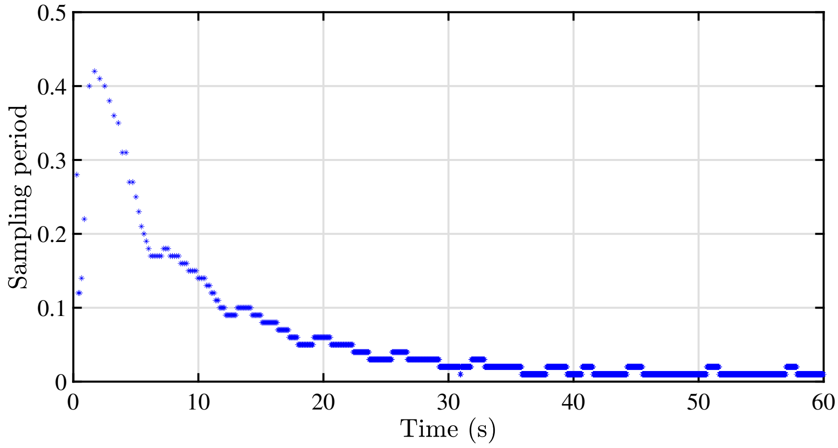

Figure 5.4: Sampling period during the implementation phase

the identifier network (5.5), the parameter δ is set to 6 and the matrix S is taken as

$$S = \begin{bmatrix} -0.5 & 0.5 \\ -0.25 & -0.25 \end{bmatrix}.$$

S is Hurwitz and $(S - \delta I_2)$ is invertible. The activation function for the identifier is chosen as $\sigma_f(\cdot) = \tanh(\cdot)$, and the initial value of the weight matrix is randomly selected from the interval $[0, 1]$. The initial states of the identifier network are taken as $\hat{x}(0) = [0.4, 0.2]^\top$. The parameters n_1 and n_2 of the identifier weight update rule are selected as 7 and 4, respectively. The matrix parameters of the identifier network are chosen heuristically. The evolution of the identification error is shown in Figure 5.1.

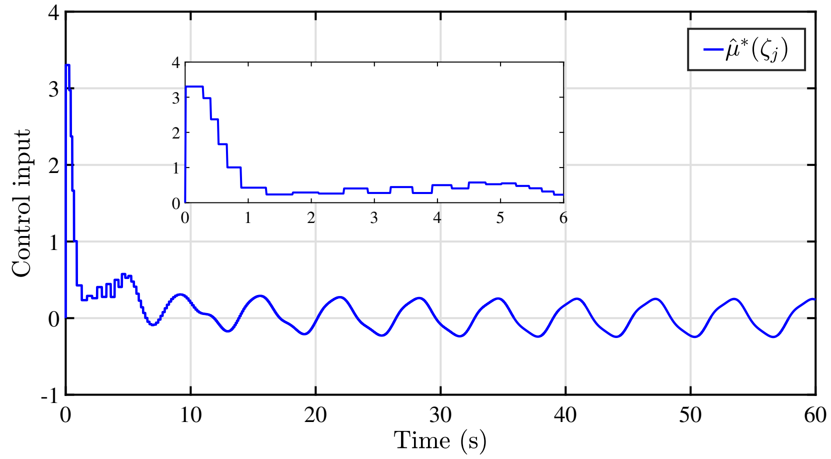

Figure 5.5: Event-triggered control input

The desired trajectory $x_r(t)$ is generated from

$$\dot{x}_r(t) = \begin{bmatrix} x_{r2} \\ -x_{r1} \end{bmatrix}, \tag{5.90}$$

with $x_r = [x_{r1}, x_{r2}]^\top \in \mathbb{R}^2$ and the initial condition $x_{r0} = [0.2, -0.2]^\top$.

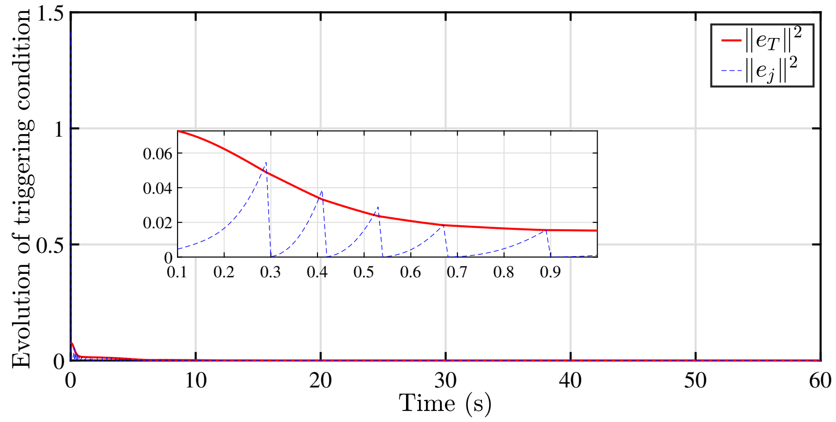

Figure 5.6: Evolution of triggering condition during the implementation phase

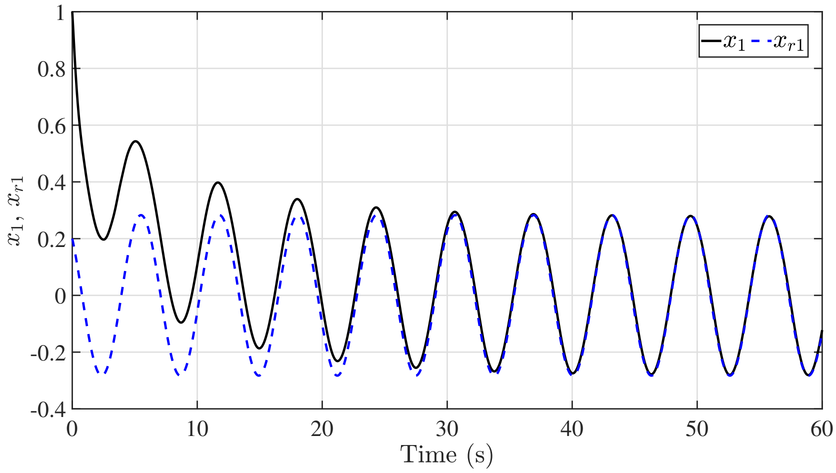

Figure 5.7: Tracking performance of x_1 for $\theta_1 = 0.9$ and $\theta_2 = -0.7$

An augmented state vector $\zeta = [\zeta_1, \zeta_2, \zeta_3, \zeta_4]^\top \in \mathbb{R}^4$ is introduced, and the following augmented system is formed

$$\dot{\zeta} = \begin{bmatrix} \zeta_2 \\ -5(\zeta_1+\zeta_3)^3 - 0.5(\zeta_2+\zeta_4) + \zeta_3 \\ \zeta_4 \\ -\zeta_3 \end{bmatrix} + \begin{bmatrix} 0 \\ 1 \\ 0 \\ 0 \end{bmatrix} u(\zeta) + L(\zeta)d(\zeta), \tag{5.91}$$

where $L(\zeta) = [1, 0, 0, 0]^\top$ and $d(\zeta) = 0.5\theta_1(\zeta_1+\zeta_3)(\zeta_2+\zeta_4)\sin(\zeta_1+\zeta_3)\cos((\zeta_2+\zeta_4)+\theta_2)$. The initial condition is $\zeta_0 = [0.8, -0.8, 0.2, -0.2]^\top$. The upper bound for $d_M(\zeta)$ is $d_M(\zeta) = |\zeta_1+\zeta_3||\zeta_2+\zeta_4|$. The auxiliary system is formulated as

$$\dot{\zeta} = \begin{bmatrix} \zeta_2 \\ -5(\zeta_1+\zeta_3)^3 - 0.5(\zeta_2+\zeta_4) + \zeta_3 \\ \zeta_4 \\ -\zeta_3 \end{bmatrix} + \begin{bmatrix} 0 \\ 1 \\ 0 \\ 0 \end{bmatrix} u(\zeta) + \begin{bmatrix} 1 \\ 0 \\ 0 \\ 0 \end{bmatrix} v(\zeta). \tag{5.92}$$

Since $\|G^+(\zeta)L(\zeta)d(\zeta)\| = 0$, one can consider $g_M(\zeta) = 0$. For the simulation, let $R = I_1$, $M = I_1$, and $Q = 5I_2$. Use $\gamma = 1.4$ and $\beta = 0.4$. The cost function (5.22) for the auxiliary system (5.92) becomes

$$J(\zeta(t)) = \int_t^\infty \mathrm{e}^{-1.4(\tau-t)}\{5\|e_r\|^2 + W(u(\zeta)) + 0.16\|\zeta\|^2 + \mathcal{B}(\zeta)\}\mathrm{d}\tau, \tag{5.93}$$

where $W(u(\zeta))$ is given in (5.23) and the control barrier function is considered as

$$\mathcal{B}(\zeta) = -\log\left(\frac{\varrho_1(x_{2_{\max}} - (\zeta_1 + \zeta_4))}{\varrho_1(x_{2_{\max}} - (\zeta_1 + \zeta_4) + 1)}\right) - \log\left(\frac{\varrho_2((\zeta_2 + \zeta_4) - x_{2_{\min}})}{\varrho_2((\zeta_2 + \zeta_4) - x_{2_{\min}}) + 1}\right), \tag{5.94}$$

where $x_{2_{\min}} = -1.1$, $x_{2_{\max}} = 3.3$, $\varrho_1 = 0.1$, and $\varrho_2 = 0.05$.

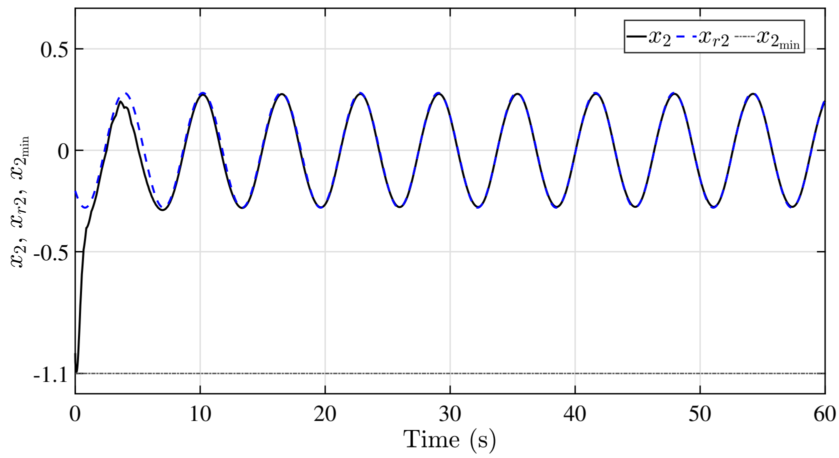

Figure 5.8: Tracking performance of x_2 for $\theta_1 = 0.9$ and $\theta_2 = -0.7$

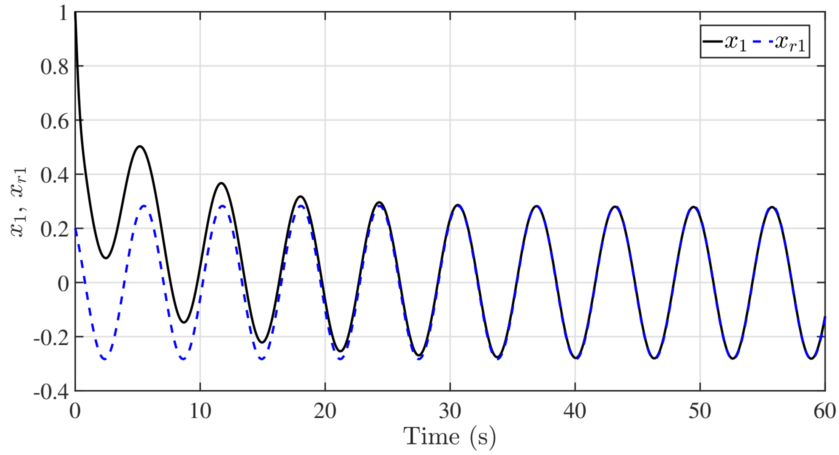

Figure 5.9: Tracking performance of x_1 for $\theta_1 = -0.5$ and $\theta_2 = 0.5$

The parameters for updating the critic weights, as specified in (5.60), are set to $l_c = 1.6$ and $l_s = 0.08$. The event-triggering rule used during training, detailed in (5.65), is configured with $(A^2 \nabla\sigma_{cM}^2 + B^2 G_M^2) = 7$ and $\eta_1 = 0.8$. The critic weight vector is initially set to zero, with probing noise applied during the first few seconds of the weight update process. The activation function is chosen as

$$\sigma_c(\zeta) = [\zeta_1^2, \zeta_1\zeta_2, \zeta_1\zeta_3, \zeta_1\zeta_4, \zeta_2^2, \zeta_2\zeta_3, \zeta_2\zeta_4, \zeta_3^2, \zeta_3\zeta_4, \zeta_4^2]^\top.$$

After 200 seconds, the critic weight vector $\hat{\omega}_c$ converges to

$$[1.85, 0.30, -0.027, 0.037, 5.99, 1.40, -0.85, 38.76, -0.27, 38.62]^\top$$

as depicted in Figure 5.2.

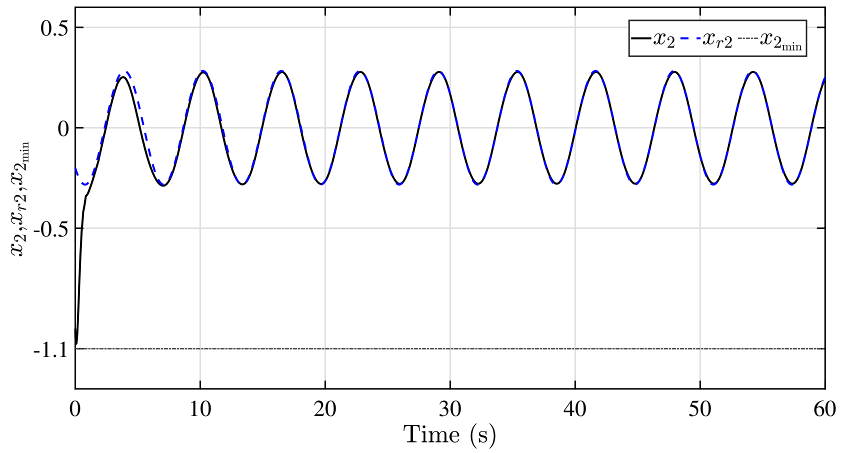

Figure 5.10: Tracking performance of x_2 for $\theta_1 = -0.5$ and $\theta_2 = 0.5$

In the learning phase, the event-triggered controller updates 19550 times, compared to 20000 updates for the time-triggered controller. This is not a significant reduction in number of triggering instant and it occurs due to the inclusion of the control barrier function into the cost function. During the implementation phase, the converged weight vector is utilized along with the triggering rule defined by equation (5.65). It is considered that $\mathcal{L} = 10$, $\theta_1 = 0.9$, and $\theta_2 = -0.7$. The constraint satisfaction by the state x_2 is shown in Figure 5.3. The event-based controller is shown in Figure 5.5. The results show that the event-based tracking controller and the states remain within their specified constraints. Figure 5.4 depicts the sampling period during the implementation phase. The relationship between the gap e_j and the threshold e_T is illustrated in Figure 5.6. The tracking performances are illustrated in Figures 5.7 and 5.8. The event-triggered tracking controller uses only 2878 state samples, whereas the conventional time-triggered method requires 6000 samples. This shows that the event-based approach significantly lowers the need for computational resources during the implementation phase.

To demonstrate the robust tracking performance, the values of θ_1 and θ_2 were changed to -0.5 and 0.5, respectively. The tracking performance of x_1 and x_2 with these new values of θ_1 and θ_2 is shown in Figures 5.9 and 5.10, respectively. The figures indicate that the tracking performance is satisfactory and that the constraint on x_2 is satisfied despite the change in the uncertainty.

5.9 Summary

In this chapter, an event-triggered robust tracking controller is designed for unmatched uncertain nonlinear systems with state and input constraints. The system's drift dynamics is considered to be unknown; to approximate the unknown drift dynamics, a neural network based identifier is designed. The robust tracking control problem of the original nonlinear system is converted to the optimal control problem of an augmented auxiliary system. The constraints in the states and input are handled by incorporating the control barrier function and nonquadratic utility function into the cost function of the augmented auxiliary system. The optimal control problem is solved using a critic neural network. The event-triggering rule is designed, and the controller is updated only when the triggering rule is violated. Furthermore, the uniformly ultimately boundedness of the identifier and critic weight approximation error, identification error, and tracking error is demonstrated. Finally, a simulation study is conducted to demonstrate the effectiveness of the proposed controller. The simulation study reveals that the controller updates more frequently when the state constraint is considered. During the learning phase, the controller does not significantly reduce the number of triggering instants. However, during the implementation phase, the number of times the controller is updated is reduced substantially despite the presence of constraints in both state and input, highlighting the effectiveness of the proposed controller.

6

Conclusions and Scope for Future Work

Contents

6.1 Conclusions

In this thesis, robust tracking controllers for different classes of nonlinear systems are designed. The thesis primarily focused on addressing robust tracking control problems under matched and unmatched uncertainties, control and state constraints, and partially unknown dynamics utilizing the event-triggered adaptive dynamic programming (ADP) approach. The thesis work yielded robust optimal tracking controllers that ensure effective performance even with limited computational resources. The key contributions and findings are briefly concluded as follows.

The first work in this thesis, as presented in Chapter 2, addressed the robust guaranteed cost tracking control problem for nonlinear systems with matched uncertainties. The original control problem is converted to the optimal control problem of a nominal augmented system and solved using a critic neural network under the ADP framework. A novel event-triggering rule is derived, and its applicability to the original system is ensured using Lyapunov analysis. The event-triggered guaranteed cost is found to be more than the time-triggered guaranteed cost. While a lower guaranteed cost cannot be calculated with the event-triggered controller, the main benefit is reducing state sampling, which aligns with the primary goal of the event-triggered control mechanism. In the simulation study, the designed controller is found to be robust to the change in uncertainties while maintaining satisfactory tracking performance.

While Chapter 2 effectively dealt with matched uncertainties, real-world systems often involve unmatched uncertainties, where the disturbances affect the system in a more complex manner. To address this, Chapter 3 extended the methodology to develop a robust tracking control strategy for nonlinear systems with unmatched uncertainties. An augmented system consisting of tracking error dynamics and the reference trajectory is formed. Then, the unmatched uncertainty is decomposed into matched and unmatched components to form an auxiliary system. The robust tracking control problem of the original system is converted to the optimal control problem of the auxiliary system and is solved using the ADP approach. The Lyapunov method demonstrated the UUB of all signals in the closed-loop system. The simulation studies have shown a significant reduction in the number of times the derived event-triggered controller updates while maintaining a satisfactory tracking performance.

Following the development of robust tracking control for systems with unmatched uncertainties, this thesis extended the approach to account for input constraints, which are critical in real-world applications. In Chapter 4, an event-triggered robust tracking controller is designed specifically for input constraint nonlinear systems with unmatched uncertainties. The tracking control problem of the original system is transformed into an optimal control problem of an auxiliary system, and the cost function is modified to incorporate the constraint in the input. The expression for the event-triggered guaranteed cost and the time-triggered guaranteed cost are derived. The controller updates only when the designed triggering rule is violated, and the controller stays within its constraint value, as shown in simulation studies.

The state constraint must be considered in addition to the control input constraint to ensure the proper safety of the controlled system. Moreover, complete knowledge of systems dynamics may not be available for most practical systems. To address this issue, Chapter 5 developed an event-triggered robust tracking controller for nonlinear systems with both input and state constraints and partially unknown dynamics. A neural network-based identifier is designed to approximate the unknown drift dynamics. The robust tracking problem is transformed into an optimal control problem for an augmented auxiliary system, where a control barrier function (CBF) and a nonquadratic utility function are added to the cost function to incorporate the state and input constraints. The simulation study has shown that the proposed controller significantly reduces the need for controller updates despite state and input constraints. However, there remains a scope to modify the triggering rule used during the learning phase to further reduce the number of event-triggering instants.

6.2 Scope for Future Work

There are several ways in which the work in this thesis can be extended and further investigated. Some of them are mentioned below.

- The work developed in this thesis needs complete or partial knowledge of system dynamics. However, the knowledge of the system dynamics may not be available in many practical applications. The work presented in this thesis can be extended to systems with completely unknown dynamics. The unknown dynamics can be approximated by designing a data-based event-triggered identifier neural network under the ADP framework, yielding an intelligent and resource-efficient controller.

- In Chapter 5, it was observed that incorporating the state constraint using the CBF into the cost function led to a substantial increase in the number of triggering instants during the learning phase. Future research could focus on modifying the triggering rule or the CBF to reduce the number of triggering instants while maintaining system performance.

- Recently, the event-based ADP approach has been successfully applied in the development of controllers for multi-agent systems [101, 102]. In multi-agent systems, the event-based ADP approach is particularly advantageous, as it allows for efficient coordination between agents without requiring continuous communication, which is often impractical in large-scale systems. The methodologies developed in this thesis can be adopted to multi-agent systems, ensuring synchronization and cooperative behaviour under dynamic uncertainties and system constraints.
- The event-triggered delay, which refers to the time required for the control update to be completed after a jump instant, may be significant in some systems. If this delay is significant, it becomes essential to consider it in the control design to ensure system stability and performance. Exploring the methods to incorporate and mitigate the effects of event-triggered delays in the event-based ADP approach is another interesting problem.
- Exploring the experimental validation of the proposed methods is a promising direction for future research. For example, mobile robots suffer from environmental uncertainties and face system constraints such as limited control inputs [43]. Hence, designing an event-triggered ADP-based tracking controller for mobile robots under system constraints and external uncertainties will ensure the practical effectiveness of the developed methodologies by yielding a robust and resource-efficient tracking controller.

A

Appendix

Contents

A few fundamental concepts that facilitate a smoother understanding of this thesis are presented below.

A.1 Lyapunov's Direct Method (Second Method)

Lyapunov's second method, often called the direct method, provides a powerful tool to study the stability of nonlinear systems without solving the system explicitly. It involves the construction of a scalar function $V(x)$, called a Lyapunov function, which is positive definite and whose derivative along the system's trajectories is negative definite or negative semi-definite.

Consider the system

$$\dot{x} = f(x), \quad x \in \mathbb{R}^n. \tag{A.1}$$

A function $V : \mathbb{R}^n \to \mathbb{R}$ is said to be a Lyapunov function if

(i) $V(x)$ is positive definite, i.e., $V(0) = 0$ and $V(x) > 0$ for $x \neq 0$,

(ii) The time derivative of $V(x)$ along the trajectories of the system, given by

$$\dot{V}(x) = \frac{\partial V}{\partial x} f(x), \tag{A.2}$$

is negative definite (or negative semi-definite).

If such a function $V(x)$ exists, the equilibrium point $x = 0$ is globally asymptotically stable. If $\dot{V}(x)$ is negative semi-definite, then the system is stable in the sense of Lyapunov.

A.2 Bellman's Principle of Optimality

The foundation of dynamic programming is Bellman's principle of optimality, which states [9]

> An optimal policy has the property that, regardless of the initial state and decision, the remaining decisions must constitute an optimal policy with regard to the state resulting from the first decision.

A.3 Persistence of Excitation

Persistence of excitation (PE) is a crucial concept in adaptive control and system identification. It describes the richness of a signal in terms of the frequency content needed to ensure the convergence of adaptive parameters.

Definition A.1. (Persistently exciting signal). A bounded signal $\phi(t) \in \mathbb{R}^n$, where $n \geq 1$ and $t \in [t_0, \infty)$, is called persistently exciting if there exist constants $T > 0$ and $\beta > 0$ such that for all $t \geq t_0$, the following condition satisfies

$$\int_t^{t+T} \phi(\tau)\phi^T(\tau)d\tau \geq \beta I_n, \quad \forall t \geq t_0, \tag{A.3}$$

where I_n is an Identity matrix of n dimension.

A.4 Comparison Lemma

The comparison lemma is utilized to compare the solution to a differential inequality with the solution of a differential equation. The lemma, which is taken from [96], is stated below.

Lemma 1. Consider the scalar differential equation

$$\dot{x} = f(t, x), \quad x(t_0) = u_0, \tag{A.4}$$

where $f(t, x)$ is continuous in t and locally Lipschitz in x, for all $t \geq 0$ and all $x \in Z \subset \mathbb{R}$. Let $[t_0, T)$ (where T could be infinity) be the maximal interval of existence of the solution $x(t)$, and suppose that $x(t) \in Z$ for all $t \in [t_0, T)$.

Let $y(t)$ be a continuous function whose upper right-hand derivative $D^+y(t)$ satisfies the differential inequality

$$D^+y(t) \leq f(t, y(t)), \quad y(t_0) \leq u_0, \tag{A.5}$$

with $y(t) \in Z$ for all $t \in [t_0, T)$. Then, $y(t) \leq x(t)$ for all $t \in [t_0, T)$.

References

[1] C. Kravaris and S. Palanki, “A lyapunov approach for robust nonlinear state feedback synthesis,” *IEEE Transactions on Automatic Control*, vol. 33, no. 12, pp. 1188–1191, 1988.

[2] C. Edwards and S. Spurgeon, *Sliding mode control: theory and applications*. Crc Press, 1998.

[3] F. Lin, “An optimal control approach to robust control design,” *International Journal of Control*, vol. 73, no. 3, pp. 177–186, 2000.

[4] M. Karimi-Ghartemani, S. A. Khajehoddin, P. Jain, and A. Bakhshai, “Linear quadratic output tracking and disturbance rejection,” *International Journal of Control*, vol. 84, no. 8, pp. 1442–1449, 2011.

[5] M. Zribi, N. Almutairi, M. Abdel-Rohman, and M. Terro, “Nonlinear and robust control schemes for offshore steel jacket platforms,” *Nonlinear Dynamics*, vol. 35, no. 1, pp. 61–80, 2004.

[6] D. Wang, H. He, and D. Liu, “Adaptive critic nonlinear robust control: A survey,” *IEEE Transactions on Cybernetics*, vol. 47, no. 10, pp. 3429–3451, 2017.

[7] H. Modares, M.-B. N. Sistani, and F. L. Lewis, “A policy iteration approach to online optimal control of continuous-time constrained-input systems,” *ISA Transactions*, vol. 52, no. 5, pp. 611–621, 2013.

[8] K. G. Vamvoudakis and F. L. Lewis, “Online actor–critic algorithm to solve the continuous-time infinite horizon optimal control problem,” *Automatica*, vol. 46, no. 5, pp. 878–888, 2010.

[9] F. L. Lewis, D. Vrabie, and V. L. Syrmos, *Optimal control*. John Wiley & Sons, 2012.

[10] F. Lewis, S. Jagannathan, and A. Yesildirak, *Neural network control of robot manipulators and non-linear systems*. CRC press, 1998.

[11] P. J. Werbos, “Foreword-adp: The key direction for future research in intelligent control and understanding brain intelligence,” *IEEE Transactions on Systems, Man, and Cybernetics, Part B (Cybernetics)*, vol. 38, no. 4, pp. 898–900, 2008.

[12] R. Padhi, N. Unnikrishnan, X. Wang, and S. N. Balakrishnan, “A single network adaptive critic (snac) architecture for optimal control synthesis for a class of nonlinear systems,” *Neural Networks*, vol. 19, no. 10, pp. 1648–1660, 2006.

[13] L. Xing, C. Wen, Z. Liu, H. Su, and J. Cai, "Event-triggered adaptive control for a class of uncertain nonlinear systems," *IEEE Transactions on Automatic Control*, vol. 62, no. 4, pp. 2071–2076, 2016.

[14] E. Garcia and P. J. Antsaklis, "Model-based event-triggered control with time-varying network delays," in *2011 50th IEEE Conference on Decision and Control and European Control Conference*. IEEE, 2011, pp. 1650–1655.

[15] P. Tabuada, "Event-triggered real-time scheduling of stabilizing control tasks," *IEEE Transactions on Automatic control*, vol. 52, no. 9, pp. 1680–1685, 2007.

[16] K. G. Vamvoudakis, "Event-triggered optimal adaptive control algorithm for continuous-time nonlinear systems," *IEEE/CAA Journal of Automatica Sinica*, vol. 1, no. 3, pp. 282–293, 2014.

[17] R. S. Sutton and A. G. Barto, *Reinforcement learning: An introduction*. MIT press, 2018.

[18] A. G. Barto, R. S. Sutton, and C. W. Anderson, "Neuronlike adaptive elements that can solve difficult learning control problems," *IEEE Transactions on Systems, Man, and Cybernetics*, vol. SMC-13, no. 5, pp. 834–846, 1983.

[19] F. L. Lewis and D. Vrabie, "Reinforcement learning and adaptive dynamic programming for feedback control," *IEEE Circuits and Systems Magazine*, vol. 9, no. 3, pp. 32–50, 2009.

[20] R. Bellman, "Dynamic programming," *Science*, vol. 153, no. 3731, pp. 34–37, 1966.

[21] W. B. Powell, *Approximate Dynamic Programming: Solving the curses of dimensionality*. John Wiley & Sons, 2007, vol. 703.

[22] R. Bellman and S. Dreyfus, "Functional approximations and dynamic programming," *Mathematical Tables and Other Aids to Computation*, vol. 13, no. 68, pp. 247–251, 1959.

[23] P. Werbos, "Beyond regression: New tools for prediction and analysis in the behavioral sciences," *Ph. D. dissertation, Harvard University*, 1974.

[24] A. Al-Tamimi, F. L. Lewis, and M. Abu-Khalaf, "Discrete-time nonlinear hjb solution using approximate dynamic programming: Convergence proof," *IEEE Transactions on Systems, Man, and Cybernetics, Part B (Cybernetics)*, vol. 38, no. 4, pp. 943–949, 2008.

[25] P. He and S. Jagannathan, "Reinforcement learning neural-network-based controller for nonlinear discrete-time systems with input constraints," *IEEE Transactions on Systems, Man, and Cybernetics, Part B (Cybernetics)*, vol. 37, no. 2, pp. 425–436, 2007.

[26] J. Si and Y.-T. Wang, "Online learning control by association and reinforcement," *IEEE Transactions on Neural networks*, vol. 12, no. 2, pp. 264–276, 2001.

[27] P. J. Werbos, "Optimal neurocontrol: practical benefits, new results and biological evidence," in *Proceedings of WESCON'95*. IEEE, 1995, p. 580.

[28] D. V. Prokhorov and D. C. Wunsch, "Adaptive critic designs," *IEEE Transactions on Neural Networks*, vol. 8, no. 5, pp. 997–1007, 1997.

[29] G. K. Venayagamoorthy, R. G. Harley, and D. C. Wunsch, "Comparison of heuristic dynamic programming and dual heuristic programming adaptive critics for neurocontrol of a turbogenerator," *IEEE Transactions on Neural Networks*, vol. 13, no. 3, pp. 764–773, 2002.

[30] P. Werbos, "Approximate dynamic programming for real-time control and neural modeling," *Handbook of intelligent control*, 1992.

[31] T. Dierks, B. T. Thumati, and S. Jagannathan, "Optimal control of unknown affine nonlinear discrete-time systems using offline-trained neural networks with proof of convergence," *Neural Networks*, vol. 22, no. 5-6, pp. 851–860, 2009.

[32] F. Liu and H. Peng, "Learning-based robust output tracking control for unknown discrete-time nonlinear systems with dynamic uncertainty," *Neurocomputing*, vol. 606, p. 128412, 2024.

[33] L. Baird, "Advantage updating (tech. rep. no. wl-tr-93-1146)," *Dayton, OH: Wright-Patterson*, 1993.

[34] K. Doya, "Reinforcement learning in continuous time and space," *Neural computation*, vol. 12, no. 1, pp. 219–245, 2000.

[35] D. Vrabie, O. C. Pastravanu, M. Abu-Khalaf, and F. L. Lewis, "Adaptive optimal control for continuous-time linear systems based on policy iteration," *Automatica*, vol. 45, pp. 477–484, 2009.

[36] Y. Zhang, L. Zou, Y. Liu, D. Ding, and J. Hu, "A brief survey on nonlinear control using adaptive dynamic programming under engineering-oriented complexities," *International Journal of Systems Science*, vol. 54, no. 8, pp. 1855–1872, 2023.

[37] D. Wang, N. Gao, D. Liu, J. Li, and F. L. Lewis, "Recent progress in reinforcement learning and adaptive dynamic programming for advanced control applications," *IEEE/CAA Journal of Automatica Sinica*, 2023.

[38] F. Lin, *Robust control design: an optimal control approach.* John Wiley & Sons, 2007, vol. 18.

[39] D. M. Adhyaru, I. Kar, and M. Gopal, "Bounded robust control of nonlinear systems using neural network–based hjb solution," *Neural Computing and Applications*, vol. 20, no. 1, pp. 91–103, 2011.

[40] D. Wang, D. Liu, and H. Li, "Policy iteration algorithm for online design of robust control for a class of continuous-time nonlinear systems," *IEEE Transactions on Automation Science and Engineering*, no. 2, pp. 627–632, 2014.

[41] D. Li and J. Dong, "Robust control for a class of nonlinear systems with input constraints based on actor-critic learning," *International Journal of Robust and Nonlinear Control*, vol. 34, no. 12, pp. 7635–7654, 2024.

[42] F. A. Cheein and G. Scaglia, "Trajectory tracking controller design for unmanned vehicles: A new methodology," *Journal of Field Robotics*, vol. 31, no. 6, pp. 861–887, 2014.

[43] S. Al Issa and I. Kar, "Design and implementation of event-triggered adaptive controller for commercial mobile robots subject to input delays and limited communications," *Control Engineering Practice*, vol. 114, p. 104865, 2021.

[44] Y. Zhang, J. Liu, and J. Yu, "Adaptive asymptotic tracking control for autonomous underwater vehicles with non-vanishing uncertainties and input saturation," *Ocean Engineering*, vol. 276, p. 114280, 2023.

[45] K. Zhang, H. Zhang, G. Xiao, and H. Su, "Tracking control optimization scheme of continuous-time nonlinear system via online single network adaptive critic design method," *Neurocomputing*, vol. 251, pp. 127–135, 2017.

[46] J. Na, Y. Lv, K. Zhang, and J. Zhao, "Adaptive identifier-critic-based optimal tracking control for nonlinear systems with experimental validation," *IEEE Transactions on Systems, Man, and Cybernetics: Systems*, vol. 52, no. 1, pp. 459–472, 2020.

[47] C. Mu, C. Sun, D. Wang, and A. Song, "Adaptive tracking control for a class of continuous-time uncertain nonlinear systems using the approximate solution of hjb equation," *Neurocomputing*, vol. 260, pp. 432–442, 2017.

[48] J.-G. Zhao, "Adaptive dynamic programming-based adaptive optimal tracking control of a class of strict-feedback nonlinear system," *International Journal of Control, Automation and Systems*, vol. 21, no. 4, pp. 1349–1360, 2023.

[49] D. Wang, D. Liu, Y. Zhang, and H. Li, "Neural network robust tracking control with adaptive critic framework for uncertain nonlinear systems," *Neural Networks*, vol. 97, pp. 11–18, 2018.

[50] J. Zhao, J. Na, and G. Gao, "Robust tracking control of uncertain nonlinear systems with adaptive dynamic programming," *Neurocomputing*, vol. 471, pp. 21–30, 2022.

[51] C. Mu, Y. Zhang, Z. Gao, and C. Sun, "Adp-based robust tracking control for a class of nonlinear systems with unmatched uncertainties," *IEEE Transactions on Systems, Man, and Cybernetics: Systems*, vol. 50, no. 11, pp. 4056–4067, 2019.

[52] X. Yang, D. Liu, Q. Wei, and D. Wang, "Guaranteed cost neural tracking control for a class of uncertain nonlinear systems using adaptive dynamic programming," *Neurocomputing*, vol. 198, pp. 80–90, 2016.

[53] D. Xu, Q. Wang, and Y. Li, "Optimal guaranteed cost tracking of uncertain nonlinear systems using adaptive dynamic programming with concurrent learning," *International Journal of Control, Automation and Systems*, vol. 18, no. 5, pp. 1116–1127, 2020.

[54] W. H. Heemels, M. Donkers, and A. R. Teel, "Periodic event-triggered control for linear systems," *IEEE Transactions on Automatic Control*, vol. 58, no. 4, pp. 847–861, 2012.

[55] K. J. Åström and B. Bernhardsson, “Comparison of periodic and event based sampling for first-order stochastic systems,” *IFAC Proceedings Volumes*, vol. 32, no. 2, pp. 5006–5011, 1999.

[56] K.-E. Åarzén, “A simple event-based pid controller,” *IFAC Proceedings Volumes*, vol. 32, no. 2, pp. 8687–8692, 1999.

[57] Q. Hong and H. Zhang, “An introduction to event-based control for networked control systems,” in *2014 IEEE International Conference on System Science and Engineering (ICSSE)*, July 2014, pp. 190–195.

[58] W. Zhu, Z.-P. Jiang, and G. Feng, “Event-based consensus of multi-agent systems with general linear models,” *Automatica*, vol. 50, no. 2, pp. 552–558, Feb. 2014. [Online]. Available: http://dx.doi.org/10.1016/j.automatica.2013.11.023

[59] M. Lemmon, “Event-triggered feedback in control, estimation, and optimization,” *Networked control systems*, pp. 293–358, 2010.

[60] W. H. Heemels, M. Donkers, and A. R. Teel, “Periodic event-triggered control for linear systems,” *IEEE Transactions on Automatic Control*, vol. 58, no. 4, pp. 847–861, 2013.

[61] N. K. Dhar, N. K. Verma, and L. Behera, “Adaptive critic-based event-triggered control for hvac system,” *IEEE Transactions on Industrial Informatics*, vol. 14, no. 1, pp. 178–188, 2017.

[62] D. Wang, L. Hu, M. Zhao, and J. Qiao, “Adaptive critic for event-triggered unknown nonlinear optimal tracking design with wastewater treatment applications,” *IEEE Transactions on Neural Networks and Learning Systems*, vol. 34, no. 9, pp. 6276–6288, 2021.

[63] S. A. Issa, A. Chakravarty, and I. Kar, “Improved event-triggered adaptive control of non-linear uncertain networked systems,” *IET Control Theory & Applications*, vol. 13, no. 13, pp. 2146–2152, 2019.

[64] S. Al Issa and I. Kar, “Event-triggered adaptive control of uncertain non-linear systems under input delay and limited resources,” *International Journal of Dynamics and Control*, vol. 9, no. 4, pp. 1703–1710, 2021.

[65] Q. Zhao, J. Sun, G. Wang, and J. Chen, “Event-triggered adp for nonzero-sum games of unknown nonlinear systems,” *IEEE Transactions on Neural Networks and Learning Systems*, vol. 33, no. 5, pp. 1905–1913, 2021.

[66] X. Wang, Z. Quan, Y. Li, and Y. Liu, “Event-triggered trajectory-tracking guidance for reusable launch vehicle based on neural adaptive dynamic programming,” *Neural Computing and Applications*, vol. 34, no. 21, pp. 18 725–18 740, 2022.

[67] A. Sahoo, H. Xu, and S. Jagannathan, “Neural network-based adaptive event-triggered control of affine nonlinear discrete time systems with unknown internal dynamics,” in *American Control Conference (ACC), 2013*. IEEE, 2013, pp. 6418–6423.

[68] ——, "Near optimal event-triggered control of nonlinear discrete-time systems using neurodynamic programming," *IEEE Transactions on Neural Networks and Learning Systems*, vol. 27, no. 9, pp. 1801–1815, 2016.

[69] M. Ha, D. Wang, and D. Liu, "Event-triggered adaptive critic control design for discrete-time constrained nonlinear systems," *IEEE Transactions on Systems, Man, and Cybernetics: Systems*, vol. 50, no. 9, pp. 3158–3168, 2018.

[70] X. Yang and H. He, "Adaptive critic designs for event-triggered robust control of nonlinear systems with unknown dynamics," *IEEE transactions on cybernetics*, vol. 49, no. 6, pp. 2255–2267, 2018.

[71] D. Wang, C. Mu, H. He, and D. Liu, "Adaptive-critic-based event-driven nonlinear robust state feedback," in *Decision and Control (CDC), 2016 IEEE 55th Conference on*. IEEE, 2016, pp. 5813–5818.

[72] ——, "Event-driven adaptive robust control of nonlinear systems with uncertainties through ndp strategy," *IEEE Transactions on Systems, Man, and Cybernetics: Systems*, vol. 47, no. 7, pp. 1358–1370, 2017.

[73] X. Yang, H. He, and Q. Wei, "An adaptive critic approach to event-triggered robust control of nonlinear systems with unmatched uncertainties," *International Journal of Robust and Nonlinear Control*, vol. 28, no. 10, pp. 3501–3519, 2018.

[74] Q. Zhang, D. Zhao, and D. Wang, "Event-based robust control for uncertain nonlinear systems using adaptive dynamic programming," *IEEE Transactions on Neural Networks and Learning Systems*, vol. 29, no. 1, pp. 37–50, 2018.

[75] L. Dong, X. Zhong, C. Sun, and H. He, "Event-triggered adaptive dynamic programming for continuous-time systems with control constraints," *IEEE Transactions on Neural Networks and Learning Systems*, vol. 28, no. 8, pp. 1941–1952, 2017.

[76] Y. Zhu, D. Zhao, H. He, and J. Ji, "Event-triggered optimal control for partially unknown constrained-input systems via adaptive dynamic programming," *IEEE Transactions on Industrial Electronics*, vol. 64, no. 5, pp. 4101–4109, 2017.

[77] X. Yang and H. He, "Event-triggered robust stabilization of nonlinear input-constrained systems using single network adaptive critic designs," *IEEE Transactions on Systems, Man, and Cybernetics: Systems*, no. 99, pp. 1–13, 2018.

[78] D. Wang, C. Mu, X. Yang, and D. Liu, "Event-based constrained robust control of affine systems incorporating an adaptive critic mechanism," *IEEE Transactions on Systems, Man, and Cybernetics: Systems*, vol. 47, no. 7, pp. 1602–1612, 2017.

[79] X. Zhong and H. He, "An event-triggered adp control approach for continuous-time system with unknown internal states," *IEEE Transactions on Cybernetics*, vol. 47, no. 3, pp. 683–694, 2017.

[80] D. Wang and D. Liu, "Learning and guaranteed cost control with event-based adaptive critic implementation," *IEEE transactions on neural networks and learning systems*, vol. 29, no. 12, pp. 6004–6014, 2018.

[81] K. G. Vamvoudakis, A. Mojoodi, and H. Ferraz, "Event-triggered optimal tracking control of nonlinear systems," *International Journal of Robust and Nonlinear Control*, vol. 27, no. 4, pp. 598–619, 2017.

[82] K. Zhang, H. Zhang, H. Jiang, and Y. Wang, "Near-optimal output tracking controller design for nonlinear systems using an event-driven adp approach," *Neurocomputing*, vol. 309, pp. 168–178, 2018.

[83] N. Xu, B. Niu, H. Wang, X. Huo, and X. Zhao, "Single-network adp for solving optimal event-triggered tracking control problem of completely unknown nonlinear systems," *International Journal of Intelligent Systems*, vol. 36, no. 9, pp. 4795–4815, 2021.

[84] D. Wang, C. Mu, X. Yang, and D. Liu, "Event-based constrained robust control of affine systems incorporating an adaptive critic mechanism," *IEEE Transactions on Systems, Man, and Cybernetics: Systems*, vol. 47, no. 7, pp. 1602–1612, 2017.

[85] X. Yang and H. He, "Event-triggered robust stabilization of nonlinear input-constrained systems using single network adaptive critic designs," *IEEE Transactions on Systems, Man, and Cybernetics: Systems*, vol. 50, no. 9, pp. 3145–3157, 2018.

[86] L. Cui, X. Xie, X. Wang, Y. Luo, and J. Liu, "Event-triggered single-network adp method for constrained optimal tracking control of continuous-time non-linear systems," *Applied Mathematics and Computation*, vol. 352, pp. 220–234, 2019.

[87] S. Xue, B. Luo, D. Liu, and Y. Gao, "Event-triggered adp for tracking control of partially unknown constrained uncertain systems," *IEEE Transactions on Cybernetics*, vol. 52, no. 9, pp. 9001–9012, 2021.

[88] A. D. Ames, S. Coogan, M. Egerstedt, G. Notomista, K. Sreenath, and P. Tabuada, "Control barrier functions: Theory and applications," in *2019 18th European control conference (ECC)*. IEEE, 2019, pp. 3420–3431.

[89] Z. Marvi and B. Kiumarsi, "Safe reinforcement learning: A control barrier function optimization approach," *International Journal of Robust and Nonlinear Control*, vol. 31, no. 6, pp. 1923–1940, 2021.

[90] C. Qin, H. Zhu, J. Wang, Y. Hou, S. Hu, D. Zhang, and Q. Xiao, "Adaptive critic learning for event-triggered safe control of nonlinear safety-critical systems," *Asian Journal of Control*, vol. 25, no. 5, pp. 3645–3659, 2023.

[91] H. Zhang, L. Cui, X. Zhang, and Y. Luo, "Data-driven robust approximate optimal tracking control for unknown general nonlinear systems using adaptive dynamic programming method," *IEEE Transactions on Neural Networks*, vol. 22, no. 12, pp. 2226–2236, 2011.

[92] S. Bhasin, R. Kamalapurkar, M. Johnson, K. G. Vamvoudakis, F. L. Lewis, and W. E. Dixon, "A novel actor–critic–identifier architecture for approximate optimal control of uncertain nonlinear systems," *Automatica*, vol. 49, no. 1, pp. 82–92, 2013.

[93] H. Modares and F. L. Lewis, "Optimal tracking control of nonlinear partially-unknown constrained-input systems using integral reinforcement learning," *Automatica*, vol. 50, no. 7, pp. 1780–1792, 2014.

[94] Y. Zhu, D. Zhao, H. He, and J. Ji, “Event-triggered optimal control for partially unknown constrained-input systems via adaptive dynamic programming,” *IEEE Transactions on Industrial Electronics*, vol. 64, no. 5, pp. 4101–4109, 2016.

[95] Q. Zhang, D. Zhao, and D. Wang, “Event-based robust control for uncertain nonlinear systems using adaptive dynamic programming,” *IEEE Transactions on Neural Networks and Learning Systems*, vol. 29, no. 1, pp. 37–50, 2016.

[96] H. K. Khalil, *Nonlinear systems; 3rd ed.* Upper Saddle River, NJ: Prentice-Hall, 2002.

[97] W. M. Haddad, V. Chellaboina, and S. G. Nersesov, *Impulsive and hybrid dynamical systems: stability, dissipativity, and control.* Princeton University Press, 2006.

[98] T. Dierks and S. Jagannathan, “Optimal control of affine nonlinear continuous-time systems,” in *Proceedings of the 2010 American Control Conference*. IEEE, 2010, pp. 1568–1573.

[99] S. E. Lyshevski, “Optimal control of nonlinear continuous-time systems: design of bounded controllers via generalized nonquadratic functionals,” in *Proceedings of the 1998 American Control Conference. ACC (IEEE Cat. No. 98CH36207)*, vol. 1. IEEE, 1998, pp. 205–209.

[100] M. Abu-Khalaf and F. L. Lewis, “Nearly optimal control laws for nonlinear systems with saturating actuators using a neural network hjb approach,” *Automatica*, vol. 41, no. 5, pp. 779–791, 2005.

[101] A. Cao, F. Wang, Z. Liu, and Z. Chen, “Model-free event-triggered optimal containment control for multiagent systems via adaptive dynamic programming,” *IEEE Transactions on Control of Network Systems*, vol. 11, no. 3, pp. 1452–1464, 2023.

[102] W. Zhao, W. Yu, and H. Zhang, “Event-triggered optimal consensus tracking control for multi-agent systems with unknown internal states and disturbances,” *Nonlinear Analysis: Hybrid Systems*, vol. 33, pp. 227–248, 2019.